Solid-Phase Combinatorial Chemistry and Scintillation Proximity Assays

Mark Christopher M^{C}Cairn

Doctor of Philosophy

Aston University

July 2003

Thesis Summary

Solid-Phase Combinatorial Chemistry and Scintillation Proximity Assays

Mark Christopher M^{c}Cairn

Doctor of Philosophy

Aston University

July 2003

The Scintillation Proximity Assay (SPA) is a method that is frequently used to detect and quantify the strength of intermolecular interactions between a biological receptor and ligand molecule in aqueous media.

This thesis describes the synthesis of scintillant-tagged-compounds for application in a novel cell-based SPA. A series of 4-functionalised-2,5-diphenyloxazole molecules were synthesised. These 4-functionalised-2,5-diphenyloxazoles were evaluated by Sense Proteomic Ltd. Accordingly, the molecules were evaluated for the ability to scintillate in the presence of ionising radiation. In addition, the molecules were incorporated into liposomal preparations which were subsequently evaluated for the ability to scintillate in the presence of ionising radiation. The optimal liposomal preparation was introduced into the membrane of HeLa cells that were used successfully in a cell-based SPA to detect and quantify the uptake of [^{14}C]methionine.

This thesis also describes the synthesis and subsequent polymerisation of novel poly(oxyethylene glycol)-based monomers to form a series of new polymer supports. These Poly(oxyethylene glycol)-polymer (POP) supports were evaluated for the ability to swell and mass-uptake in a variety of solvents, demonstrating that POP-supports exhibit enhanced solvent compatibilities over several commercial resins. The utility of POP-supports in solid-phase synthesis was also demonstrated successfully.

The incorporation of (4'-vinyl)-4-benzyl-2,5-diphenyloxazole in varying mole percentage into the monomer composition resulted in the production of chemically functionalised scintillant-containing poly(oxyethylene glycol) polymer (POP-Sc) supports. These materials are compatible with both aqueous and organic solvents and scintillate efficiently in the presence of ionising radiation. The utility of POP-Sc supports in solid-phase synthesis and subsequent *in-situ* SPA to detect and quantify, in real-time, the kinetic progress of a solid-phase reaction was exemplified successfully. In addition, POP-Sc supports were used successfully both in solid-phase combinatorial synthesis of a peptide nucleic acid (PNA)-library and subsequent screening of this library for the ability to hybridise with DNA, which was labelled with a suitable radio-isotope. This data was used to identify the dependence of the number and position of complimentary codon pairs upon the extent of hybridisation. Finally, a further SPA was used to demonstrate the excellent compatibility of POP-Sc supports for use in the detection and quantification of enzyme assays conducted within the matrix of the POP-Sc support.

Key Words: Scintillant, Polymer, PEG, PNA, Hybridisation.

"My parents to whom I am indebted eternally"

Acknowledgement

I am indebted to my friend and mentor Andrew Sutherland who has provided guidance during our working together and permitted the freedom to pursue my own passions.

I am appreciative to both Aston University and Sense Proteomics Ltd for providing financial support.

I thank Drs Anna Hine and Marcus Hughes for discussion and assistance with both radioactive studies and biological-assays. I thank Dr Steven Tonge for discussion and assistance with mass-solvent uptake studies. I also thank Mr Kevin Hughes for assistance with the operation of the scintillation counters.

My gratitude extends to Mrs Karen Farrow and Mr Peter Ashton for performing low resolution mass spectrometry and high resolution spectrometry respectively. I am thankful to Dr Mike Perry for performing nuclear magnetic resonance spectrometry and tuition in the use of the NMR-spectrometer.

I thank Siobhan Cummins and Dr Dierdre Pearce for reading this document critically.

Contents

Abbreviations

A	adenine
AIBN	azobis-*iso*-butyronitrile
ATP	adenosine 5'-triphoshate
Bhoc	benzhydryloxycarbonyl
18-C-6	18-crown-6
C	cytosine
cat	catalytic
Cbz	benzyloxycarbonyl
CLEAR	cross-linked ethoxylate acrylate resins
cpm	counts per minute
DCC	dicyclohexylcarbodiimide
DCM	dichloromethane
DIPEA	diisopropylethylamine
DMAP	4-*N,N*-dimethylaminopyridine
DME	dimethoxyethane
DMF	*N,N*-dimethylformamide
DMSO	dimethylsulfoxide
DNA	deoxyribonucleic acid
DOPE	dioleoylphosphatidylethanolamine
DOTAP	dioleoyltrimethylammonium propane
DVB	divinyl benzene
EtOH	ethanol
FACS	fluorescence activated cell sorting
Fmoc	fluorenylmethoxycarbonyl
FTIR	fourier transform infra red
G	guanine
Gly-OH	glycine
HPLC	high performance liquid chromatography
HYDRA	hydroxyl and amine polymer support
IR	infrared
LPCS	liquid phase combinatorial synthesis
MeOH	methanol
MS	mass spectroscopy
MSNT	1-(mesitylene-2-sulfonyl)-3-nitro-1H-1,2,4-tiazole
nm	nanometres
NMI	*N*-methylimidazole

NMP	1-methyl-2-pyrolidinone
Nvoc	6-nitroveratryloxycarbonyl
PAM	polyacrylamide
PC	phosphatidylcholine
PCC	pyridinium chlorochromate
PEG	poly(oxyethylene glycol)
PEGA	polyethylene glycol polyacrylamide
PNA	peptide nucleic acid
PNK	polynuceotide kinase
POEPOP	polyoxyethylene-polypropylene
POEPS	polyoxyethylene-polystryrene
PS	polystyrene
PTHF	polytetrahydrofuran
PVT	polyvinyl toluene
POP	poly(oxyethylene glycol) polymer
POP-Sc	scintillant-containing poly(oxyethylene glycol) polymer
PVA	poly(vinyl alcohol)
PyBOP	1*H*-benzotriazole-1-yl-oxy-tris-pyrrolidinophosphonium hexafluorophosphate
Pyr	pyridine
RT	room temperature
SPA	scintillation proximity assay
SPOC	solid-phase organic chemistry
SPOCC	superpermeable organic combinatorial chemistry
SPPS	solid-phase peptide synthesis
T	thymine
TBDMS	*tert*-butyldimethylsilyl
TBAF	tetrabutylammonium fluoride
t-Boc	*tert*-butoxycarbonyl
TFA	trifluoroacetic acid
THF	tetrahydrofuran
TMP	2,2,6,6-tetramethylpiperidine
TsCl	toluene sulphonyl chloride
uv	ultraviolet

Figures, Schemes and Tables

Chapter 1

Introduction

1.1 Scintillation counting

The initial stages of the drug discovery process often involve the identification of a biological receptor of interest.[1] Typically, the receptor is then screened against potential ligand molecules for non-covalent intermolecular binding interactions. Successful binding between the ligand molecule(s) and the receptor may be used to identify a lead to a potential drug candidate.[2] These intermolecular binding interactions may be investigated using potential ligand molecule(s) tagged with a radioisotope.

A radioisotope possesses an unstable nucleus. The spontaneous decay of such a nucleus results in the emission of electromagnetic radiation and/or energetic particle(s). This radioactive decay may be monitored using a suitable counting technique.[3] One such technique is scintillation counting which may be used to detect and quantify the light pulse(s) produced when ionising radiation passes through a scintillation system. The pulse amplitude is proportional to the energy of the ionising radiation and the pulse frequency is proportional to the number of radioisotope disintegrations per minute (dpm), which is subsequently converted into scintillation counts per minute (cpm).[4]

Despite the immense versatility of radioisotopes as analytical probes they possess inherent hazards associated with their application. Radioisotopes are potentially dangerous to biological organisms and may potentially contaminate the environment. The risk associated with their use may be reduced to a minimum by combining a knowledge of radioisotopes, radioactive decay with the appropriate precautions and good working practice.[5]

1.1a Radioactive Decays

An atom may be perceived as a dense central nucleus, comprised of both protons and neutrons, surrounded by a diffuse cloud of electrons. The number of electron(s) determines the chemically reactive nature of the atom whilst the number of proton(s) dictates which element is the atom.[6] The number of neutrons in the nucleus of the atom may vary and dictates which isotope of the element is the atom.

Isotopic stability is dependent upon the relative number of protons and neutrons comprising the nucleus. The greater the imbalance in the number of protons and neutrons generally the less stable is the nucleus. An unstable nucleus may decay spontaneously, to form a daughter nucleus of greater stability, by the emission of electromagnetic radiation and/or energetic particles in one of several ways.

α-Particle emission is associated with the expulsion of two protons (p) and two neutrons (n) from a nucleus. α-Particles are indistinguishable from the nuclei of helium's stable isotope. Consequently, the resultant daughter nucleus has two protons and two neutrons less than that of the parent isotope **Figure1**.[7]

$$^{226}\mathbf{Ra}\ (88p + 138n) \longrightarrow {}^{222}\mathbf{Rn}\ (86p + 136n) + {}^{4}\mathbf{He}^{2+}$$

Figure 1: α-Emission from a radium-226 nucleus.

There are two types of β-emission, β^- and β^+ particles. The type of β-particle emitted from a nucleus is primarily dependent upon the relative number of protons and neutrons comprising the nucleus. Nuclei comprised of an excess number of neutrons relative to protons spontaneously convert a neutron into a proton and an electron (β^--particle). The emission of a β^--particle results in the nucleus gaining a proton and consequently becomes positively charged. The β^--particle is emitted with a neutrino that shares the decay energy in a random manner. Therefore, the β^--particle may possess energy between zero and the maximum decay energy **Figure 2**.[8]

$$^{14}\mathbf{C}\ (6p + 8n) \longrightarrow {}^{14}\mathbf{N}\ (7p + 7n) + \beta^-$$

Figure 2: β^--emission from a carbon-14 nucleus.

Nuclei comprised of an excess number of protons relative to neutrons may spontaneously convert a proton into a neutron and a positron (β^+-particle). The emission of a β^+-particle results in the nucleus gaining a neutron **Figure 3**.[9]

$$^{11}\mathbf{C}\ (6p + 5n) \longrightarrow {}^{11}\mathbf{B}\ (5p + 6n) + \beta^+$$

Figure 3: β^+-emission from a carbon-11 nucleus.

γ-Rays are energy in the form of electromagnetic radiation that is often emitted as a secondary emission process accompanying β^+-particle emission. γ-Rays are produced when an emitted β^+-particle collides with an electron in an orbital surrounding the nucleus. The opposite charges annul one another and the total mass is converted into electromagnetic radiation (γ-rays) of a specific short wavelength (~0.001–0.1 μm).[9]

X-rays are energy in the form of electromagnetic radiation that has a wavelength slightly longer than γ-rays. X-ray emission occurs in association with the capture of an inner orbital electron into an unstable nucleus. Subsequently, a proton is converted into a neutron and the rearrangement of electrons in the atomic orbitals results in the emission of an X-ray.[8]

1.1b Detection of Radioactivity

The first use of scintillation counting to detect radioactive decay was at the beginning of the twentieth century. The collision of ionising radiation with a zinc sulphide screen was found to produce a weak flash of light (scintillation). These scintillations were observed through a low-power optical microscope and individually recorded by the experimenter.[10] Subsequently, these scintillations have been quantified using a photo-multiplier tube coupled to a zinc sulphide screen.

In the middle of the twentieth century it was discovered that a dilute solution of certain organic compounds will scintillate after electronic excitation by ionising radiation.[11] These scintillations may be detected and quantified by the photo-multiplier tube(s) of a scintillation counter.

The concentration of scintillant used in the majority of liquid scintillation systems is very low and as such scintillation resulting from the direct collision of ionising radiation with scintillant molecules is negligible. For the most part, ionising radiation that passes through a liquid scintillation system transfers the majority of its energy to solvent molecules by collision.[12] Subsequently, this energy is transferred to scintillant molecules and competing non-emissive chemical quenching species. The photons emitted by the scintillant molecules that are not absorbed by a coloured species in the scintillation system are detected by the photo-multiplier tube(s) (PMT). These photons are converted into photo-electrons at the cathode of the photo-multiplier tube and then accelerated into the dynode system for amplification. The number of electrons are multiplied by a secondary emission at successive dynodes and detected as electrical pulses at the anode. These pulses are then fed into electronic circuits for amplification (AMP) and counting. The amplitude of the electrical pulse is directly proportional to both the scintillation signal detected and inherently to the energy of the ionising radiation that produced the scintillation **Figure 4**.[13,14,15,16,17,18]

Figure 4: Schematic representation of a liquid scintillation system coupled to a scintillation counter.[19,20]

Any species in a liquid scintillation system that reduces the number of photons reaching the photo-multiplier tube(s) is known as a quenching species.[21] Successful quenching occurs when the species becomes electronically excited and then returns to its ground state by a non-radiative de-excitation process. The interception of photons prior to detection by the photo-multiplier tube(s) causes a reduction in quantum efficiency.[4]

Chemical quenching species may absorb energy that is transferred between the radioisotope and the solvent molecule(s) or a solvent molecule and scintillant molecule. The most commonly encountered

quenching species include ketones, amines and halogenated compounds. In addition, oxygen, water, acids and alkalis also quench scintillation slightly.[39]

Colour quenching commonly occurs when a coloured material that can absorb the photons emitted by the scintillant molecules is present in the liquid scintillation system.

The percentage value of the decaying nuclei that are counted (counting efficiency) may be determined using a radioactive standard of accurately known activity.[22,23] This value can be used in conjunction with the count rate to quantify the amount of radioactivity present in an assay.[24]

Scintillation counts may also originate from the passage of a charged particle, such as a β-particle, through a transparent medium, such as water, at a speed greater than that of light (2.99792458×10^8 ms^{-1}). A small proportion (<1%) of the energy of the charged particle is dissipated by the emission of electromagnetic radiation.[25,26] This electromagnetic radiation known as Cerenkov radiation, is of heterogeneous wavelength, highly directional and appears in the near-ultraviolet (uv) of the electromagnetic spectrum.[27] This phenomenon is prevalent with the use of high energy β-particle emitters, such as ^{32}P (E_{max} = 1.71 Mev), in water.[28]

Extraneous radiation such as cosmic rays and pulses that are spontaneously generated within the electrical circuit of the scintillation counter may also produce erroneous counts. Therefore, in any scintillation counting procedure, a background count rate must be determined using an identical non-radioactive material. This background reading is then subtracted from the total count rate.[29]

1.1c Photochemical Mechanism of Scintillation

The photochemical processes that take place in liquid scintillation systems may be represented in the form of a Jablonski diagram **Figure 5**.

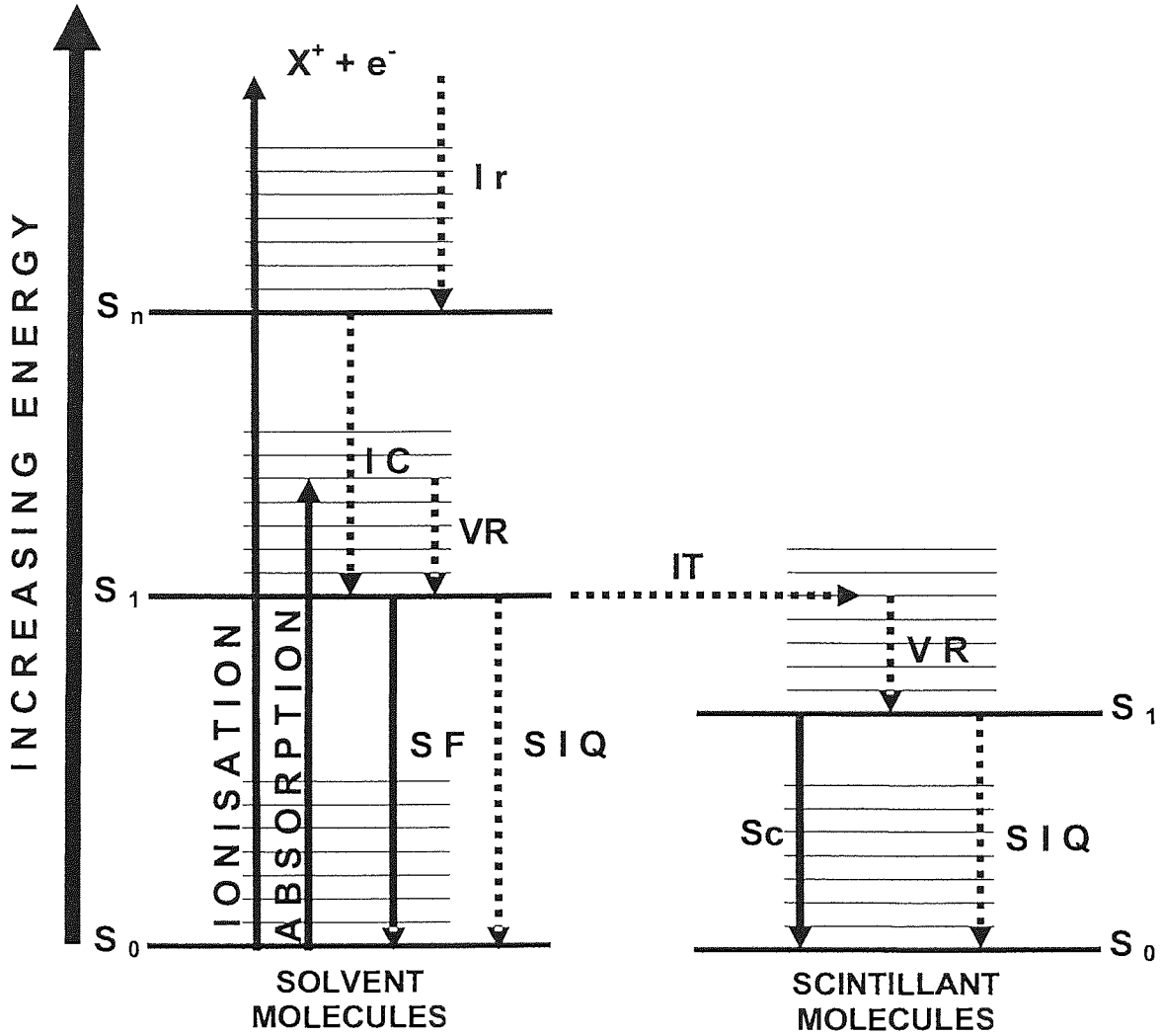

Figure 5: A Jablonski diagram for the photochemical processes operating in a liquid scintillation system.
Ir=ion recombination, VR=vibrational relaxation, SIQ=solvent/scintillant internal quenching, IC=internal conversion, IT=intermolecular transition, SF=solvent fluorescence, Sc=scintillation.

The low concentration of scintillant compound used in popular liquid scintillation systems causes the ionising radiation to transfer the majority of its energy to solvent molecules.[30] The solvent molecules that absorb energy greater than their ionisation energy expel an electron to form a solvent ion (X^+).[31] These ions recombine (Ir) with electrons rapidly to become solvent molecules in an electronically excited state S_n.

The ionising radiation may have a frequency corresponding to the difference in energy between the ground electronic state S_0 and a vibrational level of an upper electronic state S_n in the solvent molecule. Successful absorption of this energy may promote an electron from the S_0 state to a vibrational level of a S_n state.[32]

The energy of an electronically excited molecule may be dissipated by radiative (solid arrow) or non-radiative (broken arrow) de-excitation processes. The high rate ($\sim 10^{13}$ s^{-1}) of molecular collision in a solution facilitates the transfer and dissipation of energy. An electron occupying a vibrational level of the S_n state may return to the lowest excited singlet state S_1 by the dissipation of energy through non-radiative de-excitation processes of vibrational relaxation (VR), rotational relaxation, translational relaxation and internal conversion (IC).[33]

A liquid scintillation system comprised of a scintillant compound that possesses an S_1 state that is lower in energy than the S_1 state of the solvent facilitates the spontaneous transfer of energy from an electronically excited solvent molecule to a scintillant molecule. An electronically excited solvent molecule with an electron occupying the S_1 state may dissipate this energy by the radiative process of solvent fluorescence (SF) or either of the non-radiative processes of solvent internal quenching (SIQ) and intermolecular transition (IT). The IT process transfers the energy to an isoenergetic vibrational level of a scintillant molecule that is in close proximity. Subsequently this electron cascades down the vibrational levels to the S_1 state by non-radiative relaxation processes.[34]

The solvent molecules are often unable to accept the energy from this electronically excited scintillant molecule. Consequently, the electron that occupies the S_1 state frequently returns to the ground electronic state S_0 by the emission of a photon in the form of a weak flash of light or scintillation (Sc).

Alternatively, the energy populating a S_1 state may be dissipated by non-radiative de-excitation processes of vibrational relaxation, rotational relaxation and translational relaxation. This overall process is known as solvent/scintillant internal quenching (SIQ). The relative rate of non-radiative de-excitation processes versus scintillation determines the amplitude and frequency of the scintillation signal detected.

1.1d Liquid Scintillation Systems

Liquid scintillation counting has become the generally preferred method for the accurate detection and quantification of low energy β-emitting radioisotopes.[35] The majority of liquid scintillation counting systems are comprised of a dilute solution of a primary and secondary organic scintillant compound dissolved in a primary solvent in the presence of either a secondary solvent or a surfactant.[36]

Efficient liquid scintillation counting generally occurs with the use of a solvent that has an aromatic structure. The aromatic π-bonded electrons are readily excited upon collision of the ionising radiation with solvent molecules.[37] The primary solvent of choice is toluene. Toluene in contact with tritium and carbon-14 radioisotopes has been known to produce up to 15 and 120 excited solvent molecules respectively.[38] A secondary solvent is often required to solubilise the primary solvent and scintillant

compound(s) in water. The secondary solvent (e.g. dioxane or 2-ethoxy-ethanol) may either dissolve the primary solvent, primary scintillant, secondary scintillant and water or be a surfactant (e.g. triton X-100). In general, oxygen-containing solvents such as water, alcohols and ethers perform reasonably well as solvents in liquid scintillation counting systems. The use of halogenated solvents is precluded because they quench scintillation significantly.[39]

The primary scintillant molecule(s) generally used in successful scintillation counting systems are aromatic and possess extended conjugation. The commonly used primary scintillant molecules include 2,5-diphenyloxazole **1**, *p*-terphenyl **2** and 2-phenyl-5-(4-biphenyl)-1,3,4-oxadiazole **3** **Figure 6**.[40,36]

Figure 6: Commonly used primary scintillant compounds.[41]

The passage of ionising radiation through a dilute solution of each compound **1-3** dissolved in toluene displays high quantum efficiency.[42] The greater solubility in toluene of **1** (270 g/L at 25 °C) relative to **2** (8 g/L at 25 °C) and **3** (20 g/L at 25 °C) has made **1** the primary scintillant compound employed in the majority of liquid scintillation systems.[43]

Primary scintillant compounds often emit photons of a wavelength outside the detection range of the photo-multiplier tube(s) used in commercial scintillation counters.[44] Consequently, a secondary scintillant compound is frequently incorporated in the liquid scintillation system, typically at 10% concentration of the primary scintillant compound.[45,15,46,47] The secondary scintillant shifts the peak emission of the liquid scintillation system to a longer wavelength. The photons emitted by the primary scintillant are absorbed by the secondary scintillant and then re-emitted as photons of a wavelength within the detection range of the photo-multiplier tube(s).[6] Examples of commonly used secondary scintillant compounds include 1,4-di-(2-(5-phenyloxazoyl))benzene **4**, 5-naphthyl-2-phenyloxazole **5** and 2,5-di(4'-biphenyl) oxazole **6** **Figure 7**.[48,49,50]

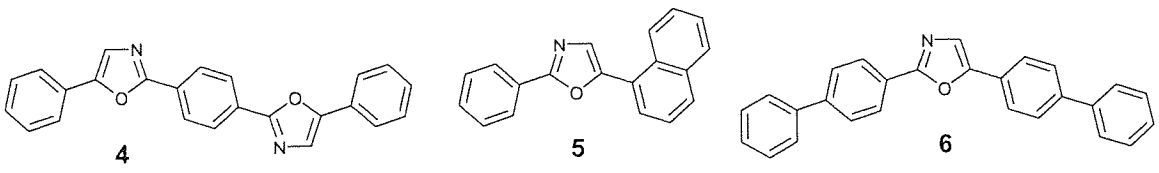

Figure 7: Commonly used secondary scintillant compounds.

1.1e Plastic Scintillation Systems

Scintillant-containing polymers have been constructed and used in place of liquid scintillation systems for the detection of ionising radiation.[51] These plastic scintillation systems are comprised of an organic scintillant compound that has been dissolved in a monomer solution or melt which is subsequently polymerised.[52] The photochemical processes that take place in a plastic scintillation system are similar to those that occur in the equivalent liquid scintillation system. Plastic scintillation systems generally employ the same scintillant compounds and polymeric analogues of solvents that are commonly used in liquid scintillation systems.

The series of alkyl benzene monomers (styrene, vinyltoluene, etc) have proved to be the most efficient polymerisable solvent analogues for the construction of plastic scintillation systems.[53] Polymers constructed from these monomers have higher fluorescence quantum efficiencies than their liquid solvent analogue. This advantage is counterbalanced by the fact that the rigidity of the polymer matrix inhibits molecular diffusion and increases self-absorption of photons. In general, these processes result in the energy transfer between the polymer matrix and scintillant molecules being less efficient than in their analogous liquid scintillation system. Consequently, plastic scintillation systems have relatively low scintillation counting efficiencies and in addition give poor experimental reproducibility.[54,55] To achieve optimum scintillation efficiency, a higher concentration of scintillant compound is often incorporated into a plastic scintillation system, relative to that required in an equivalent liquid scintillation system.

1.1f Scintillation Proximity Assay (SPA)

In 1979, it was demonstrated successfully that a species labeled with tritium may be discriminated by its proximity to a scintillant-containing polymer bead in aqueous medium.[56] This application was patented [57] and subsequently developed by Amersham Biosciences and is currently marketed as the Scintillation Proximity Assay (SPA).[58,59] SPA is a radioisotopic, sensitive, real-time and dynamic assay that may be used to detect and quantify the strength of intermolecular interactions between receptor-ligand systems.[60] SPA technology involves the use of either cerium doped yttrium silicate (Y_2SiO_5:Ce) particles or polyvinyl toluene (PVT) microspheres that have been impregnated with an organic scintillant compound.

PVT-SPA beads are prepared by precipitating a scintillant compound in the pores of the spherical polymeric beads. Typically, a batch of porous PVT-beads (~2-8 μm diameter) is mixed with a solution of 2,5-diphenyloxazole **1** dissolved in dimethylsulfoxide (DMSO) and the mixture is allowed to equilibrate. The addition of water to this system results in the precipitation of scintillant molecules within the pores of the beads **Figure 8**.

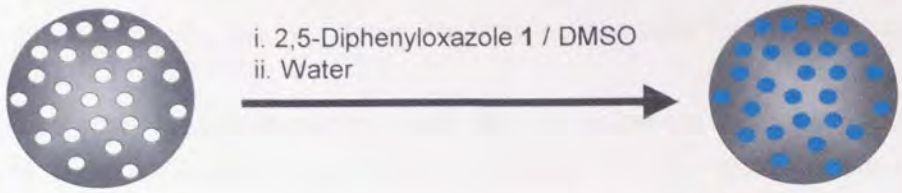

Figure 8: The preparation of a SPA-bead.

To reduce both hydrophobicity and potential non-specific binding interactions of the PVT-SPA-beads they are coated with a polyhydroxyl film **Figure 9**(**A**). A compound that has a strong affinity towards binding generic proteins is then attached covalently to the surface of these polyhydroxyl-coated SPA-beads **Figure 9**(**B**).[61,62] A biological receptor (antibodies, receptor proteins, enzymes) is then pre-coupled to these SPA-beads or captured by the SPA-bead after assay completion **Figure 9**(**C**).[60]

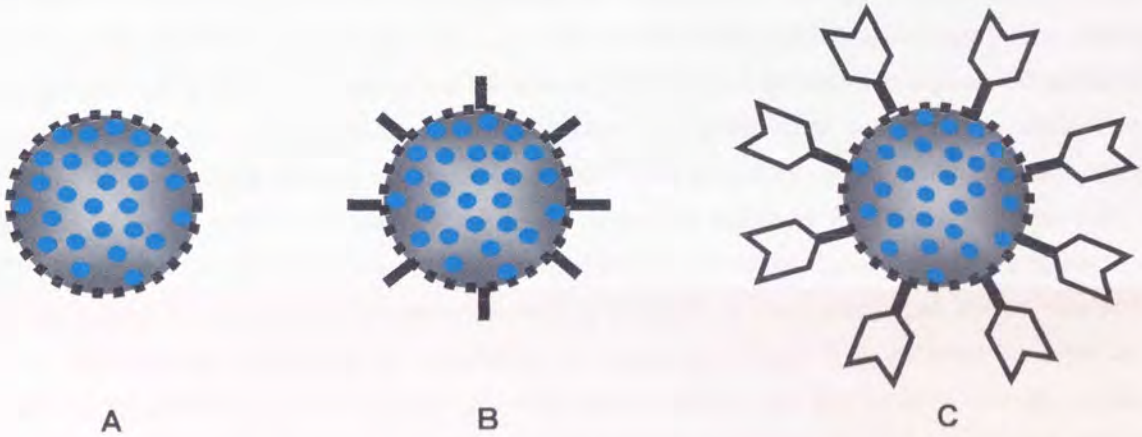

Figure 9: Schematic structures of a polyhydroxyl-SPA-bead (**A**), generic binding protein-SPA-bead (**B**) and biological receptor-SPA-bead (**C**).

Commercially available SPA-beads coupled to binding proteins include wheat germ agglutinin (WGA), streptavidin, glutathione, histidine and protein-A. Attachment of these SPA-beads to a biological receptor is achieved by tagging the receptor molecule with the appropriate molecule. These tagged receptor molecules are coupled to the SPA-beads by the formation of the following high affinity conjugates WGA-*N*-acetyl-β-D-glucosamine, biotin-streptavidin, glutathione-GST, copper chelate-histidine and Protein A-IgG.[18,63,60]

In SPA, the potential ligand molecule(s) are radioisotopically-labelled, generally with a low-medium energy β-emitter that has a short path length in an aqueous environment. Radioisotopes such as tritium, carbon-14, phosphorous-33, sulphur-35 and Iodine-125 are ideally suited for use in SPA. The β-electrons emitted from ^{3}H, ^{14}C, ^{33}P and ^{35}S in water have mean path-lengths of 1.5 μm, 58 μm, 126

μm and 66 μm respectively. The two Auger electrons emitted from ^{125}I in water have mean path-lengths of 1 μm and 17 μm.[60,61,64]

SPA may be applied to an assay format that gives either an increase or decrease in scintillation signal. A decrease in signal occurs when the radiolabel is cleaved from the substrate that is bound to the SPA-bead. This assay format has been applied to the study of hydrolase's (protease and nucleases) enzyme catalytic activity and competitive receptor binding with non-radiolabelled potential ligand molecules.

An increase in signal occurs upon attachment of a radiolabel to the substrate that is bound to the SPA-bead.[18,65] This assay format has been applied to the study of transferase, polymerase and kinase enzyme catalytic activity and receptor-radiolabelled ligand binding assays.

In general, receptor binding assays involve the incubation of a radioisotopically-labelled ligand molecule(s) with a SPA-labelled receptor in aqueous buffer.[66] These assay mixtures are monitored in a scintillation counter to detect and quantify any intermolecular binding interactions between the receptor and ligand molecule(s). Successful binding between the receptor and ligand molecule(s) brings the radiolabel into close proximity of the SPA-bead. The energy of the β-particle emitted by the radiolabel is transferred to the polymer matrix of the SPA-bead and then to a scintillant molecule. De-excitation of the electronically excited scintillant molecule results in the emission of a scintillation which may be detected and quantified using a scintillation counter.[67] The amplitude and frequency of the signal is proportional to the number of radiolabelled ligand molecules bound to the SPA-labeled receptor and thus, in a system at equilibrium, directly to the strength of the receptor-ligand binding interaction.[61]

The successful discrimination of receptor binding by proximity is dependent upon the particle emitted from a radioisotope having a short path-length in aqueous medium. The distance travelled by the particle is dependent upon the energy of the ionising radiation and the medium through which the particle travels. The SPA-bead only enables the detection of radio-labelled ligand molecules that either bind to the receptor or are sufficiently close in proximity to the bead to elicit a signal. Any radioisotope may cause a non-proximity effect but the effect is more pronounced with high energy emitting radioisotopes.[18, 64, 68, 69, 70] SPA has been utilised effectively for monitoring binding interactions continuously in an aqueous medium without the requirement to separate bound ligand molecules from those free in solution **Figure 10**.[18,35,60,67,69,71,72]

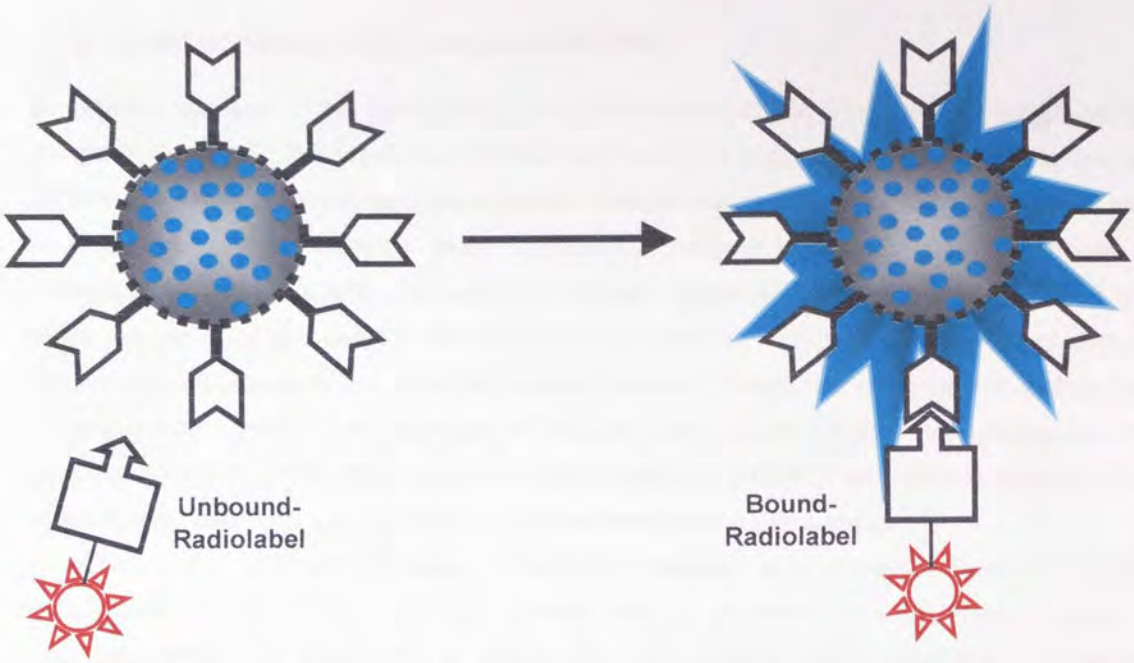

Figure 10: Schematic representation of a radiolabelled ligand molecule binding to a SPA-labelled receptor molecule.

Applications of SPA include radioimmunoassays, receptor binding assays and enzyme inhibition assays. More recently SPA has been applied to cellular adhesion molecule binding, protein-protein interactions, protein-deoxyribonucleic acid (DNA) interactions and cellular biochemistry assays.[59]

High-throughput screening laboratories required SPA to be miniaturized to enable the study of cellular biochemical processes. The SPA-96-well-microplate base is constructed from scintillant containing polystyrene which has then been chemically treated to promote cell growth. In a typical application, cells are cultured in the plate and then various radiolabelled test molecules in aqueous buffer are added to each well. Cells that successfully take up the radiolabelled molecules bring the radioisotope into close proximity with the scintillant compound contained in the base of the well. The amount of light emitted from the scintillant compound quantifies the number of radiolabelled molecules that have been taken up by the cells.[61]

1.1g Disadvantages with Commercial SPA

Despite the elegance of the SPA, it has found only limited utility in the field of combinatorial chemistry, principally because SPA-beads have limited application as supports in solid-phase organic chemistry (SPOC). SPA-beads do not possess suitable chemical functionality for the facile covalent attachment of molecules to their surfaces. Most significantly however is the fact that SPA-beads are also completely incompatible with the majority of organic solvents. The precipitated scintillant compound within the pores of the bead is incorporated non-covalently. Therefore, exposure of SPA-beads to organic solvent results in the scintillant molecules being dissolved, rendering the beads useless for subsequent SPA applications. Although SPA-beads are relatively stable in the presence of water and aqueous solutions up to 20% volume DMSO, methanol (MeOH) and ethanol (EtOH), it has been reported that, even in water, leaching may occasionally prove problematic.[71]

In addition, for comparative assays, the SPA requires each potential ligand molecule to be radioisotopically labeled with the same specific activity. In practice this would be extremely difficult, time consuming and expensive to accomplish. Alternatively, the competitive displacement of a radiolabelled ligand bound to a SPA-labelled receptor must be undertaken using non-radiolabelled potential ligand molecules. The binding activity is then estimated by loss of scintillation signal. Even if known ligands exist and can be radiolabelled an assay format based on a loss of signal is much less reliable than a format which results in an increase in scintillation signal.

1.2 Polymer Supports

Merrifield pioneered solid-phase peptide synthesis (SPPS) by utilising chloromethyl-functionalised styrene-divinylbenzene (PS-DVB) polymer resin beads.[73] The practitioners of SPPS have continued to predominantly use PS-DVB based resins.[74] Usually these resins are prepared by a suspension radical co-polymerisation reaction of a styrene monomer, DVB cross-linking monomer and a radical initiator such as azobis-*iso*-butyronitrile (AIBN) **7**.[75,76] Typically, the monomer mixture and a larger volume of an aqueous solution that contains a low concentration of stabiliser, such as polyvinyl alcohol (PVA), are stirred. This process disperses the monomer mixture as spherical micro-droplets that are suspended in the aqueous phase by continuous stirring and stabilised by PVA. The reaction vessel temperature is increased (~80 °C) to cause the thermolytic fission of AIBN **7** into free radicals **Scheme 1**.

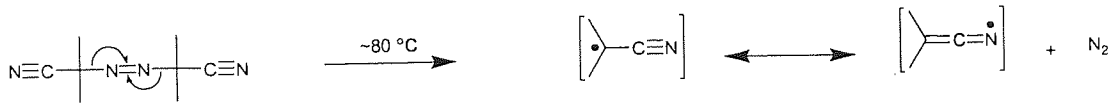

7

Scheme 1: Thermolytic fission of AIBN **7**.

These radicals initiate the polymerisation reaction by reacting with molecules of monomer to form initiator monomer radical adducts. These radicals then react with other monomer molecules to propagate the polymerisation reaction.

The monomers polymerise into discrete micro-gel regions that subsequently polymerise into an extended "infinite" network. The polymerisation reaction proceeds with an increase in insolubility of the monomer mixture, which results in the transformation of the liquid monomer micro-droplets into spherical insoluble polymer beads (a process that can take as long as 12 hours). These resin beads are collected by filtration, washed, extracted, dried and normally sieved into size ranges.

1.2a Polymer Morphology

Polymer beads may be characterised as either gel-type or macroreticular (macroporous), according to the molar quantity of cross-linking monomer used in their preparation.[74,76]

Gel-type polymers are prepared by the polymerisation of a monomer mixture that incorporates a low molar percentage (<10 typically 1 or 2 mole percent) of cross-linking monomer. These polymers comprise of a network of interpenetrating polymer chains. The polymer is adequately cross-linked to boost mechanical strength and insolubility. The degree of cross-linking is low enough to allow significant swelling when the polymer beads are brought into contact with a suitable solvent. This swelling is a consequence of the partial solvation of linear regions of the polymer matrix. Swelling allows suitable solvents and thus reagent(s) to permeate the polymer matrix.

Macroporous polymers are prepared by the polymerisation of a monomer mixture that incorporates a relatively high molar percentage (>10 typically 20 mole percent) of cross-linking monomer and an appropriate porogen. As the polymerisation reaction proceeds the porogen introduces pores between the highly cross-linked micro-gel regions of the polymer matrix. The porogens 2–ethyl-1-hexanol and toluene are used to introduce pores into the polymer matrix by early and late precipitation of the monomer mixture respectively. The resultant polymer is physically rigid and possesses a well defined internal network of pores with a large surface area (~50-1000 m^2/g) that may imbibe all solvents with negligible swelling of the polymer matrix.

1.2b Polymer Supports for Solid-Phase Synthesis

Merrifield pioneered SPPS by using a chloromethyl-functionalised PS-DVB resin **9** for the covalent attachment on the carboxyl group of an amino acid. This support-bound amino acid served as a support for sequential couplings of subsequent *N*-protected amino acid residues.[73] The chemical functionality of the resin was provided by chloromethylation of PS-DVB (2 mole percent DVB) resin **8** **Scheme 2**.

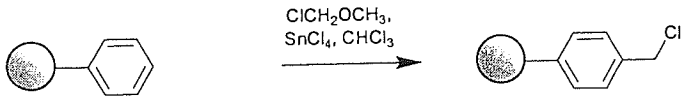

8 **9**

Scheme 2: Chloromethylation of PS-DVB resin **8**.

Alternatively, copolymerisation of styrene **10**, DVB **11** and 4-vinylbenzylchloride **12** provides polymer with a controlled loading of chloromethyl-groups that are homogeneously distributed throughout the polymer matrix **Scheme 3**.[77]

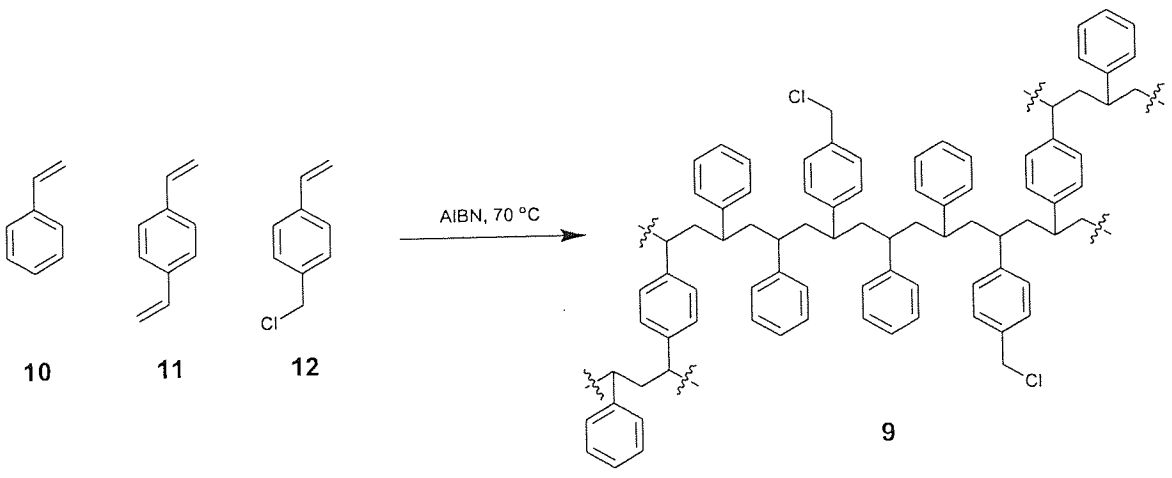

10 **11** **12** **9**

Scheme 3: Copolymerisation of styrene **10**, divinylbenzene **11** and 4-vinylbenzylchloride **12**.

The initial amino acid is attached to the resin *via* a benzyl ester linkage. This linkage is not entirely stable towards repetitive treatment with trifluoroacetic acid (TFA), used to remove *N*-protection groups prior to each amino acid coupling. Therefore, resin-linkers and amino acid *N*-protection strategies have been developed to facilitate *N*-deprotection and release of peptides under milder conditions.

In 1973, Wang constructed 4-alkoxybenzyl alcohol resin **13**.[78] This resin and a series of analogues have been synthesised by reaction of chloromethyl-PS-DVB resin **9** with the appropriate 4-hydroxybenzyl alcohol derivative **Figure 11**.[79,80]

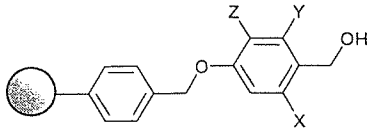

Figure 11: Structure of Wang-resin (X=H, Y=H, Z=H) **13**, HMPB-resin (X=H, Y=H, Z=OMe) **14**, SASRIN-resin (X=OMe, Y=H, Z=H) **15** [80] and HAL-resin (X=OMe, Y=OMe, Z=H) **16**.

These resins are generally used in conjunction with a fluorenylmethoxycarbonyl (Fmoc)-*N*-protection synthetic strategy. At the end of the peptide synthesis, the benzylic ester linkage is cleaved often by treatment with TFA. This cleavage is facile, compared with cleavage of a benzylic ester linkage that tethers a peptide to Merrifield's resin because the methoxy group(s) mesomeric transfer of electrons stabilise the benzylic cation that is formed upon cleavage of the peptide.

A variety of other resin linkers have been developed for use in SPPS.[81,82] Notable examples include, 2-chlorotrityl resin **17**,[83] Rink acid resin **18** (X=MeO, Y=MeO, Z=OH), Rink amide resin **19** (X=MeO, Y=MeO, $Z=NH_2$),[84] benzhydrylamine (BHA) resin **20** (X=H, Y=H, $Z=NH_2$),[85] *p*-methylbenzhydrylamine (MBHA) resin **21** (X=Me, Y=H, $Z=NH_2$),[86] Sieber resin **22**,[87] Kaiser's oxime resin **23**,[88] Kenner's safety catch resin **24** and *o*-nitrobenzyl resin **25**,[89] **Figure 12**.

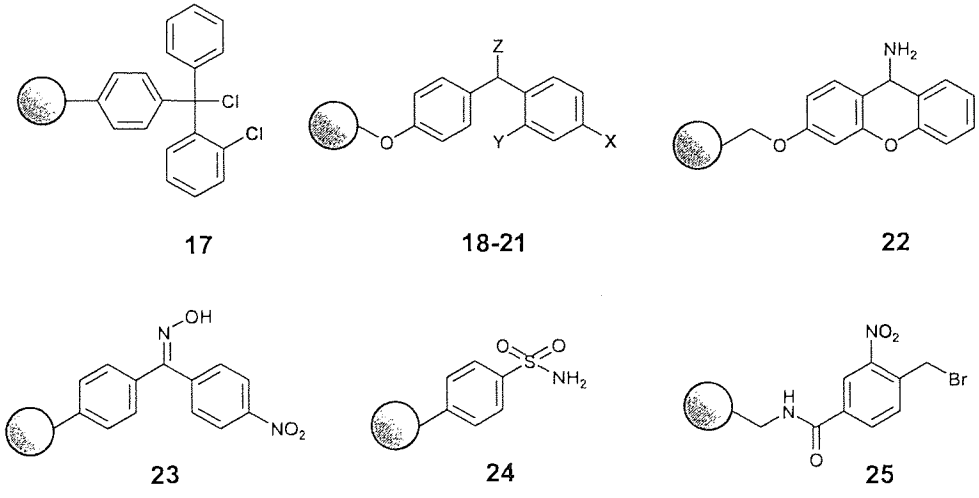

Figure 12: Polymer resins **17-25** for SPPS.

These linkers modify the local environment surrounding the reactive chemical functionality within the resin, but do not have a significant effect upon the intrinsic low-polarity of PS-DVB resins.[90]
Solution phase peptide synthesis is often conducted using polar protic solvents that solvate the nascent peptide effectively. However, these solvents do not swell the PS-DVB resins that are commonly used in SPPS significantly. Consequently SPPS that employs polar protic solvents restricts the access of the amino acid(s) and polar reagent(s) into the PS-DVB matrix, which often results in low yielding reactions. Conversely, the use of a low-polarity solvent significantly swells the PS-DVB matrix, but promotes intra-molecular folding of the polymer-supported peptide. This folding may inhibit the coupling of the next amino acid, which can result in the synthesis of peptides with incorrect sequences.

One way to overcome this incompatibility of PS-DVB resins with peptide synthesis is to increase the polarity of the polymer matrix by the covalent attachment of poly(oxyethylene glycol) (PEG). Initially this approach required the arduous synthesis and purification of orthogonally functionalised PEG prior to coupling with the resin.[91] This strategy has been superseded by the facile grafting of linear PEG onto PS-DVB resin. These composite resins are prepared by anionic graft polymerisation of ethylene oxide onto a tetraethylene glycol derived PS-DVB resin **26** (1 mmol/g, 1 mole percent DVB) **Scheme 4**.[92]
The composite resin that exhibits optimal functional group loading (0.2-0.3 mmol/g), resin crystallinity and swelling properties are grafted with PEG approximately 68 ethylene oxide units (n= ~64, ~75 wt % PEG) in length. These resins swell significantly in water and the majority of organic solvents of widely differing polarity. This property facilitates the diffusion of polar reagents that are dissolved in a suitable solvent into the polymer matrix to access the terminal hydroxyl functionality. These PEG-PS-DVB composite supports are available commercially as TentaGel resins **27**.[93]

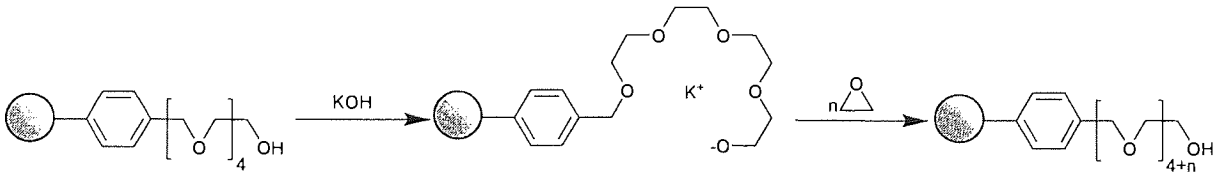

26 **27**

Scheme 4: Synthesis of TentaGel resin **27**.

The benzylic ether in TentaGel resin's is labile towards the relatively strong acidic conditions that are commonly employed in SPPS. Subsequently this linkage has been replaced with a relatively stable benzyl ethyl ether linkage.[94] However, resins of this type still have a low functional group loading per unit weight of resin (mmol functional group/g resin).

ArgoGel resins **29** address both these limitations by grafting linear PEG onto a bifurcated linkage that provides a chemically inert linker with twice the functional group loading per unit weight of resin.[95]
Chloromethyl-PS-DVB resin **9** is reacted with methyl diethylmalonate followed by reduction to provide

1,3-dihydroxy-2-methylpropane derivatised resin **28**. This resin is subsequently subjected to an anionic graft polymerisation of ethylene oxide **Scheme 5**.[96]

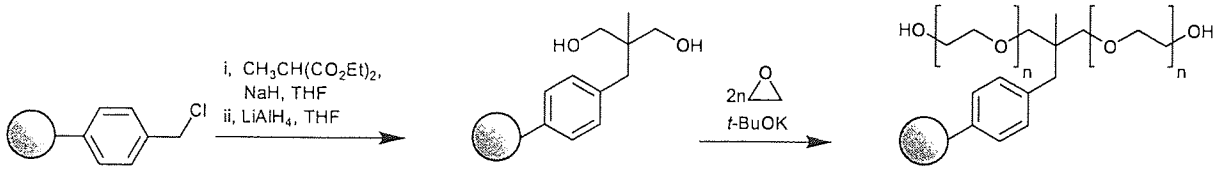

9 **28** **29**

Scheme 5: Synthesis of ArgoGel resin **29**.

The ArgoGel resin **29** that has optimal loading, crystallinity and swelling properties is comprised of a similar percentage of PEG (~75%, n=~35) as the optimal TentaGel resin **27**. However, ArgoGel resin's **29** bifurcated linkage provides approximately twice the functional group loading (0.4-0.5 mmol/g) to that of TentaGel resin **27** (0.2-0.3 mmol/g). Macroporous resins that possess high internal surface areas (>500 m^2/g) are commercially available as ArgoPore resins.[97]

The successful grafting of low-molecular weight PEG onto PS-DVB polymer beads provides a composite resin with higher functional group loading per unit weight of resin than resins derived from grafting high-molecular weight PEG.[98] A tetraethylene glycol derived resin **32** has been prepared by the hydrolysis of 4-acetoxy-PS-DVB resin **30** and subsequent Mitsunobu reaction with tetraethyleneglycol monotetrahydropyranyl (THP) ether followed by hydrolysis of the THP group from resin **31 Scheme 6**.[99]

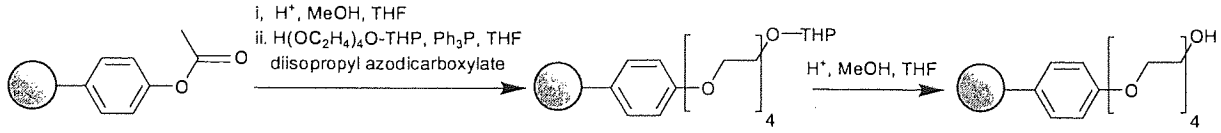

30 **31** **32**

Scheme 6: Synthesis of tetraethylene glycol derived resin **32**.

Alternatively, solid-phase dendrimer synthesis using an isocyanate monomer and aminomethlyl-functionalised resin **33** has provided a pseudo PEG-PS-DVB resin **34**. This resin has an extremely ordered and hyperbranched structure with high functional group loading per unit weight of resin **Scheme 7**.[100,101]

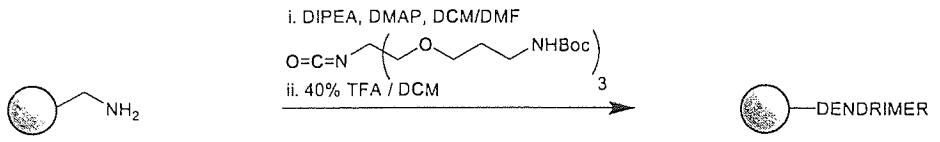

33 34

Scheme 7: Synthesis of dendrimer resin **34**.

Despite the significant and elegant work involving the grafting of PEG onto PS-DVB resins, the grafting process does not significantly alter the intrinsic hydrophobicity and molecular architecture of the polystyrene matrix. In a study focused on modifying the PS-DVB matrix, styrene has been cross-linked with short-chain-PEG.[102] α,ω-*Bis*-styryl-oligo(oxyethylene glycol) ether cross-linking monomers **36** were synthesised by reacting the corresponding oligo(ethylene glycol) **35** with 2 equivalents of 4-vinylbenzyl chloride **12** under Williamson ether synthesis conditions **Scheme 8**.

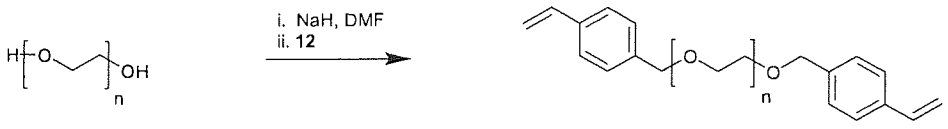

35 36

Scheme 8: Synthesis of α,ω-*bis*-styryl-oligo(oxyethylene glycol) ether cross-linking monomer **36**.

The PEG-based cross-linker **36**, styrene **10** and a chiral monomer were then subjected to a suspension radical copolymerisation reaction. The resultant resin beads exhibited greater swelling in aprotic organic solvents, superior mechanical stability and higher enantioselectivities when used in the appropriate asymmetric synthesis reaction compared with analogous PS-DVB resins.

Kurth subsequently polymerised styrene **10** with α,ω-bis-styryl-oligo(oxyethylene glycol) ethers **36** of variable ethylene glycol tether length (n=1, 2, 4, 6) and mole percentage incorporation. The resultant polymer resins were investigated in terms of their swelling and diffusion properties in aprotic solvents.[103] In this manner, it was determined that a polymeric gel-type resin's swelling behaviour is not a function of ethylene glycol tether length of the cross-linking monomer. Whilst, conversely highly cross-linked resins exhibit increased swelling with increasing ethylene glycol tether length.
The rate of diffusion through the polymer matrix is not simply dependent upon the ethylene glycol tether length of the cross-linking monomer. Although, PS-PEG resins exhibit faster diffusion rates than PS-DVB resins in solvent that does not significantly swell the polymer matrix, the opposite is observed in high swelling solvents.

In related work, Janda's group has reported the synthesis and evaluation of a series of polystyrene-based resins that have been cross-linked with polytetrahydrofuran (PTHF) derivatives **38**.[104,105,106] These PTHF-derived cross-linking monomers **38** were synthesised by reacting the corresponding

polybutylene glycol molecule **37** (n=1, n=~3.5, n=~9.5) with 2 equivalents of 4-vinylbenzyl chloride **12** under Williamson ether synthesis reaction conditions **Scheme 9**.

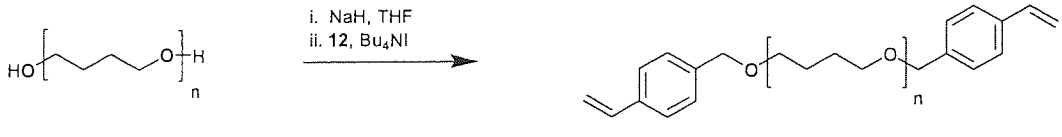

37 **38**

Scheme 9: Synthesis of PTHF-derived cross-linking monomer **38**.

The PTHF-cross-linker **38**, styrene **10** and 4-vinylbenzyl chloride **12** were then subjected to a suspension copolymerisation reaction. The resultant polymer resin beads are mechanically stable and swell in aprotic organic solvents to approximately twice the volume of analogous PS-DVB resins.
The α,ω-*bis*-styryl-oligo(oxyethylene glycol) ether **36** and PTHF **38** cross-linking monomers both possess benzylic ether linkages that are well known to be labile towards strongly acidic conditions and certain nucleophilic reagents. To circumvent this problem, a THF derived cross-linking monomer **40** was synthesised that led to the replacement of the potentially labile benzylic ether linkage with more stable phenolic ether linkages. The THF-cross-linking monomer **40** was prepared by the base hydrolysis and subsequent deprotonation of two equivalents of 4-acetoxystyrene **39**, which was then reacted with 1,4-dibromobutane **Scheme 10**.

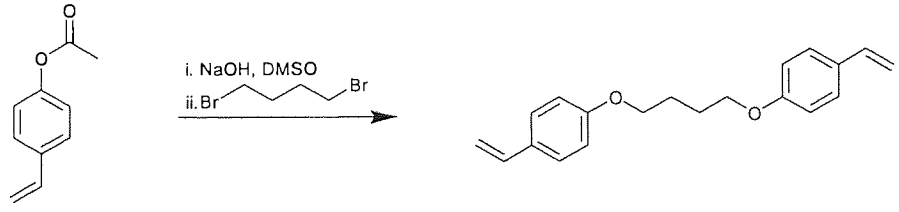

39 **40**

Scheme 10: Synthesis of THF-derived cross-linking monomer **40**.

PS-THF resins (sold commercially as Jandajel^{TM}) are chemically robust and in aprotic organic solvents swell to approximately twice the volume of analogous PS-DVB resins.[107] However, the inability of Jandajel^{TM} resin to swell in polar protic solvents restricts its use in SPPS/SPOC and precludes their use for on-bead biological screening, a process that inherently requires aqueous solvent.

Alternative polymer supports have been constructed to circumvent the limitations imposed by the intrinsic hydrophobicity of polystyrene based resins. A series of polyacrylamide (PAM) based resins **44** were designed and synthesised specifically for use in SPPS.[108] In a typical synthesis, a monomer mixture of *N*,*N*-dimethylacrylamide **41**, *N*,*N'*- bisacryloylethylenediamine **42** cross-linking monomer and *N*-tert-butoxycarbonyl (*t*-Boc)-β-alanyl-*N'*-acryloylhexamethylenediamine **43** functional monomer

(100 : 12 : 7.3 moles) is subjected to an emulsion radical copolymerisation to provide PAM resin beads **44** (0.3-0.4 mmol β-alanine/g) **Scheme 11**.

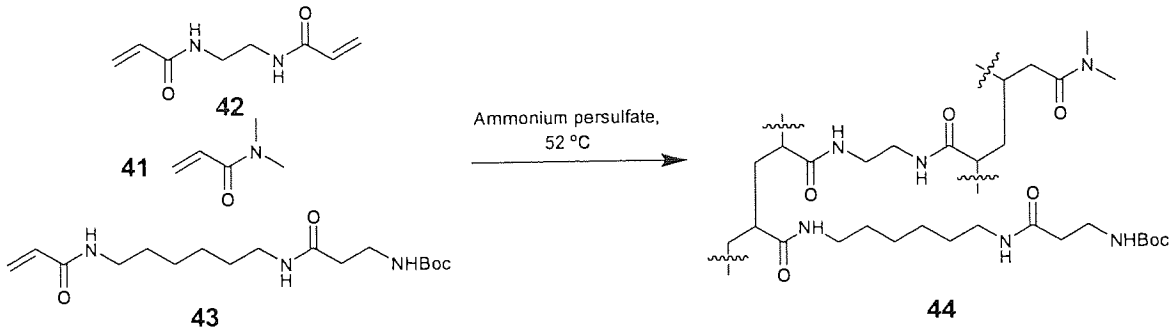

Scheme 11: Synthesis of PAM resin **44**.

The polarity of the PAM matrix and the structure of this matrix are sufficiently similar to that of a polypeptide that a single solvent may be used to solvate both the peptide and PAM resin effectively. Effective solvation of both coupling partners facilitates successful peptide synthesis.[109] Analogous resins to PAM resin **44** have been synthesised subsequently by substitution of the functionalised monomer with other acryloyl derived monomers.[110,111]

In related work, Frechet's group has prepared poly(ethylene glycol) methacrylate resin beads **47** by suspension polymerisation reaction of commercially available oligoethylene glycol monomethacrylates **45** (n=3, 7, 12) and with an ethylene dimethacrylate **46** cross-linking monomer **Scheme 12**.[112]

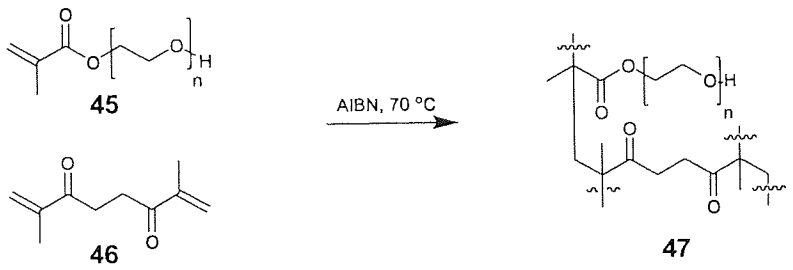

Scheme 12: Synthesis of poly(ethylene glycol) methacrylate resin **47**.

In related work, Kempe and Barany constructed a series of analogous highly Cross-Linked Ethoxylate Acrylate Resins (CLEAR) **54** from commercially available monomers. The cross-linking monomer trimethylpropane ethoxylate triacrylate **48** (>95% wt) was copolymerised with one or more of allylamine **49**, 2-aminoethyl methacrylate-HCl **50**, PEG_{400}-dimethacrylate **51**, PEG-ethyl ether methacrylate **52** and trimethylolpropane trimethacrylate **53** in the desired molar ratio **Figure 13**.[113]

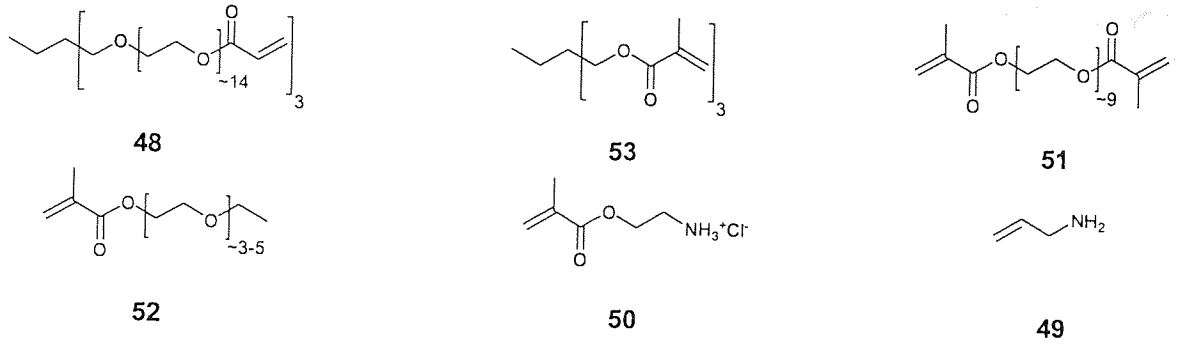

Figure 13: CLEAR monomers **48-53**.

Poly(ethylene glycol) methacrylate resin **47** and CLEAR supports **54** both exhibit excellent mechanical stability, significant swelling in aqueous solvent and a range of organic solvents of widely different polarity and also have been used in SPPS successfully. Unfortunately the polyester matrixes of both supports are labile towards many reagents and conditions commonly employed in SPOC.

Meldal's, polyethylene glycol polyacrylamide (PEGA) resin **57** is prepared by an inverse suspension copolymerisation of *bis*-2-acrylamidoprop-1-yl-PEG_{1900} **55**, 2-acrylamidoprop-1-yl-[2-aminoprop-1-yl]-PEG_{300} **56** and *N,N*-dimethylacrylamide **38** **Scheme 13**.[114]

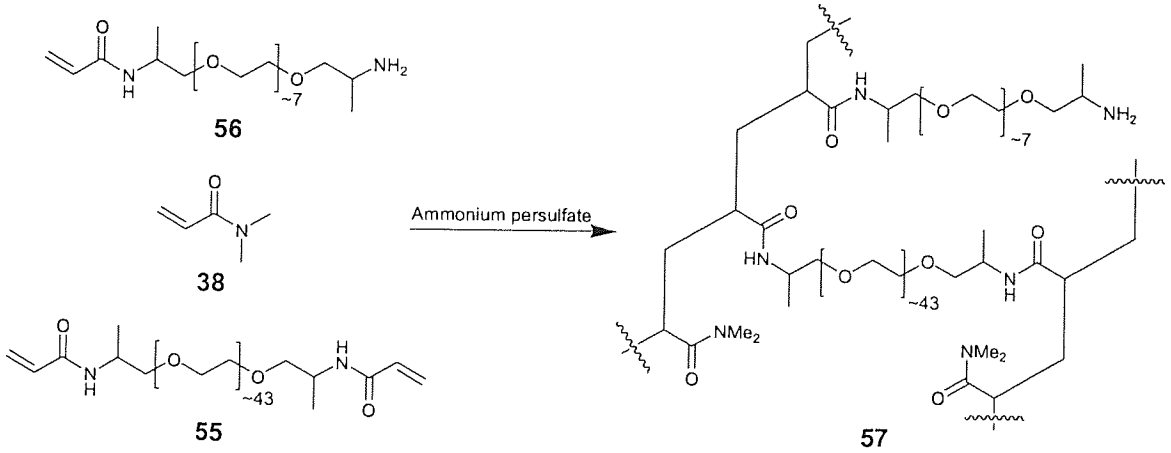

Scheme 13: Synthesis of PEGA resin **57**.

PEGA resin **57** swells significantly in solvents of widely differing polarity including water. In addition, recent work has shown that PEGA resin **57** is permeable to enzymes that cannot penetrate TentaGel **27** and ArgoGel **29** resins.[115,116,117,118] Unfortunately however, the polyamide matrix of PEGA resin **57** is moderately labile towards certain reagents and conditions commonly employed in SPOC and thus the application of this resin is primarily restricted to SPPS.

Meldal and co-workers have also prepared a hydroxyl and amine functionalised (HYDRA) polymer support by a reductive amination reaction between tris-(2-aminoethyl)amine and aldehyde-derivatised-PEG, which in turn is synthesised by a Swern oxidation of PEG_{1500}.[119] The aldehyde and amine functionalities react to produce a polymer that is subsequently reduced to provide hydroxyl (0.33-0.80 mmol/g) and amine (0.88-0.24 mmol/g) functionalised HYDRA polymer **58 Scheme 14**.

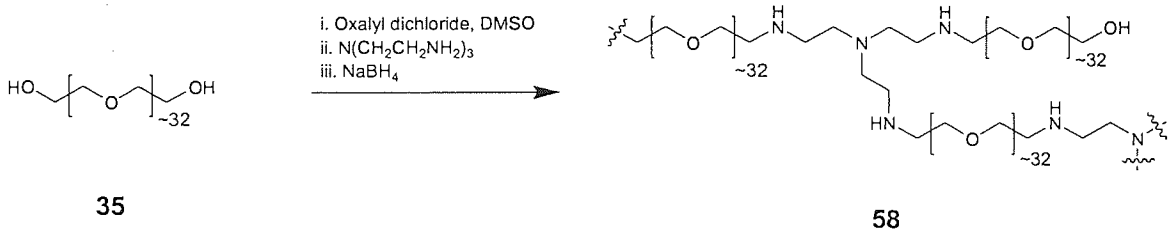

35 **58**

Scheme 14: Synthesis of HYDRA **58**.

To demonstrate the compatibility of HYDRA supports **58** with on-support biological assays, a short peptide (a known substrate of subtilisin carlsberg, a 27 kDa protease enzyme) was synthesised on a HYDRA support **58**. When the subtilisin carlsberg was incubated with its HYDRA-supported substrate, the enzyme permeated the HYDRA matrix successfully and cleaved the peptide. The subsequent synthesis of a peptide inhibitor of the enzyme, upon the hydroxyl functionality, inhibited the enzyme effectively and prevented cleavage of the peptide substrate.

A support related to HYDRA **58** is polyoxyethylene-polypropylene (POEPOP) resin **60** which is synthesised by anionic ring-opening polymerisation of epoxy-derivatised PEG (400, 900 or 1500) monomers **59 Scheme 15**.[120,121]

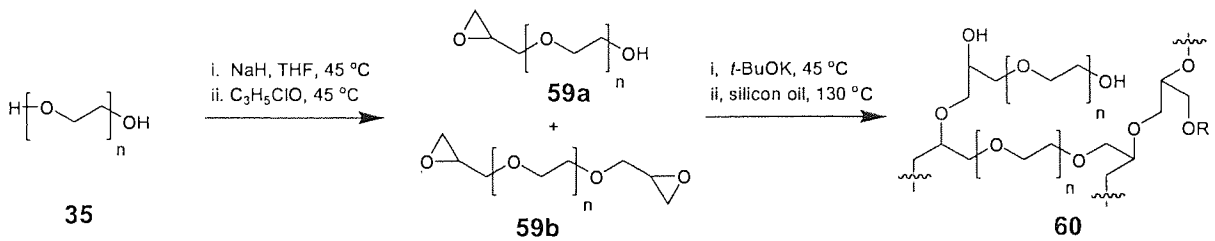

35 **59a** + **59b** **60**

Scheme 15: Synthesis of POEPOP resin **60**.

The resultant POEPOP matrix is comprised of both primary and secondary hydroxyl groups derived from mono-epoxy-PEG and polymerisation termination sites respectively. These primary and secondary hydroxyl groups may well exhibit different reactivities and it may be possible to differentiate chemically between them for library synthesis. The POEPOP matrix contains secondary ether bonds which are labile under extremely strong acidic or basic conditions.

Polyoxyethylene-polystyrene (POEPS) resin **62** is prepared by inverse suspension radical polymerisation of a mixture of styryl-derivatised PEG-based monomers **61**.[120] POEPS resin **62** benzylic

ether (n=1) linkages are labile towards protolytic conditions and many Lewis acids. This benzyl ether linkage has been substituted with the less labile phenylpropyl ether (n=3) linkage **63** to provide POEPS-3 resin **64 Scheme 16.**[122]

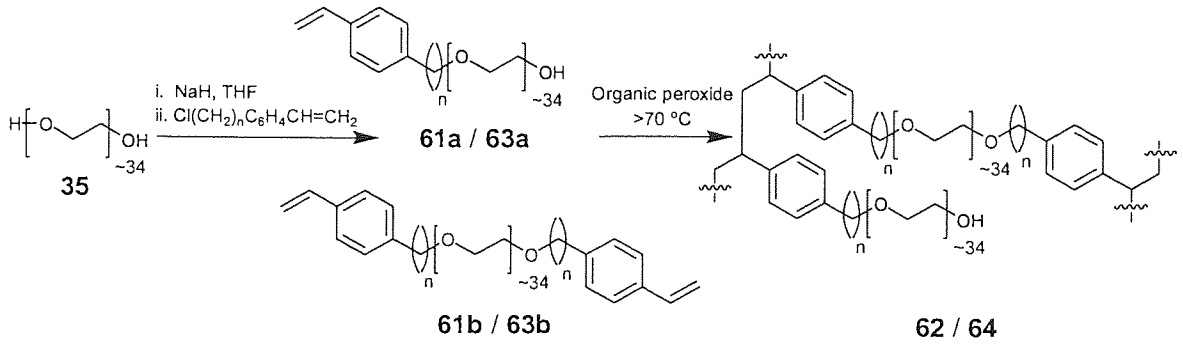

Scheme 16: Synthesis of POEPS resin **62** (n=1) and POEPS-3 resin **64** (n=3).

Superpermeable organic combinatorial chemistry (SPOCC) resins **66** contain only primary ether and primary hydroxyl functionalities.[123] These resins are prepared by Lewis acid-catalysed cationic ring-opening inverse suspension copolymerisation of oxetanyl-derivatised PEG (194, 400, 900 or 1500) monomers **65 Scheme 17.**

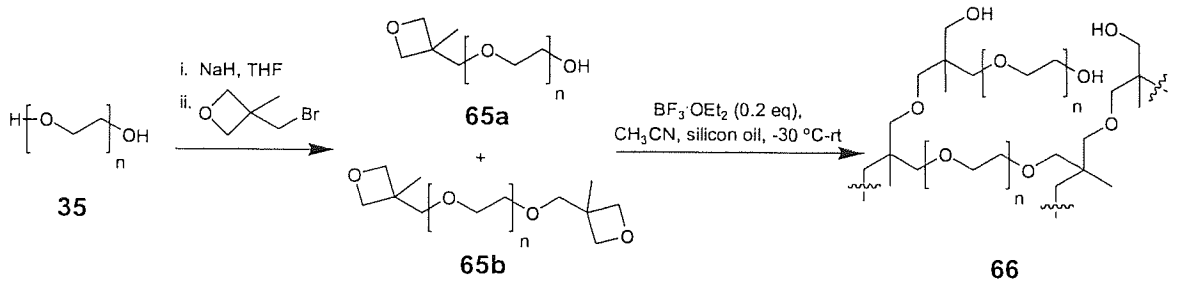

Scheme 17: Synthesis of SPOCC resin **66**.

SPOCC resins **66** are extremely stable towards aggressive reaction conditions and reagents that are commonly employed in SPOC.[124]

Copolymerisation of oxetanyl-PEG_{3000} **65** and tetravalent-silyl-monomer **67** provides $EXPO_{3000}$ resin.[125] This resin exhibits relatively low swelling (3-7 mL/g) in all solvents and is impermeable to enzymes (27 kDa). However, the silicon-carbon bonds, within the $EXPO_{3000}$ polymer matrix, may be cleaved selectively by treatment with strong acid. The resultant polymer matrix significantly swells (10-20 mL/g) in all solvents and it has been shown that the polymer is permeable to enzymes up to 27 kDa in size **Figure 14.**

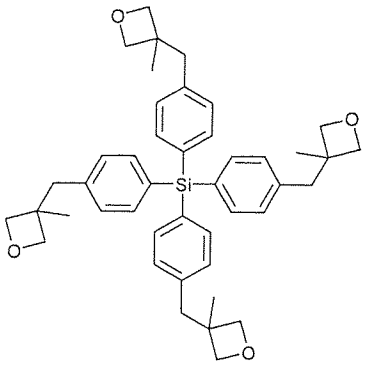

67

Figure 14: $EXPO_{3000}$ tetravalent-silyl-cross-linking monomer **67**.

A potentially significant flaw in the construction of HYDRA **58**, POEPOP **60**, POEPS **62**, POEPS-3 **64** and SPOCC **66** resins is that they are all prepared by the polymerisation of a stoichiometric mixture of non-, mono- and bis-functionalised PEG. The synthesis of the monomers, for each resin, relies upon generating a statistical mixture of non-, mono- and di-substituted PEG-based molecules. Thus complete control over the final polymer compositions is intrinsically reliant upon the same mixtures being produced reproducibly from batch to batch. The resultant polymer resins swell significantly in aqueous and organic solvent of widely differing polarities. In addition, it has been shown that these PEG-based resins are readily permeable to enzymes (22-90 kDa), enzymes of this size are often unable to penetrate TentaGel **27** and ArgoGel **29** resins[115] and have been successfully used in enzymatic synthesis,[118] inhibition assays,[115,116] and binding assays.[117,123,125,126,127]

1.3 Peptide Synthesis

Natural peptides and proteins are constructed from 19 L-α-amino acids **68** and L-proline **69**. Different peptides and proteins differ in the number of amino acid residues they contain and in the sequence in which these amino acids are bonded together **Figure 15**.

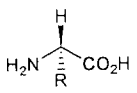

68

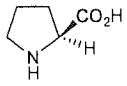

69

Figure 15: L-α-amino acids **68** and L-proline **69**.

1.3a Solution-Phase Peptide Synthesis

A condensation reaction between two different α-amino acids may generate four dipeptides and their corresponding polycondensation products **Figure 16**.

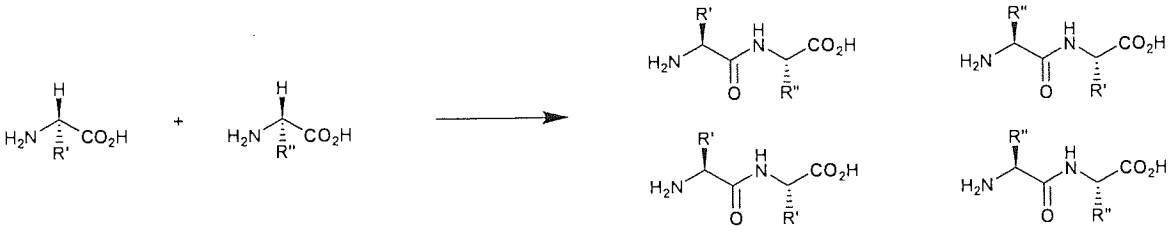

Figure 16: Dipeptides produced by an uncontrolled coupling reaction between two different L-α-amino acids.

The unambiguous sequential coupling of α-amino acid residues requires α-amino protection (P^1) of one residue and orthogonal carboxy-protection (P^2) of the other component. In addition, the amino acid side chain functionality (R', R") may require protection (P^3, P^4) that is orthogonal to either or both the other protection strategies **Figure 17**. In addition, the coupling agent employed must prevent epimerisation of chiral carbon atoms.

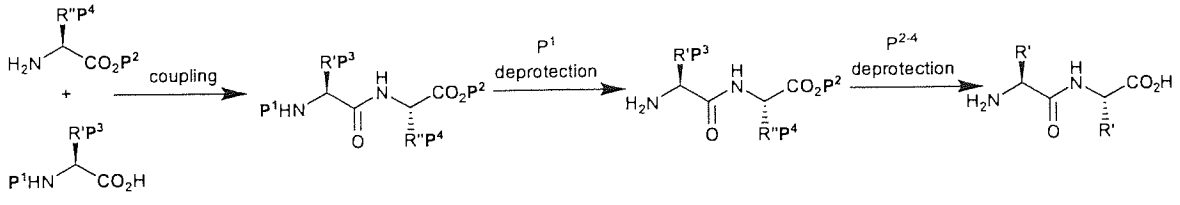

Figure 17: Unambiguous synthesis of a dipeptide.

1.3b Solid-Phase Peptide Synthesis (SPPS)

Merrifield pioneered solid-phase peptide synthesis (SPPS) by utilising a polystyrene resin bead to protect the carboxy-terminus of the growing peptide chain and facilitate purification of the resin-bound peptide intermediates by simple washing and filtration procedures.[73,128] Initially, polystyrene resin was partially chloromethylated and then nitrated. The triethylammonium salt of the benzyloxycarbonyl (Cbz) *N*-protected-amino acid was attached covalently to the chloromethyl-resin *via* a *p*-alkylbenzyl ester linkage. In this first coupling reaction it was essential that "dry" reaction conditions were employed or else hydrolysis of the polymer support to the corresponding benzyl alcohol may become a significant side reaction that competes with coupling. The unreacted chloromethyl groups were esterified by treatment with triethylammonium acetate. The Cbz-group was then cleaved selectively by treatment with hydrobromic acid/acetic acid (HBr/AcOH), prior to coupling the next Cbz-*N*-protected-amino acid using *N,N'*-dicyclohexylcarbodiimide (DCC) as the coupling agent **Figure 18**.

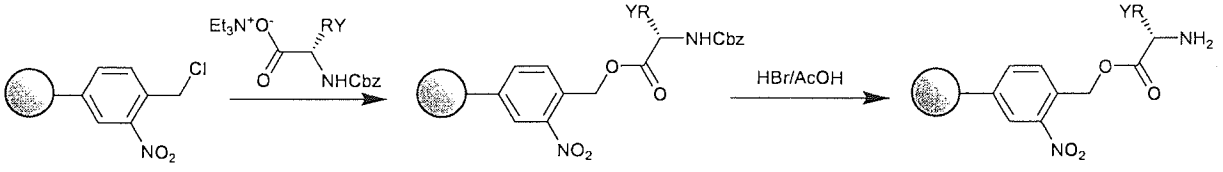

Figure 18: Initial Cbz-amino acid coupling to Merrifield resin and subsequent *N*-deprotection.

This *N*-deprotection and amino acid coupling procedure was repeated to provide a peptide of desired length and sequence. At this stage, the α-amino-protection (Cbz) and side-chain protecting groups (Y) of the product peptide were removed by treatment with HBr and the benzyl ester linkage was cleaved by saponification to release the unprotected peptide from the solid support **Figure 19**.

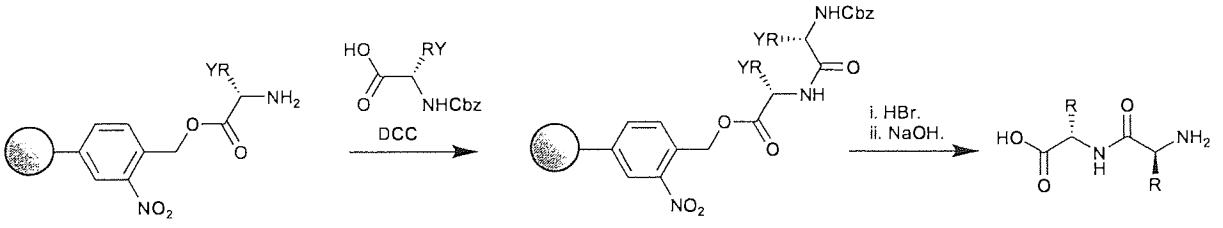

Figure 19: Solid-phase amino acid coupling and subsequent peptide deprotection/cleavage.

1.3c α-Amino Protection

The amino acid side-chain-amine and α-amino-functionality typically is protected with a substituent that reduces the nucleophilicity of the amine group by the withdrawal of electron density and/or is a bulky group that sterically hinders the amine functionality. The majority of these amine protecting groups are alkoxycarbonyl derivatives **Figure 20**.[129]

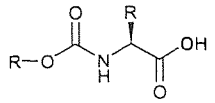

Figure 20: Alkoxycarbonyl protected derivative of alanine.

Alkoxycarbonyl protected amino acid derivatives are usually synthesised with minimal racemisation and are relatively stable towards coupling reagents commonly employed in SPPS. It is important that the protecting group can also be removed easily and in good yield. This can be achieved by acidolysis, which cleaves the alkyl-oxygen bond selectively to provide the corresponding stabilised cation and carbamic acid. The carbamic acid derivative then decarboxylates spontaneously to regenerate the unprotected amino acid.

Merrifield protected the α-amino-functionality with a benzyloxycarbonyl group **Figure 21**.

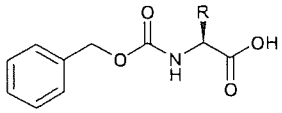

Figure 21: Structure of benzyloxycarbonyl (Cbz) protected alanine.

The Cbz-protecting group was removed by treatment with hydrobromic acid/acetic acid to regenerate the free α-amino terminus. The use of hydrobromic acid/acetic acid was superseded by the use of anhydrous liquid hydrofluoric acid (HF). Unfortunately both of these acidic reagents may cleave the benzyl ester linkage that attaches the peptide to the resin. This will result in the premature release of peptide and in addition the generation of a benzyl cation that may subsequently act as an electrophile and attack side-chains of susceptible amino acid residues electrophilically. Consequently, the benzyloxycarbonyl protection strategy was superseded by a *t*-butoxycarbonyl (*t*-Boc)-strategy. An amino acid protected with a *t*-Boc-group is more labile towards acid than the analogous Cbz-derivative and could therefore be deprotected successfully by treatment with TFA without cleavage from the resin **Figure 22**.

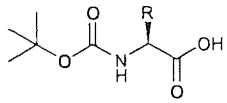

Figure 22: Structure of *t*-butoxycarbonyl (*t*-Boc)-protected alanine.

Even though less acidic conditions could be employed in the cleavage of *t*-Boc groups, the resin-peptide benzyl ester linkage was still not completely stable towards repetitive treatment with TFA conditions required in the synthesis of polypeptides. It is necessary, at each stage of synthesis, to react the nascent polymer-supported peptide with TFA to cleave the *t*-Boc groups prior to attaching the next

amino acid residue. This situation was greatly improved when Carpino developed the use of 9-fluorenylmethoxycarbonyl (Fmoc) as the amino protecting group of choice **Figure 23.**[130]

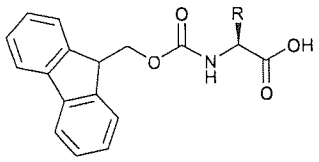

Figure 23: Structure of 9-fluorenylmethoxycarbonyl (Fmoc)-protected alanine.

An Fmoc-protected amino acid **70** is stable towards acidic reagents, but the Fmoc group may be cleaved successfully by treatment with a mild base (20% piperidine in *N,N*-dimethylformamide (DMF)). Deprotection is accomplished via formation of the stabilised 14-π-electron dibenzocyclopentadienide anion **71** which decomposes extremely rapidly to the carbamic acid derivative **72** of the amino acid and dibenzofuluene **73**. The carbamic acid derivative **72** decarboxylates spontaneously to form the unprotected amino acid **68** and the dibenzo fuluene **73** reacts with piperidine to form 1-fluoren-9-yl methylpiperidine **74**. This adduct has a characteristic uv-absorbance at 290 nano metres (nm) which may be used to estimate the loading of peptide on the resin **Figure 24.**[131]

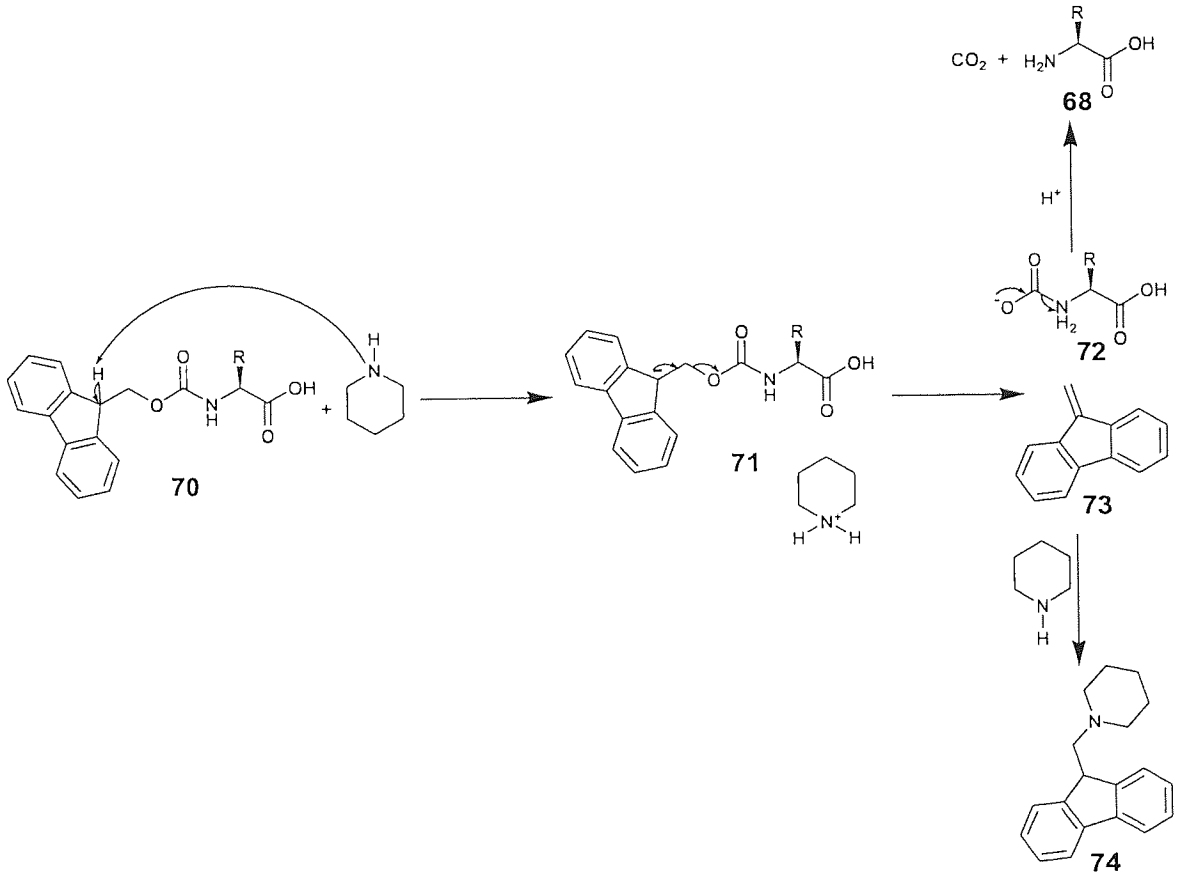

Figure 24: Cleavage of Fmoc from an Fmoc-amino acid upon treatment with piperidine.

1.3d Carboxy-Activation

The majority of resin linkers have been developed for use in conjunction with Fmoc-*N*-protection and Cbz-side chain protection strategies. These linkers are often attached to the first Fmoc-amino acid residue through either an ester or amide bond. This is commonly achieved by activation of the carboxy-group of the Fmoc-amino acid followed by reaction with the chloro (Y=Cl), hydroxyl (Y=OH) or amine ($Y=NH_2$) functionalised resin to give the corresponding Fmoc-amino acid derived support (V=O), (V=O) and (V=NH) respectively **Figure 25**.

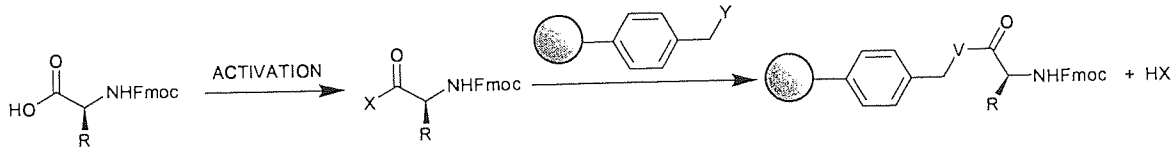

Figure 25: Activation of the carboxyl terminus of an Fmoc-protected amino acid and subsequent coupling to a resin bound hydroxyl or amine group.

Carboxy-activation as described above may also be used in peptide synthesis to couple amino acids to resin bound amino acids or peptides. Carboxy activation towards nucleophilic attack may be achieved in many ways, for example, by conversion to the corresponding acyl chloride or acyl azide. However, these activated species are synthesised from relatively aggressive reagents and have a propensity to partake in side reactions. This has resulted in alternative carboxy-activation methods being developed for use in SPPS.

The amino acid carboxy-terminal may also be activated towards nucleophilic attack by conversion into the corresponding amino acid-anhydride. Reaction of a *N*-carboxyanhydride (X=H) derivative of this type with an amino acid/peptide generates a coupled product in the form of a carbamic acid that spontaneously decarboxylates to provide the corresponding coupled peptide product **Figure 26**.[132]

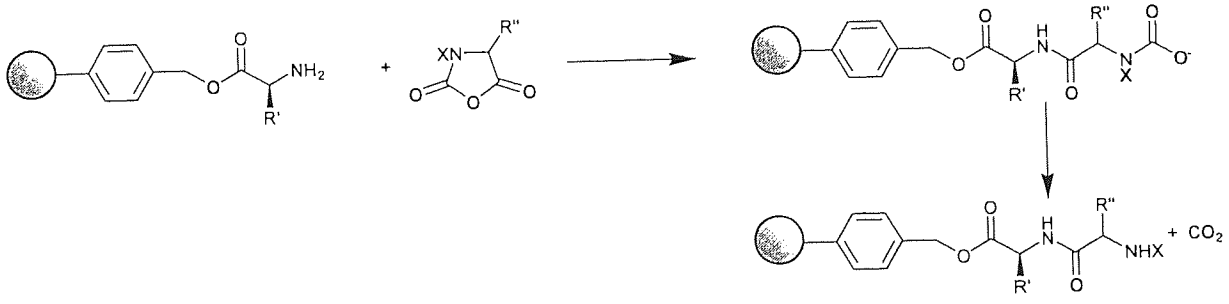

Figure 26: Reaction of a polymer-supported amino acid with an *N*-carboxyanhydride derivative of a second amino acid.

One problem with this approach is that the amino functionality of the product peptide may react with another NCA-residue if coupling of the NCA-residue with the amino acid/peptide is not complete. This will generate peptides of ambiguous length and sequence. To circumvent this potential problem, *N*-protected-NCA analogues (X=Cbz, *t*-Boc or Fmoc) have been developed.[133] These may be reacted with an amino acid/peptide to provide the corresponding *N*-protected-aminoacyl derivative. This derivative has to be deprotected prior to participating in the next coupling step.

Anhydrides

More frequently, a symmetrical anhydride is generated *in-situ* by the coupling of two equivalents of the corresponding *N*-protected amino acid **Figure 27**.[134]

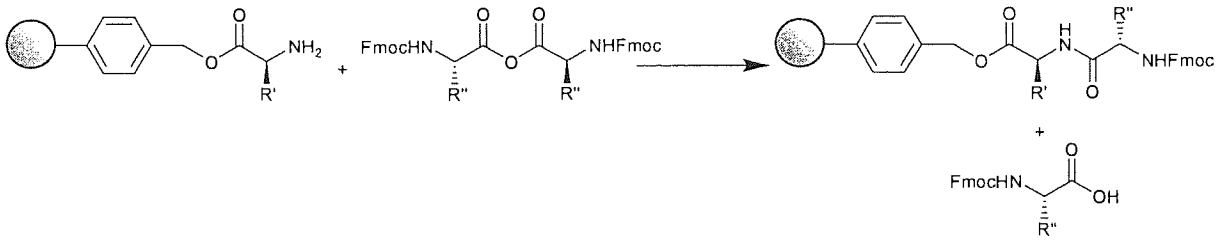

Figure 27: Reaction of a polymer supported amino acid with a symmetrical anhydride derivative of a second amino acid.

The product formed by the aminolysis of a symmetrical anhydride is unambiguous. However, it is also a wasteful process in that only half the carboxy-component is incorporated into the peptide product.

As a result, mixed anhydrides are often used in place of symmetrical anhydrides. Mixed anhydrides incorporate the desired *N*-protected amino acid and a suitable carboxylic acid component. The carboxylic acid component is often sterically hindered to facilitate unambiguous regio-selective aminolysis that results in coupling to the carbonyl carbon of the amino acid component exclusively **Figure 28**.

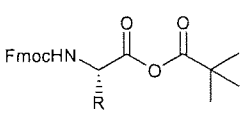

75

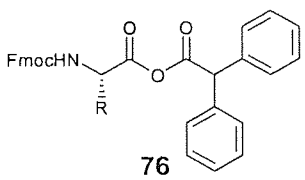

76

Figure 28: Structures of *N*-protected-amino acid mixed pivalic anhydride **75** and diphenylacetic anhydride **76**.

The use of mixed anhydrides has now been superseded by *N*-protected carboxylic-carbonic anhydrides. The less electrophilic carbonic carbon directs aminolysis to the carbonyl carbon of the amino acid component. Typically, the appropriate *N*-Fmoc protected amino acid is reacted with ethyl chloroformate to provide the corresponding carboxylic-ethyl carbonic anhydride **Figure 29**.

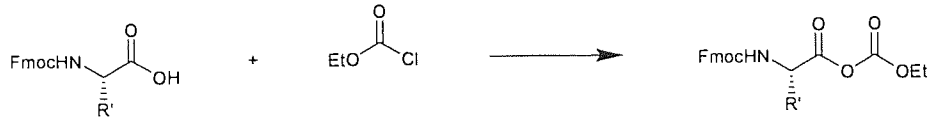

Figure 29: Synthesis of an amino acid carboxylic-carbonic anhydride.

Carboxylic-ethyl carbonic anhydrides may also be generated *in-situ* by reaction of an appropriately protected amino acid with 1-ethoxycarbonyl-2-ethoxy-1,2-dihydroquinoline (EEDQ) **77** **Figure 30**.

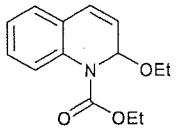

77

Figure 30: Structure of 1-ethoxycarbonyl-2-ethoxy-1,2-dihydroquinoline (EEDQ) **77**.

Carbodimide Reagents

Carbodimide reagents may also be used to activate suitably protected-amino acids towards amide and anhydride formation **Figure 31**.

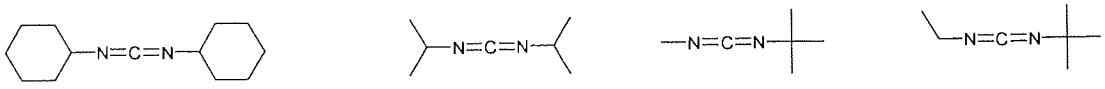

78 **79** **80** **81**

Figure 31: Structure of dicyclohexylcarbodiimide (DCC) **78**,[135] 1,3-diisopropylcarbodiimide (DIC) **79**, *t*-butyl-methylcarbodiimide **80** and *t*-butylethylcarbodiimide **81**.

The carboxyl group of an *N*-protected amino acid adds to the carbodimide functionality to provide the corresponding *O*-acylisourea, ester **82**. This intermediate may react with a second equivalent of the *N*-protected amino acid to provide the symmetrical anhydride **83** followed by aminolysis or the *O*-acylisourea **82** is directly consumed in the aminolysis reaction to provide the peptide product **84** **Figure 32**.

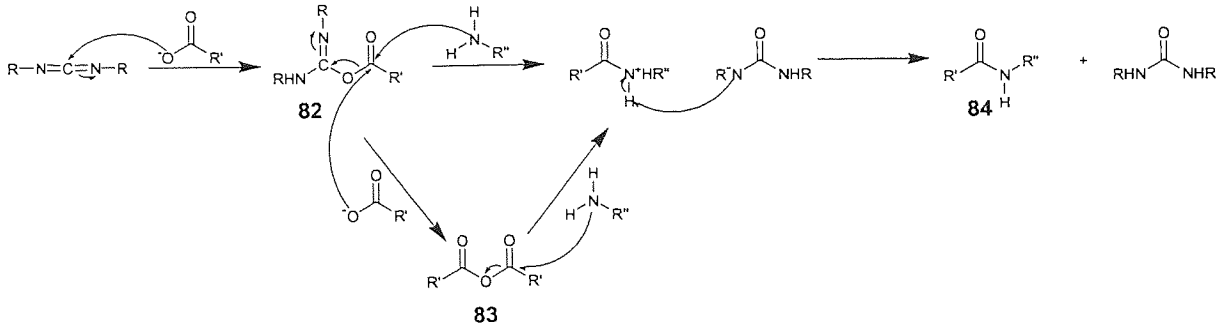

Figure 32: Mechanism of amide bond formation mediated by a carbodimide reagent.

The intermediate *O*-acylisourea **82** and symmetrical anhydride **83** are very reactive species and can cause partial racemisation of the amino acid. However, the addition of a suitable alcohol (e.g. **85-89**), that reacts rapidly with the *O*-acylisourea / symmetrical anhydride enable the corresponding ester to be formed with minimal racimisation of the amino acid **Figure 33**.[136]

Figure 33: *p*-Nitrophenol **85**, 2,4,5-trichlorophenol **86**, *N*-hydroxybenzotriazole **87**, Pentafluorophenol **88**[137] and *N*-hydroxysuccinimide **89**.[138]

The electrophilicity of the carbonyl carbon atom of the esterified amino acid approximately correlates with the acidity of the alkoxy component. The greater the acidity of the conjugate acid, the greater the stability of the corresponding alkoxide ion that is produced upon cleavage from the ester and thus the more reactive the esterified amino acid.

Coupling Reagents

A series of reagents have been developed that generate 1-hydroxybenzotriazole esters *in-situ*. The majority of these coupling reagents are based upon phosphonium or uronium salts **Figure 34**.

Figure 34: Structure of benzotriazolyloxy-tris-(dimethylamino) phosphonium hexafluorophosphate **90**, [139] 1H-benzotriazole-1-yl-oxy-tris-pyrrolidinophosphonium hexafluorophosphate (PyBOP) **91**, 2-(1H-benzotriazole-1-yl)-1,1,3,3-tetramethyluronium tetrafluoroborate **92** and 2-(1H-benzotriazole-1-yl)-1,1,3,3-tetramethyluronium hexafluorophosphate **93**.[140]

In a typical example, the coupling reagent (PyBOP) reacts with the carboxyl terminus of an *N*-protected amino acid to provide the corresponding 1-hydroxybenzotriazole ester **94**. This ester derivative then reacts with the amino terminus of a polymer-bound amino acid to provide the peptide product **95** **Figure 35**.

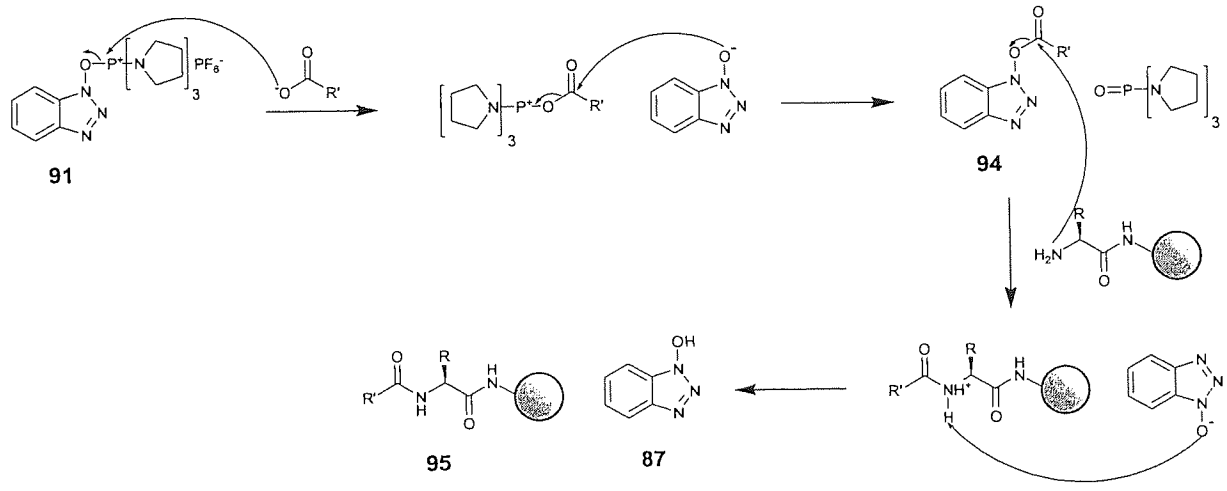

Figure 35: Mechanism of amide bond formation mediated by PyBOP **91**.

A further example of a coupling reagent is 1-(mesitylene-2-sulfonyl)-3-nitro-1H-1,2,4-triazole (MSNT) **96** which is a reagent that was developed initially for phosphotriester oligonucleotide synthesis.[141] However, MSNT has also been used to mediate the esterification reaction between Fmoc-amino acids and hydroxyl functionalised resins.[142] This coupling reagent provides higher substitution and minimum epimerisation compared with all other coupling reagents that have been tested **Figure 36**.

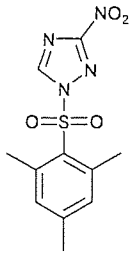

96

Figure 36: Structure of 1-(mesitylene-2-sulfonyl)-3-nitro-1H-1,2,4-triazole (MSNT) **96**.

SPPS reactions are generally driven to completion by the use of excess reagent(s) or repetition of the coupling reaction. This is achievable since purification of the supported-peptide is simply a facile filtration and washing process. Despite these precautions, unreacted residues may remain on the polymer support after the reaction(s) is complete. It is a common procedure to react unreacted amino-functionality with a suitable reagent such as acetic anhydride. This procedure terminates the growth of the peptide chain, which, in turn, prevents the synthesis of peptides with incomplete sequences.

1.3e Peptide Nucleic Acids (PNA)

Peptide nucleic acid (PNA) is a deoxyribonucleic acid (DNA) mimic in which the deoxyribose phosphate backbone has been replaced by a pseudo peptidic backbone, **Figure 37**.[143]

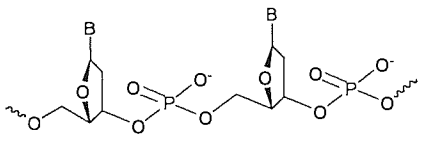

DNA

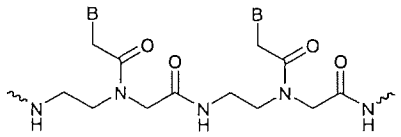

PNA

Figure 37: Structure of deoxyribonucleic acid (DNA) and peptide nucleic acid (PNA) (B= nucleobase).

PNA can form helical duplex structures with complimentary DNA, RNA or PNA base sequences through Watson-Crick base pairing in either orientation, but the anti-parallel orientation is strongly favoured **Figure 38**.[144]

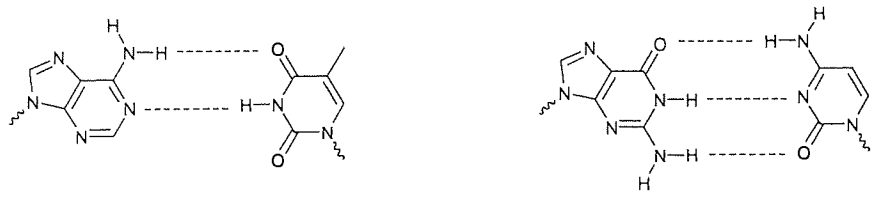

Figure 38: Hydrogen bonding between purine (adenine A, guanine G) and pyrimidine (thymine T, cytosine C) nucleobases.

These PNA-duplexes exhibit increased thermal stability (~1 °C/base pair) compared with the corresponding DNA-DNA and DNA-RNA duplexes, which may be attributed to less electrostatic repulsion between the neutral peptide backbone compared with the negatively charged phosphodiester backbone of DNA.

Synthesis of PNA

The peptide backbone of PNA is comprised of repeating *N*-(2-aminoethyl)glycine units. Each *N*-2-aminoethyl glycine unit is attached to a nucleobase (B) through a methylenecarbonyl linker **Figure 37**. This backbone is less susceptible to degradation by reagents and conditions employed commonly in solid-phase synthesis than the corresponding phosphodiester backbone of DNA. A PNA oligomer may be constructed from the corresponding PNA-monomers using existing SPPS methodologies that are used routinely in the solid-phase synthesis of peptides. An added advantage in synthesising PNA is that there is no need to be concerned about racemisation since PNA monomers are achiral **Figure 39**.

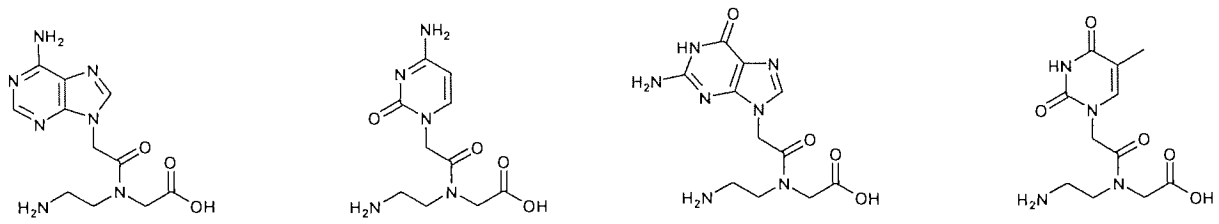

Figure 39: Structure of PNA monomers: adenine, cytosine, guanine and thymine.

1.4 Combinatorial Synthesis

Combinatorial chemistry methodologies facilitate the rapid synthesis of many compounds simultaneously. In this approach, reagents are reacted together in a systematic manner to generate collections of structurally related molecules. These combinatorial libraries are usually constructed using chemical reactions that are reliable and high yielding or the product compounds are amenable to facile purification. The combinatorial library may comprise of a collection of individual compounds or a mixture of compounds that may be synthesised using either solid-phase or solution-phase techniques.[145,146,147,148,149]

1.4a Solution-Phase Combinatorial Synthesis

Solution-phase combinatorial synthesis may have certain advantages compared with an equivalent solid-phase strategy. Solution-phase reactions are well established and do not require the development of attachment and cleavage strategies of compounds to/from a solid support. In addition, soluble library compounds may be analysed readily using conventional techniques. However, solution-phase synthesis is primarily restricted to reliable chemical reactions that react stoichiometric quantities of reagents that are of similar reactivity. In addition, the synthetic route must be very efficient and short in sequence, thus precluding the need for purification of intermediate or product compounds. Alternatively, in certain instances, the products may be amenable to a facile purification procedure for example an extraction procedure using either acidic or basic washes.[150,151,152,153,154,]

The deliberate synthesis of compounds in the solution-phase as mixtures was first described by a group at Glaxo. The indexed combinatorial compound library contained 1600-amides or esters that were synthesised by reacting 40 acid chlorides with either 40 amines or 40 alcohols respectively. Each library comprised of two sublibraries that each contain forty spatially separate compound mixtures (pool). The pools within the first and second sub-libraries were prepared by the separate reaction of each acid chloride (A) with all 40 nucleophiles (N) and each nucleophile with all 40 acid chlorides respectively **Figure 40**.[155]

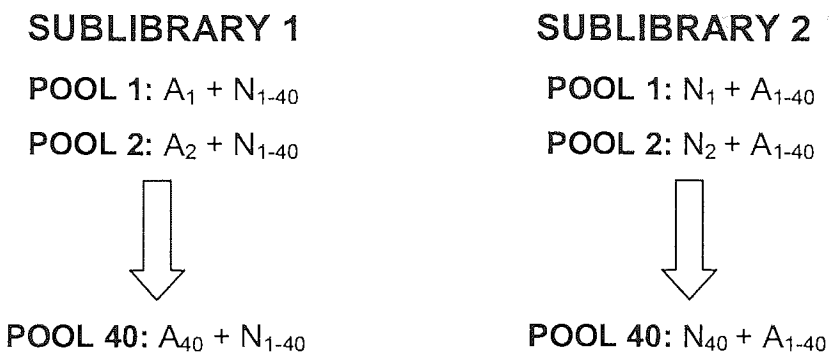

Figure 40: An indexed combinatorial compound library.

The entire library was screened for binding activity against a biological receptor molecule of interest. The pool from each sub-library that displayed the greatest activity, defined the constituent acid chloride (A) and nucleophile (N) of the library compound with the greatest inhibitory activity towards the receptor. A potential drawback of this approach is that the observed biological activity represents the cumulative activities of all the compounds in the mixture. Consequently, activity may be derived from one very potent active compound, several moderately active compounds or many relatively weakly active compounds.

Rebek *et al* reported a strategy for the synthesis and deconvolution of a compound mixture in the solution-phase.[156,157] A rigid core scaffold molecule possessing multiple functional groups was reacted with a mixture of small organic molecules. The core molecules 9,9-dimethylxanthene-2,4,5,7-tetracarboxylic acid tetrachloide **97**, cubane-1,3,5,7-tetracarboxylic acid tetrachloride **98** and 9,9-dimethylxanthene-2,4,5,7-tetraisocyanate **99**, **Figure 41**, were reacted separately with four molar equivalents of an equimolar mixture of amines in a single step.

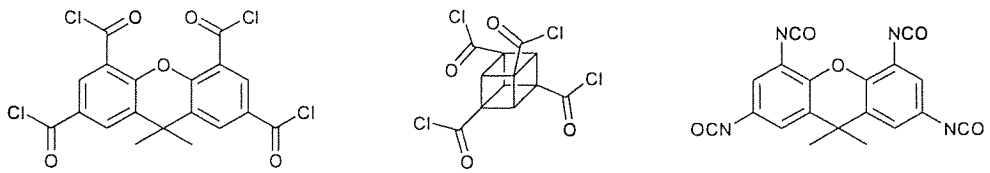

97 **98** **99**

Figure 41: Structures of xanthene **97**, cubane **98** and xanthene **99**.

The resultant product compound mixture theoretically contained every possible combination of core scaffold molecule and amine molecule. This mixture of compounds was purified by a simple liquid extraction procedure and then isolated by precipitation as a white powder. This library was analysed by electrospray ionisation-mass spectroscopy (MS) after fractionation by high-performance liquid

chromatography (HPLC) to verify the presence/absence of each potential library member.[158] This study revealed that approximately 80% of the expected compounds were present in the library.[157]
A series of sub-libraries were then constructed each omitting several different amines in their synthesis. The sublibrary compounds were dissolved in aqueous solution and then screened for the ability to inhibit the trypsin-catalysed hydrolysis of *N*-benzoyl-DL-arginine-*p*-nitroanilide. [159] The omission of an amine that is a component of the most potent biologically active compound(s) results in a reduction in the sublibrary's net activity. Iterations of this process established the identity of the four amines required for optimal activity. The most active structural isomer of this compound was then deduced by the independent synthesis and screening of each individual isomer.

The majority of solution-phase combinatorial libraries comprise of a collection of individual compounds that have been synthesised in spatially separated arrays. This approach has led to the development of several techniques for the facile purification of compound libraries in the solution-phase.
Solid-supported reagents may be employed to facilitate the isolation of pure compounds from a mixture in the solution-phase. A solid-supported reactant (R) may transform the substrate(s) to the product(s) and then be removed by filtration. A solid supported scavenger (S) couples by-product(s) or unreacted starting material(s) and is then removed by filtration. A solid-supported capture-release reagent (C) couples to the desired product compound selectively. The pure product compound may then be released selectively from the support into solution following filtration and washing procedures that remove solution-phase contaminants **Figure 42**.[160]

Figure 42: Synthesis using solid-supported reagents.[160]

In a related approach, chemically pure product compounds may be isolated from the solution-phase by employing reagents that have been labelled with a polyfluorinated tag.[161,162] These fluorous species readily partition from an organic or aqueous solvent into a fluorocarbon solvent. Fluorocarbon solvents are inherently immiscible with conventional organic and aqueous solvents.
The compound synthesis is usually conducted in an orthodox organic solvent with either the reagent(s) or substrate labelled with a suitable polyfluorinated tag. Once the reaction is complete, an appropriate fluorous solvent, which is immiscible with the organic solvent, is then added. The polyfluorinated species partition into the fluorous solvent. The three phase solvent system is then separated and the phase containing the product compound is evaporated to isolate the product compound in a relatively pure form.

Liquid-phase combinatorial synthesis (LPCS) employs linear homogeneous polymers to support the compounds in the library.[163] These polymers are often soluble in the majority of organic solvents, which permits homogenous reaction conditions to be employed. However, the propensity of the polymers to crystallise upon addition of a solvent that induces precipitation facilitates the separation and purification of the polymer-supported intermediate(s) and product(s) molecules from the reaction mixture.
Typically, the first component of each library compound is attached covalently to the polymer under homogenous reaction conditions using excess reagent(s). The homogeneous polymer solution is diluted with a solvent that induces precipitation of the polymer support. The resulting heterogeneous mixture is filtered to isolate the polymer bound molecules with excess reagents and impurities simply being washed away. This process is then repeated with the appropriate component molecules/reagents until the desired polymer supported compounds have been synthesised.[164]
Conventional analysis and screening methods may be used to establish the identity of the active library compound(s) whilst still attached to the polymer support.

Dendrimer have also been used to support compound libraries.[165] These branched oligomers possess discrete and controllable molecular architectures that often have a high functional group loading and are soluble in the majority of organic solvents. In a typical dendrimer-supported synthesis, the first component of each library compound is attached to an appropriately functionalised dendrimer. As with LPCS homogenous reaction conditions using excess reagent(s) are employed at each stage of the synthesis. The dendrimer-supported compound(s) may be purified by separation from unbound material using size exclusion chromatography. This coupling and purification procedure is repeated until the dendrimer supported library has been synthesised. Again, as with LPCS characterisation of the library compounds and all intermediates may be accomplished using routine analytical techniques.

1.4b Solid-Phase Combinatorial Synthesis

Solid-phase synthesis originates from the pioneering work of Merrifield. In 1963, Merrifield's seminal publication described the stepwise synthesis of a tetrapeptide upon the accessible surfaces of an insoluble chemically functionalised polystyrene resin bead.[73,128] In solid-phase synthesis the support serves as a terminal protecting group and also permits an excess molar amount of reagent(s) to be employed to drive reaction equilibria towards completion. Since, the compound(s) are attached to an insoluble support they may be simultaneously separated and purified from by-product(s) and excess reagent(s) by simple filtration and washing procedures. The majority of solid-phase combinatorial libraries have been synthesised as a collection of supported individual compounds using parallel-synthesis methodologies or else a complex mixture of supported compounds using a 'split and mix' synthesis strategy.

Parallel-Synthesis

Solid-phase combinatorial libraries of spatially separate compounds are often constructed using parallel synthesis techniques. Typically, a batch of polymer resin is divided into X wells of a micro-titre plate and the initial substrates A_m are attached covalently to each polymer aliquot. Coupling in this manner is followed by a purification step. The resin bound compounds are then reacted with reagents B_n to provide the intermediate compounds $(A_mB_n)_x$. After purification, these intermediate compounds are reacted with reagents C_o to provide product compounds $A_mB_nC_o$. This procedure may be repeated until a compound library of desired size and complexity of structure has been constructed **Figure 43**.

A_1	A_1	A_1	A_1	A_1	A_1	A_1	A_1	A_1
A_2	A_2	A_2	A_2	A_2	A_2	A_2	A_2	A_2
A_3	A_3	A_3	A_3	A_3	A_3	A_3	A_3	A_3

$B_{1\text{-}3}$

A_1B_1	A_1B_1	A_1B_1	A_1B_2	A_1B_2	A_1B_2	A_1B_3	A_1B_3	A_1B_3
A_2B_1	A_2B_1	A_2B_1	A_2B_2	A_2B_2	A_2B_2	A_2B_3	A_2B_3	A_2B_3
A_3B_1	A_3B_1	A_3B_1	A_3B_2	A_3B_2	A_3B_2	A_3B_3	A_3B_3	A_3B_3

$C_{1\text{-}3}$

$A_1B_1C_1$	$A_1B_1C_2$	$A_1B_1C_3$	$A_1B_2C_1$	$A_1B_2C_2$	$A_1B_2C_3$	$A_1B_3C_1$	$A_1B_3C_2$	$A_1B_3C_3$
$A_2B_1C_1$	$A_2B_1C_2$	$A_2B_1C_3$	$A_2B_2C_1$	$A_2B_2C_2$	$A_2B_2C_3$	$A_2B_3C_1$	$A_2B_3C_2$	$A_2B_3C_3$
$A_3B_1C_1$	$A_3B_1C_2$	$A_3B_1C_3$	$A_3B_2C_1$	$A_3B_2C_2$	$A_3B_2C_3$	$A_3B_3C_1$	$A_3B_3C_2$	$A_3B_3C_3$

Figure 43: Parallel-synthesis of a three component library with three positions of diversity.

The library compounds are often screened for a desired property such as the ability to bind to a biological receptor molecule. An active compound(s) identity is defined by its location in the array. In addition, the biological activity of the compounds within the library may be compared to determine any structure-activity relationship.

Several groups have designed apparatus specifically for the parallel synthesis of solid-phase compound libraries. De Witt *et al* developed apparatus for conducting solid-phase reactions under an inert atmosphere and controlled temperature in parallel.[166] The polymer resin is loaded into porous tubes and these are immersed into a solution of the appropriate reagent(s). The reagent(s) diffuse into the tubes and then into the polymer matrix of the resin beads. After the chemical reaction has taken place, the resin bound intermediate compounds are purified by washing with solvent.
Similarly, the 96-deep-well polypropylene microtiter filtration plate has been developed to facilitate the purification and separation by washing and filtration procedures of resin bound compound library intermediates and products from excess reagent(s) and impurities.[167]
More recently resin handling has been greatly simplified by the incorporation of aliquots of resin beads into plugs of high density polyethylene each plug serves as a spatially resolved reaction vessel.[168]

In 1984, Geysen developed an apparatus for the simultaneous parallel synthesis of many peptides.[169,170] The apparatus comprised of polyethylene pins arranged in an 8 x 12 array to fit in a standard 96-deep-well polypropylene micro-titre plate. Chemical functionality was introduced to the polyethylene pins (4 x 40 mm) by incubation with an acrylic acid solution (6%) and exposure to gamma irradiation. The radicals generated upon the polyethylene pin react with the acrylic acid to provide a surface coating of polyacrylate (0.15-0.2 nmol mm^{-2}). The carboxyl functionality of the polyacrylic acid was then covalently attached to a diamine linker followed by two β-alanine residues (10-100 nmol/pin) **Figure 44**. The apparatus derivatised in this way has been used successfully in the synthesis of peptide libraries.[171,172,173]

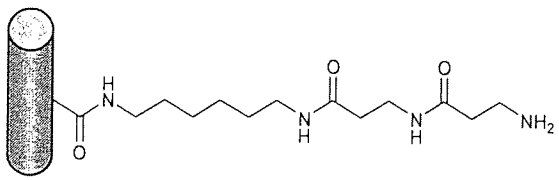

Figure 44: Diamine-β-alanine-β-alanine linker attached to a derivatised polyethylene pin.

Chiron developed and marketed this apparatus as the Multipin system.[174] The apparatus consists of a polypropylene stem that has attached a four pronged polyethylene crown (5.5 x 5.3 mm, 130 mm^2) derivatised with 2-hydroxyethyl methacrylate (HEMA). The HEMA hydroxyl functionality (1.0-7.0 μmol/crown) may be coupled to the carboxyl terminus of the initial amino acid residue and the product

peptide subsequently released by cleavage of the ester linkage by treatment with TFA. The system has been further refined and is currently marketed as "Lanterns" by Mimotopes.[175]

Geysen's pioneering work in solid-phase parallel synthesis led to a renaissance in the area of spatially addressable synthesis upon laminar solid supports.[176] An example of this is a facile method that has been developed to synthesise oligodeoxynucleotide arrays on a glass plate.[177,178] The glass plate was derivatised with hydroxyl groups and reaction channels were formed by gluing silicon rubber tubing (1.2 mm) at appropriate spacing (1-10 mm) on the glass plate. Conventional reagents for phosphoramidite or H-phosphonate synthesis were passed down each channel. The deoxynucleic acid coupled to the hydroxyl functionality of the glass plate. The tubing was then removed and the whole plate subjected to deprotection and washing procedures in a common reaction vessel. This whole procedure was repeated with the appropriate configuration of reaction channels and addition order of deoxynucleic acids to provide the desired sequence, length and location of the oligodeoxynucleotide.

In a related approach, a seminal paper was published in 1991 that described the technology of light directed spatially addressed parallel synthesis (LDS).[179] This technology incorporates orthodox solid-phase chemistry, photo-labile protecting groups and photolithography. LDS has been used to generate high-density parallel arrays of peptides on the surface of a chemically functionalised silica wafer. The surface of the silica wafer was functionalised with 3-(aminopropyl)triethoxysilane, followed by reaction with aminohexanoic acid. This amine functionality was then protected with the photo-labile 6-nitroveratryloxycarbonyl (Nvoc) group.[180] Before the first coupling step, a predetermined area of the silica wafer was irradiated (365 nm) through a photolithographic mask. The Nvoc groups were cleaved selectively to unmask amine functionality only in areas which had been illuminated **Figure 45**.

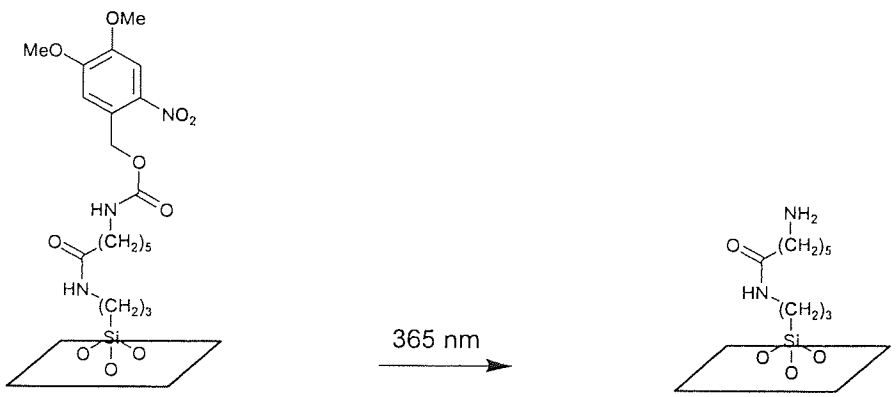

Figure 45: Cleavage of the photo-labile Nvoc-group with light (365 nm).

The entire surface of the silica wafer was then exposed to the *N*-hydroxybenzotriazole (HOBt) **87** activated ester of a Nvoc-protected **X** amino acid **A**. The activated amino acid only coupled to the free amine functionality on the silica wafer. The amino acid derived silica wafer was subsequently

reirradiated (365 nm) through a different photolithographic mask and the process repeated until library construction was complete **Figure 46**.

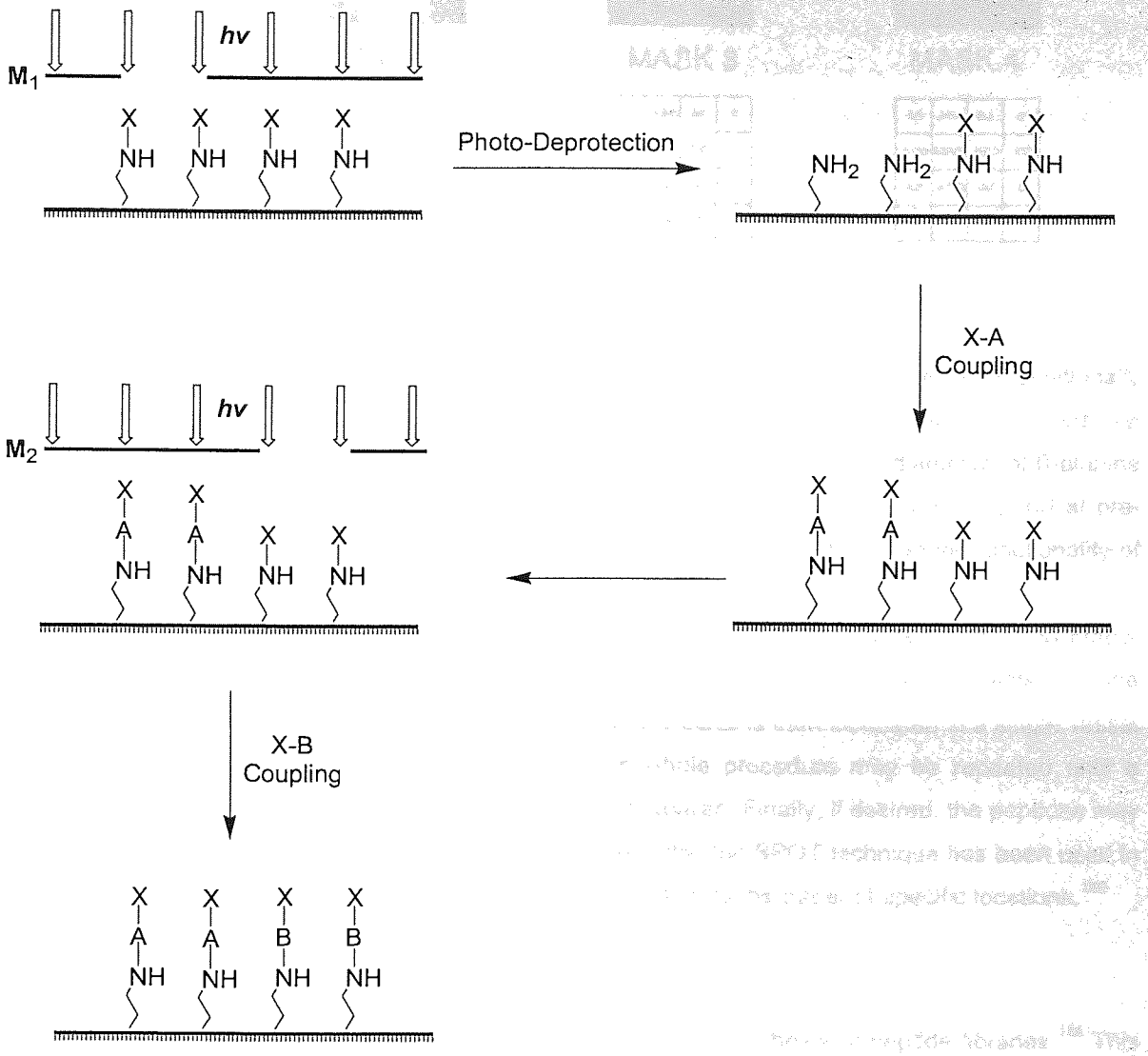

Figure 46: Light directed spatially addressed parallel peptide synthesis.

In this approach, the common washing and side chain deprotection procedures can be accomplished in a single reaction vessel. The number and pattern of photolithographic masks used in the illuminations and the addition order of amino acids dictates the length, sequence and location of the peptides synthesised upon the silica wafer **Figure 47**.

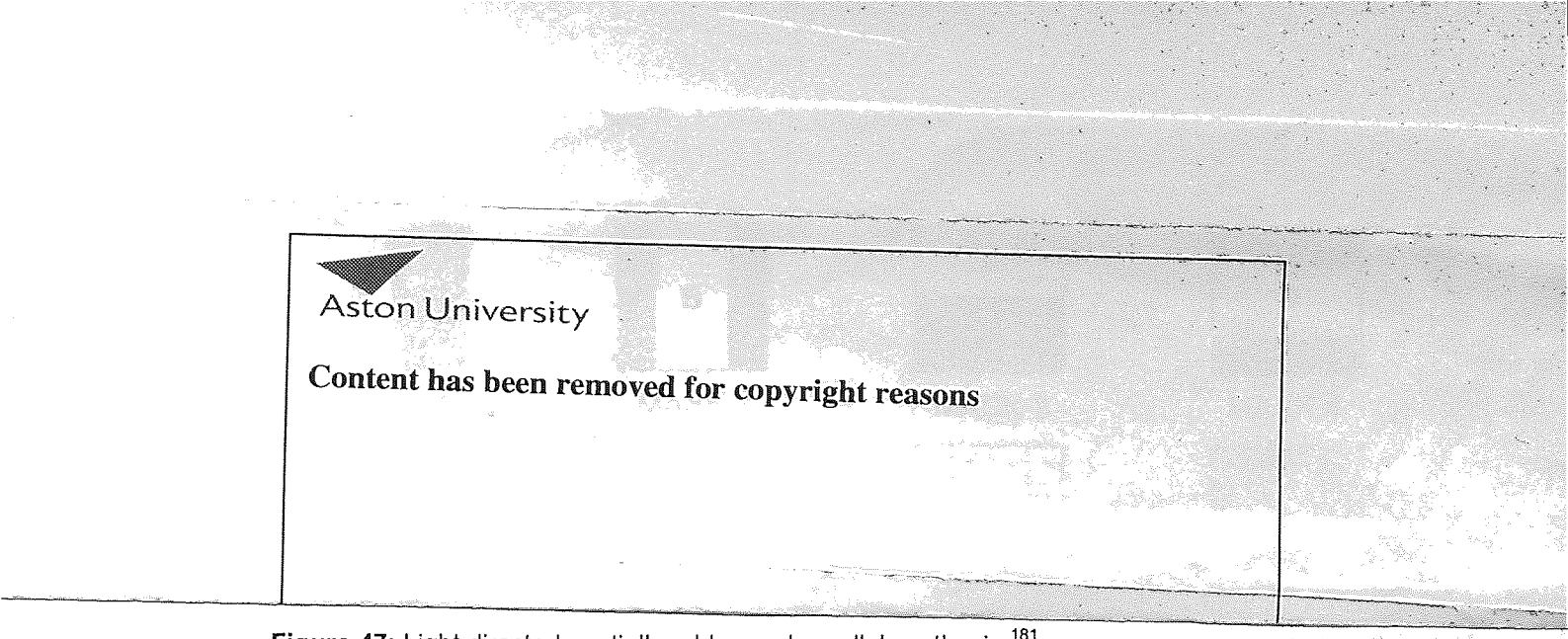

Figure 47: Light directed spatially addressed parallel synthesis.[181]

The SPOT technique has been developed for the parallel simultaneous synthesis of positionally addressable peptide libraries upon cellulose paper.[182] In a typical approach, all the accessible hydroxyl functionality of the cellulose is esterified with β-alanine. Then a droplet (~3 mm diameter) of β-alanine (5-10 nmol/spot) and coupling reagent(s) solution is pipetted on to the surface of the support at pre-defined positions (4 mm spacing). This second β-alanine residue couples to the amino functionality of the derivatised cellulose support.

The amino functionality of the *bis*-β-alanine linker is used to attach the carboxyl terminus of an Fmoc-amino acid covalently by pipetting the Fmoc-protected amino acid with appropriate reagents onto the appropriate spot on the cellulose support. The array of amino acids is then incubated in a single vessel for the common washing and deprotection steps. This whole procedure may be repeated until a peptide library of desired length and sequence has been prepared. Finally, if desired, the peptides may be cleaved from the cellulose support using TFA. More recently, the SPOT technique has been used in conjunction with ink-jet printers, which may deliver reagent(s) on to the paper at specific locations.[183]

'Split Synthesis'

In 1985, Houghten introduced the 'tea-bag' methodology for the synthesis of peptide libraries.[184] This methodology utilised labelled polypropylene mesh packets (15 x 20 mm) with pores (~74 μm) that contained an aliquot of resin. These parcels were combined and incubated with appropriate reagent(s) for common coupling, deprotection and washing procedures. In this manner, multiple peptides have been synthesised using a batch wise 'split and mix' protocol. The identity of each peptide sequence may be determined from the sequence of reactions each resin parcel has been exposed. Alternatively, a sufficient quantity (~500 μmoles) of peptide is contained within each parcel for full compound characterisation and screening.

In 1986, Geysen showed that randomisation at a specific position of a peptide sequence may be achieved in a single coupling step by the use of a mixture of amino acids. However, this procedure

often results in the production of unequal molar concentrations of peptides(s) within the library as a consequence of differing amino acid reactivities. This limitation may be circumvented by adjusting the mixture of amino acids relative concentrations to be inversely proportional to their reactivities (a kinetic mixture).[185] Unfortunately, this adjustment does not accommodate the potential preferential coupling between certain pairs of amino acid residues. This failing coupled with the advent of 'split and mix' synthesis has meant that the approach of using kinetic mixtures has not found widespread application.

'Split and Mix' Synthesis

In 1988, Furka first communicated the 'split and mix' methodology for the rapid and efficient synthesis of a peptide library. Theoretically a 'split and mix' peptide library should contain an equimolar mixture of peptides of all possible amino acid sequences. Practically, a batch of chemically functionalised resin beads is divided into a number of equal portions in separate reaction vessels. A different amino acid is coupled to each batch of resin. The beads from each reaction vessel are then recombined in a single reaction vessel for the common steps of washing and deprotection. The resin beads are randomised by thorough mixing and then divided into equally sized portions in separate reaction vessels. This whole process is repeated until the desired sequence and length of peptide has been synthesised **Figure 48**.

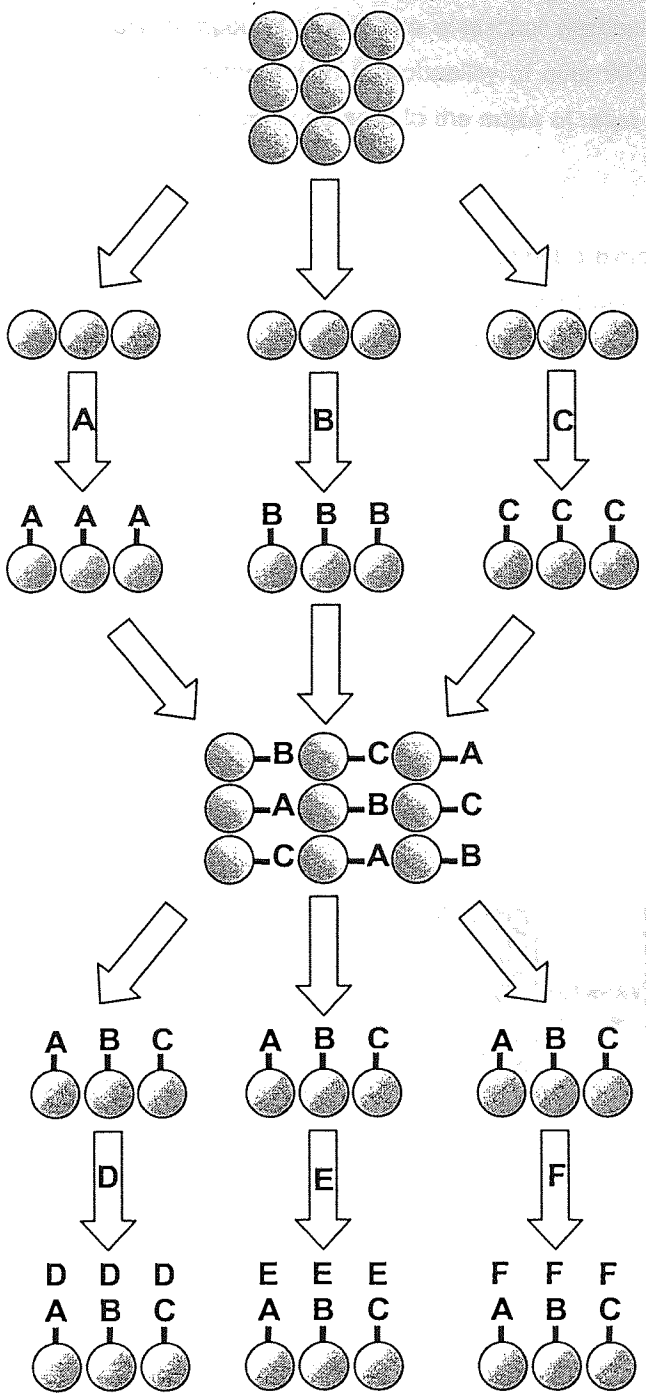

Figure 48: 'Split and mix' synthesis of a dipeptide library using six different amino acids.

The 'split and mix' procedure produces a compound library with a size that increases exponentially with the number of coupling steps. Therefore, the number of amino acids (X) and positions of diversity (Y) dictates the theoretical number (X^Y) of peptides within the library.

Provided a sufficient number of resin beads are used in the 'split and mix' synthesis each peptide will be represented.[186] However, at each splitting step of the synthesis there is the possibility for over and

under representation of each library compound due to the statistical distribution of resin. To ensure 95% of all the possible compounds are formed with a probability of over 99% it is necessary to use approximately three fold excess weight of resin compared to the mass of resin required to synthesise a single compound per resin bead.[187]

A combinatorial compound library is often screened for activity against a biological receptor molecule of interest. A resin bound compound library may be screened in the solution-phase by employing a chemically- or photo-labile linker or an orthogonal multiple-release linker. Multiple release linkers have the advantage that they enable a proportion of resin bound compound to be released sequentially into solution for screening and analysis.[188,189,190,191]

In a typical assay procedure, a resin-bound compound library is divided equally into separate wells of a micro-titre plate. A portion of each library compound is cleaved from the resin beads into solution for biological screening. The beads within a well exhibiting good biological activity are then divided into individual wells of a 96-well plate and a further aliquot of compound is released into solution for screening. This division-cleavage-screening procedure is ideally repeated until the beads have been arrayed separately. At this stage it is preferable that the individual beads should have sufficient compound still attached to them for a single assay and subsequent analysis to establish the identity of the biologically active compound(s) **Figure 49**.

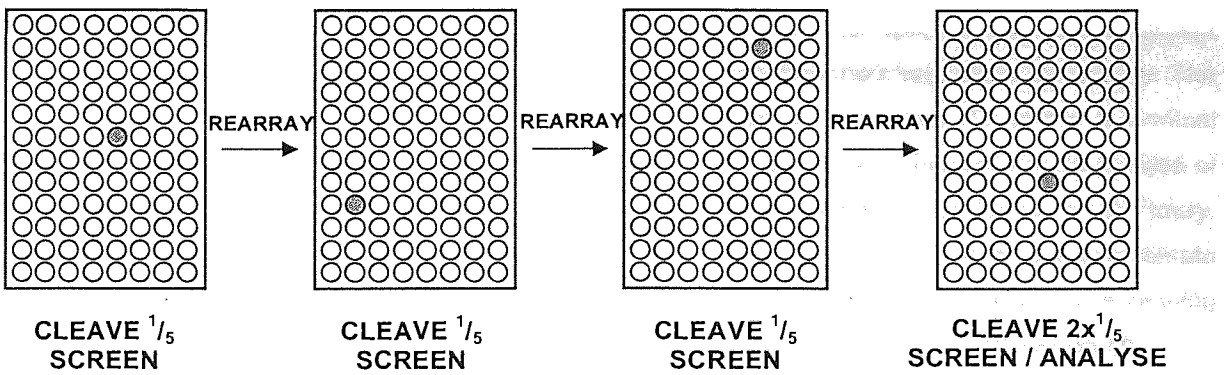

Figure 49: Screening assay using multiple cleavable linkers.

An alternative screening protocol is to screen the library compounds whilst they are still attached to the resin. This approach is commonly achieved by incubating the compound library with a receptor that has been labelled with a radioisotope, dye, chemiluminescent or fluorescent molecule.[179,186,192] The successful binding of the labelled receptor to a resin bound molecule causes the polymer bead bearing that molecule to adopt the characteristics of the label. Beads interrogated in this manner are usually isolated by micromanipulation or fluorescent activated cell sorting (FACS).[192,193] The structural identity of the resin bound compound may then be elucidated by employing a sensitive analytical or

sequencing technique after removal of the bound receptor molecule. However, unless the molecule is self-coding (e.g. a peptide or oligonucleotide) the amount of compound attached to a single bead (typically ~100 pmol) is often insufficient for definitive structural identification using conventional characterization techniques. Consequently, the identity of a library compound that is non-self coding may be established using an appropriate deconvolution strategy.

Furka established the identity of the most active peptide within a 'split and mix' library by the synthesis of either 'omission libraries' or 'amino acid tester mixtures'.[194] Libraries of this type are constructed, with the omission or inclusion of a specific amino acid respectively, and subsequently screened for activity. The importance of an amino acid when screening an omission library is implied by a reduction in total activity of the library relative to the full 'split and mix' library. Conversely, screening amino acid tester mixture gives exactly the opposite result. Iterations of either procedure may be used to determine the amino acids present in a bioactive peptide(s). The sequence of these amino acids is then established by the construction and screening of a small library of peptides where each position of diversity is defined with a known amino acid.

Houghten developed a deconvolution strategy that requires the iterative synthesis and screening of compound libraries that are fully randomised with a single position sequentially defined.[195] In this approach, a 'split and mix' peptide library is synthesised that is fully randomized (X) with only the *N*-terminal amino acid being defined. The library is constructed in the usual 'split and mix' fashion except that the sub-libraries produced from the last coupling cycle are screened separately for activity. The sub-library that exhibits the greatest activity identifies the optimal amino acid (C) at the *N*-terminal position of the peptide sequence. This sub-library is then resynthesised with the penultimate position of the peptide sequence being defined with specific amino acid, a different amino acid in each sub-library. Each sub-library is screened for activity to identify the optimal amino acid (A) at the penultimate position of the peptide sequence. This process of positional-fixed sub-library synthesis and screening is repeated until the remaining position of the active peptide sequence is identified (B) **Figure 50**.

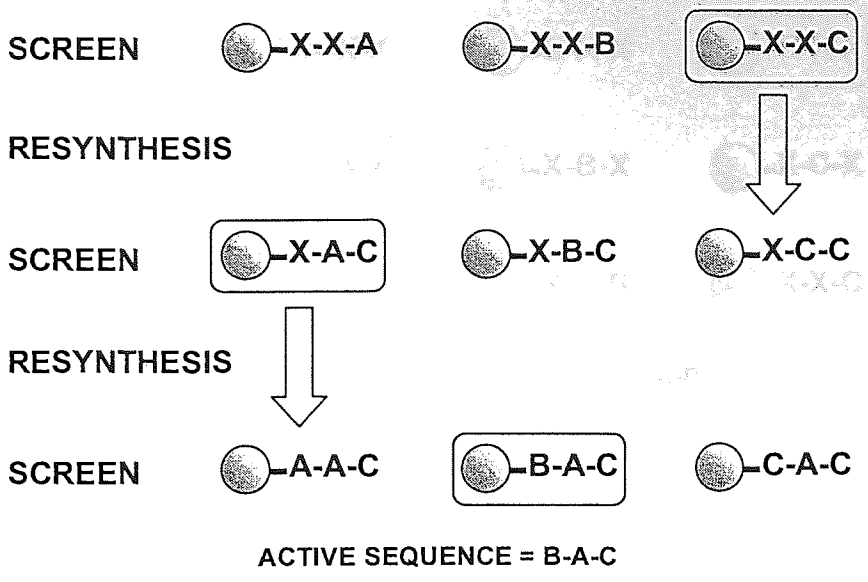

Figure 50: Iterative synthesis and screening of a tripeptide library constructed from three amino acids.

Janda's, recursive deconvolution strategy circumvents the requirement to resynthesise the active sub-library after each screening assay.[196] A fully randomised 'split and mix' library is synthesised with a portion of the resin isolated and catalogued after each coupling prior to mixing. As with Houghten's approach, the sub-libraries produced from the last amino acid coupling are screened separately to establish the identity of the *N*-terminal amino acid that provides the greatest activity. However now there is no need for a *de novo* sub-library synthesis, the optimal *N*-terminal amino acid is simply coupled to the peptide sub-libraries isolated at the previous step of the 'split and mix' synthesis. The second set of sub-libraries that result from this one coupling stage are then screened. The most active mixture defines the amino acid residue at the penultimate position of the most active peptide. This recursive synthesis and screening strategy is repeated to establish the identity and position of each amino acid within an active peptide.

In 1992, Houghten reported the technique of 'positional scanning' to establish the identity of the most active compound within a library. The library has a deconvolution strategy incorporated into the design of the library.[197,198] Specifically, a series of sub-libraries were synthesised that each have a single position defined and all other positions fully randomised (X). These sub-libraries were then screened *en masse* for a desired property. The results from this single screen enable sub-libraries that exhibit the greatest activity to be identified. This in turn identifies the preferred amino acid at each position of the most active peptide directly **Figure 51**.

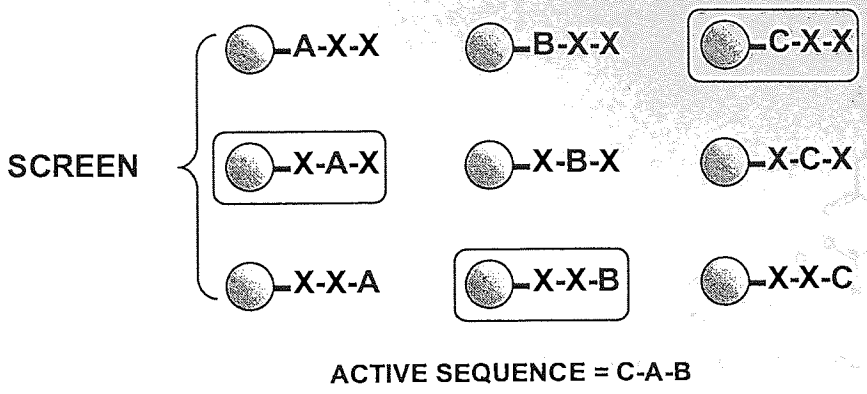

Figure 51: Positional scanning of a tripeptide library constructed from three amino acids.

Deconvolution by iterative synthesis of very large compound libraries can be an extremely arduous task. Consequently, encoding methodologies have been developed to establish the identity of a compound attached to single bead unequivocally. In this approach, tags (T_x) are attached to the resin bead at each stage of library synthesis. Once an "active" bead has been identified by screening, the tags on that bead are read using a sensitive technique to determine the identity of the library compound directly **Figure 52**.

Figure 52: A sequentially tagged bead encoding the library compound A-B-C.

The first encoding strategies employed a biopolymer as the encoding tag and a resin linker with two orthogonally protected functional groups.[192,199,200,201] These orthogonal linkers permit the sequential parallel alternating synthesis of the library compound and the encoding tag. The synthetic history and thus the identity of each library compound is encoded by the identity and location of the tag monomer in the oligomeric sequence of the biopolymer.
Typically, the peptide or oligonucleotide tagging sequence is determined using Edman micro-sequencing followed by HPLC/MS or DNA sequencing following amplification by polymerase chain reaction (PCR) respectively.

Peptides and oligonucleotides are often labile towards reagents and reaction conditions commonly employed in SPOC. Consequently, the synthesis of an encoded small-organic molecule library is limited by the susceptibility of the bio-oligomers to degradation. One way of overcoming this limitation is to employ a series of *N*-Cbz-*N*-[(dialkylcarbamoyl)methyl]glycine molecules with varying length alkyl chains as encoding tags **Figure 53**.[202]

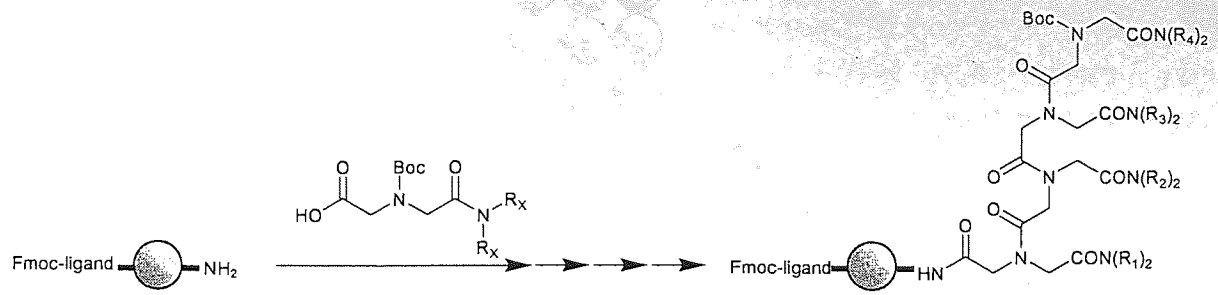

Figure 53: Sequential coupling of dialkylamine tags to encode a resin bound compound

These chemically robust tags are coupled sequentially in parallel with the synthesis of the library compound. The polyglycine encoding tag, associated with an active compound, is hydrolysed (hydrochloric acid 6 M), converted to a fluorescent dansyl sulphonamide derivative and then analysed by reverse phase HPLC. The presence or absence of each tag molecule encodes the chemical identity of the compound.

Still has employed chemically robust halogen-substituted phenoxyalkyl alcohol molecules to encode resin-bound compound libraries.[203] The length of the alkyl chain (n=3-14) and the extent of halogen substitution (X=2-5) of each haloaromatic tagging molecule gives each tag (T_1-T_{40}) a unique identity. Typically, the tag molecules (<1% loading) attached covalently to the resin via a nitrobenzyl linker and may therefore be released subsequently by irradiation (365 nm).[204, 205, 206] This method of attachment/removal has been superceded by the direct attachment of the tag molecules into the resin matrix by rhodium-catalysed carbene insertion of a diazomethyl ketone precursor of the molecular tag **Scheme 18**.[189]

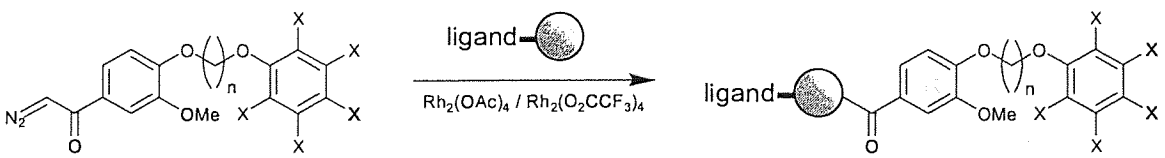

Scheme 18: Rhodium-catalysed haloaromatic tag insertion into a resin bead.

In the carbene insertion approach, the tags are attached to the resin covalently and in a non-sequential manner at each stage of the synthesis. Each tag is approximately 0.5-1% (<0.1 pmol/bead) of the concentration of the library compound **Figure 54**.

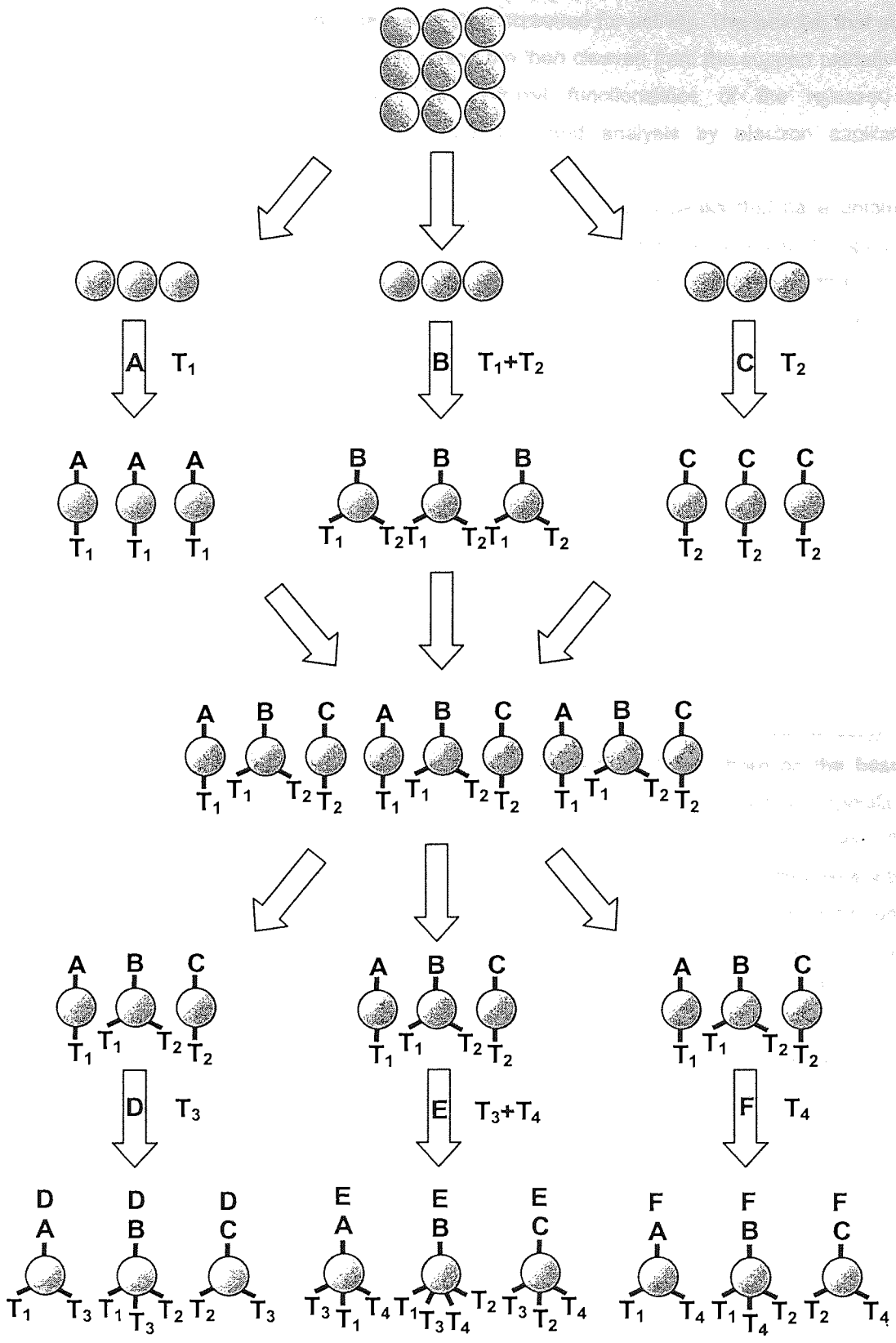

Figure 54: Non-sequential binary encoded 'split and mix' library synthesis.

The encoded library constructed in this manner is then screened for activity. The bead(s) that support an active compound(s) is isolated. The encoding tags are then cleaved from the support oxidatively by treatment with ceric ammonium nitrate. The hydroxyl functionalities of the released tags ($HO(CH_2)_nOArCl_m$) are silylated to facilitate separation and analysis by electron capillary-gas chromatography-mass spectroscopy (EC-GC-MS).
The tags have been designed so that in EC-GC-MS they give rise to peaks that have unique and approximately equally spaced retention times. Consequently, the presence or absence of a specific tag from a predetermined set of tagging molecules is identified easily. The EC-GC-MS spectrum provides a binary code that defines the synthetic history of each bead uniquely and unequivocally defines the structure of the active compound(s).

More recently, a series of resins have been synthesised by suspension polymerisation of a PS-DVB monomer mixture that incorporate a specific ratio of fluorinated monomers.[207] Beads constructed in this manner have unique infrared (IR) and Raman spectroscopic barcodes, which may serve to encode the compound attached to each bead. The ultimate application of this approach is to couple synthesis, screening and deconvolution with the speed and convenience of a FACS sorter that has been modified so that it can read the Raman spectra of individual beads.

Resin-bound compound libraries may also be encoded by the attachment of a fluorescent molecular label to the resin bead.[208] The fluorophore is attached in varying concentrations, below 0.1% of the resin loading to maintain a linear relationship between the loading of fluorphore on the bead and fluorescence intensity.[209] The intensity of the fluorescent signal may be used to encode a specific resin bead. These encoded beads may be sorted by a FACS instrument prior to each synthetic step to predetermine the synthetic reactions each bead will be exposed. The use of several fluorescent tags in varying concentration permits the potential encoding of a greater number of library compounds.[210] However, multiplexed encoding of this type is often limited to 2-3 flurophores because of the broad, asymmetrical emission profiles of conventional fluorophores which results in spectral overlap.

Multiplexed encoding has been successfully achieved by the incorporation of a predetermined size and number of zinc sulfide-capped cadmium selenide nanocrystals (quantum dots) into the polymer beads.[211] The emission wavelength of a quantum dot is dictated by its size (typically between 2-6 nm in size) and the intensity of the emission is dependent upon the number of quantum dots of a particular size present. The use of n intensity levels with m wavelengths theoretically generates (n^m-1) unique codes. Again, these pre-encoded beads may be sorted by a FACS instrument prior to each synthetic step to predetermine the synthetic reactions each bead will be exposed. Deconvolution of encoded libraries of this type, by FACS, is assured since they have been FACS sorted successfully at each stage of synthesis.

Resin-bound compound libraries have been encoded by the use of radio-frequency transponders.[212,213] This technology uses glass encapsulated semiconductor microchips that either have pre-encoded read only memories or electronically erasable, programmable read-only memories (EEPROM's).
In this approach, a microchip is placed in a porous polypropylene capsule that contains an aliquot of resin beads. A read only memory microchip transmits its binary code as a specific radio-frequency that may be detected electronically. The capsules are sorted prior to each synthetic step to predetermine the synthetic history of the resin in each capsule before the resin-bound library is screened.
Alternatively, at each step of library synthesis, a computer generates a specific binary code that may be transmitted as a specific radio-frequency and recorded by the EEPROM microchip in the capsule. After, screening, the structure of "active" capsule(s) may be determined by scanning the associated microchip to download the binary information that has recorded the synthetic history of the resin in the capsule.

A further alternative to tagging the supports used in solid-phase combinatorial chemistry is laser optical tagging. Here, a polypropylene or fluoropolymer square (10 x 10 x 2 mm) that has been radiolytically grafted with low cross-linked polystyrene, is subsequently chemically functionalised (5-8 μmol/chip).[214] The centre of the polymer square accommodates an inert alumina ceramic plate (3 x 3 mm) that has a two dimensional 16-digit bar code etched into its surface with a carbon dioxide laser. The bar code on these laser optical synthesis chips (LOSC) are read by a camera before each synthetic step. The structure of a compound synthesised on a LOSC may be deduced by reading the two dimensional bar code on the chip optically. The bar code explicitly encodes the series of reactions to which the LOSC has been exposed and thus the chemical identity of the compound it bears.

1.5a Project Aim 1: Cell-Based Scintillation Proximity Assays

The first aim of this project was to synthesise a series of scintillant-tagged-compounds for application in a novel cell-based Scintillation Proximity Assay (SPA). 2,5-Diphenyloxazole **1** was selected as the scintillant molecule of choice because it can scintillate efficiently in the presence of ionising radiation, has a chemically robust oxazole skeleton and has widespread application in scintillation counting.[215] Unfortunately, 2,5-diphenyloxazole **1** does not possess suitable chemical functionality for molecular attachment. However, 2,5-diphenyloxazole-4-carboxaldehyde **100** was synthesised by 4-lithiation of commercial 2,5-diphenyloxazole **1** followed by addition of DMF.[216] The 2,5-diphenyloxazole-4-carboxaldehyde **100** carbonyl group could be readily converted into a variety of other functional groups. The successful derivatisation of this functionality with a variety of other molecules was undertaken to provide a series of 4-functionalised-2,5-diphenyloxazole molecules **Figure 55**.

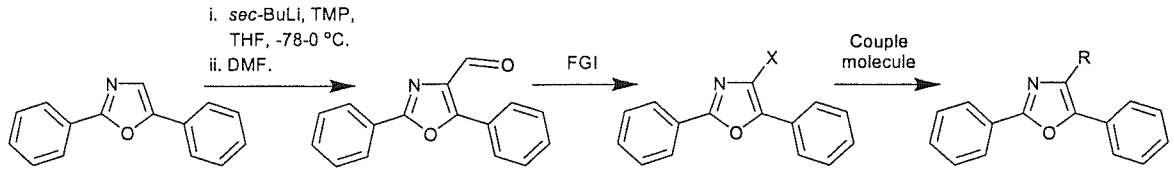

1 **100**

Figure 55: Suggested strategy for the functionalisation of 2,5-diphenyloxazole **1** and subsequent covalent attachment to a series of molecules.

These 4-functionalised-2,5-diphenyloxazole molecules were to be evaluated by Sense Proteomic Ltd. Accordingly, prior to conducting a cell-based SPA it was necessary to determine the ability of these molecules to scintillate in the presence of ionising radiation. Once this study was complete, the molecules were to be incorporated into liposomal preparations and once again evaluated for the ability to scintillate in the presence of ionising radiation. The liposome(s) that exhibited optimal properties were to be incorporated into the membrane of cells for subsequent use in a cell-based SPA to detect and quantify protein function and activity *in-vitro*.[217]

1.5b Project Aim 2: Scintillation Proximity Assays in Combinatorial Chemistry

The second project aim was to develop a polymer support for use in combinatorial solid-phase synthesis and subsequent *in-situ* SPA. Accordingly, it was necessary to synthesise a chemically-functionalised scintillant containing polymer support, which is compatible with both aqueous and organic solvents and also retains the ability to scintillate after exposure to organic solvent. It was proposed to synthesise a range of chemically-functionalised poly(oxyethylene glycol)-based monomers and cross-linking monomers that may be subsequently polymerised to provide a polymer support of controlled composition that is compatible with both organic and aqueous solvent. The co-polymerisation of such monomers would require the derivatisation of the PEG moiety with a suitable polymerisable functionality. Styrene was chosen as the preferred polymerisable unit for its compatibility with the scintillant monomer (4'-vinyl)-4-benzyl-2,5-diphenyloxazole **101**.[218] Consequently, a series of mono- (Y= OH, NH_2, OMe) and bis- (Y= styrene) styrene-functionalised oligo(oxyethylene glycol) ethers were to be synthesised **Figure 56**.

35

Figure 56: Proposed strategy for the synthesis of mono- and bis-styrene-functionalised oligo(oxyethylene glycol) ethers.

These monomers were to be co-polymerised with (4'-vinyl)-4-benzyl-2,5-diphenyloxazole **101** to generate a series of chemically functionalised PEG-based supports that incorporate scintillant covalently **Figure 57**.

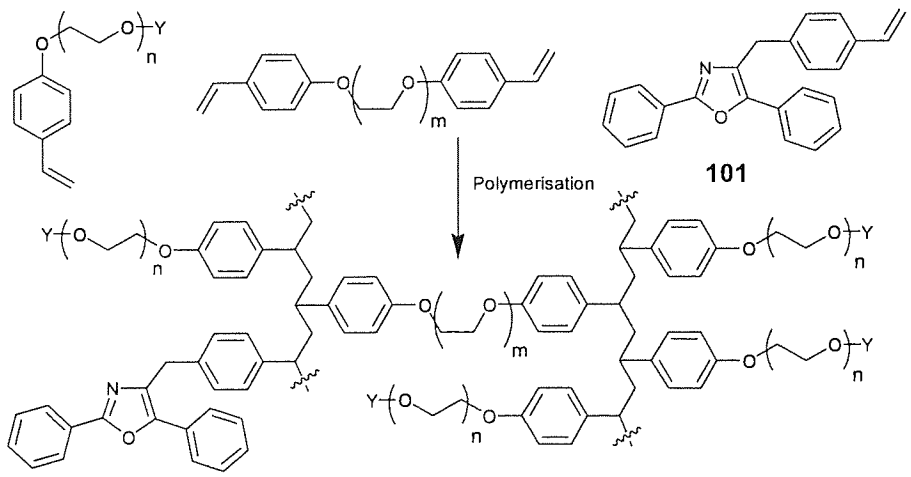

Figure 57: Proposed strategy for the co-polymerisation of mono- and bis-styrene-functionalised oligo(oxyethylene glycol) ethers and (4'-vinyl)-4-benzyl-2,5-diphenyloxazole **101**.

These PEG-based polymer supports were to be evaluated for their compatibility with both aqueous and organic solvents, their ability to scintillate in the presence of ionising radiation and their utility in solid-phase synthesis. The optimal polymer support was to be used in the solid-phase combinatorial synthesis of a compound library and subsequent *in-situ* SPA to detect and quantify non-covalent intermolecular interactions with a host that had been radiolabelled suitably. In addition, the optimal polymer support was to be evaluated for compatibility with enzymes in order to assess the feasibility of using the polymer to monitor on-support enzyme assays and also the real-time monitoring of the thermodynamic and kinetic progress of solid-phase organic reactions.

Chapter 2

Results and Discussion

2.1 Synthesis and Evaluation of 4-Functionalised-2,5-Diphenyloxazole Molecules for use in a Cell-Based Scintillation Proximity Assay

Sense Proteomic Limited required a series of scintillant-tagged-compounds to evaluate for the ability to be incorporated into liposomes, which in turn were tested for scintillation activity in the presence of ionising radiation. The liposome that exhibited optimal properties has been fused with the membrane of living cells for subsequent use in a cell-based scintillation proximity assay for studying protein function and activity *in vitro*.[217] The overall strategy is outlined schematically below **Figure 58**.

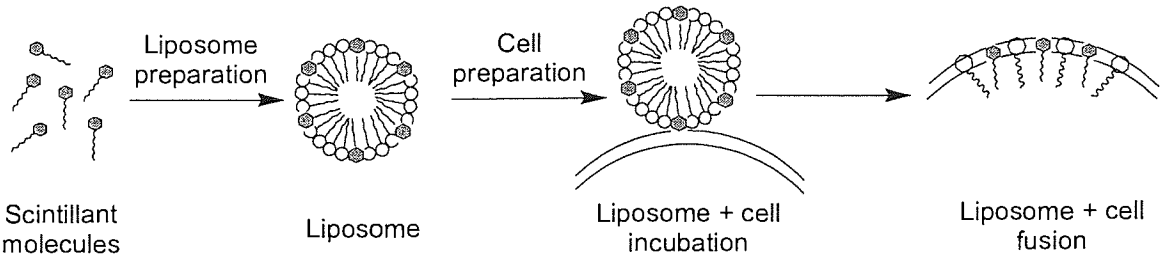

Figure 58: Schematic representation of the incorporation of scintillant molecules into lipomes and subsequent fusion with the membrane of a cell.

2.1a Synthesis of 4-Functionalised-2,5-Diphenyloxazole Molecules

The construction of scintillant-tagged compounds required the ready availability of an appropriate scintillant molecular tag. 2,5-Diphenyloxazole **1** was chosen as the scintillant moiety of choice since it is well known to scintillate in the presence of ionising radiation and also has a chemically robust oxazole skeleton. Unfortunately, 2,5-diphenyloxazole **1** possesses no suitable chemical functionality for direct molecular attachment. Previous work has shown that a variety of 4-functionalised-2,5-diphenyloxazole molecules may be synthesised by 4-lithiation of 2,5-diphenyloxazole followed by addition of an appropriate electrophile.[215,216,218]

Initial work involved the synthesis of 2,5-diphenyloxazole-4-carboxaldehyde **100** on a large scale to provide sufficient material for further transformations. Drop-wise addition of secondary-butyl lithium to a cooled solution of 2,5-diphenyloxazole **1** and tetramethylpiperidine in dry THF generated a brick red colouration as the 4-lithio-2,5-diphenyloxazole was formed. This solution was allowed to warm to 0 °C and quenched with DMF with concomitant reduction in the intensity of the colouration. Aqueous work up and trituration with diethyl ether gave 2,5-diphenyl-4-carboxaldehyde **100** as a white precipitate in a modest yield of 33% **Scheme 19**.

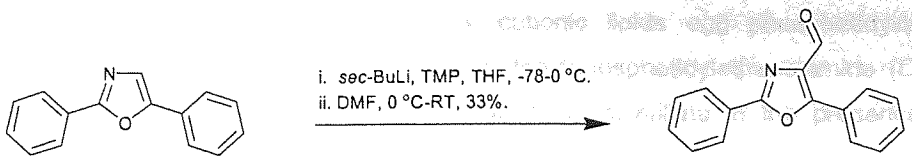

1 **100**

Scheme 19: Synthesis of 2,5-diphenyloxazole-4-carboxaldehyde **100**.

Again using methodology established previously, the addition of excess sodium borohydride to a methanolic solution of scintillant carboxaldehyde **100** provided 2,5–diphenyl-4-hydroxymethyloxazole **102** in quantitative yield **Scheme 20**.[219]

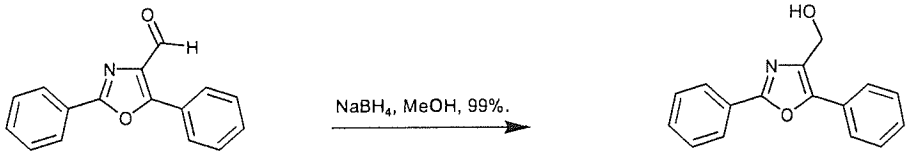

100 **102**

Scheme 20: Synthesis of 2,5–diphenyl-4-hydroxymethyloxazole **102**.

The synthetically useful scintillant bromide was synthesised by treating a solution of scintillant alcohol **102** in dichloromethane (DCM) with phosphorous tribromide to provide 4-bromomethyl-2,5-diphenyloxazole **103** in excellent yield **Scheme 21**.[215]

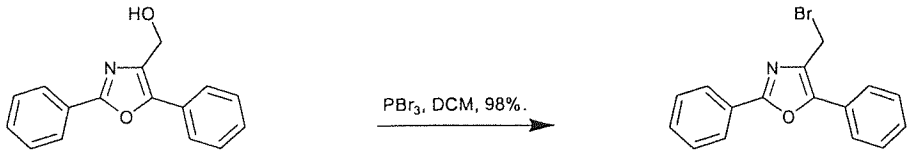

102 **103**

Scheme 21: Synthesis of 4-bromomethyl-2,5-diphenyloxazole **103**.

2.1b Synthesis of 2,5-Diphenyloxazole-Tagged Compounds

The 4-functionalised-2,5-diphenyloxazole molecules ethyl-2,5-diphenyl-4-oxazolecarboxylate **105**, 4-bromomethyl-2,5-diphenyloxazole **103**, 2,5-diphenyloxazole-4-carboxaldehyde **100** and 2,5–diphenyl-4-hydroxymethyloxazole **102** were converted, via one or multi-step syntheses into scintillant compounds **104** and **106-119**. Sense Proteomic Ltd evaluated each of these compounds for the ability to scintillate in the presence of ionising radiation (Appendix A, Table 37). In addition, attempts were made to incorporate each of these compounds, hereafter referred to as "scintilipids", into liposomal

preparations that contained one or more of the cationic lipids egg phosphatidylcholine (PC), dioleoyltrimethylammonium propane (DOTAP) and dioleoylphosphatidylethanolamine (DOPE). Each liposomal preparation was then evaluated for the ability to scintillate in the presence of ionising radiation (Appendix A, Table 37).[217]

The fusion of a cell membrane with a liposome is facilitated when the liposome is constructed from cationic lipids.[217] Accordingly, the first target was a cationic scintillant compound tetraalkylammonium salt **104** that was synthesised, in one step, by treating a solution of 4-scintillant bromide **103** in acetone with triethylamine **Scheme 22**.

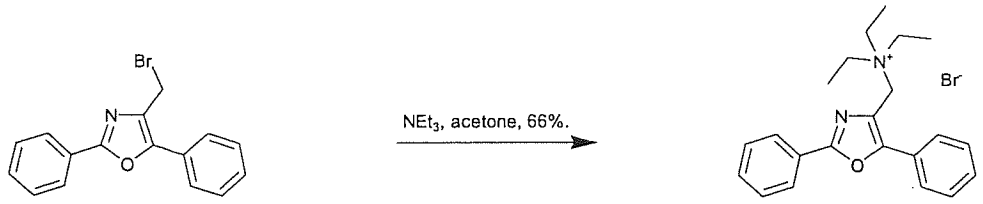

103 **104**

Scheme 22: Synthesis of 2,5-diphenyl-oxazol-4-ylmethyl-triethyl-ammonium bromide **104**.

Ethyl 2,5-diphenyl-4-oxazolecarboxylate **105** has been synthesised from commercially available ethyl benzoylacetate, previously within the research group.[215] A second cationic scintillant-containing compound was synthesised by treating a solution of scintillant ester **105** in ethanol with excess hydrazine hydrate to provide hydrazide **106** as a white precipitate. Subsequently, excess hydrogen chloride gas was bubbled through a solution of hydrazide **106** in chloroform to precipitate the corresponding hydrochloride salt **107** as a white solid **Scheme 23**.

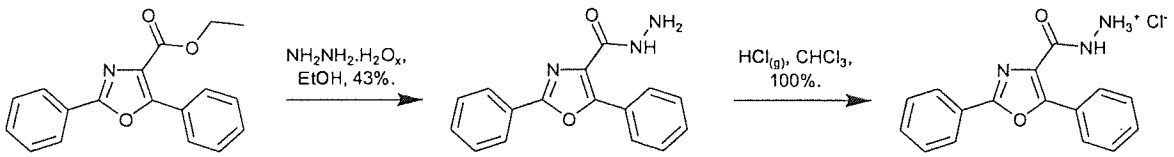

105 **106** **107**

Scheme 23: Synthesis of 2,5-diphenyl-oxazole-4-carboxylic acid hydrazide **106** and 2,5-diphenyl-oxazole-4-carboxylic acid hydrazide hydrochloride **107**.

In addition to testing **107**, hydrazide **106** had the potential to be used in an *in-situ* biological study that has literature precedent.[220] This strategy exploits the reactivity of the hydrazide functionality with ketone groups that are found within the membranes of a cell. If successful, it was hoped that treatment of a liposomal preparation containing hydrazide **106** would result in covalent attachment of the oxazole

to constituent molecules within the cell membrane to provide scintillant tagged cells that could then be used in a cell-based-SPA. A model study of this process was conducted successfully by reaction of a methanolic solution of hydrazide **106** with benzophenone in the presence of an acid catalyst to give a hydrazide-benzophenone adduct **108 Scheme 24**.

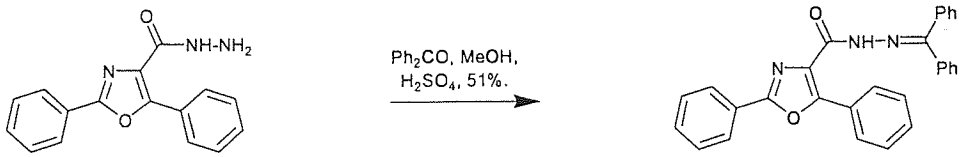

106 **108**

Scheme 24: Synthesis of 2,5-diphenyl-oxazole-4-carboxylic acid benzhydrylidene-hydrazide **108**.

Unfortunately, scintillant compounds **104**, **107** and **106** and their corresponding liposomes ("scintiliposomes") all exhibited relatively low scintillation counting efficiencies in the presence of ionising radiation (Appendix A, Table 37). A possible explanation for this may be the presence of the carbonyl functionality in scintillant compounds **106** and **107**. The conjugation of this carbonyl functionality with the oxazole ring may change the emission characteristics of the scintillant molecules and result in lower scintillation efficiency. Alternatively, the close proximity of the oxazole ring to the electron density of the carbonyl group or formal charge may cause quenching of scintillation through a charge transfer process. The situation is quite complex and prediction of scintillation efficiency is difficult, for example, previous work had shown that ester **105** scintillates with very high efficiency but aldehydic and carboxylic acid functionality at position 4 on the 2,5-diphenyloxazole skeleton resulted in very poor scintillation. The ability of a 4-functionalised-2,5-diphenyloxazole compound to scintillate in the presence of ionising radiation is thus highly dependent upon the type of chemical functionality attached at the 4-position of the heterocyclic ring.[215] In previous work ether and imide linkages have both been used to attach substituents at the 4-position of the oxazole ring, which provided compounds that exhibited very high scintillation counting efficiency in the presence of ionising radiation.[215] The ether linkage was also deemed attractive due to its chemical robustness and ready accessibility via either scintillant alcohol **102** or scintillant bromide **103**. Accordingly scintillant compounds **109-119** were all constructed with one ether linkage between the 4-position of the oxazole tag and the rest of the molecule.

Scintillant alcohol **109** was synthesised successfully by a Williamson type ether synthesis between 3-(4-hydroxyphenyl)-propan-1-ol and scintillant bromide **103**.[221] The anion of 3-(4-hydroxyphenyl)-propan-1-ol phenoxide was generated using K_2CO_3 that had been activated by the addition of a catalytic (cat) amount of 18-crown-6 (18-C-6) **Scheme 25**.[222]

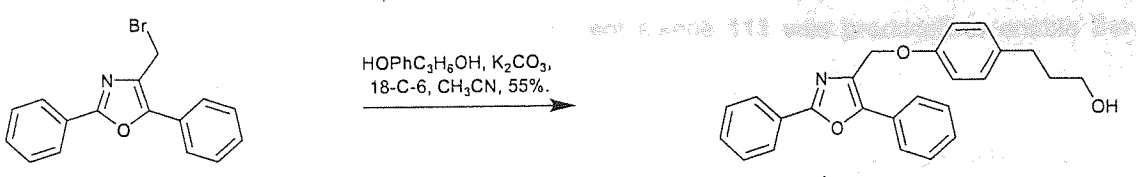

103 **109**

Scheme 25: Synthesis of 3-[4-(2,5-diphenyl-oxazole-4-ylmethyoxy)-phenyl]-propan-1-ol **109**.

At Sense Proteomic, the incorporation of scintilipid **109** into a liposomal preparation provided the corresponding 'scintiliposomes', which were monitored in a scintillation counter. The following scintiliposomes: **109**:DOTAP (469 cpm), **109**:PC (214 cpm) and **109**:DOTAP:DOPE (506 cpm) exhibited a significant number of scintillation counts compared with all other scintiliposome preparations evaluated by Sense Proteomic (Appendix A, Table 37). However, microscopic examination of the liposomal preparations that incorporated scintilipid **109** identified crystalline regions of the scintilipid within all three scintiliposomes.

The structure of scintillant alcohol **109** was modified in an attempt to circumvent the aggregation of scintilipid within the scintiliposomes. Alcohol **109** was esterified with benzoyl chloride under standard conditions, which after work-up and trituration, produced scintillant ester **110** as a white solid in good yield **Scheme 26.** [223]

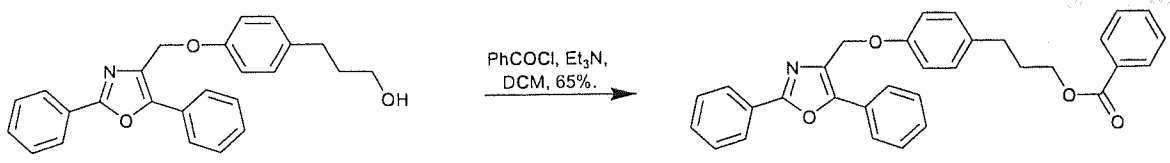

109 **110**

Scheme 26: Synthesis of benzoic acid 3-[4-(2,5-diphenyl-oxazol-4-ylmethoxy)-phenyl]-propyl ester **110**.

Ester **110** and scintiliposomes incorporating this scintilipid exhibited relatively high scintillation counting efficiency in the presence of ionising radiation. Unfortunately, microscopic examination of the scintiliposomes again revealed crystalline regions of the scintilipid. The crystallisation of the scintilipids **109** and **110** was thought to arise as a consequence of intermolecular interactions between the aromatic rings of the scintilipid molecules.[224]

Sodium borohydride was used to reduce a sample of commercially available *trans*-4-decenal to provide *trans*-4-decen-1-ol in quantitative yield.[219] A Williamson type ether synthesis between the *trans*-4-decenol and scintillant bromide **103** furnished scintillant alkene **111** as a white solid. The yield for this

coupling reaction was disappointingly low but sufficient alkene **111** was produced to enable Sense Proteomics to evaluate this compound **Scheme 27**.

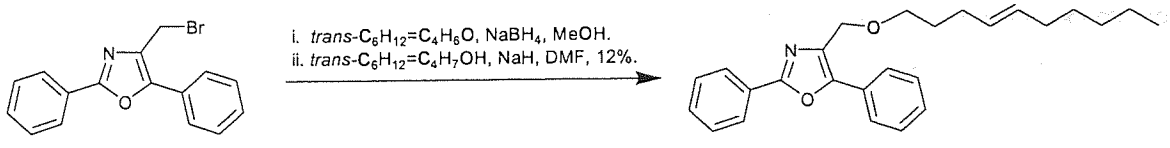

103 **111**

Scheme 27: Synthesis of 4-dec-4-enyloxymethyl-2,5-diphenyl-oxazole **111**.

Scintillant alkene **111** exhibited only a moderate scintillation counting efficiency (19%) in the presence of ionising radiation. However, incorporation of the scintillant alkene **111** into liposome preparation provided scintiliposomes **111**:DOTAP (128 cpm), **111**:PC (308 cpm) and **111**:DOTAP:DOPE (518 cpm) that exhibited significant number of scintillation counts compared with other liposome preparations evaluated (Appendix A, Table 37). In fact, **111**:PC and **111**:DOTAP:DOPE exhibited a greater number of counts than any scintiliposome of analogous composition that were evaluated. Unfortunately, microscopic analysis of these scintiliposomes again revealed that they all contained crystalline scintillant alkene **111**.

In a further attempt, to prevent crystallisation of the scintilipids within the liposomes, a set of scintilipids that contained functionalised but fully saturated side chains were prepared. Scintillant alcohol **112** was synthesised by a Williamson type ether synthesis between a silylated derivative of 6-bromo-1-hexanol and scintillant alcohol **102**. Initially, the hydroxyl functionality of 6-bromo-1-hexanol was protected by silylation with tertiary butyldimethylsilyl chloride.[225] The resultant silyl-ether was added to a solution of scintillant alkoxide in DMF, generated by treatment of **102** with sodium hydride, to give the coupled scintillant silyl-ether adduct which was then desilylated by treatment with tetrabutylammonium fluoride (TBAF) to provide alcohol **112 Scheme 28**.[225]

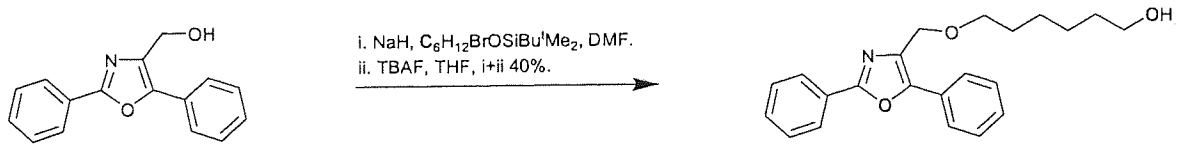

102 **112**

Scheme 28: Synthesis of 6-(2,5-diphenyl-oxazol-4-ylmethoxy)-hexan-1-ol **112**.

Surprisingly alcohol **112** gave a low scintillation counting efficiency (0.9%) but this value increased significantly upon incorporation into liposomal preparations **112**:PC (96 cpm), **112**:DOTAP (76 cpm),

112:DOTAP:DOPE (62 cpm). This encouraging result prompted the derivatisation of alcohol **112** into a number of other scintillant containing compounds, **113-118**.

Long, linear aliphatic carboxylic acids dissolved in a solvent above their critical micelle concentration frequently assemble into micelles.[226] Consequently it was anticipated that 2,5-diphenyloxazole tagged with a carboxylic acid moiety would be incorporated readily into liposomes, when introduced into liposomal preparations.

Attempts to oxidise alcohol **112** directly into the corresponding carboxylic acid **114** using either Jones reagent (CrO_3/AcOH) or $KMnO_4$ generated a variety of oxidative products. Consequently, a less vigorous two-step oxidation strategy was employed to convert alcohol **112** into carboxylic acid **114** successfully via intermediate aldehyde **113** **Scheme 29**.[227,228]

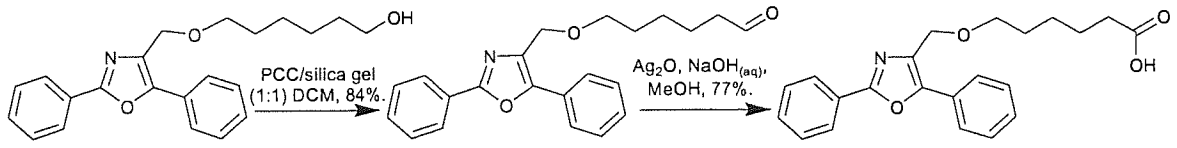

112 **113** **114**

Scheme 29: Synthesis of 6-(2,5-Diphenyl-oxazol-4-ylmethoxy)-hexanoic acid **114**.

Contrary to a previous finding that indicated that carboxylic acids quench scintillation significantly,[215] carboxylic acid **114** exhibited the greatest scintillation efficiency (93%) of all the scintillant compounds evaluated! Unfortunately, incorporation of the carboxylic acid **114** into various liposomal preparations produced scintiliposomes that only exhibited comparatively low scintillation counts (Appendix A, Table 37).

Two further strategies were proposed to attach a scintillant molecular tag covalently to the amine groups of any appropriate molecules within a cell membrane to provide scintillant-tagged cells. In the first strategy it was proposed to utilise a scintillant tag functionalised with an isocyanate group, which would be susceptible to nucleophilic attack by amines.[229] Accordingly, scintillant alcohol **112** was treated with phosphorous tribromide to provide scintillant bromide **115**. Bromide **115** was subsequently to be reacted by Sense Proteomic with sodium isocyanate in the presence of cells to generate the corresponding isocyanate precursor for covalent attachment of the scintillant tag to amine functionalities present within cell membranes **Scheme 30**.

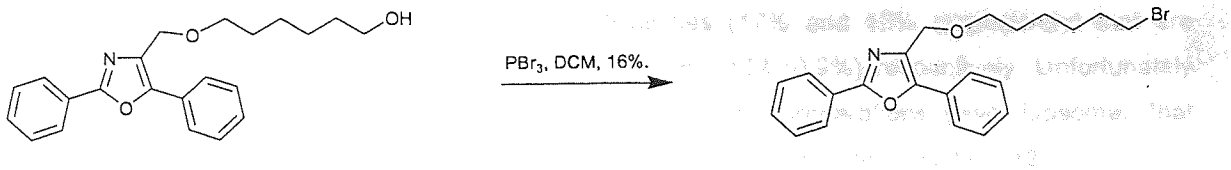

112 **115**

Scheme 30: Synthesis of 4-(6-bromo-hexyloxymethyl)-2,5-diphenyl-oxazole **115**.

In the second strategy it was proposed to generate a scintillant tag that was functionalised as an activated ester, a group which is susceptible towards nucleophilic attack by amines. Accordingly, succinic ester **116** was synthesised by the DCC mediated coupling of carboxylic acid **114** with *N*-hydroxysuccinimide in dimethoxyethane (DME) **Scheme 31**.[230,231]

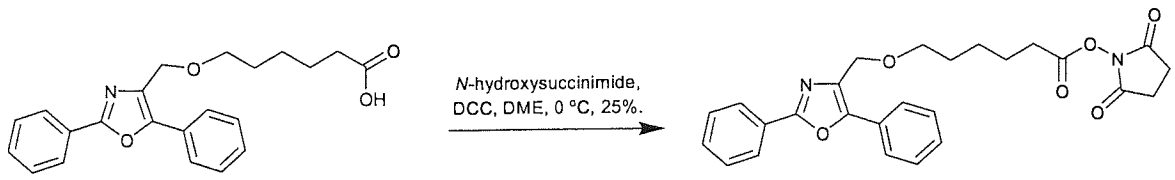

114 **116**

Scheme 31: Synthesis of 6-(2,5-diphenyl-oxazol-4-ylmethoxy)-hexanoic acid 2,5-dioxo-pyrrolidin-1-yl ester **116**.

Unfortunately, although it was possible to synthesise scintilipids **115** and **116** successfully, neither strategy for their covalent attachment to cell membranes proved successful when the appropriate coupling procedures were attempted by workers at Sense Proteomic.

Alcohol **112** was further derivatised by esterification with butyryl chloride and benzoyl chloride to provide the corresponding esters **117** (R=C_3H_7, 45%) and **118** (R=Ph, 52%) respectively **Scheme 32**.[223]

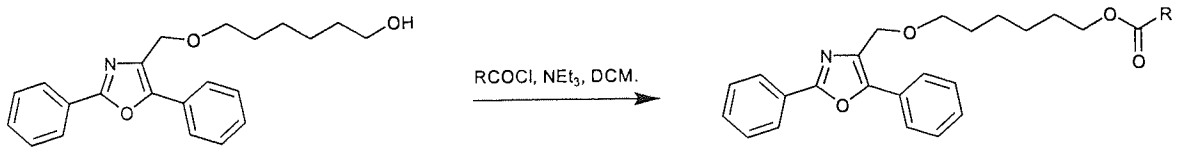

112

117 R=C_3H_7
118 R=Ph

Scheme 32: Synthesis of butyric acid 6-(2,5-diphenyl-oxazol-4-ylmethoxy)-hexyl ester **117** and benzoic acid 6-(2,5-diphenyl-oxazol-4-ylmethoxy)-hexyl ester **118**.

Esters **117** and **118** have scintillation counting efficiencies (17% and 13% respectively) that are approximately twenty and fifteen times greater than alcohol **112** (0.9%) respectively. Unfortunately however, incorporation of either of these esters into liposomal preparations gave liposomes that exhibited scintillation counts below those obtained for liposomes incorporating alcohol **112**.

Since derivatives of alcohol **112** gave no real improvements over using just precursor alcohol, an attempt was made to investigate an analogue with a slightly longer alkyl chain.
A Williamson type ether synthesis reaction between scintillant alkoxide **102** and silylated-8-bromo-1-octanol followed by treatment with TBAF gave alcohol **119**, which has an aliphatic chain length two methylene units longer in length than alcohol **112 Scheme 33**.[225]

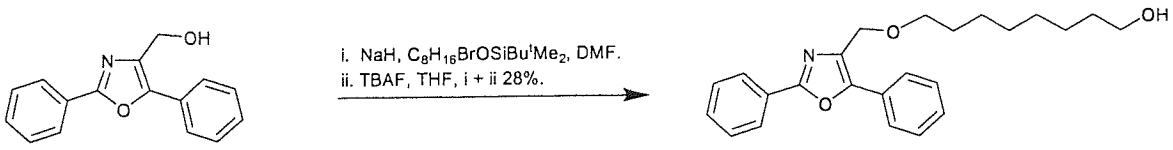

102 **119**

Scheme 33: Synthesis of 8-(2,5-diphenyl-oxazol-4-ylmethoxy)-octan-1-ol **119**.

Gratifyingly alcohol **119** exhibited a scintillation counting efficiency (21%) that is twenty five times greater than alcohol **112** (0.9%). In addition, alcohol **119** produced approximately twice the number of scintillation counts, compared with **112**, when incorporated into liposomal preparations. Scintiliposomes incorporating alcohol **119** have subsequently been used to introduce scintilipid **119** into the membrane of HeLa cells by Sense Proteomic. These cells have been used successfully in a cell-based SPA to detect and quantify the uptake of [^{14}C]methionine.[217] After this successful proof of principle experiment, Sense Proteomic filed a patent application and are currently evaluating this technology "in house".[232]

2.2 Synthesis and Evaluation of Polystyrene-Based Resins

Chemically-functionalised polystyrene-based resin beads, that incorporate scintillant molecules covalently, were required for solid-phase synthesis and a subsequent on-bead scintillation based assay. The construction of these scintillant-containing resins requires the ready availability of an appropriate scintillant monomer. 2,5-Diphenyloxazole **1** was chosen as the scintillant moiety of choice since it is well known to scintillate in the presence of ionising radiation and has a chemically robust oxazole skeleton. In addition, an efficient two step synthetic route to the scintillant monomer (4'-vinyl)-4-benzyl-2, 5-diphenyloxazole **101** has been reported previously by the Sutherland group.[218]

2.2a Synthesis of (4'-Vinyl)-4-benzyl-2,5-diphenyloxazole

(4'-Vinyl)-4-benzyl-2,5-diphenyloxazole **101** was synthesised successfully by a Stille coupling reaction between chloromethylstyrene **12** and 2,5-diphenyl-4-trimethylstannanyloxazole **120**. Firstly, Rickborn's lithiation methodology was used to generate the 4-lithio-2,5-diphenyloxazole intermediate, which was added to a solution of trimethyltin chloride in THF at -78 °C to provide 2,5-diphenyl-4-trimethylstannanyloxazole **120** as a white solid after re-crystallisation **Scheme 34**.[216]

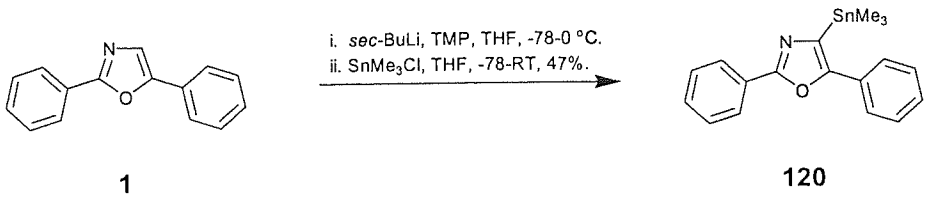

1 **120**

Scheme 34: Synthesis of 2,5-diphenyl-4-trimethylstannanyloxazole **120**.

The Stille coupling reaction between 2,5-diphenyl-4-trimethylstannanyloxazole **120** and chloromethylstyrene **12** was mediated by a palladium catalyst derived from triphenylarsine. This $Pd^{(0)}$ complex underwent oxidative addition with chloromethylstyrene **12** to form the corresponding $Pd^{(II)}$ complex. The nucleophilic stannane participated in a transmetallation reaction with the electron deficient organo-palladium centre to provide the transmetallated $Pd^{(II)}$ complex. This complex underwent reductive elimination to generate the carbon-carbon bond of the (4'-vinyl)-4-benzyl-2,5-diphenyloxazole **101** cross coupled product and regenerate the $Pd^{(0)}$ catalyst **Scheme 35**.

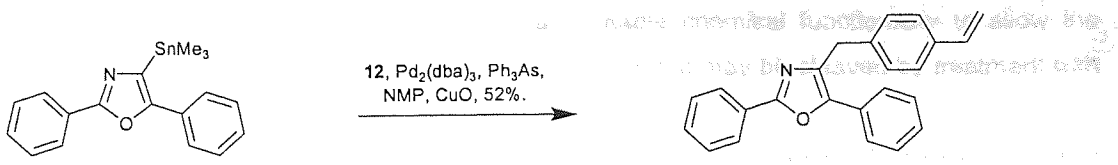

120 101

Scheme 35: Synthesis of (4'-vinyl)-4-benzyl-2,5-diphenyloxazole **101**.

2.2b Construction of Chloromethyl-Functionalised, Scintillant-Containing, Resin

The resins used in SPOC are typically constructed by a suspension polymerisation procedure. Accordingly, the monomers (4'-vinyl)-4-benzyl-2,5-diphenyloxazole **101** (1.5 mole percent), styrene **10** (85.0 mole percent), chloromethylstyrene **12** (10.9 mole percent) cross-linked with DVB **11** (2 mole percent), were combined with the free radical initiator AIBN **7**. Thermally initiated suspension polymerisation of the monomer mixture proceeded smoothly to provide chloromethyl-functionalised, scintillant-containing, gel-type resin beads **121** (0.95 mmol chloromethyl/g) **Scheme 36**.

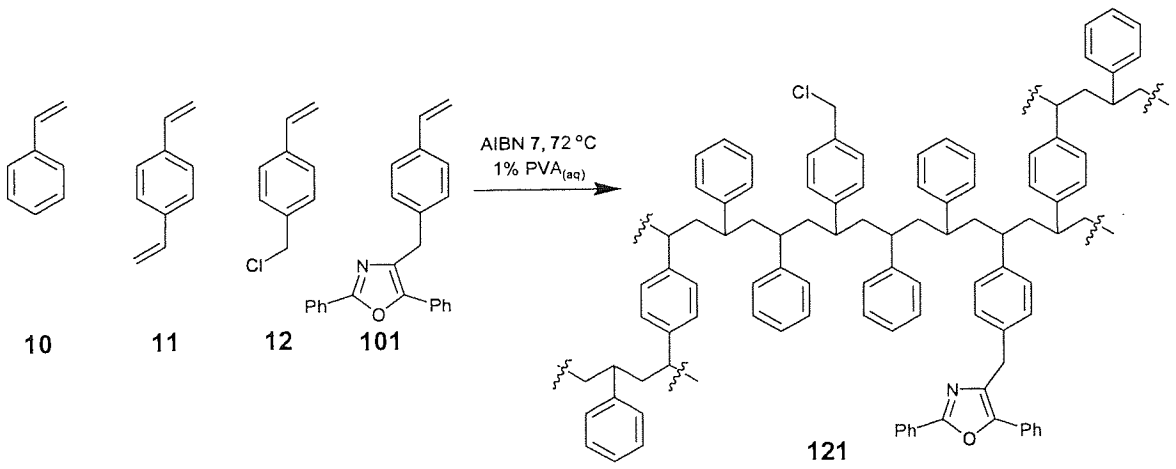

10 11 12 101 121

Scheme 36: Co-polymerisation of **10**, **11**, **12** and **101** in the construction of polymer resin **121**.

This chloromethyl functionalised, scintillant-containing, polymer resin **121** may be used as a support in SPPS. The initial *N*-protected-amino acid is usually attached covalently to the chloromethyl-resin via a *p*-alkylbenzyl ester linkage. The α-amino-protection group is then selectively cleaved by treatment with an appropriate reagent, prior to coupling the next *N*-protected-amino acid. This *N*-deprotection and amino acid coupling procedure may be repeated to provide a peptide of desired length and sequence. The product peptide often has its, side-chain protection and benzyl ester linkage cleaved in a single step by treatment with anhydrous hydrogen fluoride to release the product peptide from the solid support.

It was thought desirable to construct a resin that has suitable chemical functionality to allow the covalent attachment to an *N*-protected-amino acid via a linkage that may be cleaved by treatment with milder/less hazardous reagent(s).

The majority of such resins are provided by derivatisation of chloromethylated polystyrene resin with the appropriate linker molecule. However, it was preferred to introduce chemical functionality into the resin by incorporation of an appropriate monomer into the monomer mixture prior to polymerisation. This approach normally provides a resin with a controlled loading of functional groups that are homogeneously distributed throughout the polymer matrix.

2.2c Construction of Acetoxy-Functionalised Resins

A review of the literature revealed a method for the facile synthesis of hydroxyl functionalised polystyrene based resin.[233,234] Accordingly, the monomers 4-acetoxystyrene **39** (7 mole percent), styrene **10** (74.9 mole percent), cross-linked with DVB **11** (14.5 mole percent), combined with the free radical initiator AIBN **7** were dissolved in toluene (porogen). Thermally initiated suspension polymerisation of the monomer mixture proceeded smoothly to provide acetoxy-functionalised macroporous polystyrene resin beads **122**. Similarly, gel-type resin beads **123** were produced by co-polymerisation of 4-acetoxystyrene **39** (7.2 mole percent), styrene **10** (90.3 mole percent), cross-linked with DVB **11** (2 mole percent) **Scheme 37**.

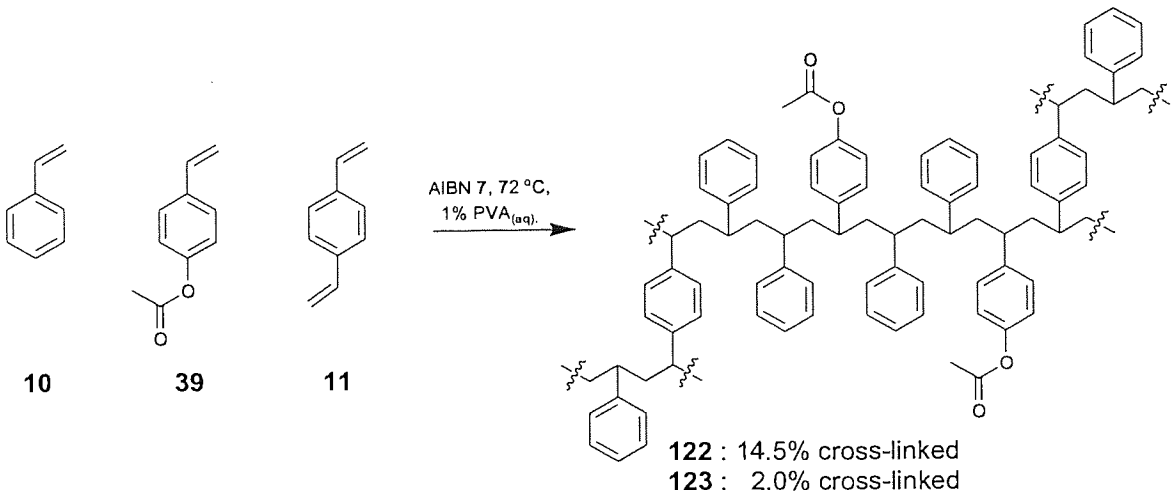

Scheme 37: Co-polymerisation of **10**, **11** and **39** in the construction of polymer resin **122** / **123**.

2.2d Hydrolysis of Acetoxy-Functionalised Resins

Following the successful construction of polymer resins **122** and **123**, it was necessary to determine if the acetate groups could be converted into hydroxyl functionality. Accordingly, polymer resins **122** and **123** were subjected to hydrolysis by treatment with an ethanolic solution of potassium hydroxide. This post-polymerisation hydrolysis reaction proceeded smoothly to provide the desired hydroxyl

functionalised polymer resins **124** and **125** respectively in quantitative yield. The efficiency of the reaction was analysed by IR-spectroscopy which showed the complete disappearance of the C=O (~1755 cm^{-1}) signal and the appearance of a strong new OH signal (~3424 cm^{-1}) **Scheme 38**.

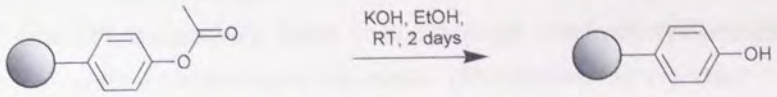

Scheme 38: Hydrolysis of resins **122** and **123** to give resins **124** and **125** respectively.

2.2e Solvent Swelling Assays of Polymer Resins

Following the successful construction of polymer resins **124** and **125** it was necessary to determine if substitution of the chloromethyl group with acetoxy and hydroxyl functionalities had significantly affected the solvent compatibility of polymer resins **122-125**. This solvent compatibility of the new supports was evaluated utilising a syringe based solvent swelling assay.[235] Accordingly, the percentage volume increase of polymer supports **121-125** in DCM, THF, toluene, DMF and water was determined **Figure 59** (Appendix B, Table 38).

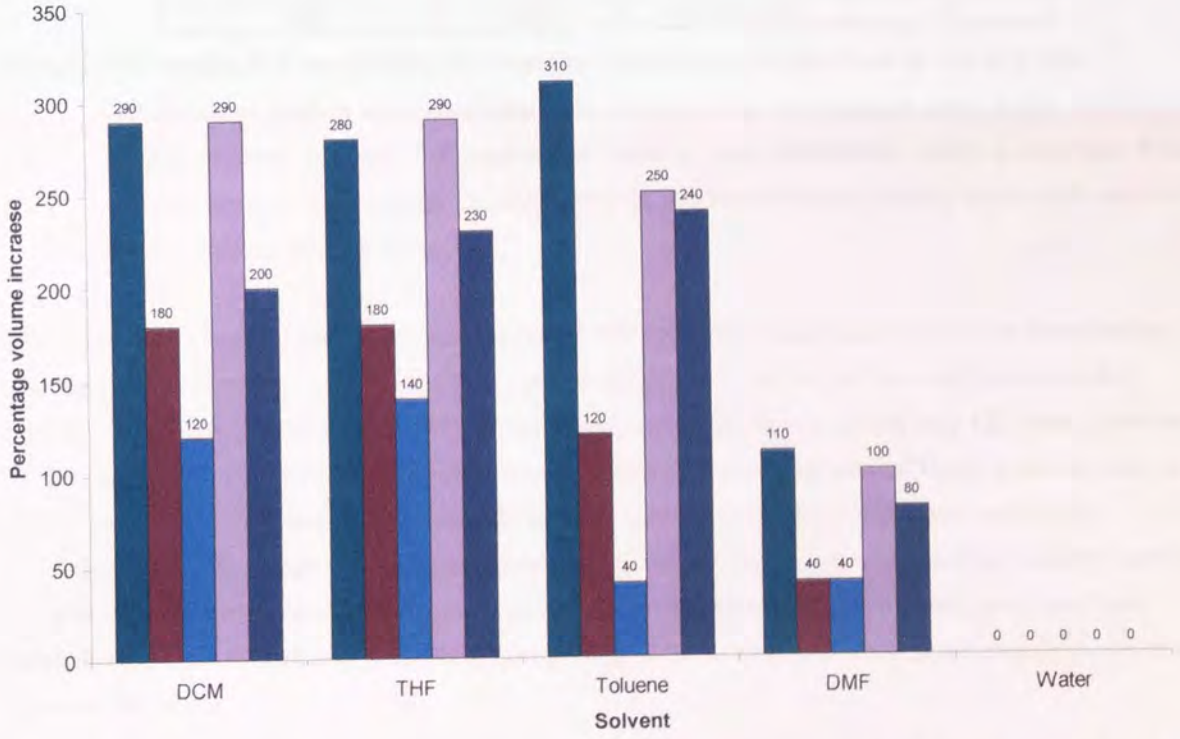

Figure 59: Graph showing percentage volume increase of polymer resins **121**, **122**, **124**, 123 and **125** upon contact with DCM, THF, toluene, DMF and water. Mean error = $^{+}$/-21%.

The swelling data obtained in this manner identified that acetoxy-functionalised gel-type resin **123** to swell to a similar degree to chloromethyl-functionalised resin **121**. As expected the acetoxy-functionalised macroporous resin **122** swelled to a lesser degree than the analogous gel-type resin **123**. The hydroxyl-functionalised resins **124** and **125** swelled to a lesser degree than their acetoxy analogues **122** and **123** respectively. Most disappointingly, the hydroxyl-functionalised resins **124** and **125** did not swell in water. In fact none of the resins **121-125** swelled in water.

2.2f Experimental Hydroxyl Loading of Polymer Resins

Having established that the hydroxyl-functionalised resins **124** and **125** are compatible with organic solvents but swell negligibly in water, it was next necessary to evaluate the utility of these supports in solid-phase synthesis. Accordingly, Fmoc-protected glycine (Fmoc-Gly-OH) was coupled to the hydroxyl functionality of the support. The experimental loading of polymer resins **124** and **125** was assessed by employing a standard Fmoc release assay **Table 1**.[235]

Polymer	Loading / mmol g^{-1}		Percentage loading [c]
	Theoretical [a]	Experimental [b]	
124	0.62	0.17 $^{+}$/-15%	27
125	0.65	0.28 $^{+}$/-10%	43

Table 1: Theoretical and experimentally determined loadings of polymer resins **124** and **125**.
[a] Theoretical loading was calculated from the monomer composition used in the construction of the polymer support. [b] Experimental loading was established using a standard Fmoc-release assay. [c] Percentage loading refers to the experimental loading value with respect to the theoretical loading value.

The theoretical hydroxyl loading of polymer resins **124** and **125**, based upon monomer composition, are calculated to be 0.62 mmol/g and 0.65 mmol/g respectively. After the Fmoc-Gly-OH coupling reaction, the experimental loading of the Fmoc derived polymer supports **126** and **127** were observed to be 0.17 mmol/g and 0.28 mmol/g respectively. These modest experimental loading values may be a consequence of the styrene based supports exhibiting limited swelling in DMF and restricted permeation of polar reagents into the polymer matrix.[103] In fact the lower experimental loading value of polymer resin **124** may be a consequence of the lesser degree of swelling in DMF compared with polymer resin **125**. In addition, the negligible swelling of these resins in water precludes their use in an aqueous bioassay.

The limitations of these PS-DVB based resins may be circumvented by increasing the polarity of the polymer matrix. This has frequently been achieved by grafting hydrophilic molecules such as polyethylene glycol (PEG) onto the polystyrene-matrix of the support.[91,92,97,103] However, the grafting of

PEG onto PS-DVB based resins does not significantly alter the intrinsic hydrophobicity and molecular architecture of the polystyrene matrix. Consequently, the polystyrene regions of the polymer matrix do not swell in an aqueous environment significantly and is impermeable to large biological molecules.[113] This precludes the screening of these resin bound compounds against large biological molecules in an aqueous environment. Thus rather than attempt to generate scintillant-containing grafted beads it was decided to try and develop a new range of polymeric materials that would be fully compatible with both organic and aqueous solvents and that could also incorporate scintillant monomer **101** for application in SPA-style assays.

2.3 Synthesis and Evaluation of Poly(Oxyethylene glycol) Polymer (POP) Supports

PEG-based polymeric supports constructed from PEG-based monomers often have a controlled loading of chemical functional groups that are homogeneously distributed throughout the polymer matrix. In addition, these polymers often exhibit superior organic and aqueous solvent compatibilities compared with both polystyrene-based supports and polystyrene-PEG grafted supports.[91,95,99,102,103,104,114,119,120,122,236] Accordingly, it was proposed that a series of PEG-based polymeric supports be constructed by the co-polymerisation of the corresponding PEG-based functional monomer and cross-linking monomer.

2.3a Synthesis of Poly(oxyethylene glycol) (PEG)-Based Cross-Linkers

A number of mono and bis-polymerisable oligo(oxyethylene glycol) ethers were required. Styrene was chosen as the preferred polymerisable unit for its compatibility with the scintillant monomer (4'-vinyl)-4-benzyl-2,5-diphenyloxazole **101**.[218,237,238,239]

In a synthesis of crown ethers, Nishimura utilised bis-tosyl PEG derivatives in a three step synthesis of two bis-styrene-functionalised oligo(oxyethylene glycol) ethers.[240] Since these styrene-containing ethers did not contain benzylic ether linkages, it was decided to use one of them, α,ω-bis-styryl-pentaethylene glycol **130**, as a cross-linking monomer for the polymer supports. A novel one step route to this target was devised based on methodology previously described by Janda.[104,105,106] Commercial 4-acetoxystyrene **39** was treated with an ethanolic solution of potassium hydroxide in the presence of commercial penta(ethylene glycol) di-*p*-toluene sulfonate (n=4). This one-pot hydrolysis and subsequent *in-situ* coupling reaction proceeded smoothly, to provide the desired product **130** in good yield (48%). Tri(ethylene glycol) di-*p*-toluene sulfonate **128** (n=2), readily synthesised from toluene sulphonyl chloride (TsCl) and tri(ethylene glycol) in excellent yield (89%), also underwent this one step hydrolysis-coupling procedure to provide cross-linking monomer **129** (n=2, 31%) **Scheme 39**.

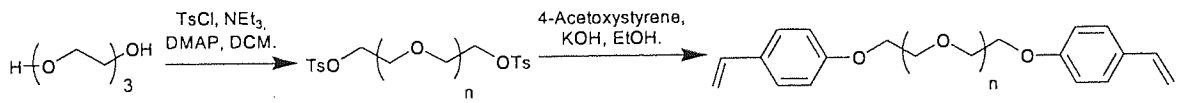

128 n=2

129 n=2
130 n=4

Scheme 39: Synthesis of α,ω-bis-styryl-oxyethylene glycols **129** and **130**.

2.3b Synthesis of PEG-Based Chemically Functionalised Monomers

PEG-based monomers that contain both the polymerisable styrene unit and suitable chemical functionality to enable the generation of chemically reactive supports were also required. Commercial

hetero-functionalised PEG is prohibitively expensive for routine large-scale production of monomers.[241] Consequently, a facile and cost effective route to mono-styrene-functionalised oligo(oxyethylene glycol) ethers was required. The synthesis of oligo(oxyethylene glycol) mono-*p*-toluene sulfonates is well documented.[242,243] Specifically, hexaethylene glycol was reacted with toluene sulfonyl chloride utilising the methodology described by Borjesson and Welch.[243] However, the work-up procedure was modified to preclude the need for purification by column chromatography. A simple extraction procedure gave pure samples of both hexaethylene glycol mono-*p*-toluene sulfonate **131** (n=5, 98%) and enabled the facile recovery of excess, unreacted hexaethylene glycol in excellent yield (70%). This synthesis and work-up procedure also proved extremely effective in the synthesis of poly(oxyethylene glycol)$_{400}$ mono-*p*-toluene sulfonate **132** (n=~8, 88%) and the recovery of excess, unreacted PEG$_{400}$ (75%).

Mono tosylates **131** and **132** were subjected to a one pot hydrolysis coupling procedure that was employed in the synthesis of the cross-linking monomers. In this approach, mono tosylates **131** and **132** were reacted with 4-acetoxystyrene **39** in the presence of an unprotected primary hydroxyl group to provide α-styryl-hexaethylene glycol **133** (n=5, 54%) and α-styryl-poly(oxyethylene glycol)$_{400}$ **134** (n=~8, 30%), respectively **Scheme 40**.

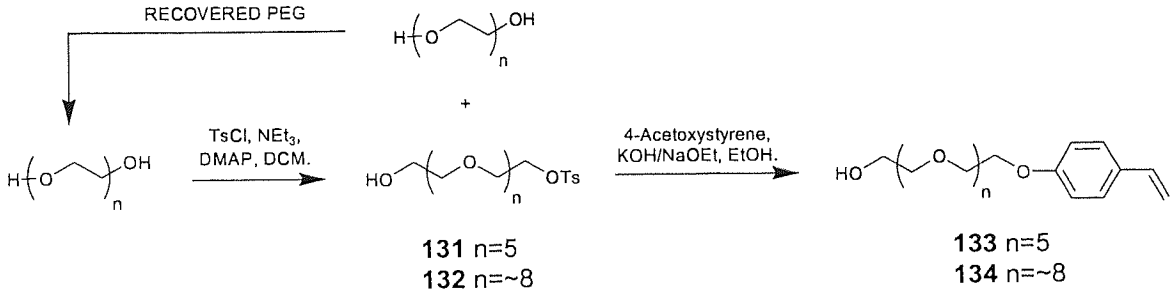

Scheme 40: Synthesis of α-styryl-oligo(oxyethylene glycol) **133** and **134**.

2.3c Polymerisation of PEG-Based Monomers

The ready availability of multi-gramme quantities of α-styryl-oligo(oxyethylene glycol) **133**, **134** and α,ω-bis-styryl-oligo(oxyethylene glycol) **129**, **130** permitted the construction of a series of novel polymer supports **135-142** of varying monomer composition and cross-linking for subsequent solvent compatibility evaluation **Scheme 41**, **Table 2**.

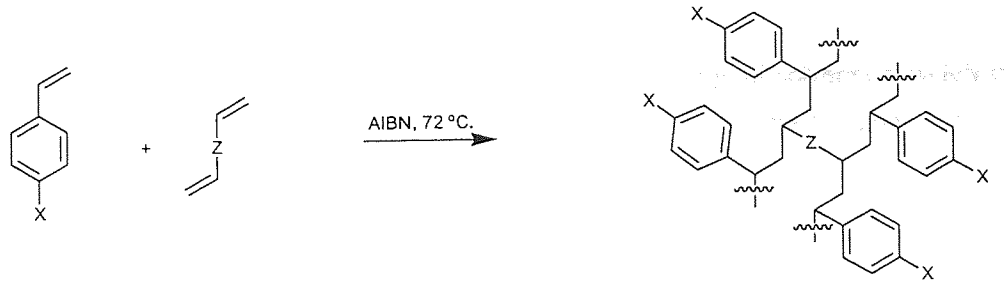

135-142

Scheme 41: Synthesis of polymer supports **135-142**.

Polymer	Functional Monomer / mole %			Cross-Linking Monomer / mole %		
	10 X=H	**133** X=$(C_2H_4O)_6OH$	**134** X=$(C_2H_4O)_{\sim 9}OH$	**11** Z=Ph	**129** Z=$PhO(C_2H_4O)_3Ph$	**130** Z=$PhO(C_2H_4O)_5Ph$
135	98	-	-	-	-	2
136	86	-	-	-	-	14
137	80	-	-	-	-	20
138	98	-	-	-	2	-
139	-	98	-	2	-	-
140	-	-	98	2	-	-
141	-	98	-	-	-	2
142	-	-	98	-	-	2

Table 2: Monomer composition of polymer supports **135-142**.

Micro-scale suspension radical polymerisation of styrene **10** cross-linked with 2, 14 and 20 mole percent α,ω-bis-styryl-penta(oxyethylene glycol) ether **130** gave beaded products **135-137**, respectively. These polymer resins were constructed for solvent compatibility evaluation to identify the mole percentage of PEG-based cross-linking monomer incorporated into the polymer that provides optimal solvent compatibility.

Micro-scale suspension radical polymerisation of styrene cross-linked with 2 mole percent α,ω-bis-styryl-tri(oxyethylene glycol) ether **129** provided resin **138**. This resin was required for comparison with resin **135** to determine the effect cross-linking monomer ethyleneoxide chain length has upon solvent compatibility.

The α-styryl-oligo(oxyethylene glycol) monomers **133** and **134** are miscible with 1% PVA solution that comprises the bulk-phase of the suspension polymerisation system. This observation prompted the bulk polymerisation of **133** and **134** with 2 mole percent DVB or PEG-based cross-linking monomer **130** to provide gel-like Poly(Oxyethylene glycol) Polymer (POP) supports **139-142**.

2.3d Solvent Swelling Assay of Polymers

The polymers **135-142** were evaluated for their ability to swell in a range of solvents of widely differing polarity. A syringe-based solvent swelling assay was employed to determine the percentage volume increase of each polymer in DMF, water and toluene.[235] For comparative purposes, commercial samples of Merrifield's resin **9**, TentaGel **27** and ArgoGel **29** were evaluated in identical manner **Figure 60** (Appendix B, Table 39).

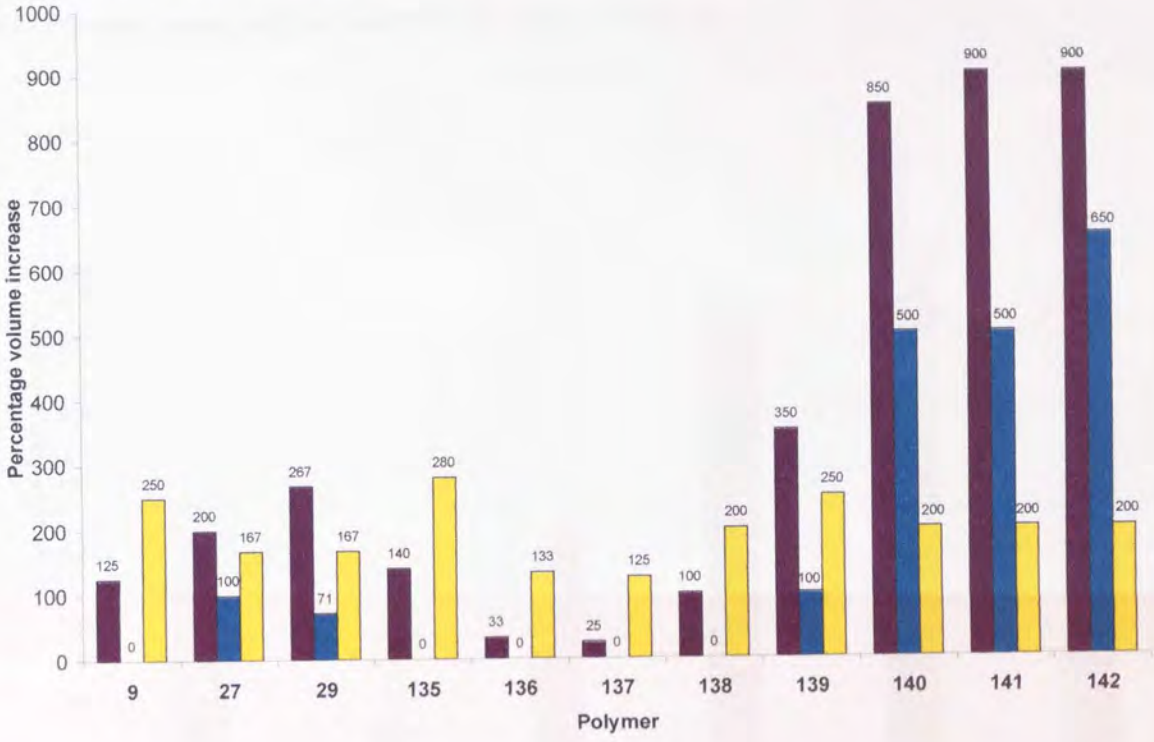

Figure 60: Graph showing the percentage volume change of polymers **135-142**, Merrifield's resin **9**, TentaGel **27** and ArgoGel **29** upon exposure to, **DMF**, **water** and **toluene**. Mean error = $^{+}$/-44%.

Polymers **140-142** that contain PEG derived monomer(s) swell to a greater extent in water than all of the other polymer supports, most notably TentaGel **27** and ArgoGel **29**, which are sold commercially as aqueous compatible supports. The predominantly styrene-based polymers **135-138** and Merrifield's resin **9** exhibit negligible swelling in water. All the polymers swell in DMF to a greater extent and with a similar overall trend to that observed in water. Interestingly, the swelling properties observed for all the polymers in toluene are very similar.

As expected and in agreement with a similar study,[103] styrene-based resins **135-137** exhibit decreased swelling characteristics with increasing degrees of PEG-based cross-linking in DMF and toluene. Similarly, a comparison of the degree of swelling of resins **135** and **138** indicates that increasing the

length of the PEG-based cross-linker, from triethylene glycol to pentaethylene glycol, results in increased swelling of the resin in DMF and toluene.

Polymers **140-142** exhibited the best swelling characteristics in water and thus seemed the most likely candidates for use in on-support aqueous-based assays. Consequently, these polymers were further evaluated for their compatibility with DCM and THF for application in SPPS. For comparative purposes, Merrifield's resin **9**, TentaGel **27** and ArgoGel **29** were also evaluated in these solvents. Again polymers **140-142** exhibited excellent compatibility with both solvents and swelled to far greater extents than the commercial controls **Figure 61** (Appendix B, Table 39).

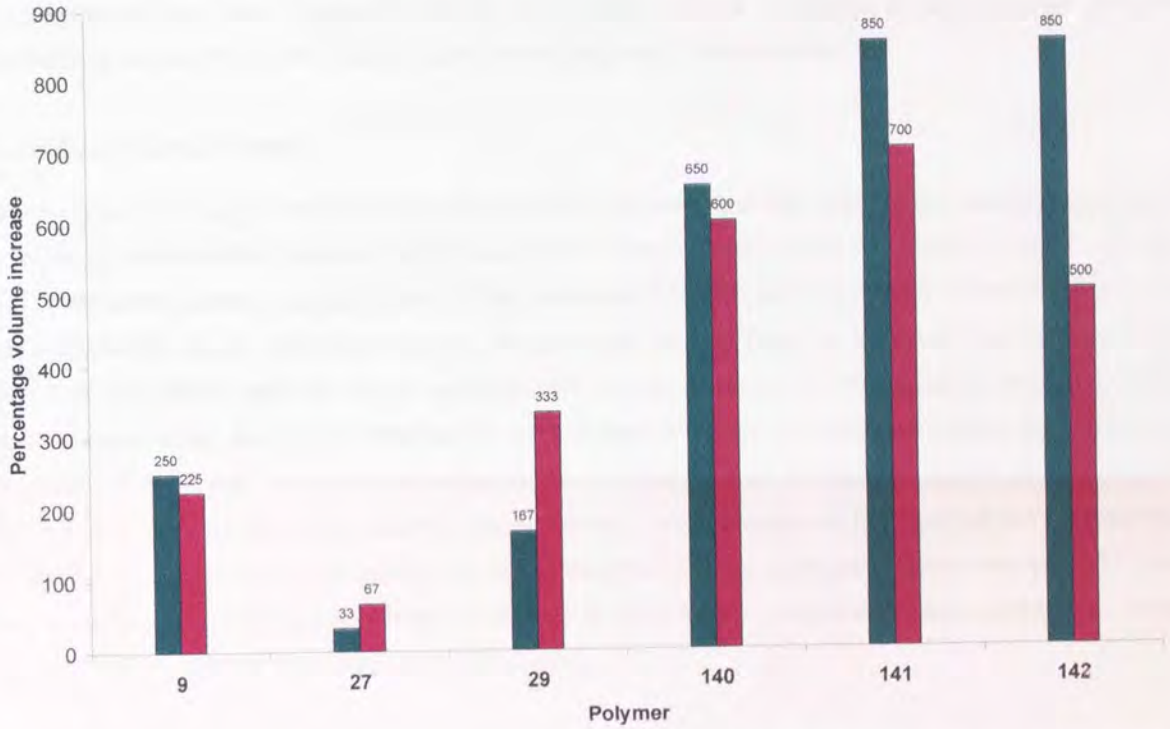

Figure 61: Graph showing the percentage volume change of polymers **140-142**, Merrifield's resin **9**, TentaGel **27** and ArgoGel **29** upon exposure to **DCM** and **THF**. Mean error = $^{+}$/-40%.

2.3e Mass-Solvent Uptake Assay

The internal matrix of polymers **140-142** was tailored with the specific intention of providing a polar matrix of increased surface energy when compared with those of the commercial resins. The effect of increasing the surface energy of a polymer is to create a thermodynamically unfavourable solid/air interface, which should cause rapid and complete wetting by spontaneous penetration of high surface energy solvents, such as water, into the polymer matrix.[244] Conventionally, the wetting of non-porous surfaces and porous solid powders by liquids may be quantified by contact angle measurements[244,245] and the Washburn technique[245,246] respectively. Unfortunately, neither technique can be used to study

gel-type polymers since swelling of the polymer causes the contact surface between the liquid and solid to vary. Although solvent swelling assays give an insight into the site accessibility of a polymer it does not quantify the amount of solvent penetrating the polymer matrix. Consequently, PEG-based polymers **140-142** were studied using a novel mass-solvent uptake assay. The assay involved bringing a solvent just into contact with the surface of a polymer sample so that the solvent penetrates the polymer matrix through capillary action. The amount of solvent penetrating the polymer matrix is quantified using a microbalance, which records the mass reading at fixed time intervals. This allows a time dependent solvation profile to be obtained for each polymer sample. In addition, the mass of solvent imbibed by the polymer sample may also be used to calculate the volume of solvent imbibed by the polymer at any time. Polymers **140-142**, Merrifield's resin **9**, TentaGel **27** and ArgoGel **29** upon exposure to water, DMF and toluene have been evaluated in this manner.

Mass-Water Uptake Assay

Equal aliquots (25 mg) of each of the POP-supports **140-142** and the commercial resins TentaGel **27**, ArgoGel **29** and Merrifield's resin **9** were analysed for mass-water uptake (Appendix C, Table 43). The final mass-water uptake values for each of the polymers **140-142** are about twice those of TentaGel **27** and ArgoGel **29** resins. The mass-solvent uptake versus time profile also demonstrates that Merrifield's resin **9** is completely hydrophobic. In addition, the profiles obtained for TentaGel **27** and ArgoGel **29** resins plateau faster than those obtained for PEG-based polymers **140-142**. A possible explanation for this observation is that there is rapid solvation of the grafted PEG-containing regions of TentaGel **27** and ArgoGel **29** and that subsequently there is little if any solvation of the hydrophobic polystyrene backbones of these resins. In contrast after the peripheral PEG surfaces of polymers **140-142** have been solvated rapidly, it appears that more time is required for complete solvent penetration to the PEG-containing cores of these polymers **Figure 62**.

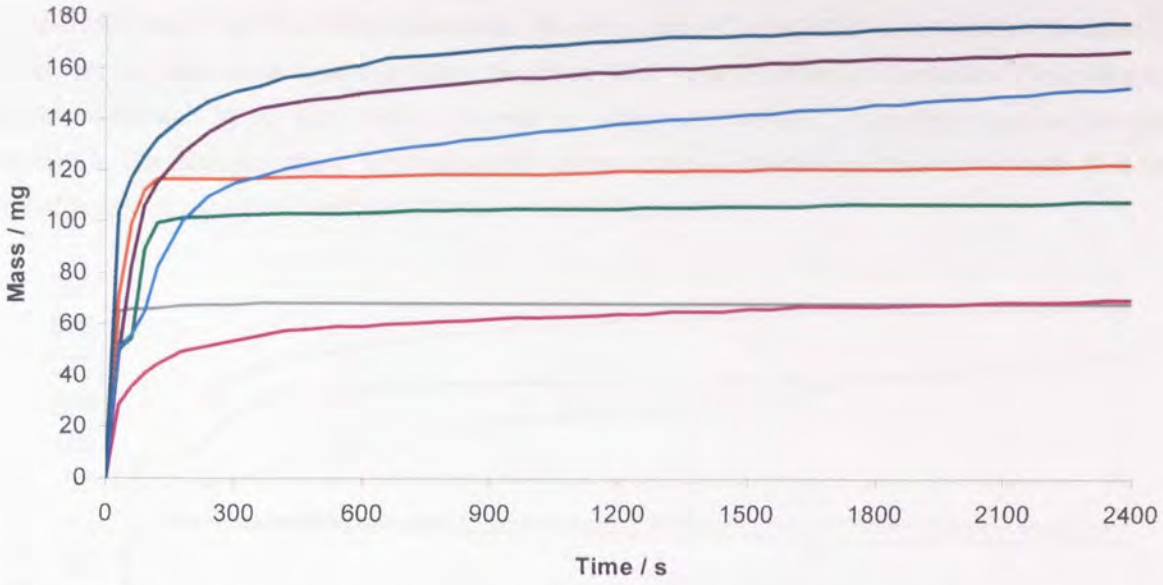

Figure 62: Graph showing mass-water up-take versus time of polymers **140**, **141** and **142** relative to the commercial control resins TentaGel **27**, ArgoGel **29**, Merrifield's resin **9** and a **blank control**. Estimated error = $^{+}$/-0.05mg.

Polymer **139** imbibes a similar final mass (50.5 mg/mg polymer) of water to both TentaGel **27** (40.5 mg/mg polymer) and ArgoGel **29** (54.5 g/mg polymer). The replacement of the DVB cross-linker in polymer **139** with α,ω-bis-styryl-pentaethylene glycol **130** gives polymer **141**, which exhibits a dramatically increased mass-water uptake that is far greater than both TentaGel **27** and ArgoGel **29**. Similarly, replacement of the α-styryl-hexaethylene glycol monomer **133** in polymer **139** with α-styryl-poly(oxyethylene glycol)$_{400}$ **134** provides polymer **140** which again exhibits a dramatically increased mass-water uptake.

In summary, increasing the ethylene oxide chain length of either the PEG-based functional monomer or the cross-linking monomer provides polymers with greater mass-water uptake. In addition, since polymer **140** (2% DVB **11** cross-linker; 98% α-styryl-poly(oxyethylene glycol)$_{400}$ monomer **134**) takes up a greater mass of water than polymer **141** (2% α,ω-bis-styryl-pentaethylene glycol **130** cross-linker; 98% α-styryl-hexaethylene glycol monomer **133**) the importance of the ethylene oxide chain length of the PEG-based monomer appears to outweigh the effects of the small amount of cross-linking monomer that is incorporated in gel-type supports such as these.

Mass-DMF Uptake Study

POP-supports **140-142** and commercial resins TentaGel **27**, ArgoGel **29** and Merrifield's resin **9** had their mass-DMF uptake versus time evaluated (Appendix C, Table 44). The polymers **140-142** imbibed final masses of DMF that are approximately double that of the three commercial resins **9**, **27** and **29**.

This observation is presumably a consequence of the greater solvent accessibility towards a PEG cross-linked matrix than the DVB cross-linked styrene cores of TentaGel **27** and ArgoGel **29** resins. Similar to the mass-water uptake profiles, the mass-DMF uptake profiles of TentaGel **27** and ArgoGel **29** resins plateau faster than those obtained for polymers **140-142**. In addition, and in complete contrast to the aqueous study, the mass-DMF uptake profile obtained for Merrifield's resin **9** is very similar to that obtained for TentaGel **27** resin in DMF **Figure 63**.

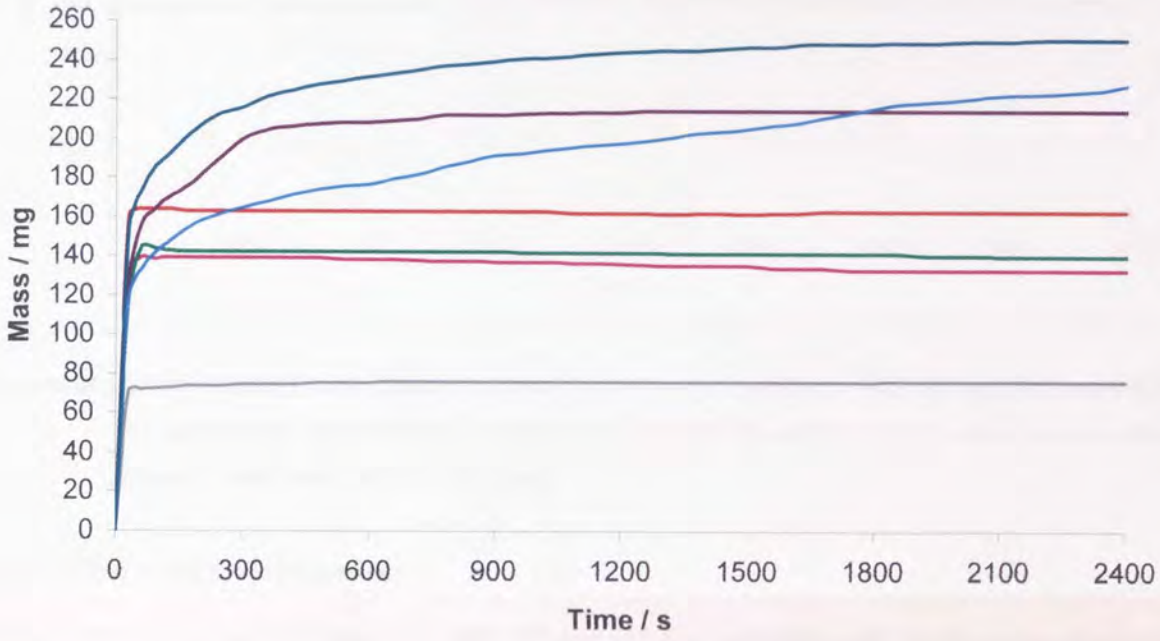

Figure 63: Graph showing mass-DMF up-take versus time of polymers **140**, **141** and **142** relative to the commercial control resins TentaGel **27**, ArgoGel **29** and Merrifield's resin **9** and a blank control. Estimated error = $^{+}$/-0.05mg.

Mass-Toluene Uptake Study

The polymers mass-toluene up-take versus time profiles indicates the imbibed final mass of toluene decreases in the order Merrifield's resin **9**, TentaGel **27**/ArgoGel **29**, **140/141/142** (Appendix C, Table 45). This order reflects the hydrophobicity of each class of polymer studied and consolidates the view of Merrifield's resin **9** behaving as a polystyrene resin, TentaGel **27** and ArgoGel **29** behaving as polystyrene resins with PEG-grafts and POP-supports **140-142** behaving predominantly as PEG-based supports with styrene grafts **Figure 64**. Interestingly, such subtleties are less apparent in the toluene swelling assay where all of the polymers evaluated give relatively similar swelling volumes (Figure 60).

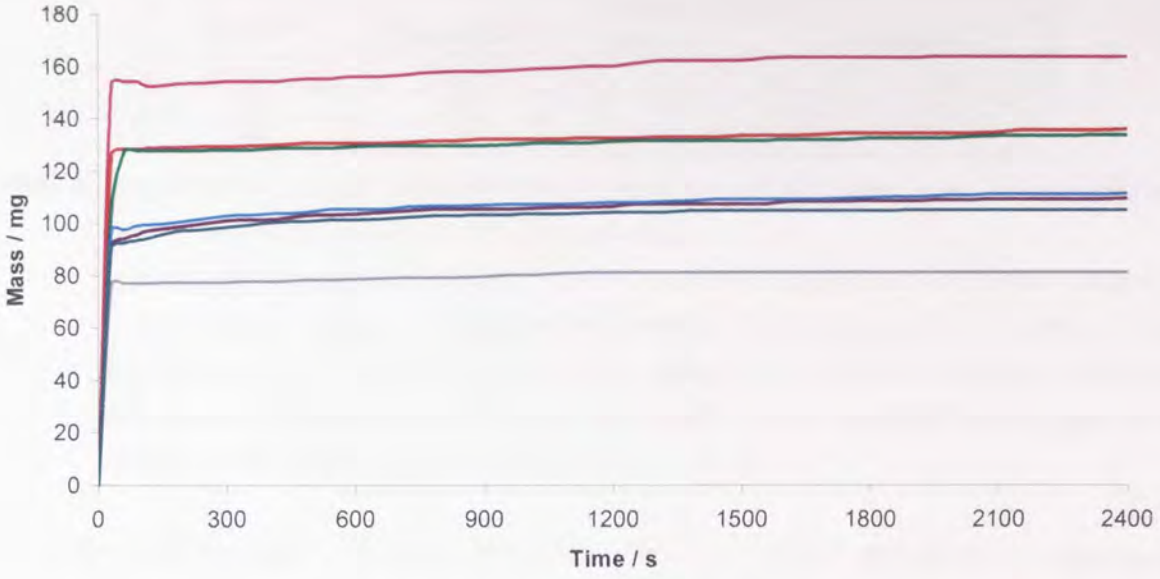

Figure 64: Graph showing mass-toluene up-take versus time of polymers **140**, **141** and **142** relative to the commercial control resins TentaGel **27**, ArgoGel **29** and Merrifield's resin **9** and a **blank control**. Estimated error = $^{+}$/-0.05mg.

2.3f SPPS on POP-Supports

Having established that POP-supports **140**, **141** and **142** are compatible with a wide range of solvents of differing polarities their utility as supports for SPPS has been evaluated. Accordingly, the coupling of Fmoc-Gly-OH to the pendant hydroxyl functionality within each of the supports was undertaken, using unsymmetrical active ester methodology, to provide the corresponding Fmoc-glycine derived supports **143**, **144** and **145** respectively.

The experimental loading of these supports was assessed by employing the Fmoc release assay.[235] The Fmoc-glycine derived supports **143**-**145** were treated with piperidine to liberate the Fmoc group as 1-fluoren-9-yl methylpiperidine **74**, which is related directly to the support loading, which was quantified by uv-vis spectroscopy by monitoring the absorbance of the assay mixture at 290 nm. This coupling/deprotection process was repeated to determine the efficiency of the second coupling reaction

After the first round of couplings, the loadings of the three POP-supports **140**, **141** and **142** were determined to be 0.65, 0.68 and 0.57 mmol/g respectively. Whilst somewhat lower than the theoretical loadings calculated for these supports these experimentally determined values are still significantly higher than the theoretical loadings reported for the commercial samples of ArgoGel **29** and TentaGel **27** used in this study, 0.47 and 0.28 mmol/g respectively. In addition, the second round of Fmoc-Gly-OH couplings gave average yields of 68% **Table 3**.

Polymer	Loading / mmol g^{-1}		
	Theoretical[a]	Coupling 1[b]	Coupling 2[b]
140	1.92	0.65 $^{+}$/-7% (34%)	0.41 $^{+}$/-10% (63%)
141	2.53	0.68 $^{+}$/-10% (27%)	0.43 $^{+}$/-18% (63%)
142	1.90	0.57 $^{+}$/-7% (30%)	0.44 $^{+}$/-19% (77%)

Table 3: Theoretical and experimentally determined loadings of POP-supports **140**, **141** and **142** after two successive rounds of Fmoc-Gly-OH coupling.

[a] Theoretical loading was calculated from the monomer composition used in the construction of the polymer support. [b] Experimental loadings for coupling 1 and coupling 2 were established using a standard Fmoc-release assay. The numbers in brackets refer to the experimental loading value for coupling 1 with respect to the theoretical loading value and for coupling 2 with respect to to the loading value for coupling 1.

The utility of POP-supports **140-142** in SPPS has been demonstrated successfully. In addition, the swelling properties and mass-solvent uptake studies have identified these POP-supports to be compatible with both water and a range of organic solvents with widely differing polarities.

2.4 Synthesis and Evaluation of Scintillant-Containing Poly(Oxyethylene glycol) Polymer (POP-Sc) Supports

A range of chemically-functionalised poly(oxyethylene glycol)-based polymeric supports that incorporate scintillant molecules covalently were required. These chemically-reactive supports were to be used in solid-phase synthesis and their in-built assay capability exploited in subsequent on-support SPA's in aqueous media. Herein is reported the construction and evaluation of poly(oxyethylene glycol) polymer supports that incorporate scintillant molecules covalently (POP-Sc supports).

POP-supports **141** and **142** incorporate α-styryl-hexaethylene glycol **133** or α-styryl-poly(oxyethylene glycol)$_{400}$ **134** respectively and are both cross-linked with 2% α,ω-bis-styryl-pentaethylene glycol **130**. These polymers exhibit similar swelling and mass-solvent uptake abilities, which are superior to all the other polymers evaluated.

The higher product yield obtained for the synthesis of monomer **133** compared with **134** prompted its preferred use in the construction of the POP-Sc supports. However, the hexaethylene glycol starting material that is used to synthesise **133** was replaced with analogous PEG_{300} that is significantly cheaper. Accordingly, α-styryl-poly(oxyethylene glycol)$_{300}$ **153** was synthesised in two steps from commercially available PEG_{300}.

The co-polymerisation of α-styryl-poly(oxyethylene glycol)$_{300}$ **153**, 2 mole percent α,ω-bis-styryl-pentaethylene glycol **130** and a varying mole percentage of (4'-vinyl)-4-benzyl-2,5-diphenyloxazole **101** provided the series of POP-Sc supports **155-160** and POP support **154**. These supports have been evaluated for their ability to swell in a variety of solvents, including water, and to scintillate in the presence of ionising radiation. Finally, the application of the optimal POP-Sc support in SPPS/SPOC is exemplified.

2.4a Synthesis of POP-Sc Supports

Monomers **101**, **130** and **153** were combined in various molar ratios with the free radical initiator AIBN **7 Table 4**.

Polymer	Mole percent monomer composition		
	153	130	101
154	98	2	0
155	97	2	1
156	96	2	2
157	94	2	4
158	92	2	6
159	90	2	8
160	88	2	10

Table 4: Mole percent monomer composition of POP support **154** and POP-Sc supports **155-160**.

Thermally initiated bulk polymerisation of each monomer mixture proceeded smoothly and resulted in the production of hydroxyl-functionalised, scintillant-containing, PEG-based gel-type POP-Sc supports **155-160** and non-scintillant containing POP support **154 Scheme 42.**

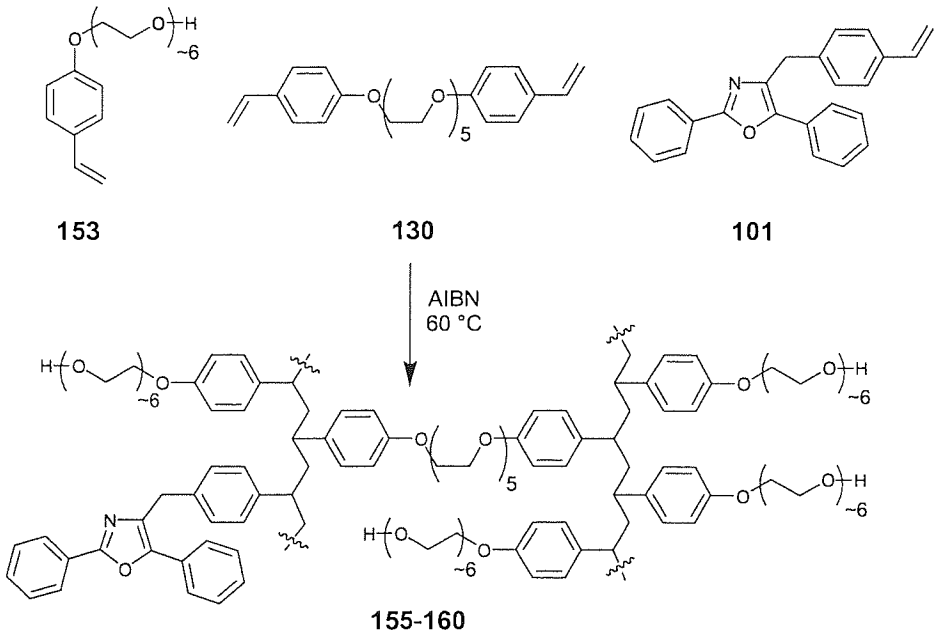

Scheme 42 Copolymerisation of α-styryl-poly(oxyethylene glycol)$_{300}$ **153**, α,ω-bis-styryl-pentaethyleneglycol **130** and (4'-vinyl)-4-benzyl-2,5-diphenyloxazole **101** used in the construction of POP-Sc supports **155-160**.

2.4b Solvent Swelling Assay

It was necessary to determine that the incorporation of the hydrophobic scintillant monomer **101** into POP-Sc supports **155-160**, albeit at relatively low levels, had not significantly affected the compatibility of these materials with a range of solvents. The solvent compatibility of each polymer was assessed by evaluating their swelling properties in water and a range of organic solvents of differing polarity. The syringe-based solvent swelling assay was employed to measure the percentage volume increase of each POP-Sc support **155-160** and control POP support **154** in toluene, water, THF, DMF and DCM (Appendix B, Table 40) **Figure 65.**

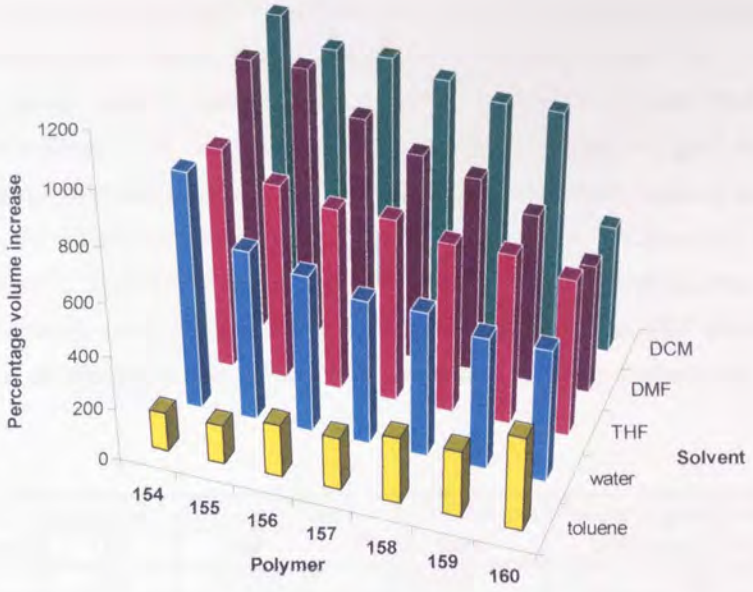

Figure 65: Graph showing the percentage volume increase of POP-Sc supports **155-160** and POP support **154** upon contact with **DCM**, **DMF**, **THF**, **water** and **toluene**. Mean error = $^{+}$/-47%.

The data obtained in this manner was used to quantify solvent accessibility into each polymer matrix and also to assess the compatibility of each POP-Sc support with the aqueous environment of a bio-assay. Each POP-Sc support, **155-160** and POP support **154**, exhibited significant swelling in water and the range of organic solvents of widely differing polarity. As might be expected, an increase in the mole percent of (4'-vinyl)-4-benzyl-2,5-diphenyloxazole **101** in the POP-Sc support monomer composition resulted in a reduction in the percentage volume increase of the support when brought into contact with polar solvent (DMF, DCM, THF, water) and an increase in swelling when the POP-Sc support was brought into contact with non-polar solvent (toluene). These encouraging results suggested that POP-Sc supports may indeed be suited for use in both SPPS/SPOC and aqueous-based assay procedures.

2.4c Scintillation Assay Development

Having established that all of the POP-Sc supports **155-160** could be used in both aqueous and organic media, it was next necessary to determine the optimal mole percentage of (4'-vinyl)-4-benzyl-2,5-diphenyloxazole **101** that should be incorporated into the POP-Sc support. A non-proximity scintillation assay was used to determine the scintillation efficiency of POP-Sc supports **155-160** when incubated with an aliquot of radioactivity in water.

A suitable radionucleotide was chosen to ensure that a significant scintillation signal would be generated even in the absence of proximity effects. An aqueous solution of [^{14}C]benzoic acid was used as the source of non-specific, medium energy β-particles (<280 μm in water [247]).

Initially, a suitable assay volume was determined using a POP-Sc support that contained 2 mole percent scintillant monomer **101**, which has been shown previously to give optimal efficiency in scintillant-containing polystyrene resins.[237,238] POP-Sc support **156** and negative control POP support **154** (~2 mg) were separately incubated with equal aliquots of the [^{14}C]benzoic acid stock solution (~120000 cpm) in varying volumes of water and monitored in a scintillation counter. POP support **154**, that contains no scintillant, gave no significant scintillation signal. Whilst POP-Sc support **156** gave a significant number of counts per minute (cpm) that decreased in value as the assay volume increased **Table 5**.

Volume water / μL	support / cpm mg^{-1}[a]		156 + Scintillation Fluid / cpm[a]	Percentage scintillation efficiency of 156[b]
	154	156		
10	243	12931	115886	16
20	93	9489	120621	11
30	103	8693	120119	10
40	87	9075	126631	10
50	156	8649	122107	10

Table 5: Effect of assay volume upon observed scintillation. Mean error = $^{+}$/-11%.

[a] Cpm values are background corrected. [b] The values for scintillation efficiency correspond to the cpm expressed as a percentage of the total cpm detected for **156** with the scintillation fluid. All values have been adjusted to accommodate the fact that a fluor based solely on 2,5-diphenyloxazole **1** gives only 70% of the cpm obtained with a multi-fluor scintillation fluid.[215]

This observation suggests that the greater the dilution of the radionucleotide the less likely it is that β-particles will encounter the scintillant molecules within the polymer support. The lowest volume of water that could fully solvate the POP-Sc matrix, whilst maximising scintillation efficiency was determined to be a volume of 20 μL.

2.4d Assay to Determine the Optimal Scintillant Content

A non-proximity scintillation assay was used to determine the optimal concentration of (4'-vinyl)-4-benzyl-2,5-diphenyloxazole **101** to incorporate in the monomer composition of the POP-Sc support to attain the highest scintillation efficiency. Accordingly POP-Sc supports **155-160** and control POP support **154** (~2 mg) were incubated with an aqueous solution of [^{14}C]benzoic acid (20 μL) and monitored in a scintillation counter **Figure 66**.

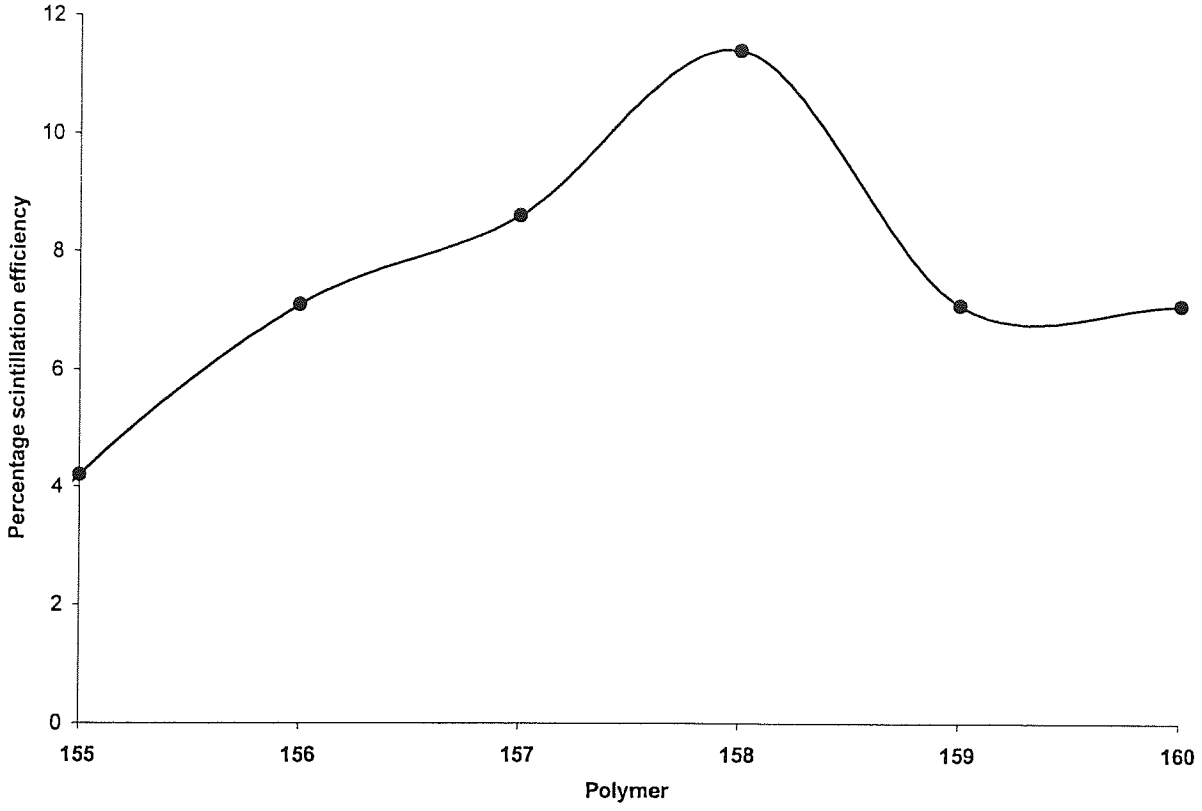

Figure 66. Graph showing the scintillation efficiency of polymers **155-160**. Mean error = $^{+}$/-7%. Scintillation efficiency is expressed as a percentage of the total cpm detected with scintillation fluid. All values have been adjusted to accommodate the fact that a fluor based solely on 2,5-diphenyloxazole **1** gives only 70% of the cpm obtained with a multi-fluor scintillation fluid.[215]

The increase in scintillation efficiency of polymers **155-158** parallels the 1-6 mole percent increase in incorporation of scintillant monomer **101** into the monomer composition. However, increasing the amount of scintillant **101** in the monomer composition from 6 to 8 or 10 mole percent, POP-Sc supports **159** and **160** respectively, results in a reduction in the scintillating efficiency of the supports, which is presumably a consequence of self quenching by the oxazole fluorophore.[248]

POP-Sc support **158**, constructed from a monomer mixture containing 6 mole percent (4'-vinyl)-4-benzyl-2,5-diphenyloxazole **101**, scintillates the most efficiently (11%) of the POP-Sc supports **155-160**.

2.4e SPPS upon POP-Sc Support

The utility of POP-Sc support **158** in SPPS was evaluated by conducting two successive couplings of Fmoc-Gly-OH to the pendant hydroxyl functionality of the support. The experimental loading of POP-Sc support **158** and the efficiency of the second coupling reaction was assessed by employing the Fmoc release assay **Table 6**.[235]

	Loading / mmol g^{-1}	Percentage loading
Theoretical	2.53	-
Coupling 1	0.81 $^{+}$/-8%	32 [a]
Coupling 2	0.79 $^{+}$/-21%	98 [b]

Table 6: Experimentally determined loadings of POP-Sc support **158** after sequential coupling reactions.

[a] The percentage of the functional sites reacted in the first coupling reaction is calculated with respect to the theoretical loading deduced from the monomer composition. [b] The percentage of the functional sites reacted in the second coupling reaction is calculated with respect to the loading calculated for the first coupling reaction.

POP-Sc support **158** modest experimental loading (32%) provides a respectable 0.81 mmol/g of hydroxyl functionality that subsequently may be reacted with excellent efficiency (98%), which suggests that POP-Sc support **158** is well-suited for use as a support for SPPS.

2.5 SPA to Detect and Quantify, in Real-Time, the Kinetic Progress of Solid Phase Organic Chemistry upon Polymer Supports that incorporate Scintillant Covalently

To date the majority of combinatorial libraries have been synthesised upon chemically-functionalised insoluble polymer resins. Solid-phase synthesis frequently requires optimisation from the analogous solution-phase strategy and the most unfavourable reactions are commonly investigated in a separate study. These optimisation studies often monitor the conversion of substrate to product during the time course of the reaction. This is achieved commonly by withdrawing a sample of resin from the reaction mixture at various time intervals. Each aliquot of resin is washed exhaustively, dried to constant mass and then analysed using one or more conventional analytical technique.[249]

Fourier Transform-Infra-Red (IR) and Fourier Transform-Raman spectroscopy are both sensitive, non-destructive, analytical techniques that provide an approximate method for real-time monitoring of solid-phase reactions. In this approach, the intensity of an absorption band, characteristic of either the substrate or product, is monitored during the course of the reaction. This strategy has allowed kinetic studies of solid-phase reactions to be undertaken successfully.[250,251,252,253]

Gel-phase- and Magic Angle Spinning-Nuclear Magnetic Resonance spectroscopy may also be used to determine the structure of a compound tethered to a solid support in a non-destructive manner.[254,255] In addition, the chemical shifts and signal intensities may be used, in a diagnostic manner, to monitor the progress of a chemical reaction upon a solid support.[256]

Mass spectroscopy is an analytical technique that is sufficiently sensitive to provide molecular weight and structural information of a compound cleaved from a single bead (10-100 pmoles).[257] This information may be used to determine the progress of the solid-phase reaction and confirm the molecular structure of the final product.[258]

All of the analytical techniques described above necessitate the removal of a sample of solid support from the assay mixture, which necessarily disturbs the reaction equilibrium. A generically applicable technique that enable both the detection and quantification in real-time of the progress of a reaction in the solid-phase would facilitate our understanding of the thermodynamic and kinetic processes that take place during solid-phase reactions.[259]

A proof of concept study has exemplified the use of the scintillation proximity phenomena to monitor solid-phase reactions upon polymer supports successfully. In this study, chloromethyl-functionalised scintillant-containing resin **121** was derivatised with a suitable linker molecule to provide appropriate chemical functionality for convenient acetylation. Accordingly, resin **121** was treated with a solution of 4-hydroxybenzyl alcohol in the presence of sodium methoxide in DMF to provide polymer resin **164**, **Scheme 43**.

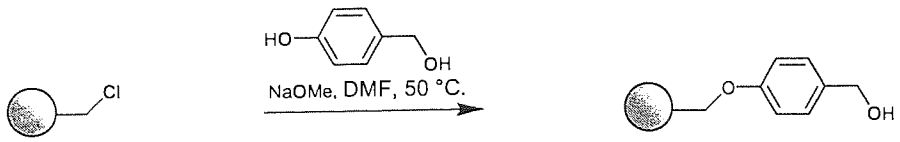

121 164

Scheme 43: Derivatisation of scintillant-containing polymer resin **121** into polymer resin **164**.

The hydroxyl loading of scintillant containing Wang resin **164** was quantified experimentally using the well established Fmoc-coupling/cleavage assay.[235] The results obtained from this study are presented in Table 7 where they are compared with those obtained previously for POP-Sc support **158**.

Polymer	Loading / mmol g^{-1}		Percentage loading [c]
	Theoretical [a]	Experimental [b]	
158	2.53	0.81 +/-8%	32
164	0.96	0.65 +/-3%	68

Table 7: Theoretical and experimental hydroxyl loading values of polymer supports **158** and **164**.
[a] Theoretical loading was calculated from the monomer composition used in the construction of the polymer support. [b] Experimental loading was established using a standard Fmoc-release assay. [c] Percentage loading refers to the experimental loading value with respect to the theoretical loading value.

The theoretical hydroxyl loading of polymer resin **164**, based upon the chloromethyl loading derived from the monomer composition, was calculated to be 0.96 mmol/g. After the Fmoc-Gly-OH coupling reaction, the experimental loading of the Fmoc derived polymer support **164** was observed to be 0.65 mmol/g (68%). This respectable value suggests that a good conversion of resin **121** into scintillant-containing Wang resin **164** had been achieved.

2.5a Acetylation of Polymer Supports

Prior to conducting a proof of concept ester hydrolysis assay, polymer supports **158** and **164** were esterified with [^{3}H]acetic anhydride in the presence of pyridine (Pyr) and a catalytic amount of 4-*N*,*N*-dimethylaminopyridine (DMAP) in DCM to give acetate derived supports **166** and **167** respectively. Similarly, polymer supports **158** and **164** were also acetylated with [^{1}H]acetic anhydride to respectively provide unlabelled polymer supports **168** and **169** as negative controls **Scheme 44**.

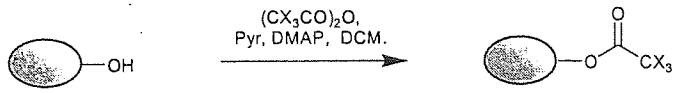

158 or 164 166-169

Scheme 44: Acetylation of polymer supports **158**, **164** with [^{3}H]acetic anhydride (X=^{3}H) and [^{1}H]acetic anhydride (X=^{1}H) to provide **166**, **167** and **168**, **169** respectively.

The acetylated polymer supports **166-169** were washed exhaustively, dried to constant mass and then evaluated for the ability to scintillate spontaneously. Accordingly, polymer supports **158**, **164** and **166-169** were monitored in a scintillation counter. As expected, the blank controls **158** and **164** and the negative controls, polymers **168** and **169**, gave no appreciable scintillation counts. However, polymers **166** and **167** scintillated spontaneously and with high values of cpm/mg of polymer. Commercial scintillation fluid was subsequently added to each scintillation vial. Monitoring the vials in a scintillation counter gave the total number of counts present in each assay system and enabled the scintillation efficiencies of the polymers **166** and **167** to be calculated **Table 8**.

Polymer	Polymer only / cpm mg^{-1}	Polymer + scintillation fluid / cpm mg^{-1}	Percent scintillation efficiency [a]
158	49	53	-
164	15	15	-
166	39550	95413	59
167	12358	24822	71
168	26	40	-
169	4	9	-

Table 8: Scintillation counting of polymer supports **158**, **164** and **166-169**. [a] Mean error = $^+$/-23%. Scintillation efficiency is expressed as a percentage of the total cpm detected with scintillation fluid. All values have been adjusted to accommodate the fact that a fluor based solely on 2,5-diphenyloxazole **1** gives only 70% of the cpm obtained with a multi-fluor scintillation fluid.[215]

The scintillation counting efficiency of 71% obtained for polymer support **167** compared very well with the value of 70% obtained for this support in the previously reported study.[238] The scintillation counting results obtained in Table 8 suggested that scintillant-containing supports would be well suited for use in a SPA to detect and quantify in real-time the thermodynamic and kinetic progress of solid-phase reactions.

2.5b Scintillation Proximity Ester-Hydrolysis Assay

Following the successful synthesis of the [^{3}H]acetylated polymer supports **166** and **167**, it was necessary to determine if the acetate groups could be hydrolysed to regenerate the hydroxyl functionality. Accordingly, [^{3}H]acetate ester derived polymer supports **166-167** and, as a quantitative control reaction [^{1}H]acetylated support **169** were subjected to a hydrolysis reaction by treatment with a solution of potassium hydroxide (0.18 M) dissolved in benzene. In addition, polymer supports **166-167** were treated with an aqueous solution of potassium hydroxide (0.18 M). 18-Crown-6 is known to bind to potassium ions selectively which in benzene has the effect of making KOH an effective base. Accordingly, equal catalytic quantities of 18-crown-6 were added to each assay solution, to enable direct comparisons of results, including the aqueous based-systems. **Scheme 45**.

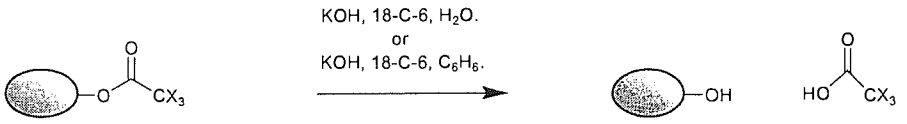

166/167/169

Scheme 45: Hydrolysis of acetate ester derived polymer supports **166**, **167** and **169**.

Prior to investigating the possibility of monitoring the hydrolysis of tritiated-polymer supports **166** and **167** by SPA, a non-radiolabelled study was performed to establish an approximate time period for the hydrolysis reaction to reach equilibrium. Accordingly, polymer **169** was treated with a solution of KOH in benzene. At known time intervals, an aliquot of resin was separated from the supernatant by filtration, washed exhaustively, dried to constant mass and then analysed by IR-spectroscopy.

Bands corresponding to both the characteristic acetate ester carbonyl (~1735 cm^{-1}) and the polystyrene C-H band (~3024 cm^{-1}) were present in the IR-spectra of each resin sample evaluated. As the ester hydrolysis reaction proceeds, a reduction in the intensity absorption of the ~1735 cm^{-1} band would be expected to be observed, whilst the ~3024 cm^{-1} band should remain constant during the course of the reaction. Consequently, the intensity of the absorption of the ~1735 cm^{-1} band relative to the ~3024 cm^{-1} band may be used to calculate the 'absorbance ratio', which quantifies approximately the extent of hydrolysis of [^{1}H]acetate ester from polymer **169 Table 9**.

Time / hr	Band absorbance / % [a]		Absorbance ratio
	~1735 cm^{-1}	~3024 cm^{-1}	~1735 cm^{-1} / ~3024 cm^{-1}
0.0	87.38	87.31	1.00
3.0	76.72	77.99	0.98
11.5	78.48	86.14	0.91
26.0	79.64	83.52	0.95
52.5	76.39	87.01	0.88
72.0	54.46	71.17	0.77

Table 9: IR-spectroscopic analysis of polymer **169** (0.008 g) following hydrolysis with a solution of KOH dissolved in benzene (1 mL, 10 M, 18-crown-6 catalytic amount).

[a] Band absorbance values are background corrected. Mean estimated error = $^{+}$/-1%.

The table shows a general reduction in value of 'absorbance ratio' with increasing time that polymer **169** was incubated with the solution of potassium hydroxide in benzene. This observation is believed to parallel the progressive hydrolysis of ester from polymer **169**.

The analogous scintillation proximity type assay was conducted to detect and quantify, in real-time, the hydrolysis of [^{3}H]acetate ester from scintillant-containing PEG-based polymer support **166** and styrene-based polymer support **167**. Polymers **166** and **167** were treated separately with both a solution of KOH/water/18-C-6 (cat) and KOH/benzene/18-C-6 (cat). These assay mixtures were then monitored in a scintillation counter (Appendix D, Table 46). The number of scintillation counts detected at a specific time for each assay mixture was converted into a percentage of the initial number of scintillation counts detected (0 hr.) (Appendix D, Table 47). These percentage values were plotted versus time for both polymer supports **166** and **167 Figure 67**.

The kinetics of each hydrolysis reaction is first order with respect to both polymer supported [^{3}H]acetate ester and KOH. However, the vast excess of KOH employed in each hydrolysis reaction renders the reaction kinetically pseudo-first-order. Each set of scintillation counting data, represented in Figure 67, fits well with a pseudo-first-order rate equation. For each assay mixture a graph of natural logarithm of (initial percentage scintillation counts/percentage scintillation counts) versus time gives a linear plot, with the gradient of each plot being equal to the pseudo-first-order rate constant (k'). This value quantifies the rate of hydrolysis of [^{3}H]acetate from the polymer support. In addition, the percentage scintillation counts value at a specific time quantifies the extent of the hydrolysis reaction at that time. Both of these parameters are dependent upon the composition of the polymer support, linker group and solvent in which the assay was performed.

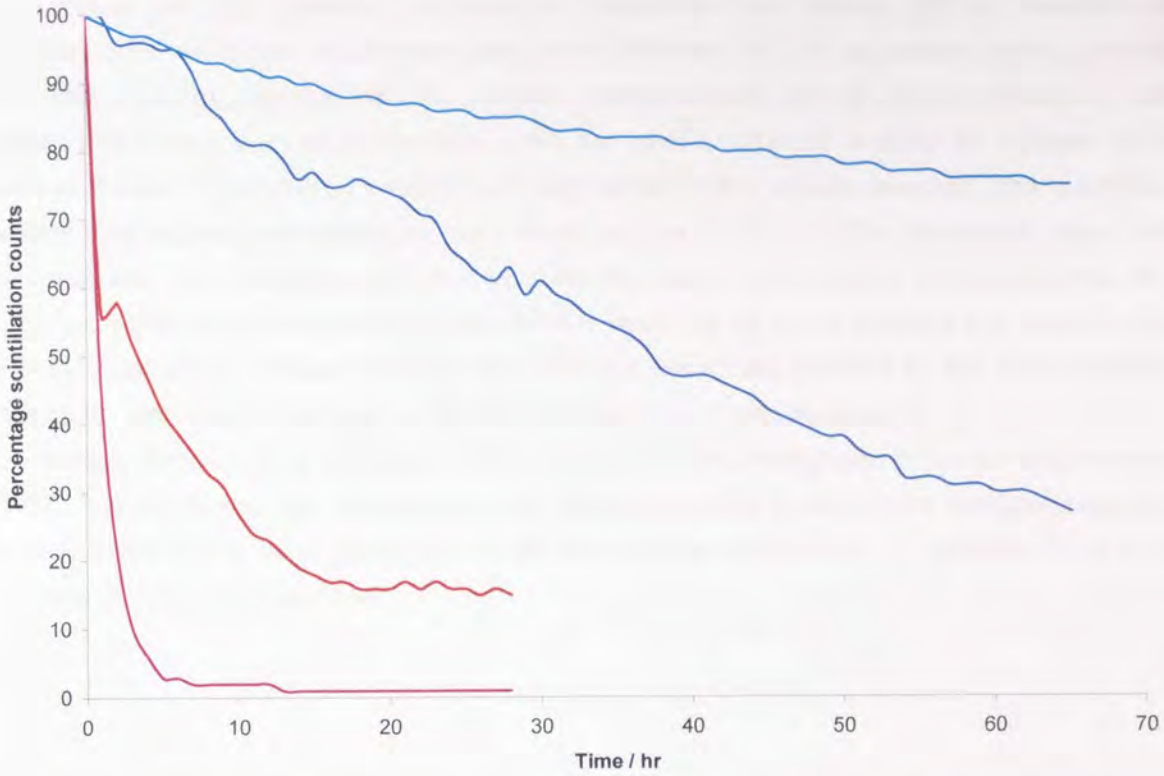

Figure 67: Scintillation counts versus time profiles for assay mixtures **167/KOH/18-C-6/water**, **166/KOH/18-C-6/water**, **166/KOH/18-C-6/benzene** and **167/KOH/18-C-6/benzene**. According to Figure 66, estimated error = $^{+}$/-7%.

The graph shows a concomitant decrease in the number of scintillation counts detected as the tritiated acetate groups are hydrolysed progressively from each polymer support and diffuse into the surrounding solvent.

The significant swelling (Figure 60) and mass-solvent uptake (Figure 64) in toluene of styrene-based polymer supports compared with PEG based supports suggests that KOH/benzene/18-C-6 (cat) will permeate into styrene-based matrices more rapidly than PEG-based matrices. This supposition fits exactly with the observation that hydrolysis of [^{3}H]acetate ester from styrene-based polymer **167** proceeds at a faster initial rate and nearer to completion (k'=0.693 hr.$^{-1}$, 99% @ 28 hr.) than observed for PEG-based support **166** (k'=0.095 hr.$^{-1}$, 85% @ 28 hr.).

In contrast, PEG-based supports in contact with water exhibit greater swelling (Figure 60, 65) and mass-water uptake (Figure 62) compared with styrene-based supports. Once again this observation was found to be in excellent agreement with the greater rate and extent (k'=0.021 hr.$^{-1}$, 37% @ 28 hr.) of hydrolysis in water of PEG-based support **166** compared with styrene based support **167** (k'=0.004 hr.$^{-1}$, 15% @ 28 hr.).

The greater rate and extent of hydrolysis of [^{3}H]acetate from polymer **167** by treatment with KOH/benzene/18-C-6 (cat) solution compared with KOH/water/18-C-6 (cat) solution is fully consistent with what would be expected from the solvation studies because the styrene-based matrix is better solvated by toluene than water. However, when the same comparison is made for polymer **166** the reverse of what is predicted by swelling and mass uptake data is actually observed. The hydrolysis of acetate from polymer **166** proceeded more slowly using a solution of KOH dissolved in water rather than benzene. This anomaly may result from the decreased nucleophilicity of the hydroxide ion in water compared with benzene. In benzene the OH^- anion will be poorly solvated and as such will be strongly nucleophilic whereas in water the hydroxide ion will be solvated by the water molecules through the formation of hydrogen bonds and may thus be a weaker nucleophile.

The findings outlined above constitute the first example of a SPA being used to monitor the progress of SPOC. It is anticipated that, with further study, these chemically-functionalised, scintillant-containing, polymer supports may be of generic use in the detection and quantification, in real-time, of the kinetic progress of solid-phase reactions.

2.6 Scintillation Proximity Hybridisation Assay

A "proof of concept" study was required to evaluate the potential generic application of POP-Sc supports in solid-phase combinatorial synthesis and subsequent *in-situ* SPA to detect and quantify non-covalent interactions between molecules in aqueous media.

It is well known that the majority of deoxyribonucleic acid (DNA) exists in a double helix that comprises of two antiparallel polynucleotide chains. The individual nucleotide monomers each incorporate one of four nitrogenous base molecules: adenine (A), guanine (G), thymine (T) or cytosine (C). These nitrogenous base molecules interact through hydrogen bonding that holds the two polynucleotide chains together in the double helix. In this manner, adenine base pairs with thymine through two hydrogen bonds and guanine base pairs with cytosine through three hydrogen bonds (Figure 38).

Similarly, a polynucleotide chain may successfully hybridise with a PNA-oligomer of complimentary nitrogenous base sequence.[260,261] The resultant PNA-DNA duplex exhibits increased thermal stability (~1 °C/base pair) compared with the corresponding DNA-DNA duplex. This feature facilitates successful PNA-DNA hybridisation assays using oligomers containing fewer nitrogenous base units. In addition, the PNA-oligomer may be constructed using existing SPPS methodology from the corresponding commercial PNA-monomers A, G, T and C.[262] These PNA-monomers commonly have their amino functionality protected with the Fmoc group and any exocyclic amine functionality is usually protected with the benzhydryloxycarbonyl (Bhoc) group **Figure 68**.[263]

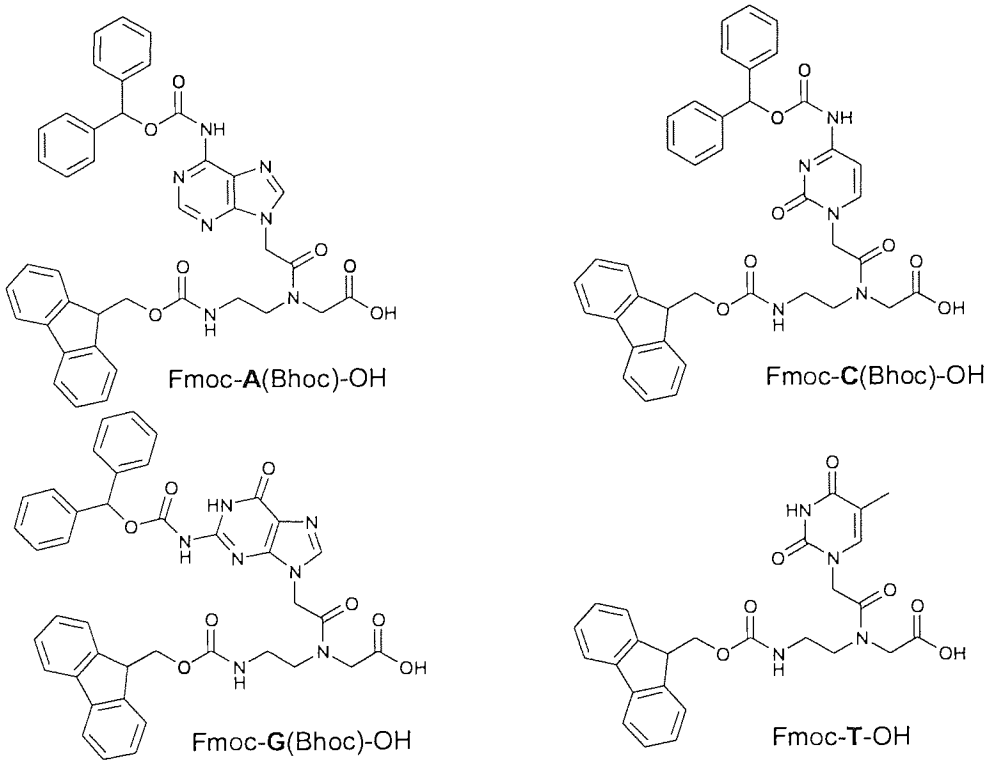

Figure 68: Structure of Fmoc-PNA(Bhoc)-OH monomers.

Having previously established that POP-Sc support **158** is compatible with Fmoc-SPPS, it was decided to utilitlise a POP-Sc support and commercial Fmoc-PNA monomers in the solid-phase synthesis of a PNA-oligomer. This oligomer was to be screened subsequently for hybridisation with complimentary DNA.

2.6a Synthesis of PEG-Based Monomer and Cross-linking Monomer

Before commencing any solid-phase synthesis of PNA-oligomers, it was necessary to construct a POP-Sc support of relatively low hydroxyl loading that is homogeneously distributed through an open polymer matrix. This low functional loading places greater distance between the hydroxyl groups, which inhibits potential inter-molecular interaction between PNA-oligomers that have been synthesised upon the hydroxyl functionality.[264] In addition, the open polymer matrix permits relatively large oligonucleotides to permeate the matrix freely and successfully hybridise with PNA-oligomers of complimentary nitrogenous base sequence.

The hydroxyl loading of a POP-Sc support may be controlled conveniently by incorporating into the monomer mixture a PEG-based monomer, which contains both a polymerisable unit and suitable inert chemical functionality at the terminal of the PEG chain. Styrene was chosen as the desired polymerisable unit for its compatibility with the other monomers **153** and **101**. The methyl ether group was selected as the preferred functionality to terminate the PEG chain for its stability towards the majority of reagents and conditions commonly employed in organic synthesis. Accordingly, α-styryl-poly(oxyethylene glycol)$_{350}$ monomethyl ether **171** was synthesised in two steps from commercial PEG-monomethyl ether$_{350}$, utilising the methodology previously employed to synthesise PEG-based monomers **129**, **130**, **133**, **134** and **153**. Specifically, PEG-monomethyl ether$_{350}$ was reacted with toluenesulfonyl chloride to produce the corresponding tosylate **170** in excellent yield (90%) and purity. This tosylate was subjected to a one-pot hydrolysis and coupling procedure with 4-acetoxystyrene to furnish the desired product **171** (43%) following purification by column chromatography **Scheme 46**.

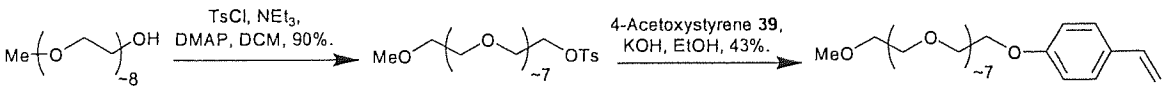

170 **171**

Scheme 46: Synthesis of α-styryl-poly(oxyethylene glycol)$_{350}$ monomethyl ether **171**.

A PEG-based cross-linking monomer that contains the polymerisable styrene unit was also required to enable the construction of a POP-Sc support with an open polymer matrix. It has been previously reported that PEG-based supports cross-linked with PEG$_{1500}$ are permeable to certain enzymes (90 kDa). Therefore, commercial PEG$_{2000}$ was utilised with the methodology previously described for the construction of cross-linking monomers **129** and **130** to provide α,ω-bis-styryl-poly(oxyethylene glycol)$_{2000}$ **173**.

2.6b Construction of POP-Sc Support

The bulk radical co-polymerisation of α-styryl-poly(oxyethylene glycol)$_{350}$ monomethyl ether **171** (87 mole percent), α-styryl-poly(oxyethylene glycol)$_{300}$ **153** (5 mole percent) and (4'-vinyl)-4-benzyl-2,5-diphenyloxazole **101** (6 mole percent) cross-linked with 2 mole percent α,ω-bis-styryl-poly(oxyethylene glycol)$_{2000}$ **173**, proceeded smoothly to provide hydroxyl-functionalised scintillant containing POP-Sc support **174 Scheme 47**.

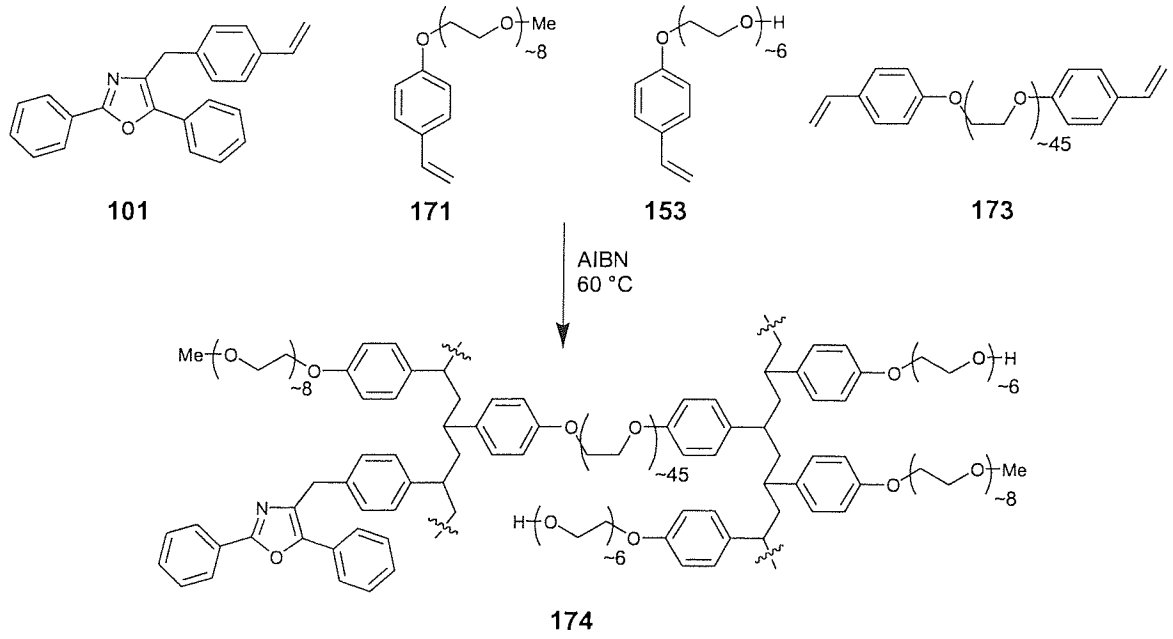

Scheme 47: Co-polymerisation of **101**, **171**, **153** and **173** in the construction of POP-Sc support **174**.

2.6c Solvent Swelling Assay

Following the successful construction of POP-Sc support **174**, it was necessary to determine if the incorporation of α-styryl-poly(oxyethylene glycol)$_{350}$ monomethyl ether **171** and α,ω-bis-styryl-poly(oxyethylene glycol)$_{2000}$ **173** into the monomer mixture had significantly affected the solvent compatibility of POP-Sc support **174**. The polymer support solvent compatibility was evaluated utilising the syringe-based solvent swelling assay. Accordingly, the percentage volume increase of POP-Sc support **174** in DCM, THF, DMF, water and toluene was determined (Appendix B, Table 41) **Figure 69**.

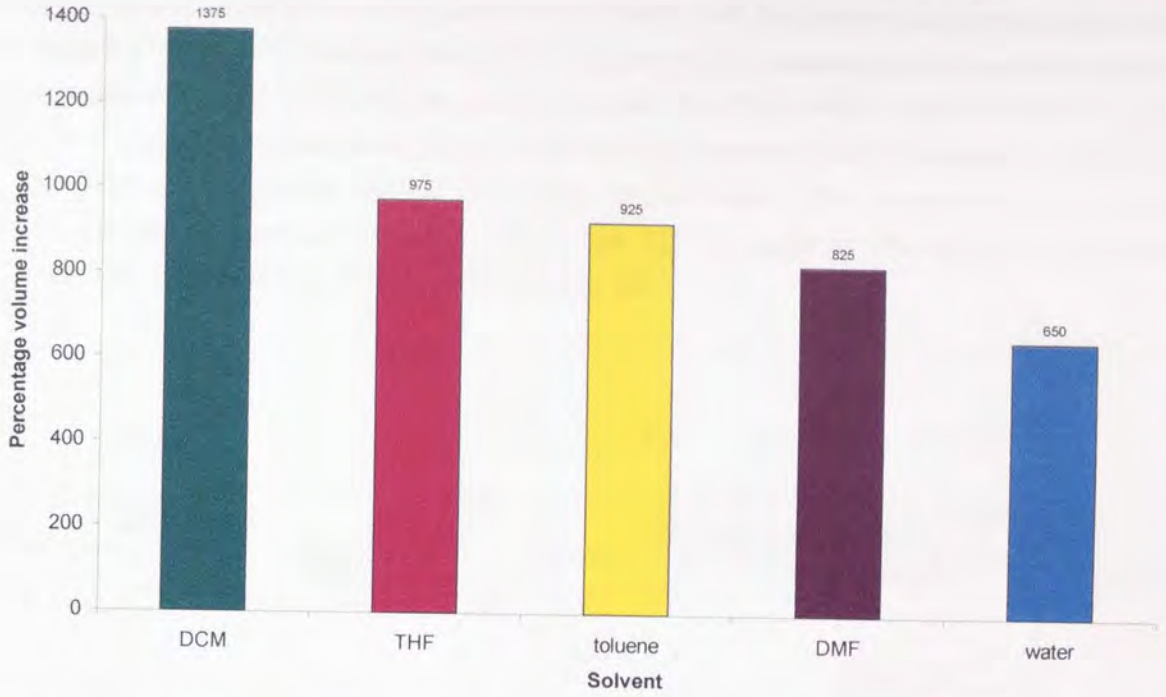

Figure 69: Graph showing the percentage volume increase of POP-Sc support **174** upon contact with **DCM**, **THF**, **toluene**, **DMF** and **water**. Mean error = $^{+}$/-17%.

The data obtained in this manner was used to quantify solvent accessibility into the polymer matrix and also determine solvent compatibility compared with optimal POP-Sc support **158**. POP-Sc support **174** exhibited excellent swelling in water and a range of solvents commonly employed in SPOC. In fact this polymer swells to a greater degree than POP-Sc support **158** in all solvents evaluated in this assay.

2.6d Solid-Phase PNA Synthesis

Having established that POP-Sc support **174** is compatible with both aqueous and organic solvent, it was next necessary to evaluate the utility of this polymer in the solid-phase synthesis of a PNA-oligomer. It was elected to synthesise a PNA-oligomer ten thymine base units in length. The corresponding PNA(T_{10})-DNA(A_{10}) duplex has a calculated melting temperature of approximately 50 °C, which permitted the hybridisation assays to be conducted conveniently at room temperature (RT). In addition, thymine has no exocyclic amine functionality that requires protection with a Bhoc group. At the end of the PNA-oligomer synthesis the Bhoc group is normally removed by treatment with TFA. This final step was deemed undesirable since TFA may also facilitate cleavage of the ester linkage that tethers the PNA-oligomer to the POP-Sc support.

The PNA-oligomer ten thymine base units in length was synthesised successfully upon POP-Sc support **174**. The initial Fmoc-PNA(T)-OH monomer was reacted with MSNT **96** to generate *in-situ* the corresponding activated ester, which subsequently reacted with the hydroxyl functionality within POP-Sc support **174**.[142,265] The resultant Fmoc-PNA(T) derived POP-Sc support had any unreacted hydroxyl functionality capped by treatment with acetic anhydride. The Fmoc-PNA(T) derived POP-Sc support had the Fmoc groups cleaved selectively by treatment with piperidine, prior to coupling the next Fmoc-PNA(T)-OH monomer using PyBOP **91** as the coupling agent. This deprotection and coupling procedure was repeated sequentially to provide the POP-Sc supported PNA-oligomer ten thymine base units in length, POP-Sc-PNA(T_{10}) **175 Scheme 48**.

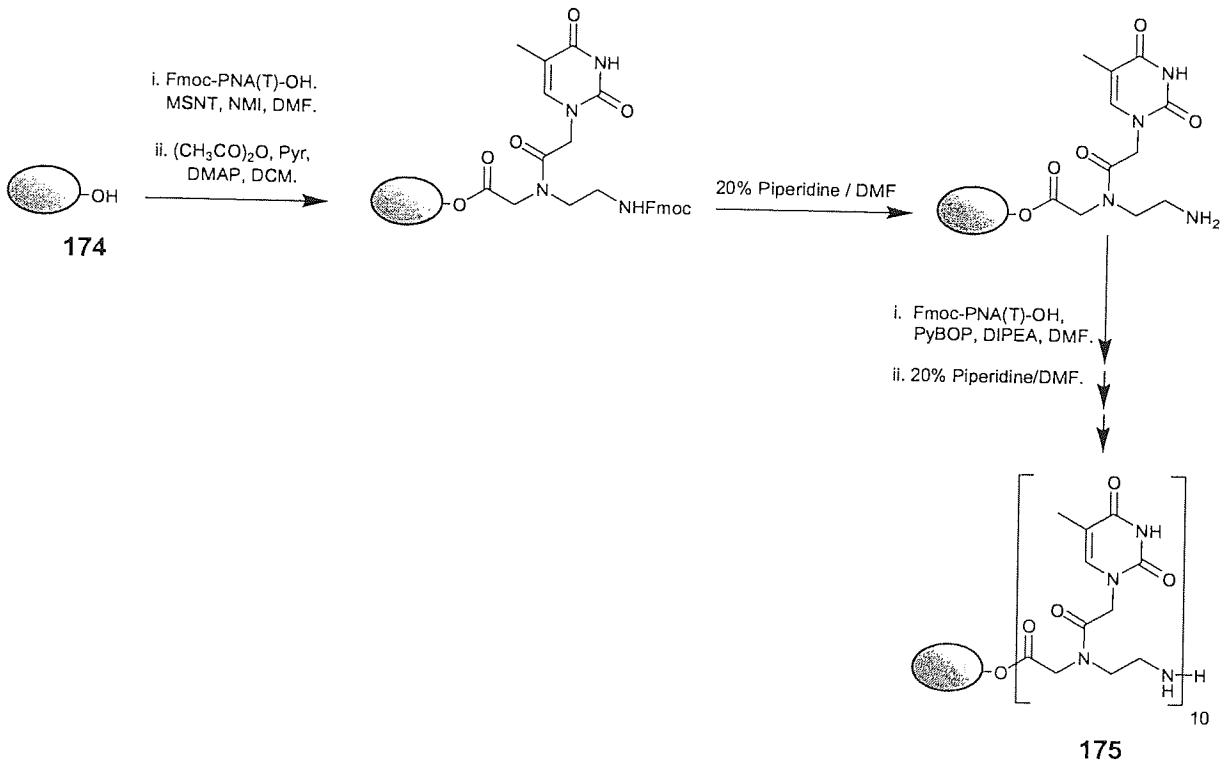

Scheme 48: Synthesis of POP-Sc supported PNA-oligomer ten thymine base units in length **175**.

Following the coupling of each Fmoc-PNA(T)-OH monomer, a standard Fmoc-release assay was employed to determine the experimental hydroxyl loading (Exp) of POP-Sc support **174** and the efficiency of the subsequent Fmoc-PNA(T)-OH coupling reactions **Table 10**.[235]

Coupling	Exp	1[a]	2[b]	3[b]	4[b]	5[b]	6[b]	7[b]	8[b]	9[b]	10[b]
Loading / mmol g^{-1}	0.09	0.03	0.03	0.03	0.03	0.03	0.03	0.03	0.03	0.03	0.03
Percentage efficiency	-	33	100	100	100	100	100	100	100	100	100

Table 10: Fmoc-loading results for ten sequential couplings of Fmoc-PNA(T)-OH to POP-Sc support **174**. Estimated error = $^{+}$/-20%.

[a] The percentage of the functional sites reacted in the first coupling reaction is calculated with respect to the theoretical loading deduced from the monomer composition. [b] The percentage of the functional sites reacted in the coupling reaction is calculated with respect to the loading calculated for the first coupling reaction.

The theoretical hydroxyl loading of POP-Sc support **174**, based upon monomer composition, is calculated to be 0.09 mmol/g. After the first Fmoc-PNA(T)-OH coupling reaction, the experimental loading of the Fmoc derived POP-Sc support was observed to be 0.03 mmol/g (33%) and the efficiency of subsequent Fmoc-PNA(T)-OH coupling reactions were observed to be quantitative.

2.6e Scintillation Proximity Hybridization Assay

Having successfully synthesised POP-Sc-PNA(T_{10}) **175**, it was next necessary to evaluate the ability of this polymer to detect non-covalent interactions in a scintillation proximity type assay. In a proof of concept study, the scintillation proximity phenomena was used to detect and quantify the hybridisation between POP-Sc supported PNA(T_{10}) **175** and the complimentary oligonucleotide ten adenine base units in length that had been radio-labeled with phosphorous-33 (^{33}P-DNA(A_{10})).

The phosphorous-33 emits β^{-}-particles in water that have a mean path length of 126 μm. This path-length in aqueous media successfully discriminates non-proximity effects. The POP-Sc support only detects phosphorous-33 that either binds or is sufficiently close in proximity to the polymer. This should ensure a significant scintillation signal is generated only when the ^{33}P-DNA(A_{10}) successfully hybridises to the PNA(T_{10})-oligomer that is tethered to the POP-Sc support.

Initially, DNA(A_{10}) was radio-labelled at the 5' termini with ^{33}P from [γ-^{33}P]-adenosine 5'-triphoshate (ATP) using the enzyme bacteriophage T4 polynucleotide kinase (PNK).[266] To provide a negative control, an oligonucleotide ten thymine base units in length DNA(T_{10}) was also radiolabelled with ^{33}P and to provide a blank control all the reagents were combined in the absence of oligonucleotide. A standard DE81 assay was conducted to determine the amount of oligonucleotide that had been successfully labeled with phosphorous-33.[267]

The mixtures containing ^{33}P-DNA(A_{10}), ^{33}P-DNA(T_{10}) and blank control were dissolved in 6 x SSPE buffer and then added in duplicate to both POP-Sc-PNA(T_{10}) **175** and POP-Sc **174**. The resultant assay mixtures were monitored in a scintillation counter. The successful hybridisation between the POP-Sc-PNA(T_{10}) **175** and a ^{33}P-DNA-oligomer will bring the radiolabel into close proximity with the POP-Sc support and elicit a significant scintillation signal. The non-specifically bound material and

buffer solution were separated from POP-Sc-PNA$(T)_{10}$ **175** by centrifugation and the polymer was then monitored in a scintillation counter. This washing-counting and centrifugation-counting process was repeated using successive washes of 4 x SSPE, 2 x SSPE and water to progressively reduce the number of non-specific intermolecular interactions. Finally all the polymer supports were individually immersed in scintillation fluid and monitored in the scintillation counter to determine the maximum number of counts obtainable from each assay mixture **Figure 70** (Appendix E Table 48, 49).

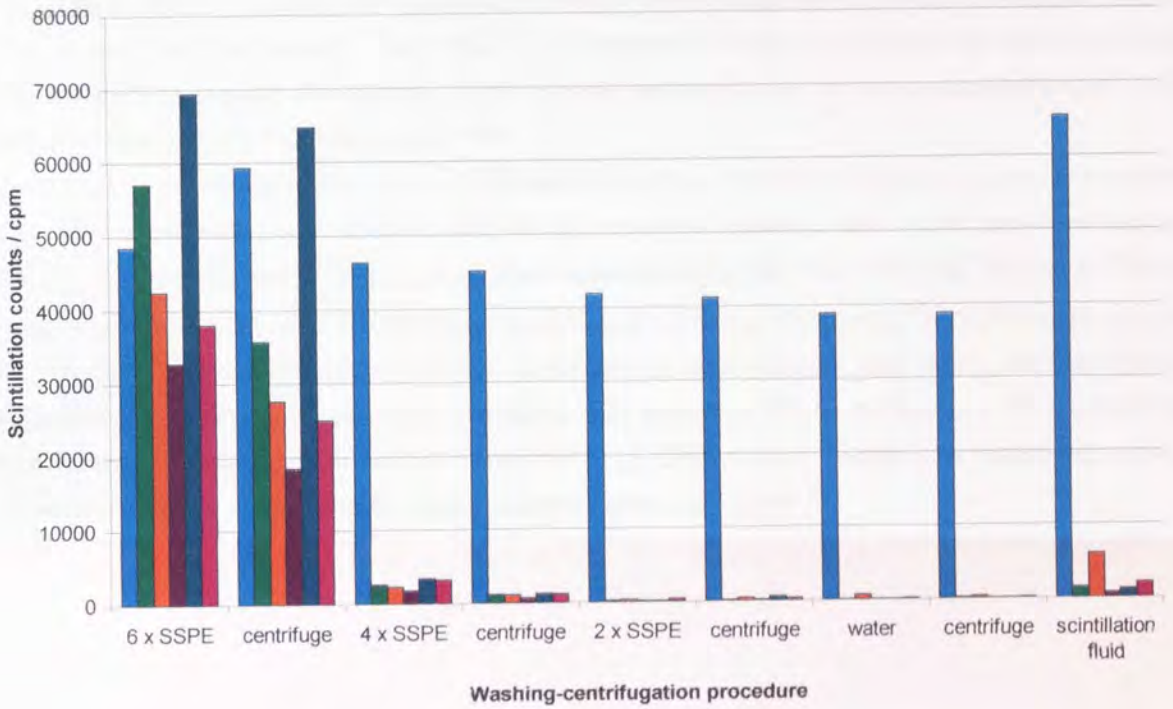

Figure 70 Graph showing the scintillation counts per minute detected for **175 + ^{33}P-DNA(A_{10})**, **175 + ^{33}P-DNA(T_{10})**,[a] **175 + [^{33}P]ATP**, **174 + ^{33}P-DNA(A_{10})**, **174 + ^{33}P-DNA(T_{10})**,[a] **174 + [^{33}P]ATP**. Scintillation counts over 10000 cpm have a mean error = $^{+}$/-10%. All values have been adjusted to accommodate the fact that a fluor based solely on 2,5-diphenyloxazole **1** gives only 70% of the cpm obtained with a multi-fluor scintillation fluid.[215 a] The calculated value has been increased by a factor of 1.6 $^{+}$/-4% to accommodate the fact that DNA(T_{10}) was labelled to a lesser extent than DNA(A_{10}) as determined by the DE81 assay.[267]

These scintillation counting results show that, after extended washing only the assay mixture containing POP-Sc-PNA(T_{10}) **175** and ^{33}P-DNA(A_{10}) generated a significant scintillation signal. The negative and blank controls all produced negligible scintillation counts after the first washing procedure with 4 x SSPE. In fact the excellent signal to noise ratio obtained after one wash increased significantly after two further washing procedures. Most importantly the assay mixture containing POP-Sc-PNA(T_{10})

and ^{33}P-DNA(A_{10}) displayed excellent scintillation counting efficiency (59%) compared with the cpm detected after the addition of scintillation fluid.

2.6f Polynucleotide Kinase-Kinetic Assay

A previous study demonstrated that POP-Sc support **174** exhibits excellent compatibility with aqueous and organic solvents (Figure 69) and that the polymer matrix is permeable to oligonucleotides of ten base units in length (Figure 70). It was next desired to evaluate the compatibility of this support with enzymes in order to evaluate the feasibility of using POP-Sc supports to monitor on-support enzyme assays. In a "proof of concept" kinetic study, an attempt was made to exploit the scintillation proximity phenomenon to quantify the activity of the enzyme bacteriophage T4 polynucleotide kinase (PNK) within the matrix of the POP-Sc support **174**.

Five mixtures containing DNA(A_{10})-6 x SSPE were incubated with POP-Sc-PNA(T_{10}) **175**. The polymer was then separated from unbound material by repeated washing with water and centrifugation procedures. The hybridised DNA(A_{10}) was then radio-labelled at the 5' termini with ^{33}P from [γ-^{33}P]ATP using the enzyme PNK. This was achieved by adding a solution of PNK and [γ^{33}P]ATP to each polymer sample. Each sample was incubated at 37 °C for various time intervals, after which, the polymer was subjected to a washing-centrifugation procedure with water (37 °C) to remove any ^{33}P material that was not covalently attached to the hybridised DNA(A_{10}). Each polymer sample was then monitored in a scintillation counter and the results obtained are presented in **Figure 71**.

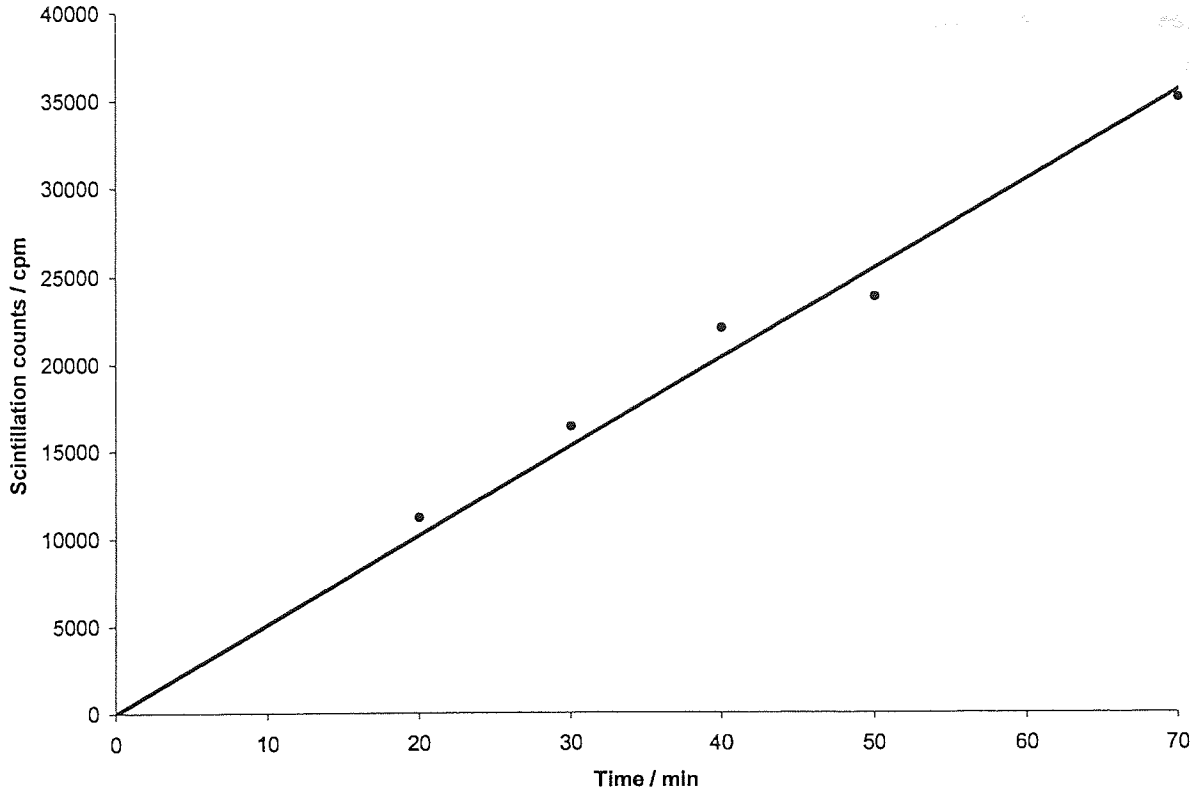

Figure 71: Graph showing the scintillation counts per minute detected following the POP-Sc supported PNA(T_{10}) **175** hybridisation assay with DNA(A_{10}) and subsequent *in-situ* ^{33}P-radiolabelling using PNK with time. Mean error deviation from linear plot = $^{+}$/-7%.
All values have been adjusted to accommodate the fact that a fluor based solely on 2,5-diphenyloxazole **1** gives only 70% of the cpm obtained with a multi-fluor scintillation fluid.[215]

As the graph shows clearly, there is an increase in the number of scintillation counts detected with increasing time. This indicates that the enzyme, PNK (140 kDa),[268] is able to permeate the polymer matrix of the POP-Sc support and carry out the 5' phosphorylation of the hybridised DNA(A_{10}). The real-time *in-situ* nature of this assay provides information about the activity of the PNK within the polymer matrix. In a single negative control experiment POP-Sc(T_{10}) **175** was incubated with DNA(T_{10}) and equal aliquots of both PNK and [γ^{33}P]ATP for seventy minutes. The straight line plot obtained for the *in-situ* phosphorylation reaction enables the rate of on-support phosphorylation to be calculated. By converting cpm to pmoles it is possible to determine the activity of the PNK in terms of pmoles/minute. After seventy minutes the cpm obtained for the DNA labelling experiment was 24656 cpm (Table 32). The cpm obtained after this time for the negative control experiment was 6753 cpm (Table 32). Consequently, the background corrected cpm for the PNK assay after 70 minutes is 17903 cpm. The POP-Sc support **174** was observed to scintillate with 41% efficiency (Appendix E, Table 49). Consequently, the efficiency corrected cpm for the PNK assay after 70 minutes is 43666 cpm. Since

the activity of the [γ^{33}P]ATP used in the experiment was 4519431 cpm per pmole. After 70 minutes, 9.6618×10^{-3} pmoles of ^{33}P had been incorporated into the POP-Sc support corresponding to a rate of 1.38×10^{-4} pmoles/min.

2.7 Scintillation Proximity Hybridisation Assay of a POP-Sc-PNA-Library

Previously, it has been established that POP-Sc support **174** is well suited for use in solid-phase PNA synthesis utilising standard Fmoc chemistry procedures and can be used to detect and quantify non-covalent interactions in a scintillation proximity hybridisation assay. In an extension of this work, it was decided to utilise a POP-Sc polymer to support the synthesis of a PNA combinatorial library and subsequently to screen this library using a scintillation proximity hybridisation assay with a DNA oligonucleotide of known sequence with the same number of nitrogenous bases, which has been labelled with a suitable radioisotope. In this model study, the sequence of the DNA was chosen to be a known compliment of one of the library molecules to be synthesised.

2.7a Synthesis of PEG-Based Monomer

Despite the successful synthesis and hybridisation assay of PNA(T_{10}) upon POP-Sc support **174**, it was deemed necessary to replace the hydroxyl functionality of the polymer support. These hydroxyl groups had been utilised previously to attach the initial Fmoc-PNA monomer to the support covalently via an ester linkage. An ester linkage of this type is potentially susceptible to cleavage by monoketopiperazine formation upon removal of the Fmoc group after attachment of the first Fmoc-PNA-monomer. In addition, the penultimate step of the synthesis involves treatment with TFA to remove any Bhoc protecting groups. It was thought that exposure to TFA in this step may have resulted in cleavage of the PNA-oligomer from the polymer support.

Before commencing the synthesis of the PNA-library, it was decided to construct an analogous polymer to POP-support **174** that had the hydroxyl functionality replaced with amine functionality. The initial Fmoc-PNA-monomer would then be attached via an amide linkage, which is far less susceptible to cleavage under the reaction conditions employed in the PNA-library synthesis.

To enable the construction of a polymer support with a controlled amine loading that is homogeneously distributed through the polymer matrix, a PEG-based amine functionalised monomer was required. Accordingly, the intermediate monomer α-styryl-poly(oxyethylene glycol)$_{350}$ phthalimide **177** was synthesised in two steps from α-styryl-poly(ethylene glycol)$_{300}$ **153** that had been synthesised previously. Specifically, α-styryl-poly(ethylene glycol)$_{300}$ **153** was reacted with a solution of toluenesulfonyl chloride, triethylamine and catalytic amount of DMAP in DCM to furnish the desired tosylate product **176** (93%). Purification of tosylate **176** was achieved by a facile washing procedure and subsequent employment of a nucleophilic scavenger resin (Polymer Laboratories PL-EDA (ethylenediamine) MP-resin 0.85 g, >3.3 mmol/g)). Tosylate **176** was then subjected to a Gabriel type synthesis by reaction with potassium phthalimide in wet DMF to provide pure α-styryl-poly(oxyethylene glycol)$_{350}$ phthalimide **177** (76%). Again purification of the phthalimide **177** was accomplished by a simple washing procedure **Scheme 49**.

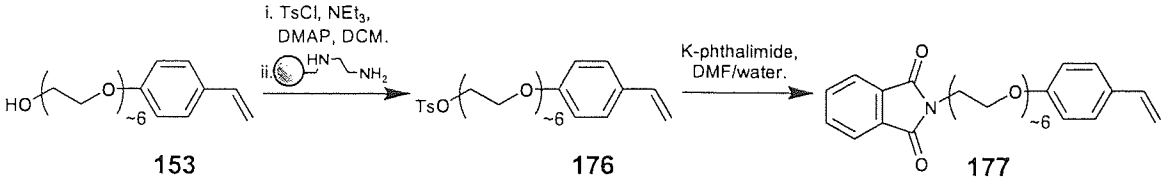

Scheme 49: Synthesis of PEG-based phthalimide monomer **177**.

Unfortunately although hydrazinolysis of the phthalimido group to the corresponding amine was successful it was accompanied by reaction of the double bond of the styrene moiety presumably by reduction under the vigorous reaction conditions employed (excess NH_2NH_2, EtOH, 80 °C). The disappearance of the styrenic double bond was evidenced by the disappearance of the signals corresponding to the terminal olefin in the ^1H NMR spectra of the crude product. With the, perhaps not unexpected, failure of the hydrazinolysis step in the presence of the styrenic double bond it was decided to form the polymeric support from phthalimide **177** and subsequently carry out a post-polymerisation hydrazinolysis step.

2.7b Construction of POP-Sc Support

The monomers α-styryl-poly(oxyethylene glycol)$_{350}$ phthalimide **177** (6 mole percent), α-styryl-poly(oxyethylene glycol)$_{350}$ monomethyl ether **171** (86 mole percent), (4'-vinyl)-4-benzyl-2,5-diphenyloxazole **101** (6 mole percent) cross-linked with α,ω-bis-styryl-poly(oxyethylene glycol)$_{2000}$ **173** (2 mole percent), were combined with the free radical initiator AIBN 7. Thermally initiated bulk polymerisation of this mixture proceeded smoothly to produce the phthalimide-functionalised, scintillant-containing, POP-Sc support **178 Scheme 50**.

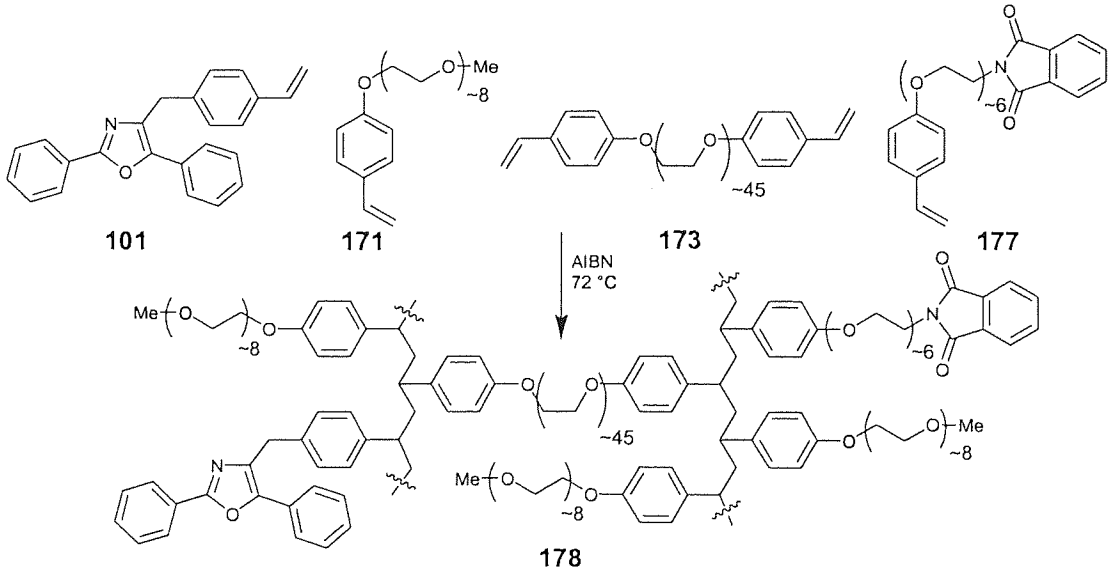

Scheme 50: Co-polymerisation of **101**, **171**, **173** and **177** in the construction of POP-Sc support **178**.

2.7c Hydrazinolysis of POP-Sc Support

Following the successful construction of POP-Sc support **178**, it was necessary to determine if the phthalimide groups could be converted into amine functionality. Accordingly, POP-Sc support **178** was subjected to hydrazinolysis by treatment with a solution of hydrazine hydrate in dioxane. Gratifyingly, this post-polymerisation hydrazinolysis reaction worked extremely well and the desired amine functionalised PEG-based support **179** was formed in quantitative yield **Scheme 51**. The efficiency of the reaction was analysed by IR-spectroscopy which showed the complete disappearance of the imide C=O signal and the appearance of a strong new NH_2 stretch.

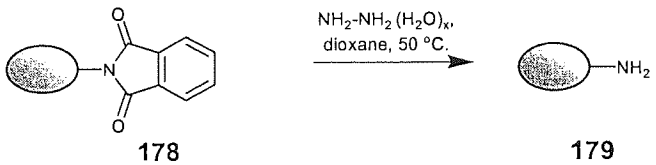

178 **179**

Scheme 51: Synthesis of amine functionalised PEG-based support **179**.

2.7d Solvent Swelling Assay

Following the successful construction of POP-Sc support **179**, it was necessary to determine if the substitution of the hydroxyl with amine functionality had significantly affected the solvent compatibility of POP-Sc support **179**. The solvent compatibility of the new support was evaluated utilising the syringe-based solvent swelling assay. Accordingly, the percentage volume increase of POP-Sc support **179** in DCM, THF, DMF, water and toluene was determined **Figure 72** (Appendix B, Table 42).

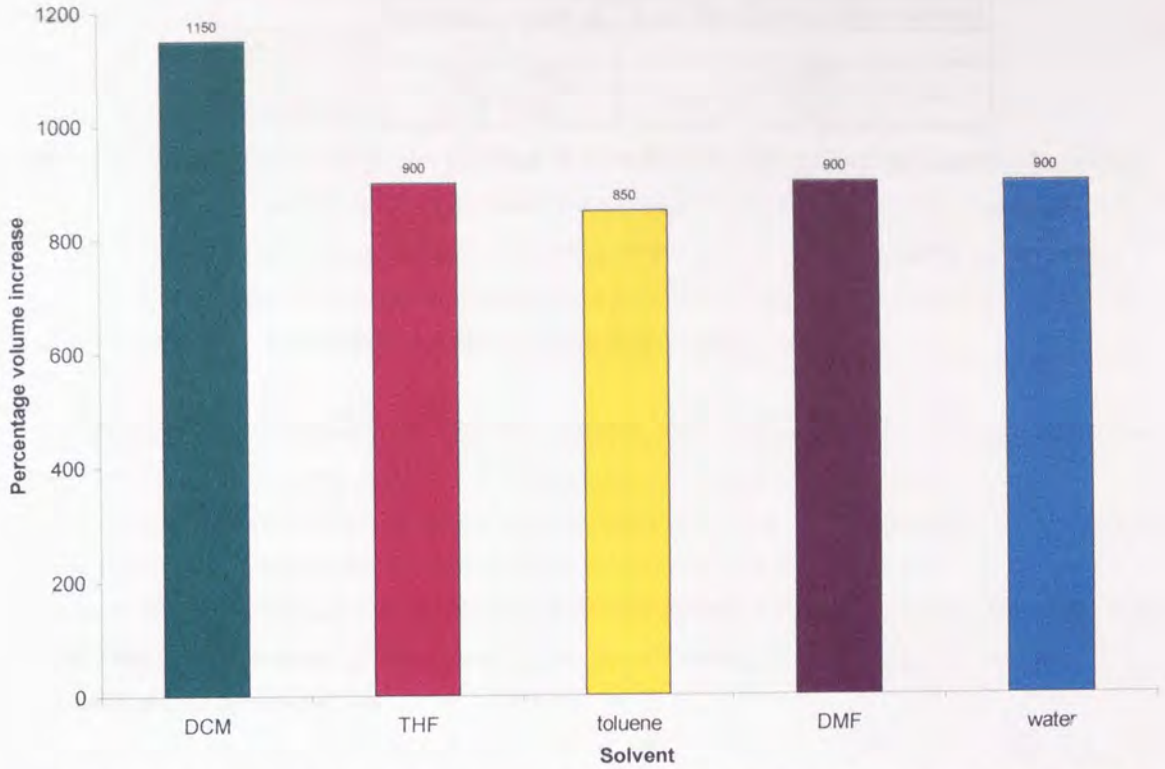

Figure 72: Graph showing the percentage volume increase of POP-Sc **179** upon contact with **DCM**, **THF**, **toluene**, **DMF** and **water**. Mean error = $^{+}$/-47%.

The swelling data obtained in this manner demonstrated that the amine functionalised POP-Sc support **179** swells significantly and to a similar extent as the analogous hydroxyl-functionalised POP-Sc support **174** in all the solvents evaluated. In addition, evaluation of POP-Sc support **179** in a variety of solvents provides percentage volume increase values that are more uniform in value, which suggests it may perform well in multi-step syntheses employing a variety of solvents.

2.7e Experimental Amine Loading of POP-Sc Support

Having established that POP-Sc support **179** is compatible with both aqueous and organic solvents, it was next necessary to evaluate the utility of this amine functionalised polymer **179** in solid-phase synthesis. Accordingly, two successive couplings of Fmoc-Gly-OH to the pendant amine functionality of the support were undertaken. As in previous work the experimental loading of POP-Sc support **179** and the efficiency of the second coupling reaction was assessed by employing the Fmoc release assay **Table 11**.[235]

	Loading / mmol g^{-1}	% of functional sites reacted
Theoretical	0.11...	-
Coupling 1	0.13 $^{+}$/-3%	126[a]
Coupling 2	0.13 $^{+}$/-3%	100[b]

Table 11: Experimentally determined loadings of POP-Sc **179** after sequential coupling reactions.

[a] The percentage of the functional sites reacted in the first coupling reaction is calculated with respect to the theoretical loading deduced from the monomer composition. [b] The percentage of the functional sites reacted in the second coupling reaction is calculated with respect to the loading calculated for the first coupling reaction.

The theoretical amine loading of POP-Sc support **179**, based upon monomer composition, is calculated to be 0.11 mmol/g. After the first Fmoc-Gly-OH coupling reaction, the experimental loading of the Fmoc derived POP-Sc support **180** was observed to be 0.13 mmol/g (126%). This value suggests the more favourable polymerisation of monomer **177** than one or more of the other monomers **101**, **171**, **173** used in the construction POP-Sc **178**. The excellent efficiency (100%) of the second Fmoc-Gly-OH coupling reaction suggests that POP-Sc **179** is well-suited for use as a support in the solid-phase synthesis.

2.7f Solid Phase PNA-Library Synthesis

Having previously established the exceptional compatibility of POP-Sc support **174** in both solid-phase PNA synthesis and subsequent scintillation proximity hybridisation assay, the utility of amino-functionalised polymer support **179** in the solid-phase synthesis of a PNA-combinatorial library was evaluated. It was elected to construct a library of PNA-oligomers each of which was to be nine nitrogenous base units in length, which comprises a three codon sequence. This library of 64 PNA-oligomers was constructed successfully from the four commercial Fmoc-PNA monomers using well established SPPS techniques. Accordingly, 64 POP-Sc-support **179** samples were accurately weighed into a parallel array (A1-H8) of separate reaction vessels. The Fmoc-PNA-OH monomers were reacted with PyBOP **91** to generate the corresponding activated ester *in-situ*, which was added to the appropriate POP-Sc sample.[142] Any un-reacted amine functionality on the resultant Fmoc-PNA derived POP-Sc support was capped by subsequent treatment with acetic anhydride. This coupling/capping procedure was followed by the selective cleavage of the Fmoc group by treatment with piperidine. The coupling and deprotection procedure was repeated using the appropriate PNA-monomers in succession to provide the 64 member three codon PNA-library shown in Table 12. As a blank control, three POP-Sc support **179** samples that were not subjected to any PNA coupling procedures were included in the array I1-I3 **Table 12**.

	1	2	3	4	5	6	7	8
A	$A_3A_3A_3$	$A_3G_3A_3$	$T_3A_3A_3$	$T_3G_3A_3$	$G_3A_3A_3$	$G_3G_3A_3$	$C_3A_3A_3$	$C_3G_3A_3$
B	$A_3A_3T_3$	$A_3G_3T_3$	$T_3A_3T_3$	$T_3G_3T_3$	$G_3A_3T_3$	$G_3G_3T_3$	$C_3A_3T_3$	$C_3G_3T_3$
C	$A_3A_3G_3$	$A_3G_3G_3$	$T_3A_3G_3$	$T_3G_3G_3$	$G_3A_3G_3$	$G_3G_3G_3$	$C_3A_3G_3$	$C_3G_3G_3$
D	$A_3A_3C_3$	$A_3G_3C_3$	$T_3A_3C_3$	$T_3G_3C_3$	$G_3A_3C_3$	$G_3G_3C_3$	$C_3A_3C_3$	$C_3G_3C_3$
E	$A_3T_3A_3$	$A_3C_3A_3$	$T_3T_3A_3$	$T_3C_3A_3$	$G_3T_3A_3$	$G_3C_3A_3$	$C_3T_3A_3$	$C_3C_3A_3$
F	$A_3T_3T_3$	$A_3C_3T_3$	$T_3T_3T_3$	$T_3C_3T_3$	$G_3T_3T_3$	$G_3C_3T_3$	$C_3T_3T_3$	$C_3C_3T_3$
G	$A_3T_3G_3$	$A_3C_3G_3$	$T_3T_3G_3$	$T_3C_3G_3$	$G_3T_3G_3$	$G_3C_3G_3$	$C_3T_3G_3$	$C_3C_3G_3$
H	$A_3T_3C_3$	$A_3C_3C_3$	$T_3T_3C_3$	$T_3C_3C_3$	$G_3T_3C_3$	$G_3C_3C_3$	$C_3T_3C_3$	$C_3C_3C_3$
I	Blank	Blank	Blank					

Table 12: POP-Sc supported PNA-ninemer (three codon) library.

2.7g Scintillation Proximity Hybridisation Assay of a POP-Sc-PNA-Library

Having synthesised a combinatorial PNA-library, it was then necessary to screen the library for the ability to hybridise with a DNA oligonucleotide that had a nitrogenous base sequence which was fully complimentary to a single library member. Accordingly, the scintillation proximity phenomena was used to detect and quantify the non-covalent interactions between the PNA-library members and a DNA oligonucleotide nine adenine base units in length, which had been radio-labeled with phosphorous-33 (^{33}P-DNA(A_9)) in a manner similar to that previously described for ^{33}P-DNA(A_{10}).

Equal aliquots of ^{33}P-DNA(A_9), dissolved in 6 x SSPE buffer, was added to the POP-Sc supported PNA library. The non-specifically bound material was separated from the POP-Sc supported library by centrifugation and the library was then monitored in a scintillation counter (Appendix F, Table 50). This was followed by a washing-centrifugation-counting procedure using successive washes of 4 x SSPE (Appendix F, Table 51), 2 x SSPE (Appendix F, Table 52) and water (Appendix F, Table 53). However, the scintillation counting results obtained showed that the majority of the library members including the negative control, POP-Sc-PNA(A_9), generated significant scintillation signals (Appendix F, Table 50-53). An attempt was made to disrupt these non-specific hybridisation interactions by employing a more vigorous washing procedure. Accordingly, aliquots of water were added to the PNA-library which was successively incubated at 25 °C (Appendix F, Table 54), 30 °C (Appendix F, Table 55) and 40 °C (Appendix F, Table 56), to disrupt PNA-DNA interactions with melting temperatures below 40 °C. A subsequent scintillation counting procedure showed that this modified washing procedure failed to reduce the number of non-specific interactions. It was thought possible that the polymer matrix was binding the ^{33}P-DNA(A_9) or [γ^{33}P]ATP non-specifically. It is well known that formamide may disrupt non-specific nitrogenous base interactions.[269] Accordingly, the PNA-library was washed three times with 50% formamide/2 x SSPE buffer and then the library was again monitored in a scintillation counter (Appendix F, Table 57-59) **Figure 73**.

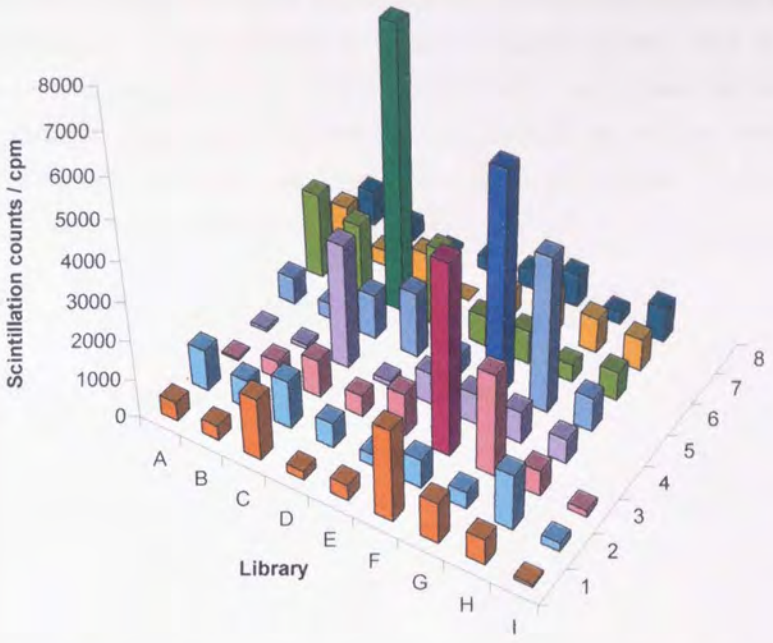

Figure 73: Graph showing the number of scintillation counts per minute detected for the POP-Sc supported PNA-library hybridisation assay with ^{33}P-DNA(A_9). Mean error = $^{+}$/-9%.
All values have been adjusted to accommodate the fact that a fluor based solely on 2,5-diphenyloxazole **1** gives only 70% of the cpm obtained with a multi-fluor scintillation fluid.[215]

The formamide washing procedure reduced the number of non-specific interactions significantly. Unfortunately, despite a significant scintillation signal being observed for POP-Sc-PNA(T_9) (4871 cpm, column F3), a greater number of scintillation counts were produced by POP-Sc-PNA($G_3T_3T_3$) (5646 cpm, column F5) and POP-Sc-PNA(G_9) (7164 cpm, column C6). In fact, the 6 library members that exhibit the greatest number of cpm all contain only thymine and guanine nitrogenous bases.
It is well known that PNA oligomers that are rich in purine, especially guanine, have a tendency to aggregate and have low solubility in aqueous solutions.[262] Aggregate formation of this type may have led to the non-specific adsorption of ^{33}P-radiolabeled material.

2.7h Scintillation Signal Dependence upon the Position and Number of Codon Mismatches

Following the evaluation of all the scintillation counting data obtained from screening the POP-Sc-PNA-library against ^{33}P-DNA(A_9), it was decided to utilise a subset of this data to investigate the dependence of the number and position of complimentary codon pairs upon the ability of the PNA-oligomer and ^{33}P-DNA(A_9) to hybridise. Accordingly, the counts per minute obtained, when ^{33}P-DNA(A_9) was incubated with POP-Sc supported PNA codon sequences $T_3T_3T_3$, $A_3T_3T_3$, $T_3T_3A_3$, $T_3A_3T_3$, $A_3A_3T_3$, $T_3A_3A_3$ and $A_3A_3A_3$ were plotted **Figure 74**.

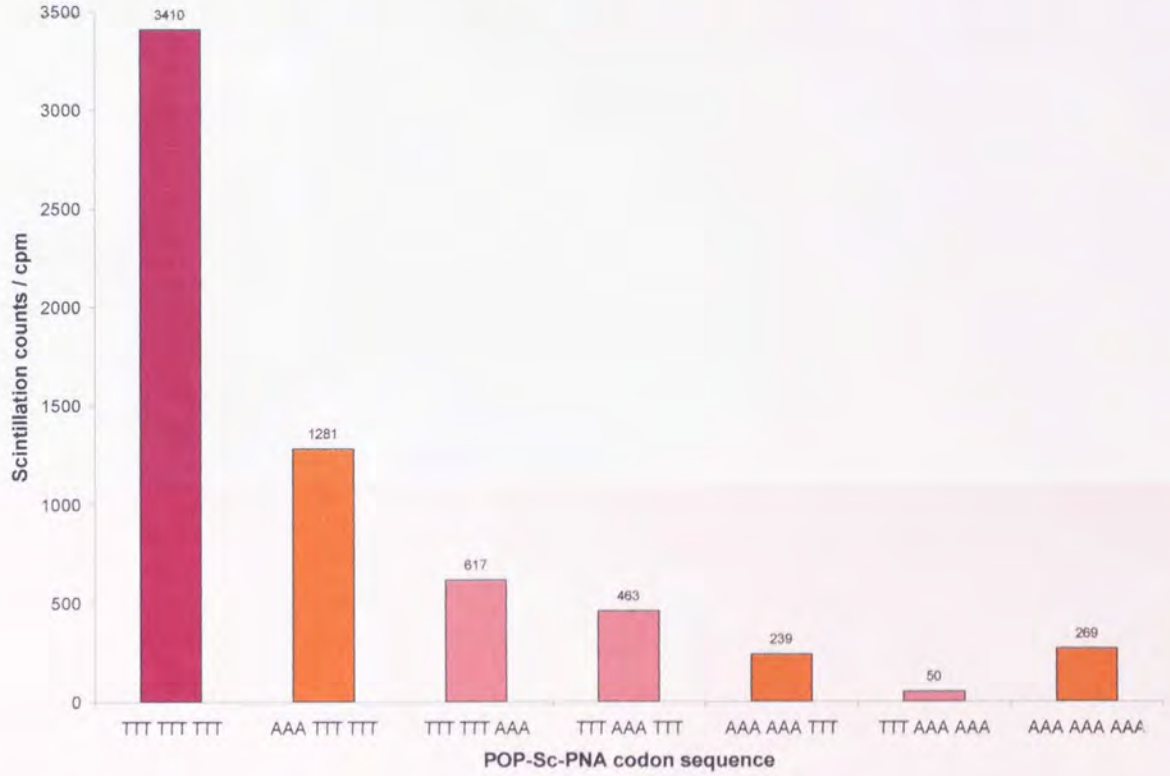

Figure 74: Graph showing the scintillation counts per minute detected for the hybridisation assay of ^{33}P-DNA(A_9) with POP-Sc-PNA codon sequences $T_3T_3T_3$, $A_3T_3T_3$, $T_3T_3A_3$, $T_3A_3T_3$, $A_3A_3T_3$, $T_3A_3A_3$ and $A_3A_3A_3$. Mean error = $^{+}$/-9%.
All values have been adjusted to accommodate the fact that a fluor based solely on 2,5-diphenyloxazole **1** gives only 70% of the cpm obtained with a multi-fluor scintillation fluid.[215]

This graph shows clearly, that for codons involving T and A only, the fully complementary PNA codon sequence $T_3T_3T_3$ exhibits the greatest scintillation signal. The substitution of a single thymine codon (T_3) with a non-complimentary adenine codon (A_3) resulted in a significant reduction in the scintillation

counts detected. Further, it may be deduced that substitution of the codon in the centre of the PNA sequence results in the greatest disruption of hybridisation, followed by the 5' end of the PNA whilst the codon closest to the polymer support causes the least disruption of hybridisation.

The scintillation data obtained with the PNA-oligomers containing two adenine codons and one thymine codon have been included for completeness. However, the insignificant hybridisation between these PNA-oligomers and ^{33}P-DNA(A_9) at room temperature in each case provides only very low number of scintillation counts that can not be interpreted with confidence. Similarly, as expected, the negative control POP-Sc-PNA(A_9) also produced very low levels of scintillation.

2.7i Scintillation Proximity Hybridisation Assay with Nitrogenous Base Mismatch

Having determined that a non-complementary codon in the second position of the PNA-ninemer causes the greatest disruption to PNA-DNA hybridisation, it was elected to utilise the SPA to investigate the effect that a one and two base mismatch in the central codon has upon the extent of hybridisation. Accordingly, two further POP-Sc supported PNA-oligomers of nitrogenous base sequence T_4AT_4 and $T_4A_2T_3$ were synthesised and subsequently subjected to the scintillation proximity hybridisation assay with ^{33}P-DNA(A_9), in identical fashion to that described previously for the POP-Sc-PNA-library **Figure 75** (Appendix F, Table 60).

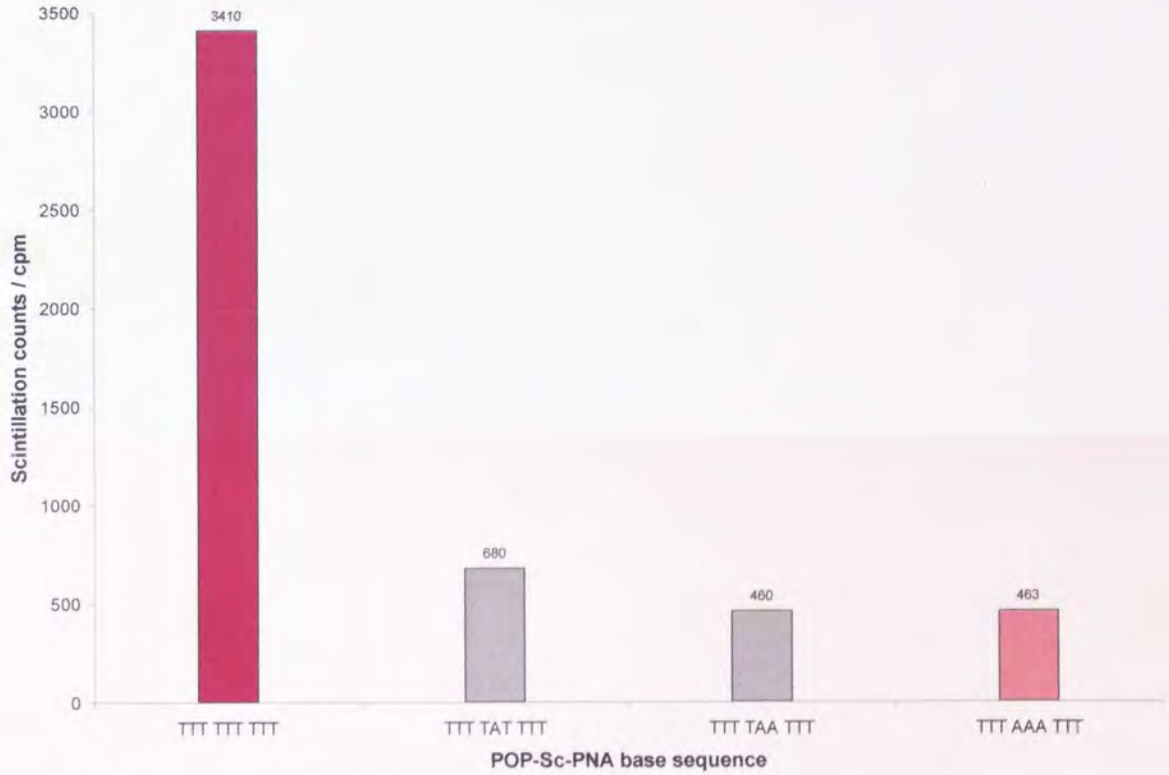

Figure 75: Graph showing the number of scintillation counts per minute detected in the hybridisation assay of ^{33}P-DNA(A_9) with POP-Sc-PNA sequences T_9, T_4AT_4, $T_4A_2T_3$ and $T_3A_3T_3$. Mean error = $^{+}$/-9%. All values have been adjusted to accommodate the fact that a fluor based solely on 2,5-diphenyloxazole **1** gives only 70% of the cpm obtained with a multi-fluor scintillation fluid.[215]

The graph in Figure 75 shows clearly that substitution of the central thymine base unit in POP-Sc-PNA(T_9) with an adenine base unit, POP-Sc-PNA(T_4AT_4), results in a significant reduction in the number of scintillation counts obtained. However, substitution of a second thymine base unit, POP-Sc-

PNA ($T_4A_2T_3$), and third thymine base unit, POP-Sc-PNA($T_3A_3T_3$), causes only a slight reduction in scintillation counts compared with the scintillation counts observed with POP-Sc-PNA (T_4AT_4). The extent of this reduction is insufficiently great to be able to differentiate between one, two and three base mismatches in the central codon of POP-Sc-PNA (T_9).

Chapter 3

Conclusion

3.1 Cell-Based Scintillation Proximity Assay

The series of 4-functionalised-2,5-diphenyloxazole compounds were synthesised efficiently. 2,5-diphenyloxazole-4-carboxaldehyde **100** was synthesised by 4-lithiation of commercial 2,5-diphenyloxazole **1** followed by reaction with DMF. 2,5-Diphenyloxazole-4-carboxaldehyde **100** was readily converted into the synthetically useful 2,5-diphenyl-4-hydroxymethyloxazole **102** and subsequently into 4-bromomethyl-2,5-diphenyloxazole **103**. These 4-functionalised-2,5-diphenyloxazole molecules **100-103** and ethyl-2,5-diphenyl-4-oxazolecarboxylate **105**, were converted, via one or multi-step syntheses into scintillant-tagged compounds **104**, **106-119** successfully.

Evaluation of these "scintilipid" compounds by Sense Proteomic Ltd for the ability to scintillate in the presence of ionising radiation was successful. The scintillation efficiency of each scintilipid, in the presence of ionising radiation, was found to be dependent upon the type of chemical functionality attached at the 4-position of the oxazole ring. In previous work an ether linkage had been used to attach a substituent at the 4-position of the oxazole ring, which provided compounds that exhibited very high scintillation counting efficiency in the presence of ionising radiation. The ether linkage was readily accessed via either scintillant alcohol **102** or scintillant bromide **103**. Accordingly, scintillant-tagged compounds, **109-119**, were all constructed successfully with one ether linkage between the 4-position of the oxazole tag and the remainder of the molecule. These scintillant-tagged-compounds **109-119**, were found to scintillate with varying efficiencies, but all were of greater efficiency than the other scintillant-tagged-compounds evaluated.

Sense Proteomic incorporated each "scintilipid" into liposomal preparations. These liposomal preparations were found to have varying scintillation efficiencies in the presence of ionising radiation. These ability to scintillate did not necessarily replicate the scintillation efficiency observed for the scintilipid alone. In addition, microscopic examination of the liposomal preparations identified crystalline regions of scintilipid within the "scintiliposomes" of many liposomal preparations. The propensity to form crystalline regions of scintilipid in the scintiliposome was not observed to be related to the structure of the scintilipid.

The scintiliposome that incorporated scintilipid **119** exhibited optimal properties. Sense Proteomic fused scintiliposome **119** with the membrane of living HeLa cells and subsequently used these "scinticells" in a cell-based scintillation proximity assay to detect and quantify the uptake of [^{14}C]methionine *in-vitro* successfully.[217] This novel, cell-based scintillation proximity assay is anticipated to find application in high throughput screening for studying protein function and activity *in vitro*.

3.2 Scintillation Proximity Assay in Combinatorial Chemistry

The preparation of aqueous compatible polymer supports that incorporate scintillant covalently and their subsequent use in scintillation proximity assays has been exceptionally successful.

Initially, chemically-functionalised monomers, α-styryl-oligo(oxyethylene glycols) **133**, **134**, **153**, **171**, **177** and cross-linking monomers, α,ω-bis-styryl-oligo(oxyethylene glycols) **129**, **130**, **173** were synthesised successfully. Commercial PEG samples were reacted with toluene sulfonyl chloride followed by a one-pot hydrolysis and subsequent *in-situ* coupling reaction with 4-acetoxystyrene to provide the desired PEG-based monomers in good yields and purities.

Styrene, DVB, α-styryl-oligo(oxyethylene glycol) **133**, **134** and α,ω-bis-styryl-oligo(oxyethylene glycol) **129**, **130** were co-polymerised in varying molar ratios to provide polymer supports **135-142**.

PEG-based POP-supports **140-142** swelled significantly in a range of organic solvents, of widely differing polarities, and water. In addition, POP-supports **140-142** imbibed a mass of solvent that generally consolidated the observed percentage volume increase values observed. POP-supports **140-142** were subjected to two sequential peptide coupling reactions and were shown to have respectable experimental loadings and coupling efficiencies.

A range of hydroxyl-functionalised poly(oxyethylene glycol)-based polymeric supports that incorporate varying mole percentage of (4'-vinyl)-4-benzyl-2,5-diphenyloxazole **101** were synthesised successfully to provide POP-Sc supports **155-160**. Each POP-Sc support, **155-160**, exhibited significant swelling in water and a range of organic solvents of widely differing polarity. An increase in the mole percent of scintillant monomer **101** in the POP-Sc support monomer composition resulted in a slight reduction in the percentage volume increase of the support when brought into contact with polar solvent (DMF, DCM, THF, water) and an increase in swelling when the POP-Sc support was brought into contact with non-polar solvent (toluene). A non-proximity scintillation assay established POP-Sc support **158** to have the highest scintillation efficiency (11%), upon exposure to ionising radiation, of all the POP-Sc supports **155-160** evaluated. POP-Sc support **158** was found to have a modest experimental loading (32%) but this still provides a respectable 0.81 mmol/g of hydroxyl functionality that subsequently was reacted with excellent efficiency (98%).

The scintillation proximity phenomenon was used successfully to detect and quantify in real-time the thermodynamic and kinetic progress of the hydrolysis of [^{3}H]acetate ester from scintillant-containing polymer supports **166** and **167**. Initially, Wang resin **164** and POP-Sc support **158** were esterified with [^{3}H]acetic anhydride to give [^{3}H]acetate derived supports **166** and **167** respectively. These [^{3}H]acetylated polymer supports **166** and **167** scintillated spontaneously and with high efficiency. Polymers **166** and **167** were treated separately with both a solution of KOH/water/18-C-6 (cat) and KOH/benzene/18-C-6 (cat) and each solution monitored, in real time, in a scintillation counter. A

concomitant decrease in the number of scintillation counts was detected as the tritiated acetate groups were hydrolysed progressively from the polymer support and diffused into the surrounding solvent.

The application of POP-Sc support **174** in solid-phase combinatorial synthesis and subsequent *in-situ* SPA to detect and quantify non-covalent interactions between molecules in aqueous media also proved successful. A PNA-oligomer ten thymine base units in length was synthesised upon POP-Sc support **174** successfully. The experimentally determined hydroxyl loading of POP-Sc support **174** was observed to be 0.03 mmol/g (33%) and the efficiency of the nine subsequent Fmoc-PNA(T)-OH coupling reactions were observed to be quantitative. The scintillation proximity phenomena was used to detect and quantify the hybridisation between the POP-Sc supported PNA oligomer ten thymine base units in length **175** and complimentary DNA ten adenine base units in length with 59% efficiency. Moreover a signal (complimentary DNA) : noise (uncomplimentary DNA) ratio was found to be in the order of 200 :1

The scintillation proximity phenomenon was also used to establish the biocompatibility of POP-Sc support **174** and quantify successfully the activity of the enzyme bacteriophage T4 polynucleotide kinase (PNK) within the matrix of the POP-Sc support **174**. The enzyme was found to both permeate and function within the matrix of POP-Sc support **174** to effect the 5' phosphorylation of DNA that was hybridised to the complimentary PNA of **175**.

A novel amine functionalised POP-Sc support **179** was also constructed, that swelled significantly in all the solvents evaluated, The amine loading of POP-Sc support **179** and the efficiency of the second Fmoc-Gly-OH coupling reaction were both found to be quantitative. Using support **179**, a 64 member PNA-combinatorial library nine nitrogenous base units in length was synthesised successfully. The PNA-library was screened for the ability to hybridise with ^{33}P-DNA(A_9). A significant scintillation signal was observed for the fully complimentary immobilised PNA sequence POP-Sc-PNA(T_9). However, a greater number of scintillation counts were observed by POP-Sc-PNA($G_3T_3T_3$) and POP-Sc-PNA(G_9). These unexpected scintillation signals may be a consequence of the aggregation of guanine residues within the polymer matrix, which may have led to the non-specific adsorption of ^{33}P-radiolabeled material.

A subset of this scintillation counting data was used to assess the dependence of the number and position of complimentary codon pairs upon the ability of the PNA-oligomer and ^{33}P-DNA(A_9) to hybridise. A significant reduction in the number of scintillation counts was detected when a single thymine codon was substituted with a non-complimentary adenine codon. Further, it was deduced that substitution of a non-complementary codon in the second position of the PNA-oligomer that was nine base units in length caused the greatest disruption to PNA-DNA hybridisation, followed by the 5' end of the PNA whilst the codon closest to the polymer support caused the least disruption of hybridisation.

In addition, it was determined that substitution of the central thymine base in POP-Sc-PNA (T_9) with an adenine base unit (T_4AT_4) resulted in significant reduction in the number of scintillation counts obtained. However substitution of a second ($T_4A_2T_3$) and third thymine base with an adenine base ($T_3A_3T_3$) caused only a slight reduction in scintillation counts compared with the scintillation counts observed with POP-Sc-PNA (T_4AT_4).

It is anticipated that these aqueous and organic compatible, scintillant-containing POP-Sc supports may have potential application in the solid-phase synthesis of combinatorial libraries and subsequent *in-situ* screening of these libraries against biological targets of interest using the scintillation proximity phenomena. This synthesis and screening strategy has significant advantages over other synthesis/screening strategies and has the potential to identify lead compounds against novel drug targets.

Chapter 4

Experimental

4.1 General Information

All reactions involving moisture-sensitive reagents were conducted in oven dried (120 °C) glassware. Dichloromethane (DCM), and triethylamine (TEA) were distilled from calcium hydride. Tri(ethylene glycol), Hexa(ethylene glycol), poly(oxyethylene glycol)$_{300}$, poly(oxyethylene glycol)$_{400}$, poly(oxyethylene glycol)$_{350}$ monomethyl ether and poly(oxyethylene glycol)$_{2000}$ were heated at 120 °C under high vacuum for 1 h. All other reagents were used as received from Aldrich or Lancaster. ArgoGel resin (0.47 mmol/g) was purchased from Aldrich, Merrifield's resin 2% DVB (100-200 mesh, 0.89 mmol/g) and TentaGel resin (0.27 mmol/g) were purchased from Novabiochem. Radiolabelled chemicals were obtained from Amersham International plc or Sigma-Aldrich and the Optiphase 'Highsafe' 2 liquid scintillation cocktail from Wallac Scintillation Products (Fisher chemicals). DNA sequences were purchased form MWG-Biotech AG. T4 polynucleotide kinase enzyme and buffer were purchased from Promega. An aqueous solution of PVA refers to a 1% wt/wt aqueous solution of poly(vinyl alcohol) (87-89% hydrolysed, average M_W 85,000–146,000). A 20 x SSPE solution refers to NaCl (175.3 g), $NaH_2PO_4.2H_2O$ (31.2 g), EDTA disodium salt (7.4 g) dissolved in water (994 mL) and NaOH (6 mL, 10 M) with gentle heating, which had the final pH adjusted to 7.4 with NaOH.

All reaction mixtures were stirred magnetically and conducted under an atmosphere of nitrogen unless otherwise stated. Where appropriate, reactions were monitored by thin layer chromatography using Merck silica gel 60 F_{254} precoated glass plates, which were visualized with uv light and then developed using either iodine, a solution of 10% phosphomolybdic acid in ethanol, or an aqueous solution of potassium permanganate. Flash column chromatography was carried out using Fluka silica gel 60 (0.035-0.070 μm, 220-440 mesh). The micro-scale suspension polymerisation reactions (described in General Procedure 4) were carried out using a Radleys Discovery Technologies Ltd. Carousel Reaction Station. The mass-solvent uptake assays (described in General Procedure 6) were performed using a conventional microbalance. ^{1}H NMR and ^{13}C NMR spectra were recorded on a Brucker AC300 spectrometer. Deuterated chloroform ($CDCl_3$) and deuterated dimethyl sulfoxide (d_6-DMSO) were used as the solvents and chemical shift values (δ) are reported in parts per million relative to the residual signals of these solvents (δ 7.24 and δ2.54 for ^{1}H and δ 77.0 and δ40.45 for ^{13}C respectively). Coupling constants are reported in Hertz. ^{13}C NMR spectra were recorded using the PENDANT program.[270] Low-resolution mass spectra were recorded using a Finnigan LCQ ion-trap spectrometer using atmospheric pressure chemical ionisation (APCI). High-resolution mass spectra were recorded by Mr Peter Ashton (School of Chemistry, Birmingham University) using a Micromass LCT mass spectrometer in the electrospray mode using a mobile phase of methanol (200 μL/min) and lock mass to correct the mass scale. Elemental analyses were performed by Medac Ltd., Brunel Science Centre, Cooper's Hill Lane, Engelfield Green, Egham, Surrey, UK. Infra-red spectra were recorded on a Perkin Elmer Paragon 1000 FT-IR spectrometer as a either a thin film or a gel pressed between two sodium chloride plates or as a solid suspended in a potassium bromide disk. Scintillation counting was conducted using a Canberra Packard 1600TR liquid scintillation analyser.

4.2 General Procedures

General procedure 1: Suspension polymerisation

Monomers were combined and stirred at room temperature (15 min). AIBN was added to the monomer mixture and stirring continued (10 min). This monomer mixture was added to a stirred aqueous solution of 1% PVA (700 mL) under a nitrogen atmosphere and the resultant suspension stirred (30 min). The temperature was increased (72 °C) and stirring continued (4 hrs). The mixture was cooled to room temperature and the polymeric product poured into a sieve (38 μm). The beaded polymeric product was washed with copious amounts of water until the effluent became clear. The beaded polymer was transferred to a sintered funnel and washed with distilled water (2 x 500 mL), MeOH (500 mL), MeOH/THF 1:1 (500 mL), THF (500 mL), MeOH/THF 1:1 (500 mL) and MeOH (500 mL). The polymer was dried under suction and then transferred to a soxhlet thimble and extracted with dioxane over night. The polymer was transferred to a sintered funnel and washed with MeOH/THF 1:1 (500 mL) and MeOH (500 mL). The beaded product was dried under reduced pressure to constant mass (80 °C, 4 hrs). The dry polymer was transferred to a sieve shaker and shaken over night to provide polymer beads in the range: [250–150 μm], [75–38 μm], [<38 μm].

General procedure 2: Fmoc-Gly-OH coupling to hydroxyl functionalised polymer supports

2,6-Dichlorobenzoyl chloride, pyridine and Fmoc-Gly-OH in DMF were added to the polymer and the resultant mixture stirred overnight. The polymer was collected by filtration and washed *in-situ* with DCM (30 mL), DCM/MeOH 1:1 (30 mL) and MeOH (30 mL) in triplicate. The Fmoc-Gly-OH derived polymer was pre-dried under suction before being dried to constant mass.

General procedure 3: Fmoc release assay

A sample of Fmoc-Gly derived polymer (1-2 mg) was weighed accurately into a sample vial. A 20% solution of piperidine in DMF (3.00 mL) was added to the vial and the resultant suspension agitated using a Pasteur pipette. The suspension in the vial was filtered through a plug of cotton wool into a quartz cuvette. The absorption at 290 nm of the 1-fluoren-9-ylmethylpiperidine adduct was measured against a 20% piperidine/DMF blank. The above protocol was repeated 4 times for each polymer sample and the average absorbance per mg of each sample calculated. The loading (mmol/g) of each polymer was determined by dividing the average absorbance per mg at 290 nm by 1.65.[235]

Each assay mixture absorbance with respect to the average absorbance was determined as a percentage, which were averaged to provide the mean error. Alternatively for a single assay, it was assumed absorption and mass are accurate to 0.01 units and 0.001 g respectively that gives an error of 0.006mmol/g, which was calculated as a percentage of the experimental loading of the polymer support.

General procedure 4: Micro-scale suspension polymerisation

Monomers were combined and stirred at room temperature (15 min). AIBN was added to the monomer mixture and stirring continued (10 min). This monomer mixture (~1.0–1.5 mL) was added to a stirred aqueous solution of 1% PVA (10 mL) under a nitrogen atmosphere and the resultant suspension stirred for 30 min. The temperature was increased to 72 °C and stirring continued for a further 4 hr. The mixture was cooled to room temperature, and the polymeric product collected by filtration. The beaded polymeric product was washed with distilled water (3 x 50 mL), MeOH (50 mL), MeOH/THF 1/1 (50 mL), THF (50 mL) and MeOH (50 mL), and was then dried to constant mass.

General procedure 5: Bulk polymerisation

The monomers and AIBN were placed into a glass vial (1.5 mL). The vial was held in an ultra-sound bath for 2 min. Nitrogen gas was bubbled through the monomer mixture for 5 min and the vial was then placed in an oven at 60 °C overnight. The resulting polymer gel was removed from the vial and broken into small irregular shaped particles (~1 mm in diameter) using a spatula, washed with THF (30 mL), MeOH/THF 1:1 (30 mL) and MeOH (30 mL) in triplicate and dried to constant mass.

General procedure 6: Mass-solvent uptake assay

The polymer (25 mg) was packed into the bottom of a polypropylene disposable syringe (1 mL), with the tip removed, housing a nylon frit (0.45 μm). The syringe was suspended from a microbalance and the balance reading set at zero. A reservoir containing solvent was placed below the syringe and the reservoir raised until the solvent was just brought into contact with the bottom of the syringe. A mass reading was recorded. When the solvent was water, the surface tension of the water (72.3 mN/m) was lowered below that of the plastic syringe and frit assembly by addition of TWEEN 20 (1% v/v). For each solvent studied, a blank control assay was carried out. This procedure was identical in every respect to that described above except that no polymer sample was placed in the syringe. This procedure allowed for the 'wetting' of the syringe/frit assembly by the solvent to be taken into account. The mass readings have an estimated error of $^{+}$/-0.05 g.

General Procedure 7: Acetylation of Fmoc-derived polymer supports

A solution of acetic anhydride, DMAP and pyridine in DCM was added to the polymer support, and the resultant mixture was incubated for 2 hours. The polymer was collected by centrifugation and washed *in-situ* twice with DCM (3 mL), DCM/MeOH 1:1 (3 mL), MeOH (3 mL). The polymer was placed in a vacuum oven at 35 °C and dried to constant mass.

General Procedure 8: Solvent swelling assay

The readings of initial and final volume both have an estimated error of $^{+}$/-0.005 mL.

4.3 Synthesis of 4-Functionalised-2,5-Diphenyloxazole Molecules

2,5-Diphenyloxazole-4-carboxaldehyde 100

sec-Butylithium (1.3 M, 57.4 mL, 75 mmol) was added drop-wise, over 30 minutes, to a solution of 2,5-diphenyloxazole **1** (15.000 g, 67.8 mmol) and 2,2,6,6-tetramethylpiperidine (TMP) (1.1 mL, 6.8 mmol) in tetrahydrofuran (THF) (80 mL), which was cooled (-78 °C) and stirred. The reaction mixture was allowed to warm to 0 °C and DMF (5.2 mL, 67.8 mmol) was added to the reaction mixture which was stirred whilst warming to room temperature over-night. A saturated ammonium chloride aqueous solution was added to the reaction mixture. The organic portion was separated from the aqueous portion, dried over anhydrous magnesium sulfate and concentrated under reduced pressure to give an orange gum (22.840 g). The gum was triturated with diethyl ether to give a white solid. The white solid was collected by filtration, washed with cold diethyl ether and dried to constant mass to give 2,5-diphenyloxazole-4-carboxaldehyde **100** (5.480 g, 33%). IR (KBr disc): ν_{max}/cm^{-1} 3053 (w, C-H aromatic), 2827 (w, C-H aliphatic), 1700 (s, C=O), 1654 (m), 1646 (m), 1636 (m), 1617 (w), 1577 (w), 1560 (s, C=C aromatic), 1542 (s, C=C aromatic), 1508 (w), 1490 (s), 1458 (m), 1447 (m) 1399 (w), 1300 (w), 1212 (m), 1178 (w), 1150 (w), 1070 (m), 1022 (m), 923 (w), 848 (w), 784 (s), 711 (s) and 697 (s). ^{1}H NMR (300 MHz, $CDCl_3$): δ_H 7.49-7.55 (6H, m), 8.13-8.16 (4H, m) and 10.16 (1H, s). ^{13}C NMR (75 MHz, $CDCl_3$, PENDANT)[270]: δ_C 126.8 (CH), 127.7 (CH), 128.9 (CH), 129.0 (CH), 131.2 (CH), 131.3 (CH), 185.1 (CH, carbonyl), remaining quaternary carbon signals too small to be resolved. LRMS (APCI): *m/z* 250 (100%, $[M + H]^+$), ($C_{16}H_{11}NO_2$ requires M^+ 249).

2,5–Diphenyl-4-hydroxymethyloxazole 102

Sodium borohydride (0.490 g, 12.9 mmol) was added, in portions, to a solution of 2,5-diphenyloxazole-4-carboxaldehyde **100** (0.800 g, 3.2 mmol) in methanol (30 mL). The reaction mixture was then stirred at room temperature overnight. Water (50 mL) was added to the reaction mixture and concentrated under reduced pressure to remove the methanol. The resulting slurry was extracted with ethyl acetate (3 x 50 mL). The combined organic extracts were washed with brine (50 mL), dried over anhydrous magnesium sulfate and concentrated under reduced pressure to give 2,5–diphenyl-4-hydroxymethyloxazole **102** (0.800 g, 99%) as a white solid. IR (KBr disc): ν_{max}/cm^{-1} 3244 (s, O-H), 2927 (m, C-H aliphatic), 2874 (m, C-H aliphatic), 1734 (w), 1718 (w), 1700 (w), 1684 (w), 1653 (w), 1636 (w), 1594 (m, C=C aromatic), 1558 (m, C=C aromatic), 1548 (s, C=C aromatic), 1488 (s), 1446 (s), 1374 (w), 1351 (w), 1324 (w), 1285 (w), 1195 (w), 1183 (w), 1129 (w), 1096 (w), 1070 (m), 1041 (m), 1026 (s), 1008 (s), 953 (m), 925 (w), 837 (m), 778 (s), 761 (s), 724 (m) and 705 (s). ^{1}H NMR (300 MHz, d_6-DMSO): δ_H 4.61 (2H, d, *J*=5.3), 5.39 (1H, t, *J*=5.3), 7.38-7.55 (6H, m), 7.84 (2H, d, *J*=7.3) and 8.06 (2H, dd, *J*=7.1 7.9). ^{13}C NMR (75 MHz, d_6-DMSO, PENDANT)[270]: δ_C 55.8 (CH_2), 125.7 (CH), 125.8 (CH), 126.7 (C), 127.8 (C), 128.4 (CH), 128.9 (CH), 129.0 (CH), 130.5 (CH), 137.3 (C), 146.8 (C) and 158.5 (C). LRMS (APCI): *m/z* 252 (19%, $[M + H]^+$) ($C_{16}H_{13}O_2N$ requires M^+ 251), 234 (100%).

4-Bromomethyl-2,5-diphenyloxazole 103

Phosphorus tribromide (0.66 mL, 7.0 mmol) was added to a solution of 2,5–diphenyl-4-hydroxymethyloxazole **102** (5.000 g, 19.9 mmol) in DCM (30 mL) and the resultant mixture stirred overnight. Water (20 mL) was added to the reaction mixture and the organic phase separated. The aqueous phase was extracted with DCM (3 x 20 mL). The combined organic extracts were washed with saturated sodium chloride solution (2 x 20 mL), dried over anhydrous magnesium sulfate and concentrated under reduced pressure to give 4-bromomethyl-2,5-diphenyloxazole **103** (6.130 g, 98%) as a white solid. IR (KBr disc): ν_{max}/cm^{-1} 3087 (w, C-H aromatic), 3060 (w, C-H aromatic), 3016 (m, C-H aliphatic), 2980 (m, C-H aliphatic), 2927 (m, C-H), 2874 (w, C-H), 1592 (m, C=C aromatic), 1552 (m, C=C aromatic), 1486 (s), 1446 (s), 1320 (w), 1269 (w), 1212 (s), 1151 (w), 1107 (m), 1089 (m), 1069 (m), 1024 (m) , 908 (m), 832 (w), 771 (s), 701 (s, C-Br), 886 (s, C-Br) and 667 (s). ^{1}H NMR (300 MHz, $CDCl_3$): δ_H 4.66 (2H, s), 7.41-7.54 (6H, m), 7.76 (2H, d, *J*=8.7) and 8.09 (2H, dd, *J*=8.3 11.5). ^{13}C NMR (75 MHz, $CDCl_3$, PENDANT)[270]: δ_C 25.5 (CH_2), 126.2 (CH), 126.5 (CH), 126.9 (C), 127.7 (C), 128.8 (CH), 129.0 (CH), 129.1 (CH), 130.7 (CH), 133.6 (C), 147.7 (C), remaining quaternary carbon signal too small to be resolved; LRMS (APCI): *m/z* 314 (100%, $[M + H]^+$) ($C_{16}H_{12}ON^{79}Br$ requires M^+ 313), 316 (71%, $[M + H]^+$) ($C_{16}H_{12}ON^{81}Br$ requires M^+ 315).

2,5-Diphenyl-oxazol-4-ylmethyl-triethyl-ammonium bromide 104

Triethylamine (2.2 mL, 15.9 mmol) was added to a solution of the 4-bromomethyl-2,5-diphenyloxazole **103** (0.500 g, 1.59 mmol) in acetone (50 mL) and the resultant solution was stirred at room temperature (5 hours). The resultant precipitate was collected by filtration, washed *in-situ* with acetone (2 x 10 mL) and subsequently dried *in vacuo* to give scintilipid **104** (0.490 g, 66%). IR (KBr disc): ν_{max}/cm^{-1} 3495 (s, N-H), 3360 (s, N-H), 3056 (m, C-H aromatic), 2974 (m, C-H aliphatic), 2942 (m, C-H aliphatic), 1653 (m, C=C aromatic), 1558 (m, C=C aromatic), 1484 (s), 1474 (s), 1448 (m), 1392 (m), 1374 (m), 1328 (w), 1273 (w), 1156 (m), 1097 (m), 1076 (m), 1003 (m), 941 (w), 900 (w), 797 (s), 784 (s), 717 (s), 704 (m) and 669 (m). ^{1}H NMR (300 MHz, $CDCl_3$): δ_H 1.36 (9H, t, *J*=7.2), 3.54 (6H, q, *J*=7.2), 4.92 (2H, s), 7.45-7.60 (6H, m), 7.81 (2H, d, *J*=7.1), 8.03 (2H, dd, *J*=6.6 7.7). ^{13}C NMR (75 MHz, $CDCl_3$, PENDANT)[270]: δ_C 7.8 (CH_3), 52.1 (CH_2), 53.4 (CH_2), 125.0 (C), 125.9 (C), 126.3 (CH), 127.6 (CH), 128.7 (CH), 129.3 (CH), 130.1 (CH), 131.1 (CH), 152.2 (C), 160.8 (C), Remaining quaternary carbon signals too small to be resolved. LRMS (ES^+): *m/z* 335 (100%, $[M + H]^+$) ($C_{22}H_{27}ON_2^+$ requires M^+ 335).

2,5-Diphenyl-oxazole-4-carboxylic acid hydrazide 106

Hydrazine hydrate (4.00 mL, 128.42 mmol) was added to a solution of the ethyl-4-carboxylate-2,5-diphenyloxazole **105** (1.000 g, 4.789 mmol) in ethanol (40 mL) and the resultant solution stirred overnight. The resultant white precipitate was collected by filtration and dried to constant mass to give

scintilipid **106** (0.160 g, 12%) as white solid. The filtrate was stirred at room temperature for a further two days to give a second crop scintilipid **106** (0.357 g, 27%) which was filtered and dried to constant mass. This procedure was repeated to isolate a third crop scintilipid **106** (0.047 g, 4%) as white solid. IR (KBr disc): ν_{max}/cm^{-1} 3323 (m, N-H), 3255 (m, N-H), 3070 (m, C-H aromatic), 1669 (s, C=O), 1616 (s, C=C aromatic), 1589 (s, C=C aromatic), 1569 (m), 1506 (s, C=C aromatic), 1448 (s), 1338 (m), 1250 (m), 1222 (s), 1070 (m), 1038 (m), 1012 (w), 1000 (w), 933 (s), 856 (w), 807 (w), 772 (s), 703 (s) and 681 (s). ^{1}H NMR (300 MHz, $CDCl_3$): δ_H 4.06 (2H, s), 7.39-7.50 (6H, m), 8.08 (2H, dd, *J*=7.1, 5.9), 8.35 (2H, d, *J*=6.9) and 8.41 (1H, s). ^{13}C NMR (75 MHz, $CDCl_3$, PENDANT)[270]: δ_C 126.6 (CH), 128.0 (CH), 128.4 (CH), 128.8 (CH), 129.9 (CH), 130.9 (CH), 162.0 (C), Remaining quaternary signals remain too small to be resolved. LRMS (APCI): *m/z* 280 (53%, $[M + H]^+$) ($C_{16}H_{13}O_2N_3$ requires M^+ 279), 248 (100%).

2,5-Diphenyl-oxazole-4-carboxylic acid hydrazide hydrochloride 107

Hydrogen chloride gas (excess), generated from sodium chloride and concentrated sulfuric acid, was bubbled into scintilipid **106** (0.357 g, 1.28 mmol) dissolved in chloroform (30 mL). The scintilipid **107** (0.379 g, quantitative yield) was collected by filtration and dried to constant mass. IR (thin film, NaCl plate): ν_{max}/cm^{-1} 3202 (m, br, N-H), 3060 (m, C-H aromatic), 2861 (s, br, N-H), 2608 (m, br, N-H), 1684 (s, C=O), 1654 (m, C=C aromatic), 1647 (m), 1636 (m), 1616 (m), 1590 (s, C=C aromatic), 1570 (s, C=C aromatic), 1560 (s, C=C aromatic), 1541 (m), 1534 (m), 1484 (s), 1458 (s), 1449 (m), 1232 (m), 1178 (m), 1156 (m), 1129 (m), 1054 (m), 1027 (w), 982 (m), 922 (w), 861 (w), 776 (m), 759 (m), 707 (s) and 688 (s). ^{1}H NMR (300 MHz, d_6-DMSO): δ_H 7.53-7.61 (6H, m), 8.13 (2H, dd, *J*=6.2, 6.4) and 8.26 (2H, d, *J*=6.0). ^{13}C NMR (75 MHz, $CDCl_3$, PENDANT)[270]: δ_C 125.6 (C), 126.2 (C), 126.5 (CH), 127.7 (CH), 128.6 (CH), 129.1 (CH), 130.4 (CH), 131.5 (CH), 152.7 (C), 158.7 (C) and 159.9 (C). LRMS (APCI): *m/z* 280 (100%, $[M - Cl]^+$) ($C_{16}H_{14}O_2N_3^+$ requires M 280).

2,5-Diphenyl-oxazole-4-carboxylic acid benzhydrylidene-hydrazide 108

A solution of benzophenone (0.131 g, 0.13 mmol) and sulfuric acid (3 drops, catalytic amount) in methanol (20 mL) was added to a suspension of **106** (0.200 g, 0.70 mmol) in methanol (20 mL), under a nitrogen atmosphere, and allowed to stir at room temperature (2 days) causing the formation of a white precipitate. The white precipitate was filtered and dried (0.096 g, 30%) and the filtrate returned to stir for a further three days which produced a second crop of white precipitate (0.033 g, 10%) and a further three days of stirring the filtrate gave a final crop of product (0.036 g, 11%). IR (KBr disc): ν_{max}/cm^{-1} 3304 (m, N-H), 3058 (w, C-H aromatic), 1695 (s, C=O), 1654 (m), 1590 (m, C=C aromatic), 1570 (m, C=C aromatic), 1507 (s, C=C aromatic), 1442 (m), 1327 (m), 1226 (m), 1206 (s), 1118 (m), 1087(w), 1070 (m), 1024 (w), 946 (w), 921 (w), 881(s), 844 (w), 770 (m), 760 (m), 724 (w), 705 (s) and 686 (s). ^{1}H NMR (300 MHz, $CDCl_3$): δ_H 7.37-7.49 (12H, m), 7.73 (6H, m), 8.47 (2H, d, *J*=7.2) and 10.45

(1H, s). ^{13}C NMR (75 MHz, $CDCl_3$, PENDANT)[270]: δ_C 126.0 (C), 126.3 (CH), 126.9 (C), 129.0 (CH), 128.0 (CH), 128.1 (CH), 128.3 (CH), 128.5 (CH), 128.7 (CH), 129.3 (C), 129.6 (CH), 129.8 (CH), 130.0 (CH), 130.9 (CH), 132.4 (C), 136.8 (C), 153.3 (C), 154.7 (C), 156.9 (C) and 158.0 (C=O). LRMS (APCI): *m/z* 444 (100%, $[M + H]^+$) ($C_{29}H_{21}N_3O_2$ requires M^+ 443).

3-[4-(2,5-Diphenyl-oxazole-4-ylmethyoxy)-phenyl]-propan-1-ol 109

4-bromomethyl-2,5-diphenyloxazole **103** (0.492 g, 1.57 mmol) was added to a solution of 3-(4-hydroxyphenyl)-propan-1-ol (0.248 g, 1.63 mmol), K_2CO_3 (1.273 g, 16.30 mmol) and 18-Crown-6 (catalytic amount) in acetonitrile (25 mL) and refluxed for 16 hours. The mixture was poured into water (30 mL) and extracted with diethyl ether (3 x 30 mL). The combined organic extracts were washed with an aqueous solution of hydrochloric acid (20%) (2 x 30 mL), dried over anhydrous magnesium sulfate and concentrated under reduced pressure to furnish the crude product (0.651 g). The crude product was triturated with diethyl ether to furnished the scintilipid **109** (0.330 g, 55%) as a white solid. IR (KBr disc): ν_{max}/cm^{-1} 3363 (m, O-H), 3059 (w, C-H aromatic), 3025 (w, C-H aromatic), 2935 (m, C-H aliphatic), 2865 (m, C-H aliphatic), 1714 (w), 1670 (w), 1609 (m, C=C aromatic), 1581 (w, C=C aromatic), 1553 (w), 1510 (s, C=C aromatic), 1486 (m), 1448 (m), 1395 (w), 1279 (m), 1233 (s), 1178 (m), 1111 (w), 1089 (w), 1070 (m), 1040 (m), 1010 (m), 912 (w), 860 (w), 831 (w), 801 (w), 776 (m), 712 (m) and 691 (s). ^1H NMR (300 MHz, $CDCl_3$): δ_H 1.87 (2H, pentet, *J*=7.0), 2.66 (2H, t, *J*=7.0), 3.67 (2H, t, *J*=7.0), 5.15 (2H, s), 7.00 (2H, d, *J*=8.6), 7.13 (2H, d, *J*=8.6), 7.30-7.60 (6H, m), 7.77 (2H, d, *J*=7.1) and 8.10 (2H, dd, *J*=5.5, 7.7). ^{13}C (75 MHz, $CDCl_3$, PENDANT)[270]: δ_C 31.2 (CH_2), 34.4 (CH_2), 62.3 (CH_2), 62.9 (CH_2), 114.9 (2 x CH), 126.3 (CH), 126.4 (CH), 127.2 (C), 127.9 (C), 128.8 (CH), 129.0 (CH), 129.4 (CH), 130.5 (CH), 132.7 (C) and 134.4 (C). LRMS (APCI): *m/z* 386 (64%, $[M + H]^+$) ($C_{25}H_{23}NO_3$ requires M^+ 385), 234 (100%).

Benzoic acid 3-[4-(2,5-dihenyl-oxazol-4-ylmethoxy)-phenyl]-propyl ester 110

Benzoyl chloride (0.13 mL, 0.15 g, 1.09 mmol) was added to a solution of **109** (0.400 g, 1.04 mmol) in DCM (10 mL). Triethylamine (0.29 mL, 0.21 g, 2.08 mmol) was added to the reaction mixture and the solution was stirred (3 hours). The reaction mixture was poured into water (20 mL) and extracted with ethyl acetate (3 x 20 mL). The combined organic extracts were dried over anhydrous magnesium sulfate, filtered and concentrated under reduced pressure to furnish yellow oil. The oil was allowed to stand for 16 hours after which time a yellow solid had formed (0.511 g). The yellow solid was triturated with hexane to give a white solid which was collected by filtration and dried to constant mass to give scintilipid **110** (0.330 g, 65%) as a white solid. IR (thin film, NaCl plate): ν_{max}/cm^{-1} 3051 (w, C-H aromatic), 2927 (s, C-H aliphatic), 1716 (s, C=O), 1608 (w, C-H aromatic), 1510 (s, C=C aromatic), 1494 (m), 1449 (m), 1273 (s), 1233 (s), 1176 (m), 1116 (m), 1069 (m) and 1026 (m). ^1H NMR (300 MHz, $CDCl_3$): δ_H 2.07 (2H, pentet, *J*=7.0), 2.73 (2H, t, *J*=7.0), 4.33 (2H, t, *J*=7.0), 5.14 (2H, s), 7.00

(2H, d, *J*=8.5), 7.14 (2H, d, *J*=8.5), 7.30-7.60 (9H, m), 7.76 (2H, d, *J*=7.0), 8.03 (2H, d, *J*=7.0) and 8.10 (2H, m). ^{13}C NMR (75 MHz, $CDCl_3$, PENDANT)[270]: δ_C 30.4 (CH_2), 31.4 (CH_2), 63.0 (CH_2), 68.2 (CH_2), 114.6 (CH), 115.1 (CH), 126.3 (CH), 126.5 (CH), 128.4 (CH), 128.8 (CH), 128.9 (CH), 129.0 (CH), 129.5 (CH), 132.9 (CH), 133.7 (CH), Remaining quaternary signals remain too small to be resolved. LRMS (APCI): *m/z* 490 (100%, $[M + H^+]$) ($C_{32}H_{27}NO_4$ requires M^+ 489).

4-Dec-4-enyloxymethyl-2,5-diphenyl-oxazole 111

trans-4-Decenal (1.0 mL, 5.5 mmol) was added to a solution of sodium borohydride (1.033 g, 27.30 mmol) in methanol (10 mL) and stirred for 16 hours. The mixture was poured into water (30 mL) and extracted with ethyl acetate (2 x 25 mL). The combined organic extracts were washed with brine (2 x 50 mL), dried over anhydrous magnesium sulfate, filtered and concentrated under reduced pressure to furnish crude product *trans*-4-decenol as yellow oil (0.947 g). IR (thin film, NaCl plate): ν_{max}/cm^{-1} 3358 (m, O-H), 2954 (s, C-H alkene), 2925 (s, C-H aliphatic), 2855 (s, C-H aliphatic), 1731 (w, C=O), 1416 (w), 1377 (w), 1333 (w), 1275 (w), 1120 (w), 1070 (w) and 969 (w).

A solution of 4-bromomethyl-2,5-diphenyloxazole **103** (1.906 g, 6.07 mmol) in DMF (20 mL) was added to a suspension of sodium hydride (1.457 g, 60.70 mmol) and *trans*-4-decen-1-ol (0.947 g, 6.07 mmol) in DMF. The resultant mixture was stirred at room temperature for 16 hours. The reaction was quenched cautiously with water (50 mL) and extracted with diethyl ether (3 x 30 mL). The combined organic extracts were washed with brine (20 mL), dried over anhydrous magnesium sulfate, filtered and concentrated under reduced pressure to furnish a yellow solid. Trituration with diethyl ether precipitated the unreacted oxazole which was removed by filtration through a pad of celite. The filtrate was concentrated under reduced pressure to furnish the crude product **111** as yellow oil. Purification by flash column chromatography (gradient elution: hexane (100 mL), 20% ethyl acetate in hexane (200 mL)) furnished the pure **111** (0.284 g, 12%) as a colourless solid. IR (KBr disk): ν_{max}/cm^{-1} 3051 (w, C-H aromatic), 2879 (m, C-H aliphatic), 1484 (w), 1466 (w), 1444 (w), 1355 (w), 1275 (w), 1240 (w), 1173 (w), 1147 (m), 1113 (s, C-O), 1062 (m), 1031 (m), 947 (w), 840 (w), 774 (w) and 690 (s). ^1H NMR (300 MHz, $CDCl_3$): δ_H 0.86 (3H, t, *J*=7.0), 1.20-1.40 (6H, m), 1.71 (2H, pentet, *J*=7.0), 1.93-208 (4H, m), 3.63 (2H, t, *J*=6.5), 4.64 (2H, s), 5.39 (2H, m), 7.30-7.50 (6H, m), 7.79 (2H, d, *J*=8.0) and 8.10 (2H, dd, *J*=4.0, 7.7). LRMS (APCI): *m/z* 390 (12%, $[M + H^+]$) ($C_{26}H_{31}NO_2$ requires M^+ 389), 234 (100%).

6-(2,5-Diphenyl-oxazol-4-ylmethoxy)-hexan-1-ol 112

6-Bromo-1-hexanol (1.486 g, 8.21 mmol), *tert*-butyldimethylsilyl chloride (TBDMS-Cl) (1.361 g, 9.03 mmol), imidazole (0.615 g, 9.03 mmol) and DCM (20 mL) were combined and stirred under an atmosphere of nitrogen at room temperature for 20 hours. The mixture was poured into water (200 mL) and extracted with DCM (3 x 50 mL). The combined organic extracts were washed with brine (2 x 50 mL), dried over anhydrous magnesium sulfate, filtered and concentrated under reduced pressure to

furnish the crude product. The crude product was isolated as orange oil (2.361 g, 98%). This product was used directly without any further purification. IR (thin film, NaCl plate): ν_{max}/cm^{-1} 2920 (s, C-H aliphatic), 2860 (m, C-H aliphatic), 2820 (s, C-H aliphatic), 1450 (m), 1440 (m), 1370 (s), 1330 (s), 1250 (m), 1100 (s), 1000 (w), 930 (w), 910 (w), 850 (s) and 780 (s). ^{1}H NMR (300 MHz, $CDCl_3$): δ_H 0.02 (6H, s), 0.87 (9H, s), 1.33-1.52 (6H, m), 1.84 (2H, pentet, *J*=6.9), 3.37 (2H, t, *J*=6.9) and 3.58 (2H, d, *J*=6.5). ^{13}C (75 MHz, $CDCl_3$, PENDANT)[270]: δ_C -5.4 (2 x CH_3), 18.3 (C), 24.9 (CH_2), 25.6 (3 x CH_3), 27.9 (CH_2), 32.4 (CH_2), 32.5 (CH_2), 33.7 (CH_2) and 62.5 (CH_2). LRMS (APCI): *m/z* 295 (92.5%, $[M + H]^+$) ($C_{12}H_{27}{}^{79}BrOSi$ requires M^+ 294), 297 (100%, $[M + H]^+$) ($C_{12}H_{27}{}^{81}BrOSi$ requires M^+ 296).

The silyl ether (2.361 g, 8.03 mmol) was added to a suspension of sodium hydride (1.921 g, 80.30 mmol) and 2,5–diphenyl-4-hydroxymethyloxazole **102** (1.818 g, 7.24 mmol) in DMF (30 mL) and stirred for 3 hours. The reaction was quenched cautiously with water (50 mL) and the aqueous phase extracted with ethyl acetate (3 x 30 mL), the addition of brine was required to break up emulsions that formed during this extraction procedure. The combined organic extracts were washed with brine (2 x 20 mL), dried over anhydrous magnesium sulfate, filtered and concentrated under reduced pressure to furnish the crude product (3.880 g, 104%) as yellow oil. This product was reacted on without further purification. IR (thin film, NaCl plate): ν_{max}/cm^{-1} 3040 (w, C-H aromatic), 3020 (w, C-H aromatic), 2410 (w, C-H aliphatic), 2320 (w, C-H aliphatic), 1550 (w), 1500 (m, C=C aromatic), 1480 (m), 1440 (m), 1360 (m), 1280 (m), 1240 (s), 1170 (m), 1090 (m), 1070 (m), 1020 (m), 970 (m), 920 (m), 780 (s) and 770 (s). ^{1}H NMR (300 MHz, $CDCl_3$,): δ_H 0.02 (6H, s), 0.87 (9H, s), 1.25-2.02 (8H, m), 3.55-3.63 (4H, m), 4.62 (2H, s), 7.36-7.49 (6H, m), 7.78 (2H, d, *J*=7.4) and 8.09 (2H, m). LRMS (APCI): *m/z* 466 (36%, $[M + H]^+$) ($C_{28}H_{39}NO_3Si$ requires M^+ 465), 394 (100%).

Oxazole silyl ether (3.880 g, 8.03 mmol, maximum theoretical quantity), TBAF (4.630 g, 17.7 mmol) and THF (30 mL) were combined. The reaction mixture was stirred at room temperature under an atmosphere of nitrogen for 16 hours. The reaction mixture was poured into water (50 mL) and extracted with ethyl acetate (2 x 30 mL). The combined organic extracts were washed with a saturated aqueous ammonium chloride solution (2 x 20 mL), brine (2 x 20 mL), dried over anhydrous magnesium sulfate, filtered and concentrated under reduced pressure to furnish the crude product a yellow oil **112** (3.209 g). Purification by flash column chromatography (gradient elution 20% ethyl acetate in hexane (400 mL) followed by 40% ethyl acetate in hexane (500 mL), furnished pure alcohol **112** as a pale yellow waxy solid (1.127 g, 40% for the two steps from silyl ether). IR (thin film, NaCl plate): ν_{max}/cm^{-1} 3386 (s, O-H), 3059 (w, C-H aromatic), 2930 (s, C-H), 2857 (s, C-H), 1594 (w, C=C aromatic), 1551 (m, C=C aromatic), 1485 (m), 1447 (m), 1377 (s), 1346 (s), 1279 (s), 1090 (s), 1070 (s), 1026 (m), 920 (w), 775 (m), 764 (m), 706 (s) and 690 (s). ^{1}H (300 MHz, $CDCl_3$): δ_H 1.35-1.45 (4H, m), 1.54 (2H, p, *J*=6.6), 1.66 (2H, pentet, *J*=6.6), 3.61 (4H, tt, *J*=6.6 6.6), 4.63 (2H, s), 7.36-7.48 (6H, m), 7.79 (2H, d, *J*=7.3) and 8.10 (2H, dd, *J*=5.3 7.9). ^{13}C NMR (75MHz, $CDCl_3$, PENDANT)[270]: δ_C 25.3 (CH_2), 25.8

(CH_2), 29.4 (CH_2), 32.4 (CH_2), 62.4 (CH_2), 64.9 (CH_2), 70.3 (CH_2), 126.0 (CH), 126.2 (CH), 128.6 (CH), 128.7 (CH), 129.3 (CH) and 130.2 (CH). LRMS (APCI): *m/z* 352 (50%, $[M + H]^+$) ($C_{22}H_{25}O_3N$ requires M^+ 351), 234 (100%).

6-(2,5-Diphenyl-oxazol-4-ylmethoxy)-hexanoic acid 114

Pyridinium chlorochromate (PCC)/silica gel (1:1) (4.600 g, 10.67 mmol) was added to a solution of scintilipid **112** (2.500 g, 7.12 mmol) in DCM (30 mL) and left to stir overnight. The reaction mixture was diluted with ether and filtered through celite and silica before being concentrated under reduced pressure to furnish the crude aldehyde **113** as yellow oil (2.087 g, 84%). This product was used directly without further purification.

A sample, purified by eluting through a silica column (20% ethyl acetate in hexane) was isolated as slightly yellow oil. Spectroscopic analysis of this oil gave the following data. IR (thin plate, NaCl plate): ν_{max}/cm^{-1} 3059 (m, C-H aromatic), 2933 (s, C-H aliphatic), 2860 (s, C-H aliphatic), 2718 (w), 1722 (s, C=O), 1696 (m), 1594 (w, C=C aromatic), 1551 (m, C=C aromatic), 1486 (s), 1447 (s), 1377 (w), 1346 (w), 1319 (w), 1279 (w), 1214 (w), 1177 (w), 1133 (w), 1091 (s), 1069 (m), 1025 (m), 1011 (w), 950 (w), 921 (w), 776 (s), 765 (m), 707 (s), 691 (s), 675 (m) and 660 (w). ^{1}H NMR (300 MHz, $CDCl_3$): δ_H 1.40-1.66 (6H, m), 2.31-2.41 (2H, m), 3.61 (2H, t, *J*=6.2), 4.63 (2H, s), 7.35-7.49 (6H, m), 7.77 (2H, d, *J*=7.4), 8.10 (2H, m) and 9.72 (1H, s).

Silver (I) oxide (1.574 g, 6.79 mmol) was added to a solution of aldehyde **113** (1.580 g, 4.53 mmol) in methanol (30 mL) followed by the drop-wise addition of $NaOH_{(aq)}$ (2 M, 30 mL). The reaction mixture was placed under a nitrogen atmosphere and stirred at room temperature for 6 hours. The reaction mixture was filtered through celite, and acidified (20% $HCl_{(aq)}$) which turned the yellow solution cloudy. The solution was extracted with diethyl ether (3 x 50 mL), dried over anhydrous magnesium sulfate, filtered and concentrated under reduced pressure to give yellow oil which solidified on standing open to the atmosphere. Trituration of the yellow solid with hot diethyl ether (50 mL) gave a yellow solution and a white solid. The white solid was isolated by filtration and washed with cold diethyl ether (30 mL). The filtrate was basified (2 M $NaOH_{(aq)}$) and the aqueous phase separated then acidified (20% $HCl_{(aq)}$) and extracted with diethyl ether (2 x 30 mL). Charcoal was added to the diethyl ether extracts and the resultant mixture gently warmed before being filtered through celite and concentrated under reduced pressure to give an opaque oil which solidified to a white solid on standing open to the atmosphere overnight. The two solids were identical and thus were combined to give a single pure product **114** (1.27 g, 77%). IR (KBr disc): ν_{max}/cm^{-1} 3060 (w, C-H aromatic), 2930 (s, C-H aliphatic), 2856 (s, C-H aliphatic), 2581 (m, br, O-H), 1716 (s, C=O), 1596 (w, C=C aromatic), 1546 (m, C=C aromatic), 1488 (s), 1450 (m),1420 (w), 1350 (w), 1326 (m), 1307 (m), 1217 (m), 1183 (s), 1090 (s), 1014 (m), 911 (m), 780 (m), 761 (m), 707 (s) and 688 (s). ^{1}H NMR (300 MHz, $CDCl_3$): δ_H 1.41-1.49 (2H, m), 1.65 (4H, pp, *J*=6.6 7.4), 2.33 (2H, t, *J*=7.4), 3.61 (2H, t, *J*=6.6), 4.64 (2H, s), 7.34-7.51 (6H, m), 7.77 (2H, d, *J*=7.5)

and 8.1 (2H, dd, *J*=5.25 7.86). ^{13}C NMR (75MHz, $CDCl_3$, PENDANT)[270]: δ_C 24.5 (CH_2), 25.7 (CH_2), 29.3 (CH_2), 33.9 (CH_2), 65.1 (CH_2), 70.2 (CH_2), 126.2 (CH), 126.5 (CH), 128.4 (CH), 128.6 (CH), 128.8 (CH), 128.8 (CH), remaining quaternary carbon signals remain too small to be resolved. LRMS (APCI): *m/z* 366 (1%, $[M + H]^+$) ($C_{22}H_{23}O_4N$ requires M^+ 365), 234 (100%).

4-(6-Bromo-hexyloxymethyl)-2,5-diphenyl-oxazole 115

PBr_3 (30 µL, 0.316 mmol) was added to a solution of **112** (0.317 g, 0.90 mmol) in DCM (10 mL) under a nitrogen atmosphere and the resultant solution was stirred at room temperature for 2 days. DCM (30 mL) was added to the reaction mixture and washed with water (3 x 30 mL). The organic fractions were combined and dried over anhydrous magnesium sulfate, filtered and evaporated to give yellow oil (0.25 g). The oil was eluted through a silica column (20% Ethyl acetate in hexane) (200 mL) to isolate product **115** (0.059 g, 16%) as yellow oil. IR (thin film, NaCl plate): ν_{max} /cm^{-1} 3060 (w, C-H aromatic), 2934 (s, C-H aliphatic), 2859 (s, C-H aliphatic), 1719 (w), 1596 (w, C=C aromatic), 1552 (m, C=C aromatic), 1486 (m), 1448 (m), 1376 (w), 1346 (w), 1319 (w), 1242 (m), 1176 (w), 1092 (s), 1070 (m), 1026 (w), 1012 (w), 951 (w), 921 (w), 776 (m), 764 (m), 707 (s), 691 (s) and 675 (m). ^{1}H NMR (300 MHz, $CDCl_3$,): δ_H 1.41 (4H, m), 1.65 (2H, p, *J*=6.7), 1.82 (2H, p, *J*=6.7), 3.35 (2H, t, *J*=6.7), 3.61 (2H, t, *J*=6.7), 4.63 (2H, s), 7.36-7.49 (6H, m), 7.78 (2H, d, *J*=7.3), 8.10 (2H, dd, *J*=6.7 7.7). ^{13}C NMR (75 MHz, $CDCl_3$, PENDANT)[270]: δ_C 25.4 (CH_2), 27.9 (CH_2), 29.5 (CH_2), 32.7 (CH_2), 33.7 (CH_2), 65.2 (CH_2), 70.3 (CH_2), 126.1 (CH), 126.4 (CH), 127.3 (C), 128.3 (C), 128.5 (CH), 128.7 (CH), 128.8 (CH) and 130.3 (CH). LRMS (APCI): *m/z* 428 (100%, $[M + H]^+$) ($C_{22}H_{22}{}^{79}BrNO_3$ requires M^+ 427), 430 (100%, $[M + H]^+$) ($C_{22}H_{22}{}^{81}BrNO_3$ requires M^+ 429).

6-(2,5-Diphenyl-oxazol-4-ylmethoxy)-hexanoic acid 2,5-dioxo-pyrrolidin-1-yl ester 116

To a cooled (0 °C) solution of **114** (1.200 g, 3.29 mmol) and *N*-hydroxysuccinimide (0.378 g, 3.29 mmol) in dimethoxyethane (DME) (25 mL), was added, in a drop-wise fashion, a solution of dicyclohexylcarbodimide (0.746 g, 3.62 mmol) in DME (10 mL). The resultant solution was stirred at 0 °C for a further 2 hours before being allowed to warm to room temperature whereupon stirring was continued over night. The urea by-product was removed from the reaction mixture by filtration and the filtrate concentrated under reduced pressure to furnish the crude product **116** (1.727 g) as opaque yellow oil. Purification by flash column chromatography (gradient elution 20% ethyl acetate in hexane (500 mL) followed by 40% ethyl acetate in hexane (500 mL)) furnished the product contaminated with unreacted **114**. The combined fractions were washed with 2 M sodium hydroxide solution (50 mL), dried over anhydrous magnesium sulfate, filtered and concentrated under reduced pressure to give yellow oil. Trituration of the oil with diethyl ether caused a white solid to precipitate which was collected by filtration **116** (0.381 g, 25%). IR (KBr disc): ν_{max} /cm^{-1} 2928 (m, C-H aliphatic), 2855 (m, C-H aliphatic), 1811 (w, C=O), 1782 (m, C=O), 1737 (s, C=O), 1619 (w, C=C aromatic) 1551 (w, C=C

aromatic), 1485 (w), 1447 (w), 1367 (w), 1205 (m), 1068 (m), 777 (w), 707 (w) and 691 (w). ^{1}H NMR (300 MHz, $CDCl_3$): δ_H 1.50-108 (6H, m), 2.57 (2H, t, *J*=7.3), 2.79 (4H, s), 3.62 (2H, t, *J*=6.3), 4.63 (2H, s), 7.35-7.49 (6H, m), 7.77 (2H, d, *J*=7.1) and 8.10 (2H, dd, *J*=6.5, 7.7). ^{13}C NMR (75MHz, $CDCl_3$, PENDANT)[270]: δ_C 24.4 (CH_2), 25.6 (CH_2), 29.2 (CH_2), 30.9 (CH_2), 65.3 (CH_2), 70.1 (CH_2), 126.2 (CH), 126.4 (CH), 128.6 (CH), 128.8 (CH), 128.9 (CH), 130.3 (CH), remaining quaternary carbon signals too small to be resolved. LRMS (APCI): *m/z*: 461 (13%, $[M - H]^+$), 220 (100%), 463 (15%, $[M + H]^+$), 234 (100%) ($C_{26}H_{26}O_6N_2$ requires M^+ 462).

Butyric acid 6-(2,5-diphenyl-oxazol-4-ylmethoxy)-hexyl ester 117

Butyryl chloride (0.176 g, 1.65 mmol) was added to a stirred solution of **112** (0.580 g, 1.65 mmol) in DCM (20 mL). To this solution was added triethylamine (0.334 g, 3.30 mmol) and stirring was continued for 16 hours. The reaction mixture was poured into water (20 mL) and extracted with ethyl acetate (3 x 20 mL). The combined organic extracts were washed with brine (20 mL), dried over anhydrous magnesium sulfate and concentrated under reduced pressure to furnish crude ester **117** (0.747 g, 107%) as yellow oil. Activated charcoal was added to a solution of **117** in diethyl ether (30 mL) and the resultant mixture gently warmed. The solution was filtered through a pad of celite and concentrated under reduced pressure to yield pure ester **117** (0.312 g, 45%) as pale yellow oil. IR (thin film, NaCl plate): ν_{max}/cm^{-1} 3059 (w, C-H aromatic), 2934 (s, C-H aliphatic), 2859 (s, C-H aliphatic), 1732 (s, C=O), 1594 (w, C=C aromatic), 1550 (w, C=C aromatic), 1485 (m), 1448 (m), 1346 (w), 1254 (w), 1178 (m), 1091 (m), 1070 (m), 1026 (m) and 920 (w). ^{1}H NMR (300 MHz, $CDCl_3$): δ_H 0.92 (3H, t, *J*=7.3), 1.35 (4H, br, s), 1.61 (6H, m), 2.25 (2H, t, *J*=7.5), 3.60 (2H, t, *J*=6.5), 4.03 (2H, t, *J*=6.7), 4.63 (2H, s), 7.30-7.60 (6H, m) 7.78 (2H, d, *J*=7.2) and 8.10 (2H, dd, *J*=6.5 7.7). ^{13}C NMR (75 MHz, $CDCl_3$, PENDANT)[270]: δ_C 13.4 (CH_3), 18.2 (CH_2), 25.5 (CH_2), 28.3 (CH_2), 29.3 (CH_2), 36.0 (CH_2), 63.9 (CH_2), 64.8 (CH_2), 70.1 (CH_2), 125.9 (CH), 126.2 (CH), 127.0 (C), 128.0 (C), 128.3 (CH), 128.5 (CH), 130.1 (CH), 133.9 (C), 148.5 (C), 159.4 (C) and 173.4 (C). LRMS (APCI): *m/z* 422 (100%, $[M + H]^+$) ($C_{26}H_{31}NO_4$ requires M^+ 421).

Benzoic acid 6-(2,5-diphenyl-oxazol-4-ylmethoxy)-hexyl ester 118

Scintilipid **112** (0.501 g, 1.43 mmol) was dissolved in DCM (10 mL) and placed under an atmosphere of nitrogen. Benzoyl chloride (0.17 mL, 0.20 g, 1.43 mmol) was added and the mixture stirred for ten minutes at room temperature. Triethylamine (0.3 mL, 0.217 g, 2.15 mmol) was then added and the resultant mixture was stirred at room temperature for 16 hours. The mixture was poured into water (20 mL) and extracted with diethyl ether (2 x 20 mL). The combined organic extracts were dried over anhydrous magnesium sulfate, filtered and concentrated under reduced pressure to furnish the crude product **118** as yellow oil. This oil was allowed to stand for 16 hours after which time a yellow solid had formed (0.599 g). Purification by flash column chromatography (20% ethyl acetate in hexane (200 mL))

furnished pure ester **118** (0.340 g, 52%) as colourless oil. IR (thin film, NaCl plate): ν_{max}/cm^{-1} 3059 (w, C-H aromatic), 2934 (m, C-H aliphatic), 2858 (m, C-H aliphatic), 1716 (s, C=O), 1600 (w, C=C aromatic), 1552 (w, C=C aromatic), 1485 (m), 1450 (m), 1314 (m), 1274 (s), 1175 (w), 1095 (m), 1069 (m) and 1026 (m). ^{1}H NMR (300 MHz, $CDCl_3$): δ_H 1.46-1.71 (8H, m), 3.62 (2H, t, *J*=6.5), 4.28 (2H, t, *J*=6.7), 4.64 (2H, s), 7.30-7.60 (9H, m), 7.80 (2H, m), 8.02 (2H, d, *J*=7.3) and 8.09 (2H, dd, *J*=5.5, 7.7). LRMS (APCI): *m/z* 456 (100%, $[M + H]^+$) ($C_{29}H_{29}NO_4$ requires M^+ 455).

8-(2,5-Diphenyl-oxazol-4-ylmethoxy)-octan-1-ol 119.

8-Bromo-1-octanol (1.000 g, 4.80 mmol), TBDMS-Cl (0.993 g, 6.60 mmol), imidazole (0.458 g, 6.70 mmol) and DCM (30 mL) were combined and stirred under an atmosphere of nitrogen at room temperature for 20 hours. The mixture was poured into water (200 mL) and extracted with DCM (3 x 50 mL). The combined organic extracts were washed with brine (2 x 50 mL), dried over anhydrous magnesium sulfate, filtered and concentrated under reduced pressure to furnish the crude product. The silyl ether was isolated as colourless oil (1.512 g, 98%). IR (thin film, NaCl plate): ν_{max}/cm^{-1} 2928 (s, C-H aliphatic), 2855 (s, C-H aliphatic), 1461 (m), 1387 (w), 1360 (w), 1254 (m), 1100 (m), 1005 (w) and 938 (w). ^{1}H NMR (300 MHz, $CDCl_3$): δ_H 0.02 (6H, s), 0.87 (9H, s), 1.29-1.5 (6H, m), 1.83 (2H, p, *J*=7.0), 3.36 (2H, t, *J*=7.0) and 3.58 (2H, t, *J*=6.5). ^{13}C NMR (75 MHz, $CDCl_3$, PENDANT)[270]: δ_C -5.3 (2 x CH_3), 18.3 (C), 23.7 (CH_2), 25.3 (CH_3), 27.9 (CH_2), 28.4 (CH_2), 28.9 (CH_2), 32.7 (CH_2), 33.7 (CH_2), 63.2 (CH_2) and 71.0 (C).

The silyl ether (1.211 g, 3.75 mmol) and 2,5–diphenyl-4-hydroxymethyloxazole **102** (0.988 g, 3.94 mmol) were added to a suspension of sodium hydride (0.900 g, 37.49 mmol) in DMF (30 mL) and stirred at room temperature for 2 hours. The reaction was quenched cautiously with water (50 mL) and the aqueous phase extracted with ethyl acetate (3 x 30 mL). The combined organic extracts were washed with brine (2 x 50 mL), dried over anhydrous magnesium sulfate, filtered and concentrated under reduced pressure to furnish the crude product as yellow oil (2.997 g). This product (containing some ethyl acetate) was reacted on without further purification. ^{1}H NMR (300 MHz, $CDCl_3$): δ_H 0.00 (6H, s), 0.85 (9H, s), 1.21 (8H, m), 1.45 (2H, t, *J*=6.6), 1.62 (2H, t, *J*=6.8), 3.51-4.60 (4H, m), 4.59 (2H, s) and 7.3-8.2 (10H, m).

Oxazole silyl ether (2.838 g, 3.75 mmol, maximum theoretical quantity), TBAF (1.656 g, 6.33 mmol), THF (30 mL) were combined and stirred at room temperature for 16 hours. The reaction mixture was poured into water (50 mL) and extracted with ethyl acetate (2 x 50mL). The combined organic extracts were washed with a saturated aqueous ammonium chloride solution (2 x 50 mL), brine (2 x 50 mL), dried over anhydrous magnesium sulfate, filtered and concentrated under reduced pressure. Purification by flash column chromatography (gradient elution 20% ethyl acetate in hexane followed by 40% ethyl acetate in hexane) furnished pure alcohol as a yellow oil (0.737 g, 52% for the two steps

from silyl ether). The yellow oil was dissolved in 40% ethyl acetate in hexane (20 mL) and warmed gently for 10 minutes with activated charcoal (1 g as a decolourising agent). The mixture was filtered through a pad of celite and concentrated under reduced pressure to furnish the pure product **119** as pale yellow oil (0.397 g, 28% for the two steps from silyl ether). IR (KBr disk): ν_{max}/cm^{-1} 3359 (m, O-H), 3058 (w, C-H aromatic), 2928 (s, C-H aliphatic), 2854 (s, C-H aliphatic), 1956 (w), 1890 (w), 1810 (w), 1594 (m, C=C aromatic), 1551 (m, C=C aromatic), 1486 (s), 1463 (m), 144 (s), 1377 (m), 1347 (m), 1321 (m), 1280 (m), 1180 (w), 1158 (w), 1133 (w), 1091 (s), 1070 (s), 1026 (s), 1008 (m), 951 (w), 920 (w), 844 (w), 775 (s), 763 (s), 707 (s), 691 (s), 675 (s) and 659 (m). ^{1}H NMR (300 MHz, $CDCl_3$): δ_H 1.30 (8H, br, s), 1.53-1.67 (4H, m), 3.60 (4H, t, *J*=6.5), 4.63 (2H, s), 7.30-7.60 (6H, m), 7.78 (2H, d, *J*=8.0) and 8.09 (2H, dd, *J*=5.3 7.9). ^{13}C (75 MHz, $CDCl_3$, PENDANT)[270]: δ_C 25.5 (CH_2), 26.0 (CH_2), 29.2 (CH_2), 29.5 (CH_2), 32.5 (CH_2), 56.6 (CH_2), 62.5 (CH_2), 64.9 (CH_2), 70.4 (CH_2), 125.9 (CH), 126.1 (CH), 127.0 (C), 128.0 (C), 128.4 (CH), 128.6 (CH), 130.2 (CH), 130.3 (CH), 133.9 (C), 148.6 (C) and 159.4 (C). LRMS (APCI): *m/z* 380 (31%, $[M + H]^+$) ($C_{24}H_{29}NO_3$ requires M^+ 379), 234 (100%).

4.4 Synthesis and Evaluation of Polystyrene-Based Resins

2,5-Diphenyl-4-trimethylstannanyloxazole 120

To a solution of 2,5-diphenyloxazole **1** (15.000 g, 67.80 mmol) and 2,2,6,6-tetramethylpiperidine (1.1 mL, 0.960 g, 6.80 mmol) in tetrahydrofuran (150 mL) cooled to -78 °C, *sec*-butyllithium (1.3 M, 56 mL, 73.3 mmol) was added over 30 minutes.

The solution was allowed to warm to 0 °C over 30 minutes and the resultant solution of 4-lithio-2,5-diphenyloxazole, was added via cannula to a solution of trimethyltin chloride (13.490 g, 67.70 mmol) in tetrahydrofuran (70 mL) at -78 °C. The reaction mixture was allowed to warm to room temperature before being quenched with saturated ammonium chloride solution (150 mL). The organic layer was separated, dried over magnesium sulfate and concentrated under reduced pressure to give a brick red solid.

Column chromatography (hexane/ethyl acetate 10%, 500 mL) gave 2,5-diphenyl-4-trimethylstannanyloxazole as a yellow solid. Recrystallisation from methanol gave 2,5-diphenyl-4-trimethylstannanyloxazole **120** as white needle like crystals (12.082 g, 47%). Mp 80-82 °C, IR (KBr disc): ν_{max}/cm^{-1} 3057 (m, C-H aromatic), 2980 (m, C-H aliphatic), 2906 (m, C-H aliphatic), 1604 (w, C=C, aromatic), 1540 (s, C=C, aromatic), 1482 (s), 1446 (s), 1340 (m), 1283 (w), 1186 (m), 1157 (w), 1144 (w), 1081(m), 1057 (m), 1025 (m), 974 (m), 918 (w), 773 (s), 729 (m), 705 (s) and 686 (s). ^{1}H NMR (300 MHz, $CDCl_3$): δ_H 0.36 (9H, s, d {unresolved dd from coupling to Sn^{117} and Sn^{119}}, *J*=56.0), 7.25-7.35 (6H, m), 7.59 (2H, d, *J*=7.7) and 8.06 (2H, d, *J*=7.3). ^{13}C NMR (75 MHz, $CDCl_3$, PENDANT)[270]: δ_C –9.0 (CH_3, d, *J*=–363.9 CH_3 signal split into a doublet by Sn^{119}), -8.9 (CH_3), -8.9 (CH_3, d, *J*=363.9, CH_3 signal split into a d by Sn^{117}), 32.1 (C), 125.4 (CH), 126.0 (CH), 127.4 (C), 127.9 (CH), 128.3 (CH), 129.4 (C), 129.6 (CH), 135.7 (C) and 157.2 (C). ^{119}Sn NMR (112 MHz, $CDCl_3$): $\delta_{Sn}{}^{119}$ 254.38 (dectet, 2 outermost bands are too small to be observed, *J*=56.0). ^{117}Sn NMR ($CDCl_3$, 107 MH_Z): $\delta_{Sn}{}^{117}$ -0.27 (dectet, 2 outermost bands too small to be observed, *J* 56.0). LRMS (APCI): *m/z* 386 (100%, $[M + H]^+$) ($C_{18}H_{19}ONSn$ requires M^+ 384).

(4'vinyl)-4-benzyl-2, 5-diphenyloxazole 101

A solution of *tris*-(dibenzylideneacetone) dipalladium (0) (0.060 g, 0.13 mmol, {5 mol percent Pd}) and triphenylarsine (0.160 g, 0.50 mmol {20 mol percent ligand}) in 1-methyl-2-pyrrolidinone (NMP) (25 mL) was warmed slowly to 40 °C and stirred for 1 hour. To this solution was added 4-vinylbenzyl chloride **12** (0.37 mL, 0.40 g, 2.6 mmol) and the solution stirred at 40 °C for a further 1 hour. A solution of 2,5-diphenyl-4-trimethylstanyloxazole **120** (1.000 g, 2.60 mmol) and copper (II) oxide (0.207 g, 2.60 mmol) in NMP (25 mL) was added to the reaction mixture and resultant solution stirred at 65 °C overnight. The reaction mixture was cooled to room temperature and stirred with 10% aqueous potassium fluoride solution (100 mL) and diethylether (50 mL) for 1.5 hours, filtered through celite and rinsed with diethyl

ether (3 x 50 mL). The aqueous phase was separated, diluted with water (50 mL) and extracted with diethyl ether (3 x 50 mL). The combined organic extracts were washed with saturated ammonium chloride (2 x 50 mL), dried over magnesium sulfate and concentrated under reduced pressure to give a yellow solid. Column chromatography (hexane/diethyl ether 5%, 1 L) gave (4'vinyl)-4-benzyl-2, 5-diphenyloxazole **101** (0.452 g, 52%) as a white solid. Mp 106-108°C, IR (KBr): ν_{max}/cm^{-1} 3055 (m, C-H aromatic), 3016 (m, C-H aromatic), 2918 (m, C-H aliphatic), 1595 (m, C=C aromatic), 1546 (m, C=C aromatic), 1511 (m, C=C aromatic), 1487 (s), 1446 (m), 1426 (m), 1404 (m), 1368 (w), 1317 (w), 1266 (w), 1173 (w), 1158 (w), 1120 (w), 1085 (w), 1068 (m), 1027 (m), 995 (m), 952 (w), 901 (s), 820 (s), 797 (m), 766 (s) and 690 (s). ^{1}H NMR (300 MHz, $CDCl_3$): δ_H 4.24 (2H, s), 5.23 (1H, d, *J*=10.9), 5.74 (1H, d, *J*=17.6), 6.73 (1H, dd, *J*=10.9 17.6), 7.33-7.51 (10H, m), 7.65 (2H, d, *J*=7.3) and 8.14 (2H, dd, *J*=7.9, 6.7). ^{13}C NMR (75 MHz, $CDCl_3$, PENDANT)[270]: δ_C 32.8 (CH_2), 113.2 (CH_2), 125.5 (CH), 126.3 (CH), 126.4 (CH), 127.4 (C), 128.0 (CH), 128.5 (CH), 128.6 (CH), 128.8 (CH), 130.1 (CH), 135.6 (C), 135.8 (C), 136.5 (CH), 138.2 (C), remaining quaternary signals too small to be resolved. LRMS (APCI): *m/z* 338 (100%, $[M + H]^+$) ($C_{24}H_{19}NO$ requires M^+ 337).

Chloromethyl, Scintillant Containing, Gel-type Polystyrene Resin, 121

Styrene **10** (63.0 mL, 57.2 g, 549 mmol), 80% pure divinylbenzene **11** (2.3 mL, 2.1 g, 13 mmol, {ethylstyrene 3.2 mmol}), 4-vinylbenzylchloride **12** (9.9 mL, 10.8 g, 71 mmol), AIBN **7** (0.700 g, 4.27 mmol) and (4'vinyl)-4-benzyl-2,5-diphenyloxazole **101** (3.360 g, 10.00 mmol) were stirred at 609 rpm in a 1% PVA solution (700 mL) according to General Procedure 1 to give beaded product **121** in the ranges : [150-75 µm, 20.049 g, 27%], [75-38 µm, 5.490 g, 8%], [<38 µm, 0.888 g, 12%]. IR (KBr, 150-75 µm): ν_{max}/cm^{-1} 3051 (m, C-H aromatic), 3024 (m, C-H aromatic), 2922 (s, C-H aliphatic), 2838 (m, C-H aliphatic), 1940 (w), 1871 (w), 1798 (w), 1655 (w), 1599 (m, C=C aromatic), 1577 (w), 1544 (w, C=C aromatic), 1510 (w, C=C aromatic), 1491 (s), 1446 (s), 1368 (w), 1320 (w), 1263 (w), 1178 (w), 1151 (w), 1111 (w), 1066 (m), 1024 (m), 904 (m), 835 (m) and 753 (s, C-Cl).

Acetoxy, Macroporous Polystyrene Resin 122

Styrene **10** (23.0 mL, 20.8 g, 202 mmol), 80% pure divinylbenzene **11** (6.9 mL, 6.3 g, 39 mmol, {ethylstyrene 10 mmol}), 4-acetoxystyrene **39** (3.0 mL, 3.2 g, 19 mmol) AIBN **7** (0.350 g, 2.10 mmol) and toluene (33 mL) were stirred at 320 rpm in a 1% PVA solution (700 mL) according to general procedure 1 to give beaded product **122** in the ranges : [>250 µm, 0.032 g, 1%], [250-150 µm, 12.822 g, 42%], [150-75 µm, 6.925 g, 23%], [75-38 µm, 0.392 g, 1%], [<38 µm, 0.106 g, 1%]. IR (KBr, 150-75 µm): ν_{max}/cm^{-1} 3060 (m, C-H aromatic), 3016 (m, C-H aromatic), 2918 (s, C-H aliphatic), 2847 (m, C-H aliphatic), 1940 (w), 1869 (w), 1798 (w), 1767 (m), 1750 (m, C=O), 1652 (w), 1718 (w), 1696 (w), 1674 (w), 1652 (w), 1599 (m, C=C aromatic), 1576 (w), 1563 (w), 1493 (m), 1457 (m), 1439 (m), 1422 (w), 1364 (m), 1178 (m), 1107 (w), 1071 (w), 1018 (m), 960 (w), 934 (w), 903 (m), 827 (m), 792 (w), 748 (m), 694 (m) and 663 (m).

Acetoxy, Gel-type Polystyrene Resin 123

Styrene **10** (27.4 mL, 24.8 g, 236 mmol), 80% pure divinylbenzene **11** (0.9 mL, 0.9 g, 5 mmol, {ethylstyrene 1.3 mmol}), 4-acetoxystyrene **39** (3.0 mL, 3.2 g, 19 mmol) AIBN **7** (0.350 g, 2.14 mmol) were stirred at 317 rpm in 1% PVA solution (700 mL) according to general procedure 1 to give beaded product **123** in the range : [150-75 μm, 3.375 g, 12%], [75-38 μm, 0.366 g, 1%], [<38 μm, 0.097 g, 1%]. IR (KBr, 150-75 μm): ν_{max}/cm^{-1} 3422 (m), 3060 (m, C-H aromatic), 3016 (m, C-H aromatic), 2923 (s, C-H aliphatic), 2847 (m, C-H aliphatic), 1945 (w), 1869 (w), 1803 (w), 1755 (s, C=O), 1655 (m), 1600 (m, C=C aromatic), 1493 (s), 1442 (s), 1364 (m), 1187 (s, C-O), 1160 (s), 1067 (m), 1018 (s), 905 (m), 836 (w), 751 (s) and 685(s).

Phenoxy, Macroporous Polystyrene Resin 124

Potassium hydroxide (0.126 g, 1.91 mmol) was added to a suspension of macroporous 4-acetoxystyrene resin **122** (75-150 μm, theoretical loading=0.62 mmol/g, 0.206 g, 0.13 mmol) in ethanol (20 mL) and the mixture stirred for 2 days. Aqueous hydrochloric acid (30 mL, 2 M) was added and the resin filtered, washed with water (30 mL), ethanol (2 x 30 mL) and dried under suction. The resin was extracted with acetone in soxhlet apparatus overnight and dried under reduced pressure to give the phenoxy-macroporous resin **124** (0.074 g) as white spherical beads. IR (KBr): ν_{max}/cm^{-1} 3422 (m, O-H), 3060 (w, C-H aromatic), 3007 (w, C-H aromatic), 2924 (s, C-H aliphatic), 2854 (m, C-H aliphatic), 1944 (w), 1869 (w), 1801 (w), 1750 (w), 1732 (w), 1655 (m), 1597 (m, C=C aromatic), 1541 (m, C=C aromatic), 1489 (m), 1441 (s), 1377 (m), 1320 (m), 1182 (w), 1147 (w), 1089 (m), 1067 (m), 1022 (m), 960 (w), 903 (w), 839 (w), 743 (s) and 658 (s).

Phenoxy, Gel-type Polystyrene Resin 125

Potassium hydroxide (0.276 g, 4.92 mmol) was added to a suspension of 4-acetoxy-gel-type-resin **123** (75-150 μm, theoretical loading=0.65 mmol/g, 0.500 g, 0.33 mmol) in ethanol (20 mL) and the mixture stirred for 2 days. Aqueous hydrochloric acid (30 mL, 2 M) was added and the resin filtered, washed with water (30 mL), ethanol (2 x 30 mL) and dried under suction. The resin was extracted with acetone in soxhlet apparatus overnight and dried under reduced pressure to give phenoxy-gel-type-resin **125** (0.3506 g) as white spherical beads. IR (KBr disc): ν_{max}/cm^{-1} 3545 (m), 3415 (s, O-H), 3051 (m, C-H aromatic), 3024 (m, C-H aromatic), 2924 (s, C-H aliphatic), 2847 (m, C-H aliphatic), 1945 (w), 1869 (w), 1798 (w), 1740 (w), 1600 (m, C=C aromatic), 1559 (w), 1541 (w), 1511 (m, C=C aromatic), 1491 (m), 1450 (m), 1364 (w), 1324 (w), 1258 (w), 1169 (m), 1102 (w), 1067 (w), 1027 (m), 905 (m), 828 (m), 755 (s), 697 (s) and 650 (s).

Solvent swelling assay upon polymers 121-125

The polymer was packed into the bottom of a polypropylene disposable syringe (1 mL), with the tip removed, housing a nylon frit (0.45 μm). A reservoir containing solvent was placed below the syringe and the reservoir raised until the solvent was just brought into contact with the bottom of the syringe. A volume reading was recorded when there was no further volume increase (Appendix B, Table 38).

Polymer 126: Fmoc-Gly-OH coupling to macroporous polymer 124

2,6-Dichlorobenzoylchloride (0.04 mL, 0.3 mmol), pyridine (anhydrous, 0.04 mL, 0.5 mmol), resin **124** (0.100 g, 0.06 mmol) and Fmoc-Gly-OH (0.083 g, 0.28 mmol) in DMF (anhydrous, 10 mL) were combined according to General Procedure 2 to give polymer **126** as a cream polymer (0.070 g). IR (KBr disc): ν_{max}/cm^{-1} 3421 (m, O-H), 3433 (m, N-H), 3060 (m, C-H aromatic), 3024 (m, C-H aromatic), 2922 (s, C-H aliphatic), 2847 (C-H, aliphatic), 1940 (w), 1874 (w), 1794 (w), 1776 (w), 1736 (w), 1719 (w), 1701 (w), 1683 (w), 1652 (w), 1600 (m, C=C aromatic), 1510 (m, C=C aromatic), 1492 (m), 1448 (m), 1364 (w), 1342 (w), 1258 (w), 1168 (m), 1102 (w), 1062 (w), 1026 (w), 903 (m), 827 (m), 796 (w), 755 (m) and 697 (s).

Polymer 127: Fmoc-Gly-OH coupling to gel-type polymer 125

2,6-Dichlorobenzoylchloride (0.05 mL, 0.4 mmol), pyridine (anhydrous, 0.06 mL, 0.8 mmol), resin **125** (0.200 g, 0.13 mmol) and Fmoc-Gly-OH (0.116 g, 0.39 mmol) in DMF (anhydrous, 10 mL) were combined according to General Procedure 2 to give polymer **127** as a cream polymer (0.159 g). IR (KBr disc): ν_{max}/cm^{-1} 3422 (m, br, O-H, N-H), 3059 (m, C-H aromatic), 3024 (m, C-H aromatic), 2920 (C-H aliphatic), 2848 (C-H, aliphatic), 1944 (w), 1870 (w), 1735 (w), 1712 (w), 1701 (w), 1600 (m, C=C aromatic), 1576 (w), 1505 (m, C=C aromatic), 1492 (m), 1450 (m), 1364 (w), 1342 (w), 1258 (w), 1199 (m), 1169 (m), 1068 (w), 1028 (w), 906 (w), 830 (w), 757 (m), and 697 (s).

Fmoc-release assay of macroporous polymer resin 126

Polymer resin **126** was weighed accurately, in quadruplicate, into a sample vial and treated according to General Procedure 3 **Table 13**.

Mass / g	Absorption @ 290 nm	Absorption @ 290 nm / mg
0.0010	0.248	0.248
0.0010	0.311	0.311
0.0013	0.311	0.239
0.0009	0.317	0.352
Average		0.288

Table 13: Fmoc-release assay of macroporous polymer resin **126**. Mean error = $^{+}$/-15%.

The average loading of polymer resin **124** was established to be 0.17 mmol/g (27%).[235]

Fmoc-release assay of gel-type polymer resin 127

Polymer resin **127** was weighed accurately, in quadruplicate, into a sample vial and treated according to General Procedure 3 **Table 14**.

Mass / g	Absorption @ 290 nm	Absorption @ 290 nm / mg
0.0013	0.497	0.382
0.0011	0.507	0.461
0.0008	0.441	0.551
0.0011	0.497	0.452
Average		0.462

Table 14: Fmoc-release assay of gel-type polymer resin **127**. Mean error = $^{+}$/-10%.

The average loading of polymer resin **125** was established to be 0.28 mmol/g (43%).[235]

4.5 Synthesis of Poly(Oxyethylene glycol) Polymer (POP) Supports

Tri(ethylene glycol) di-*p*-toluene sulfonate 128

A solution of TsCl (21.643 g, 111.30 mmol) in DCM (100 mL) was added drop-wise over 2 h to an ice cooled solution of tri(ethylene glycol) (5.00 mL, 37.1 mmol), triethylamine (31.3 mL, 223 mmol) and DMAP (0.046 g, 0.37 mmol) in DCM (200 mL) and the resultant mixture left to stir overnight whilst warming to room temperature. The reaction mixture was washed with distilled water (2 x 200 mL), saturated sodium bicarbonate solution (2 x 100 mL) and saturated citric acid solution (2 x 100 mL), dried over anhydrous sodium sulfate and concentrated under reduced pressure to give tri(ethylene glycol) di-*p*-toluene sulfonate **128** as a pale yellow oil (15.107 g, 89%) which was reacted on without further purification. IR (thin film): ν_{max}/cm^{-1} 2877 (w, br, C-H aliphatic), 1597 (w, C=C aromatic), 1497 (w, C=C aromatic), 1450 (w), 1400 (w), 1354 (s, $-SO_2O-$), 1189 (m), 1176 (s, $-SO_2O-$), 1124 (w), 1096 (w), 1012 (m), 921 (m), 817 (m), 776 (m) and 663 (s). ^{1}H NMR (300 MHz, $CDCl_3$): δ_H 2.40 (6H, s), 3.48 (4H, s), 3.61 (4H, t, *J*=3.0), 4.10 (4H, t, *J*=3.0), 7.31 (4H, d, *J*=9.0) and 7.75 (4H, d, *J*=9.0). ^{13}C NMR (75 MHz, $CDCl_3$, PENDANT)[270]: δ_C 21.7 (CH_3), 69.1 (CH_2), 69.6 (CH_2), 71.0 (CH_2), 128.6 (CH), 130.6 (CH), 133.0 (C) and 145.7 (C). LRMS (APCI): *m/z* 459 (21%, $[M + H]^+$). HRMS (EI): *m/z* 481.0967 ($[M + Na]^+$); calculated for $C_{20}H_{26}O_8NaS_2$ 481.0957.

α,ω-bis-Styryl-tri(ethylene glycol) 129

4-Acetoxystyrene (1.00 mL, 6.3 mmol) was added to a solution of potassium hydroxide (0.524 g, 7.94 mmol) dissolved in EtOH (13 mL) and the resultant mixture stirred at room temperature for 1 h. A solution of sodium ethoxide (0.548 g, 7.73 mmol) in EtOH (13 mL) was added and the resultant mixture brought to reflux for 1 h. A solution of tri(ethylene glycol) di-*p*-toluene sulfonate **128** (1.437 g, 3.13 mmol) in EtOH (40 mL) was added and the reaction mixture subsequently refluxed overnight. The reaction mixture was concentrated under reduced pressure, suspended in distilled water (50 mL) and extracted with Et_2O (3 x 100 mL). The combined organic fractions were dried over anhydrous sodium sulfate and concentrated under reduced pressure. Flash column chromatography (20% v/v ethyl acetate in hexane) gave α,ω-bis-styryl-tri(ethylene glycol) **129** as a white solid (0.342 g, 31%). Mp 68-69°C, IR (thin film): ν_{max}/cm^{-1} 3085 (w, C-H aromatic), 3041 (w, C-H aromatic), 2975 (w, C-H), 2934 (m, C-H aliphatic), 2903 (s, C-H aliphatic), 1626 (m, C=C), 1605 (m, C=C aromatic), 1574 (w, C=C aromatic), 1510 (s, C=C aromatic), 1452 (w), 1421 (w), 1409 (w), 1385 (w), 1330 (w), 1300 (w), 1286 (m), 1244 (s), 1178 (s), 1132 (s), 1070 (s), 1054 (m), 1026 (w), 1006 (w), 991 (m), 927 (s), 905 (s), 882 (s), 838 (s), 816 (m) and 728 (w). ^{1}H NMR (300 MHz, $CDCl_3$) δ_H 3.72 (4H, s), 3.83 (4H, t, *J*=4.1), 4.09 (4H, t, *J*=4.1), 5.13 (2H, d, *J*=11.0), 5.61 (2H, d, *J*=17.5), 6.66 (2H, dd, *J*=17.5 11.0), 6.87 (4H, d, *J*=8.4) and 7.32 (4H, d, *J*=8.4). ^{13}C NMR (75 MHz, $CDCl_3$, PENDANT)[270]: δ_C 67.2 (2 x CH_2), 69.5 (CH_2), 70.6 (CH_2), 111.3 (CH_2), 114.4 (CH), 127.1 (CH), 130.3 (C), 136.0 (CH) and 158.4 (C). LRMS

(APCI): *m/z* 355 (100%, $[M + H]^+$). HRMS (EI): *m/z* 377.1731 ($[M + Na]^+$); calculated for $C_{22}H_{26}O_4Na$ 377.1729. Found C=74.4; H=7.5; O=18.1; $C_{22}H_{26}O_4$ requires C=74.6, H=7.4, O=18.0.

α,ω-bis-Styryl-penta(ethylene glycol) 130

Using the same procedure as described for α,ω-bis-styryl-tri(ethylene glycol) **129**, 4-acetoxystyrene (2.8 mL, 17 mmol) was reacted sequentially with ethanolic solutions of potassium hydroxide (1.452 g, 22.00 mmol) and sodium ethoxide (1.518 g, 21.42 mmol). An ethanolic solution of penta(ethylene glycol) di-*p*-toluene sulfonate (5.000 g, 8.68 mmol) was then added to the refluxing reaction mixture to give α,ω-bis-styryl-penta(ethylene glycol) **130**, after flash column chromatography (60% v/v ethyl acetate in hexane), as a white solid (1.818 g, 48%). Mp 73-74 °C. IR (thin film): ν_{max}/cm^{-1} 3078 (w, C-H aromatic), 3042 (w, C-H aromatic), 2971 (w, C-H aliphatic), 2936 (m, C-H aliphatic), 2900 (m, C-H aliphatic), 2860 (m, C-H aliphatic), 1626 (m, C=C), 1604 (m, C=C aromatic), 1581 (w), 1560 (w), 1511 (s, C=C aromatic), 1456 (m), 1408 (w), 1360 (w), 1324 (w), 1299 (m), 1248 (s), 1179 (m), 1110 (s, C-O), 1064 (s), 994 (w), 951 (m), 925 (m), 907 (m), 840 (s), 814 (m) and 725 (w). ^{1}H NMR (300 MHz, $CDCl_3$): δ_H 3.62-3.65 (12H, m), 3.78 (4H, t, *J*=4.6), 4.06 (4H, t, *J*=4.6), 5.09 (2H, d, *J*=11.0), 5.57 (2H, d, *J*=17.6), 6.62 (2H, dd, *J*=17.6 11.0), 6.83 (4H, d, *J*=8.6) and 7.29 (4H, d, *J*=8.6). ^{13}C NMR (75 MHz, $CDCl_3$, PENDANT)[270]: δ_C 63.4 (CH_2), 67.3 (CH_2), 69.5 (CH_2), 70.5 (CH_2), 70.6 (CH_2), 111.4 (CH_2), 114.5 (CH), 127.1 (CH), 130.4 (C), 136.0 (CH) and 158.4 (C). LRMS (APCI): *m/z*: 443 (100%, $[M + H]^+$). HRMS (EI): *m/z* 465.2264 ($[M + Na]^+$); calculated for $C_{26}H_{34}O_6Na$ 465.2253.

Hexa(ethylene glycol) mono-*p*-toluene sulfonate 131

Using the same procedure as described for tri(ethylene glycol) di-*p*-toluene sulfonate **128**, a solution of TsCl (9.970 g, 0.05 mol) in DCM (75 mL) was added to a solution of hexa(ethylene glycol) (60.390 g, 0.205 mol), triethylamine (28.90 mL, 0.2 mol) and DMAP (0.316g, 2.56 mmol) in DCM (150 mL) to give hexa(ethylene glycol) mono-*p*-toluene sulfonate **131** as a pale yellow oil (20.403 g, 92%) which was reacted on without further purification. IR (thin film): ν_{max}/cm^{-1} 3478 (s, O-H), 2874 (s, br, C-H aliphatic aromatic), 1940 (w), 1644 (m), 1598 (m, C=C aromatic), 1494 (m, C=C aromatic), 1454 (s), 1398 (m), 1353 (s), 1293 (m), 1249 (m), 1211 (m), 1177 (s), 1097 (s, C-O), 1017 (s), 924 (s), 818 (s), 777 (s), 706 (w) and 665 (s). ^{1}H NMR (300 MHz, $CDCl_3$): δ_H 2.36 (3H, s), 2.98 (1H, s), 3.51-3.62 (22H, m), 4.08 (2H, t, *J*=4.7), 7.26 (2H, d, *J*=8.2), and 7.71 (2H, d, *J*=8.2). ^{13}C NMR (75 MHz, $CDCl_3$, PENDANT)[270]: δ_C 21.5 (CH_3), 61.5 (CH_2), 68.6 (CH_2), 69.2 (CH_2), 70.1 (CH_2), 70.4 (CH_2), 70.5 (CH_2), 70.6 (CH_2), 72.5 (CH_2), 127.8 (CH) and 129.7 (CH). LRMS (APCI) *m/z*: 437 (100%, $[M + H]^+$). HRMS (EI): *m/z* 459.1653 ($[M + Na]^+$); calculated for $C_{19}H_{32}O_9NaS$ 459.1665.

The distilled water from the aqueous work-up was combined and concentrated under reduced pressure to give a white precipitate suspended in oil. The suspension was stirred with diethyl ether (200 mL)

overnight and the filtrate concentrated under reduced pressure to give recovered hexa(ethylene glycol) ether as a colourless oil (31.85 g, 83%). Spectroscopic analysis of this material was identical with that of the starting material and thus the recovered material was used in subsequent reactions without further purification.

Poly(oxyethylene glycol)$_{400}$ mono-*p*-toluene sulfonate 132

Using the same procedure as described for tri(ethylene glycol) di-*p*-toluene sulfonate **128**, a solution of TsCl (6.809 g, 0.045 mol) in DCM (60 mL) was added to a solution of poly(oxyethylene glycol)$_{400}$ (50.0 mL, 140 mmol), triethylamine (19.3 mL, 140 mmol) and DMAP (0.216 g, 1.75 mmol) in CH_2Cl_2 (250 mL) to give poly(oxyethylene glycol)$_{400}$ mono-*p*-toluene sulfonate **134** as a pale yellow oil (18.794 g, 88%) which was reacted on without further purification. IR (thin film): ν_{max}/cm^{-1} 3475 (m, O-H), 2873 (m, C-H aliphatic), 1649 (w), 1597 (w, C=C), 1453 (m), 1353 (s, -SO_2O-), 1293 (w), 1249 (w), 1189 (m), 1177 (s, -SO_2O-), 1098 (s, C-O), 1018 (m), 924 (m), 819 (w), 777 (w) and 664 (m). ^{1}H NMR (300 MHz, $CDCl_3$): δ_H 2.35 (3H, s), 2.48-3.60 (35H, m), 4.06 (2H, t, *J*=4.9), 5.22 (1H, s), 7.25 (2H, d, *J*=8.1), and 7.69 (2H, d, *J*=8.1). ^{13}C NMR (75 MHz, $CDCl_3$, PENDANT)[270]: δ_C 21.4 (CH_3), 61.4 (CH_2), 68.4 (CH_2), 69.0 (CH_2), 70.1 (CH_2), 70.3 (CH_2), 70.4 (CH_2), 72.3 (CH_2), 127.7 (CH), 129.6 (CH), 132.7 (C), and 144.6 (C). LRMS (APCI): *m/z* 613 (100%, $[M + H]^+$), 657 (90%, $[M + C_2H_4O + H]^+$), 569 (82%, $[M - C_2H_4O + H]^+$), 701 (69%, $[M + 2(C_2H_4O) + H]^+$), 525 (57%, $[M - 2(C_2H_4O) + H]^+$), 745 (43%, $[M + 3(C_2H_4O) + H]^+$), 481 (27%, $[M - 3(C_2H_4O) + H]^+$).

Using the same procedure as described for hexa(ethylene glycol) mono-*p*-toluene sulfonate **131**, unreacted poly(oxyethylene glycol)$_{400}$ was recovered as a very pale yellow oil (31.500 g, 75%). Spectroscopic analysis of this material was identical with that of the starting material and thus the recovered material was used in subsequent reactions without further purification.

α-Styryl-hexa(ethylene glycol) 133

Using the same procedure as described for α,ω-bis-styryl-tri(ethylene glycol) **129**, 4-acetoxystyrene (0.50 mL, 3.1 mmol) was reacted with an ethanolic solution of potassium hydroxide (0.828 g, 12.55 mmol) at room temperature and then under reflux. An ethanolic solution of hexa(ethylene glycol) mono-*p*-toluene sulfonate **131** (1.728 g, 3.14 mmol) was added to the refluxing reaction mixture to give α-styryl-hexa(ethylene glycol) **133**, after flash column chromatography (5% v/v EtOH in DCM), as a pale yellow oil (0.651 g, 54%). IR (thin film): ν_{max}/cm^{-1} 3443 (m, O-H), 2872 (s, C-H aliphatic), 1627 (w, C=C), 1606 (m, C=C aromatic), 1510 (s, C=C aromatic), 1454 (m), 1408 (w), 1350 (m), 1324 (w), 1289 (m), 1249 (s), 1176 (m), 1114 (s, C-O), 1067 (s, C-O), 991 (w), 947 (w) and 838 (m). ^{1}H NMR (300 MHz, $CDCl_3$): δ_H 3.37-3.53 (20H, m), 3.64 (2H, t, *J*=4.6), 3.92 (2H, t, *J*=4.6), 4.93 (2H, d, *J*=10.9), 5.42 (1H, d, *J*=17.6), 6.48 (1H, dd, *J*=10.9, 17.6), 6.69 (2H, d, *J*=8.8) and 7.14 (2H, d, *J*=8.8). ^{13}C NMR (75

MHz, $CDCl_3$, PENDANT)[270]: δ_C 60.1 (CH_2), 62.3 (CH_2), 66.2 (CH_2), 68.4 (CH_2), 69.0 (CH_2), 69.3 (CH_2), 69.5 (CH_2), 71.5 (CH_2), 110.3 (CH_2), 113.4 (CH), 126.2 (CH), 129.2 (C), 135.1 (CH) and 157.5 (C). LRMS (APCI): *m/z* 385 (100%, $[M + H]^+$). HRMS (EI): *m/z* 407.2050 ($[M + Na]^+$). Calculated for $C_{20}H_{32}O_7Na$ 407.2046.

α-Styryl-poly(oxyethylene glycol)$_{400}$ 134

Using the same procedure as described for α,ω-bis-styryl-tri(ethylene glycol) **129**, 4-acetoxystyrene (0.87 mL, 5.4 mmol) was reacted with an ethanolic solution of potassium hydroxide (0.677 g, 10.80 mmol) at room temperature and then under reflux. An ethanolic solution of poly(oxyethylene glycol)$_{400}$ mono-*p*-toluene sulfonate **132** (3.323 g, 5.43 mmol) was added to the refluxing reaction mixture to give α-styryl-poly(oxyethylene glycol)$_{400}$ **134**, after flash column chromatography (5% v/v EtOH in DCM), as a pale yellow oil (0.803 g, 29%). IR (thin film): ν_{max}/cm^{-1} 3477 (m, O-H), 3087 (w, C-H aromatic), 3042 (w, C-H aromatic), 2872 (s, C-H aliphatic), 1627 (m, C=C), 1607 (s, C=C aromatic), 1574 (w), 1462 (m), 1454 (m), 1410 (w), 1350 (m), 1300 (m), 1249 (s), 1176 (m), 1110 (s, C-O), 993 (m), 948 (m), 839 (m) and 731 (w). ^1H NMR (300 MHz, $CDCl_3$): δ_H 3.38-3.52 (32H, m), 3.65 (2H, t, *J*=5.0), 3.93 (2H, t, *J*=5.0), 4.93 (1H, d, *J*=10.8), 5.42 (1H, d, *J*=17.6), 6.46 (1H, dd, *J*=10.8 17.6), 6.69 (2H, d, *J*=8.5) and 7.14 (2H, d, *J*=8.5). ^{13}C NMR (75 MHz, $CDCl_3$, PENDANT)[270]: δ_C 60.9 (CH_2), 63.0 (CH_2), 66.9 (CH_2), 69.1 (CH_2), 69.7 (CH_2), 69.9 (CH_2), 70.1 (CH_2), 72.1 (CH_2), 111.0 (CH_2), 114.1 (CH), 126.8 (CH), 129.9 (C), 135.6 (CH) and 158.0 (C). LRMS (APCI): *m/z* 517 (100%, $[M + H]^+$), 473 (82%, $[M - (C_2H_4O)]^+$), 429 (26%, $[M - 2(C_2H_4O)]^+$). HRMS (EI): *m/z* 451.2326 (29%, $[M - 2(C_2H_4O) + Na]^+$); calculated for $C_{22}H_{36}O_8Na$ 451.2308, 495.2579 (89%, $[M - (C_2H_4O) + Na]^+$); calculated for $C_{24}H_{40}O_9Na$ 495.2570, 539.2809 (100%, $[M + Na]^+$); calculated for $C_{26}H_{44}O_{10}Na$ 539.2832.

Polymer 135: Styrene 10, 2% cross-linked with α,ω-bis-styryl-penta(ethylene glycol) 130

Styrene **10** (920 μL, 7.9 mmol), α,ω-bis-styryl-penta(ethylene glycol) **130** (0.071 g, 0.16 mmol) and AIBN 7 (0.011 g, 0.06 mmol) were combined according to General Procedure 4 to give polymer **135**, after washing, as a white beaded product (0.223 g, 25%). IR (KBr disc): ν_{max}/cm^{-1} 3081 (w), 3058 (m, C-H aromatic), 3024 (m, C-H aromatic), 2920 (s, C-H aliphatic), 2845 (s, C-H aliphatic), 1943 (w), 1870 (w), 1830 (w), 1802 (w), 1773 (w), 1751(w), 1734 (w), 1718 (w), 1700 (w), 1685 (w), 1663 (w), 1601 (m, C=C aromatic), 1582 (m), 1560 (w), 1542 (w), 1508 (s, C=C aromatic), 1492 (s), 1451 (s), 1364 (w), 1301 (w), 1244 (m), 1177 (w), 1112 (m, C-O), 1066 (m), 1027 (m), 905 (w), 829 (w), 756 (s), 695 (s) and 536 (s).

Polymer 136: Styrene 10, 14% cross-linked with α,ω-bis-styryl-penta(ethylene glycol) 130

Styrene **10** (810 μL, 6.9 mmol), α,ω-bis-styryl-penta(ethylene glycol) **130** (0.500 g, 1.13 mmol) and AIBN 7 (0.011 g, 0.06 mmol) were combined according to General Procedure 4 to give polymer **136**,

after washing, as a white beaded product (0.985 g, 80%). IR (KBr disc): ν_{max}/cm^{-1} 3051 (m, C-H aromatic), 3016 (m, C-H aromatic), 2924 (s, C-H aliphatic), 2856 (s, C-H aliphatic), 1944 (w), 1869 (w), 1802 (w), 1735 (w), 1719 (w), 1701 (w), 1686 (w), 1655 (w), 1638 (w), 1601 (s, C=C aromatic), 1581 (m), 1560 (w), 1543 (w), 1510 (s, C=C aromatic), 1493 (s), 1449 (s), 1359 (m), 1346 (m), 1293 (m), 1241 (s), 1178 (s), 1100 (s, C-O), 1058 (s, C-O), 1023 (s, C-O), 938 (m), 903 (m), 826 (s), 746 (s) and 692 (s).

Polymer 137: Styrene 10, 20% cross-linked with α,ω-bis-styryl-penta(ethylene glycol) 130

Styrene **10** (750 μL, 6.4mmol), α,ω-bis-styryl-penta(ethylene glycol) **130** (0.724 g, 1.64 mmol) and AIBN **7** (0.011 g, 0.06 mmol) were combined according to General Procedure 4 to give polymer **137**, after washing, as a white beaded product (1.000 g, 71%) IR (KBr disc): ν_{max}/cm^{-1} 3051(s, C-H aromatic), 3025 (s, C-H aromatic), 2919 (s, C-H aliphatic), 2856 (s, C-H aliphatic), 1944 (w), 1870 (w), 1802 (w), 1751 (w), 1718 (w), 1701 (w), 1685 (w), 1654 (w), 1648 (w), 1637 (w), 1609 (s, C=C aromatic), 1582 (m), 1560 (w), 1542 (w), 1508 (s, C=C aromatic), 1493 (s), 1450 (s), 1350 (m), 1297 (m), 1244 (s), 1176 (s), 1100 (s, C-O), 1058 (s), 1027 (s), 908 (s), 826 (s), 756 (s) and 697 (s).

Polymer 138: Styrene 10, 2% cross-linked with α,ω-bis-styryl-tri(ethylene glycol) 129

Styrene **10** (226 μL, 2.0 mmol), α,ω-bis-styryl-tri(ethylene glycol) **129** (0.014 g, 0.04 mmol) and AIBN **7** (0.013 g, 0.01 mmol) were combined according to General Procedure 4 to give polymer **140**, after washing, as a white beaded product (0.195 g, 89%). IR (thin film): ν_{max}/cm^{-1} 3051 (m, C-H aromatic), 3025 (m, C-H aromatic), 2927 (s, C-H aliphatic), 2856 (m, C-H aliphatic), 1945 (w), 1874 (w), 1843 (w), 1794 (w), 1745 (m), 1710 (m), 1652 (m), 1563 (s, C=C aromatic), 1510 (m, C=C aromatic), 1457 (m), 1368 (w), 1231 (w), 1124 (w), 1067 (w), 1023 (w), 912 (w), 832 (w), 752 (s) and 685 (s).

Polymer 139: α-Styryl-hexa(ethylene glycol) 133, 2% cross-linked with DVB 11

α-Styryl-hexa(ethylene glycol) **133** (0.741 g, 1.93 mmol), DVB **11** (0.006 g, 0.04 mmol) and AIBN **7** (0.003 g, 0.02 mmol) were combined according to General Procedure 5 to give, after washing, polymer **139** as an opaque white gel (0.566 g, 76%). IR (gel compressed between NaCl discs): ν_{max}/cm^{-1} 3439 (s, O-H), 3025 (m, C-H aromatic), 2920 (s, C-H aliphatic), 2847 (s, C-H aliphatic), 1961 (w), 1883 (w), 1729 (m), 1696 (w), 1643 (m), 1610 (s, C=C aromatic), 1586 (m), 1550 (w), 1506 (s, C=C aromatic), 1488 (s), 1470 (s), 1451 (s), 1417 (s), 1359 (m), 1333 (s), 1306 (m), 1249 (m), 1102 (s, C-O), 1067 (s, C-O), 1040 (s, C-O), 943 (m), 819 (m) and 774 (m).

Polymer 140: α-Styryl-poly(oxyethylene glycol)$_{400}$ 134, 2% cross-linked with DVB 11

α-Styryl-poly(oxyethylene glycol)$_{400}$ **134** (0.301 g, 0.56 mmol), DVB **11** (0.002 g, 0.01 mmol) and AIBN **7** (0.001 g, 0.004 mmol) were combined according to General Procedure 5 to give, after washing,

polymer **140** as a clear gel (0.155 g, 51%). IR (gel compressed between NaCl discs): ν_{max}/cm^{-1} 3370 (m, O-H), 3076 (w, C-H aromatic), 3033 (w, C-H aromatic), 2909 (s, C-H aliphatic), 2867 (s, C-H aliphatic), 1657 (w), 1634 (w), 1608 (m, C=C aromatic), 1577 (w), 1510 (s, C=C aromatic), 1457 (m), 1351 (m), 1302 (m), 1247 (s), 1109 (s, C-O), 947 (m) and 832 (m).

Polymer 141: α-Styryl-hexa(ethylene glycol) 133, 2% cross-linked with α,ω-bis-styryl-penta(ethylene glycol) 130

α-Styryl-hexa(ethylene glycol) **133** (0.500 g, 1.30 mmol), α,ω-bis-styryl-penta(ethylene glycol) **130** (0.012 g, 0.03 mmol) and AIBN **7** (0.002 g, 0.01 mmol) were combined according to General Procedure 5 to give, after washing, polymer **141** as a clear gel (0.210 g, 41%). IR (gel compressed between NaCl discs): ν_{max}/cm^{-1} 3414 (s, O-H), 3025 (S, C-H aromatic), 2954 (s, C-H aliphatic), 2918 (s, C-H aliphatic), 2847 (s, C-H aliphatic), 2599 (m), 2537 (m), 2484 (m), 2093 (w), 2049 (w), 1962 (m), 1887 (w), 1723 (w), 1639 (s), 1607 (s, C=C aromatic), 1501 (s, C=C aromatic), 1484 (w), 1451 (w) and 1417 (w).

Polymer 142: α-Styryl-poly(oxyethylene glycol)$_{400}$ 134, 2% cross-linked with α,ω-bis-styryl-penta(ethylene glycol) 130

α-Styryl-poly(oxyethylene glycol)$_{400}$ **134** (0.331 g, 0.64 mmol), α,ω-bis-styryl-penta(ethylene glycol) **130** (0.006 g, 0.01 mmol) and AIBN **7** (0.001 g, 0.01 mmol) were combined according to General Procedure 5 to give, after washing, polymer **142** as a clear gel (0.168 g, 50%). IR (gel compressed between NaCl discs): ν_{max}/cm^{-1} 3416 (s, O-H), 3025 (m, C-H aromatic), 2920 (s, C-H aliphatic), 2847 (s, C-H aliphatic), 1648 (m), 1634 (m), 1611 (s), 1586 (m), 1519 (s), 1505 (s), 1488 (m), 1466 (s), 1452 (s), 1098 (s, C-O), 1069 (s, C-O) and 1040 (s, C-O).

Solvent swelling assay upon polymers 9, 27, 29 and 135-142

The polymers **9, 27, 29 and 135-142** (0.02-0.05 mL) were packed into the bottom of a polypropylene disposable syringe (1 mL), with the tip removed, housing a nylon frit (0.45 μm). A reservoir containing solvent was placed below the syringe and the reservoir raised until the solvent was just brought into contact with the bottom of the syringe. A volume reading was recorded when there was no further volume increase (Appendix B, Table 39).

Mass solvent uptake assay of polymers 9, 27, 29 and 135-142

The polymers **9**, **27**, **29** and **135-142** were evaluated with water (Appendix C, Table 43), DMF (Appendix C, Table 44) and toluene (Appendix C, Table 45) according to general procedure 6.

Polymer 143: Fmoc-Gly-OH coupling to polymer 140

2,6-Dichlorobenzoylchloride (0.10 mL, 0.7 mmol), pyridine (anhydrous, 0.13 mL, 1.6 mmol), polymer **140** (0.135 g, 0.26 mmol) and Fmoc-Gly-OH (0.230 g, 0.78 mmol) in DMF (anhydrous, 3.00 mL) were combined according to General Procedure 2 to give, after washing, Polymer **143** as a cream polymer (0.041 g).

Polymer 146: Fmoc-release assay of polymer resin 143

Polymer resin **143** was weighed accurately, in quadruplicate, into a sample vial and treated according to General Procedure 3 **Table 15**.

Mass / g	Absorption @ 290 nm	Absorption @ 290 nm / mg
0.0025	2.441	0.976
0.0022	2.258	1.026
0.0018	2.073	1.152
0.0013	1.476	1.135
Average		1.072

Table 15: Fmoc-release assay of polymer **143**. Mean error = $^{+}$/-7%.

The average loading of polymer resin **140** was established to be 0.65 mmol/g (34%).[235]

20% piperidine/DMF (7.0 mL) was added to the remainder of the resin **143** (0.072 g) and the resultant mixture stirred (1 hr). The polymer was collected by filtration and washed *in-situ* with DCM (3 x 30 mL), DCM/MeOH 1:1 (30 mL) and MeOH (3 x 30 mL). The polymer was pre-dried under suction before being dried to constant mass to give polymer **146** (0.042 g).

Polymer 149: Fmoc-Gly-OH coupling to polymer 146

2,6-Dichlorobenzoylchloride (0.03 mL, 0.2 mmol), pyridine (anhydrous, 0.04 mL, 0.5 mmol), polymer **146** (0.042 g, 0.08 mmol) and Fmoc-Gly-OH (0.072 g, 0.242 mmol) in DMF (anhydrous, 2.00 mL) were combined according to General Procedure 3 to give, after washing, Polymer **149** as a orange polymer (0.055 g).

Fmoc-release assay of polymer resin 149

Polymer resin **149** was weighed accurately, in quadruplicate, into a sample vial and treated according to General Procedure 3 **Table 16**.

Mass / g	Absorption @ 290 nm	Absorption @ 290 nm / mg
0.0036	2.600	0.722
0.0035	2.390	0.683
0.0047	2.541	0.541
0.0033	2.506	0.759
Average		0.676

Table 16: Fmoc-release assay of polymer **149**. Mean error = $^{+}$/-10%.

The average efficiency of the second Fmoc-Gly-OH coupling to polymer **140** was established to be 0.41 mmol/g (63%).[235]

Polymer 144: Fmoc-Gly-OH coupling polymer 141

2,6-Dichlorobenzoylchloride (0.10 mL, 0.7 mmol), pyridine (anhydrous, 0.13 mL, 1.6 mmol), polymer **141** (0.101 g, 0.26 mmol) and Fmoc-Gly-OH (0.228 g, 0.77 mmol) in DMF (anhydrous, 3.00 mL) were combined according to General Procedure 3 to give, after washing, Polymer **144** as a cream polymer (0.115 g).

Polymer 147: Fmoc-release assay of gel-type polymer resin 144

Polymer resin **144** was weighed accurately, in quadruplicate, into a sample vial and treated according to General Procedure 4 **Table 17**.

Mass / g	Absorption @ 290 nm	Absorption @ 290 nm / mg
0.2600	2.367	0.9104
0.0011	1.279	1.1627
0.0019	2.255	1.1868
0.0015	1.890	1.2600
Average		1.1230

Table 17: Fmoc-release assay of polymer **144**. Mean error = $^{+}$/-10%.

The average loading of polymer resin **141** was established to be 0.68 mmol/g (27%).[235]

20% piperidine/DMF (7 mL) was added to the remainder of the resin (0.137 g) and the resultant mixture stirred (1 hr). The polymer was collected by filtration and washed *in-situ* with DCM (3 x 30 mL), DCM/MeOH 1:1 (30 mL) and MeOH (3 x 30 mL). The polymer was pre-dried under suction before being dried to constant mass to give polymer **147** (0.074 g).

Polymer 150: Fmoc-Gly-OH coupling to polymer 147

2,6-Dichlorobenzoylchloride (0.07 mL, 0.5 mmol), pyridine (anhydrous, 0.09 mL, 1.1 mmol), polymer **147** (0.074 g, 0.188 mmol) and Fmoc-Gly-OH (0.167 g, 0.56 mmol) in DMF (anhydrous, 2.0 mL) were combined according to General Procedure 3 to give, after washing, Polymer **150** as a orange polymer (0.090g).

Fmoc-release assay of gel-type polymer resin 150

Polymer resin **150** was weighed accurately, in quadruplicate, into a sample vial and treated according to General Procedure 4 **Table 18**.

Mass / g	Absorption @ 290 nm	Absorption @ 290 nm / mg
0.0035	2.526	0.722
0.0035	2.423	0.692
0.0018	1.695	0.942
0.0052	2.510	0.483
Average		0.710

Table 18: Fmoc-release assay of polymer **150**. Mean error = $^{+}$/-18%.

The average efficiency of the second Fmoc-Gly OH coupling to polymer **141** was established to be 0.43 mmol/g (63%).[235]

Polymer 145: Fmoc-Gly-OH coupling to polymer 142

2,6-Dichlorobenzoylchloride (0.10mL, 0.7 mmol), pyridine (anhydrous, 0.13 mL, 1.6 mmol), polymer **142** (0.136 g, 0.26 mmol) and Fmoc-Gly-OH (0.230 g, 0.78 mmol) in DMF (anhydrous, 3.0 mL) were combined according to General Procedure 3 to give, after washing, polymer **145** as a cream polymer (0.061 g).

Polymer 148: Fmoc-release assay of gel-type polymer resin 145

Polymer resin **145** was weighed accurately, in quadruplicate, into a sample vial and treated according to General Procedure 4 **Table 19**.

Mass / g	Absorption @ 290 nm	Absorption @ 290 nm / mg
0.0028	2.312	0.826
0.0018	1.867	1.037
0.0025	2.279	0.912
0.0021	1.997	0.951
Average		0.932

Table 19: Fmoc-release assay of polymer **145**. Mean error = $^{+}$/-7%.

The average loading of polymer resin **142** was established to be 0.57 mmol/g (30%).[235]

20% piperidine/DMF (7.0 mL) was added to the remainder of polymer **145** (0.0.087 g) and the resultant mixture stirred (1 hr.). The polymer was collected by filtration and washed *in-situ* with DCM (3 x 30 mL), DCM/MeOH 1:1 (30 mL) and MeOH (3 x 30 mL). The polymer was pre-dried under suction before being dried to constant mass to give polymer **148** (0.042 g).

Polymer 151: Fmoc-Gly-OH coupling to polymer 148

2,6-Dichlorobenzoylchloride (0.03 mL, 0.2 mmol), pyridine (anhydrous, 0.04 mL, 0.5 mmol), polymer **148** (0.042 g, 0.08 mmol) and Fmoc-Gly-OH (0.071 g, 0.239 mmol) in DMF (anhydrous, 2.0 mL) were combined according to General Procedure 3 to give, after washing, Polymer **151** as a orange polymer (0.063 g).

Fmoc-release assay of gel-type polymer 151

Polymer resin **151** was weighed accurately, in quadruplicate, into a sample vial and treated according to General Procedure 4 **Table 20**.

Mass / g	Absorption @ 290 nm	Absorption @ 290 nm / mg
0.0054	2.587	0.479
0.0034	2.416	0.711
0.0018	1.716	0.953
0.0030	2.364	0.788
Average		0.733

Table 20: Fmoc-release assay of polymer resin **151**. Mean error = $^{+}$/-19%.

The average efficiency of the second Fmoc-Gly-OH coupling to polymer **145** was established to be 0.44 mmol/g (77%).

4.6 Synthesis of Scintillant-Containing Poly(Oxyethylene glycol) Polymer (POP-Sc) Supports

Poly(oxyethylene glycol)$_{300}$ mono-*p*-toluene sulfonate 152

Using the same procedure as described for triethylene glycol di-*p*-toluene sulfonate **128**, a solution of TsCl (35.120 g, 0.18 mol) in DCM (100 mL) was added to a solution of poly(oxyethylene glycol)$_{300}$ (217.000 g, 0.72 mol), triethylamine (102.0 mL, 720 mmol) and DMAP (1.114 g, 9.00 mmol) in DCM (400 mL) to give poly(oxyethylene glycol)$_{300}$ mono-*p*-toluene sulfonate **152** as a yellow oil (73.050 g, 89%). IR (thin film): ν_{max}/cm^{-1} 3463 (m, O-H), 3060 (w, C-H aromatic), 3033 (w, C-H aromatic), 2872 (m, C-H aliphatic), 1597 (w, C=C aromatic), 1453 (w), 1353 (s), 1292 (w), 1248 (w), 1189 (m), 1177 (s), 1098 (s, C-O), 1036 (m), 1017 (m), 923 (m), 818 (m), 777 (m) and 665 (m). ^{1}H NMR (300 MHz, $CDCl_3$): δ_H 2.37 (3H, s), 3.01 (2H, s), 3.50-3.62 (24H, m), 4.08 (2H, t, *J*=4.8), 7.27 (2H, d, *J*=7.5) and 7.72 (2H, d, *J*=7.5). ^{13}C NMR (75 MHz, $CDCl_3$, PENDANT)[270]: δ_C 21.4 (CH_3), 61.4 (CH_2), 68.4 (CH_2), 69.0 (CH_2), 70.0 (CH_2), 70.2 (CH_2), 70.3 (CH_2), 70.4 (CH_2), 70.5 (CH_2), 72.5 (CH_2), 76.6 (CH_2), 77.0 (CH_2), 77.4 (CH_2), 127.7 (CH), 129.6 (CH), 132.8 (C), and 144.6 (C). LRMS (APCI): *m/z* 481 (100%, $[M + H]^+$), 525 (99%, $[M + H]^+$), 570 (81%, $[M + C_2H_4O + H]^+$), 437 (60%, $[M - C_2H_4O + H]^+$), 614 (55%, $[M + 2(C_2H_4O) + H]^+$), 658 (41%, $[M + 3(C_2H_4O) + H]^+$), 393 (26%, $[M - 2(C_2H_4O) + H]^+$), 702 (17%, $[M + 4(C_2H_4O) + H]^+$), 349 (10%, $[M - 3(C_2H_4O) + H]^+$). HRMS (EI): *m/z* 415.1423 (33%, $[M - 2(C_2H_4O) + Na]^+$); calculated for $C_{17}H_{28}O_8NaS$ 451.1403, 459.1674 (73%, $[M - (C_2H_4O) + Na]^+$); calculated for $C_{19}H_{32}O_9NaS$ 459.1665, 503.1925 (100%, $[M + Na]^+$); calculated for $C_{21}H_{36}O_{10}NaS$ 503.1927, 547.2194 ([68%, $M + (C_2H_4O) + Na]^+$); calculated for $C_{23}H_{40}O_{11}NaS$ 547.2189, 591.2491 (28, $M + 2(C_2H_4O) + Na)^+$); calculated for $C_{25}H_{44}O_{12}NaS$ 591.2451.

α-Styryl-poly(oxyethylene glycol)$_{300}$ 153

Using the same procedure as described for α,ω-bis-styryl-triethylene glycol **129**, an ethanolic solution of poly(oxyethylene glycol)$_{300}$ mono-*p*-toluene sulfonate (56.750 g, 0.13 mmol) was added to an ethanolic solution of 4-acetoxystyrene (20.0 mL, 125 mmol) and potassium hydroxide (15.650 g, 250 mol) to give, after flash column chromatography (5% v/v EtOH in DCM), α-styryl-poly(oxyethylene glycol)$_{300}$ **153** as a pale yellow oil (22.930 g, 46%). IR (thin film): ν_{max}/cm^{-1} 3454 (s, O-H), 3085 (w, C-H aromatic), 3040 (w, C-H aromatic), 2893 (s, C-H alipahatic), 1628 (m, C=C), 1607 (s, C=C aromatic), 1574 (m, C=C aromatic), 1511 (s, C=C aromatic), 1454 (s), 1410 (m), 1350 (s), 1290 (s), 1249 (s), 1176 (s), 1113 (s, C-O), 993 (m), 946 (m), 838 (m) and 731. ^{1}H NMR (300 MHz, $CDCl_3$): δ_H 2.97 (1H, s), 3.43-3.57 (36H, m), 3.69 (2H, t, *J*=4.5), 3.97 (2H, t, *J*=4.8), 4.97 (1H, d, *J*=10.9), 5.45 (1H, d, *J*=17.7), 6.50 (1H, dd, *J*=10.9 17.7), 6.72 (2H, d, *J*=8.7) and 7.18 (2H, d, *J*=8.7). ^{13}C NMR (75 MHz, $CDCl_3$, PENDANT)[270]: δ_C 57.3 (CH_2), 61.0 (CH_2), 63.1 (CH_2), 67.0 (CH_2), 69.2 (CH_2), 69.7 (CH_2), 70.0 (CH_2), 70.1 (CH_2), 70.1 (CH_2), 72.3 (CH_2), 111.1 (CH_2), 114.2 (CH), 126.9 (CH), 130.1 (C), 135.8 (CH)

and 158.1 (C). LRMS (APCI): *m/z* 517 (100%, $[M + H]^+$), 561 (71%, $[M + (C_2H_4O) + H]^+$), 473 (56%, $[M - (C_2H_4O) + H]^+$), 429 (29%, $[M - 2(C_2H_4O) + H]^+$), 385 (12%, $[M - 3(C_2H_4O) + H]^+$). HRMS (EI): *m/z* 451.2325 (22%, $[M - 2(C_2H_4O) + Na]^+$). calculated. for $C_{22}H_{36}O_8Na$ 451.2308, 495.2572 (50%, $[M - (C_2H_4O) + Na]^+$); calculated for $C_{24}H_{40}O_9Na$ 495.2570, 511.2317 (21%, $[M - (C_2H_4O) + K]^+$); calculated for $C_{24}H_{40}O_9K$ 511.2309, 539.2827 (100%, $[M + Na]^+$), calculated. for $C_{26}H_{44}O_{10}Na$ 539.2832, 555.2574 (56%, $[M + K]^+$), calculated. for $C_{26}H_{44}O_{10}K$ 555.2572, 583.3098 (44%, $[M + (C_2H_4O) + Na]^+$); calculated. for $C_{28}H_{48}O_{11}Na$ 583.3094, 599.2861 (29%, $[M + (C_2H_4O) + K]^+$); calculated for $C_{28}H_{48}O_{11}K$ 599.2834.

POP support 154: α-Styryl-poly(oxyethylene glycol)$_{300}$ 153, cross-linked with 2 mole percent α,ω-bis-styryl-pentaethylene glycol 130

α-Styryl-poly(oxyethylene glycol)$_{300}$ **153** (0.120 g, 0.23 mmol), α,ω-bis-styryl-pentaethylene glycol **130** (0.002 g, 0.01 mmol) and AIBN **7** (0.0004 g, 0.003 mmol) were combined according to General Procedure 5 to give, after washing, polymer **154** as a clear gel (0.049 g, 40%). IR (gel compressed between NaCl discs): ν_{max}/cm^{-1} 3417 (s, O-H), 3045 (w, C-H aromatic), 3016 (w, C-H aromatic), 2918 (w, C-H aliphatic), 2847 (w, C-H aliphatic), 1973 (w), 1659 (m), 1650 (m), 1632 (m), 1614 (s, C=C aromatic), 1514 (m, C=C aromatic), 1504 (s, C=C aromatic), 1470 (s), 1454 (s), 1412 (m), 1373 (m), 1352 (m), 1306 (m), 1254 (m), 1178 (m), 1094 (m, br, C-O), 951 (m) and 838 (m).

POP-Sc support 155: α-Styryl-poly(oxyethylene glycol)$_{300}$ 153, 1 mole percent (4'vinyl)-4-benzyl-2,5-diphenyloxazole 101, cross-linked with 2 mole percent α,ω-bis-styryl-pentaethylene glycol 130

α-Styryl-poly(oxyethylene glycol)$_{300}$ **153** (0.133 g, 0.32 mmol), α,ω-bis-styryl-pentaethylene glycol **130** (0.002 g, 0.01 mmol), (4'vinyl)-4-benzyl-2,5-diphenyloxazole **101** (0.001 g, 0.003 mmol) and AIBN **7** (0.0004 g, 0.003 mmol) were combined according to General Procedure 5 to give, after washing, polymer **155** as a clear gel (0.067 g, 49%). IR (gel compressed between NaCl discs): ν_{max}/cm^{-1} 3384 (s, O-H), 3069 (w, C-H aromatic), 3025 (w, C-H aromatic), 2918 (s, C-H aliphatic), 2865 (s, C-H aliphatic), 1652 (m), 1634 (m), 1608 (m, C=C aromatic), 1581 (m, C=C aromatic), 1550 (m), 1505 (m, C=C aromatic), 1452 (m), 1244 (m), 1096 (s, C-O), 1067 (s, C-O) and 1036 (s, C-O).

POP-Sc support 156: α-Styryl-poly(oxyethylene glycol)$_{300}$ 153, 2 mole percent (4'vinyl)-4-benzyl-2,5-diphenyloxazole 101, cross-linked with 2 mole percent α,ω-bis-styryl-pentaethylene glycol 130

α-Styryl-poly(oxyethylene glycol)$_{300}$ **153** (0.117 g, 0.23 mmol), α,ω-bis-stryl-pentaethylene glycol **130** (0.002 g, 0.01 mmol), (4'vinyl)-4-benzyl-2,5-diphenyloxazole **101** (0.002 g, 0.01 mmol) and AIBN **7** (0.0004 g, 0.003 mmol) were combined according to General Procedure 5 to give, after washing,

polymer **156** as a clear gel (0.029 g, 24%). IR (gel compressed between NaCl discs): ν_{max}/cm^{-1} 3407 (m, O-H), 3060 (w, C-H aromatic), 3025 (w, C-H aromatic), 2918 (s, C-H aliphatic), 2873 (s, C-H aliphatic), 1652 (m), 1610 (m, C=C aromatic), 1581 (w, C=C aromatic), 1559 (w), 1541 (w), 1510 (s, C=C aromatic), 1458 (m), 1352 (m), 1297 (m), 1247 (s), 1178 (m), 1109 (s, C-O), 947 (m), 832 (m) and 703 (w).

POP-Sc support 157: α-Styryl-poly(oxyethylene glycol)$_{300}$ 153, 4 mole percent (4'vinyl)-4-benzyl-2,5-diphenyloxazole 101, cross-linked with 2 mole percent α,ω-bis-stryl-pentaethylene glycol 130

α-Styryl-poly(oxyethylene glycol)$_{300}$ **153** (0.121 g, 0.23 mmol), α,ω-bis-styryl-pentaethylene glycol **130** (0.002 g, 0.01 mmol), (4'vinyl)-4-benzyl-2,5-diphenyloxazole **101** (0.003 g, 0.01 mmol) and AIBN 7 (0.0004 g, 0.003 mmol) were combined according to General Procedure 5 to give, after washing, polymer **157** as a clear gel (0.074 g, 59%). IR (gel compressed between NaCl discs): ν_{max}/cm^{-1} 3382 (s, O-H), 3060 (w, C-H aromatic), 3033 (w, C-H aromatic), 2919 (s, C-H aliphatic), 2847 (s, C-H aliphatic), 1964 (m), 1660 (s), 1650 (s), 1633 (s), 1614 (s, C=C aromatic), 1584 (s, C=C aromatic), 1554 (w), 1504 (s, C=C aromatic), 1488(s), 1470 (s), 1454 (s), 1417 (s), 1386 (s), 1372 (s), 1359 (s), 1244 (s) and 1095 (s, br, C-O).

POP-Sc support 158: α-Styryl-poly(oxyethylene glycol)$_{300}$ 153, 6 mole percent 2 (4'vinyl)-4-benzyl-2,5-diphenyloxazole 101, cross-linked with 2 mole percent α,ω-bis-styryl-pentaethylene glycol 130

α-Styryl-poly(oxyethylene glycol)$_{300}$ **153** (0.084 g, 0.16 mmol), α,ω-bis-styryl-pentaethylene glycol **130** (0.0026 g, 0.004 mmol), (4'vinyl)-4-benzyl-2,5-diphenyloxazole **101** (0.004 g, 0.01 mmol) and AIBN 7 (0.0003 g, 0.002 mmol) were combined according to General Procedure 5 to give, after washing, polymer **158** as a clear gel (0.048 g, 54%). IR (gel compressed between NaCl discs): ν_{max}/cm^{-1} 3422 (s, O-H), 3060 (w, C-H aromatic), 3035 (w, C-H aromatic), 2923 (s, C-H aliphatic), 2865 (s, C-H aliphatic), 1741 (w), 1719 (w), 1701 (w), 1652 (m), 1634 (m), 1610 (m, C=C aromatic), 1581 (w, C=C aromatic), 1559 (w), 1541 (w), 1510 (s, C=C aromatic), 1458 (m), 1352 (m), 1297 (m), 1247 (s), 1173 (m), 1113 (s, C-O), 948 (m), 885 (s), 831 (m) and 708 (w).

POP-Sc support 159: α-Styryl-poly(oxyethylene glycol)$_{300}$ 153, 8 mole percent 2,5-diphenyl-4-(4'-vinylbenzyl)oxazole 101, cross-linked with 2 mole percent α,ω-bis-styryl-penta(ethylene glycol) 130

α-Styryl-poly(oxyethylene glycol)$_{300}$ **153** (0.128 g, 0.25 mmol), α,ω-bis-stryl-pentaethylene glycol **130** (0.002 g, 0.01 mmol), (4'vinyl)-4-benzyl-2,5-diphenyloxazole **101** (0.007 g, 0.02 mmol) and AIBN 7 (0.0005 g, 0.003 mmol) were combined according to General Procedure 5 to give, after washing,

polymer **159** as a clear gel (0.043 g, 34%). IR (gel compressed between NaCl discs): ν_{max}/cm^{-1} 3405 (s, O-H), 3060 (w, C-H aromatic), 3025 (w, C-H aromatic), 2920 (s, C-H aliphatic), 2847 (s, C-H aliphatic), 1965 (w), 1648 (s), 1634 (s), 1614 (s, C=C aromatic), 1581 (m, C=C aromatic), 1555 (m), 1515 (s), 1504 (s, C=C aromatic), 1488 (s), 1470 (s), 1454 (s), 1430 (s), 1417 (m), 1373 (m), 1355 (m), 1244 (m), 1096 (s, C-O), 952 (m), 889 (m), 827 (m) and 663 (s).

POP-Sc support 160: α,ω-Styryl-poly(oxyethylene glycol)$_{300}$ 153, 10 mole percent (4'vinyl)-4-benzyl-2,5-diphenyloxazole 101, cross-linked with 2 mole percent α,ω-bis-styryl-pentaethylene glycol 130

α-Styryl-poly(oxyethylene glycol)$_{300}$ **153** (0.083 g, 0.16 mmol), α,ω-bis-styryl-pentaethylene glycol **130** (0.0016 g, 0.004 mmol), (4'vinyl)-4-benzyl-2,5-diphenyloxazole **101** (0.0062 g, 0.018 mmol) and AIBN 7 (0.0003 g, 0.002 mmol) were combined according to General Procedure 5 to give, after washing, polymer **160** as a clear gel (0.026 g, 28%). IR (gel compressed between NaCl discs): ν_{max}/cm^{-1} 3406 (s, O-H), 3051 (w, C-H aromatic), 3025 (w, C-H aromatic), 2928 (s, C-H aliphatic), 2847 (s, C-H aliphatic), 1971(w), 1652 (m), 1645 (m), 1611 (s, C=C aromatic), 1581 (m, C=C aromatic), 1550 (w), 1506 (s, C=C aromatic), 1466 (s), 1454 (s), 1350 (m), 1324 (m), 1301 (m), 1247 (m), 1178 (m), 1096 (s, br, C-O), 952 (w), 889 (w), 832 (w) and 779.

Solvent swelling assay upon polymers 154-160

The polymers **154-160** were packed into the bottom of a polypropylene disposable syringe (1 mL), with the tip removed, housing a nylon frit (0.45 μm). A reservoir containing solvent was placed below the syringe and the reservoir raised until the solvent was just brought into contact with the bottom of the syringe. A volume reading was recorded when there was no further volume increase (Appendix B, Table 40).

Scintillation Assay Development

A stock solution was prepared by dissolving [^{14}C]benzoic acid (0.021 mg, 1.62 μCi) in distilled water (445 μL). An aliquot of this stock solution (10 μL) was added to 0, 10, 20, 30 and 40 μL of distilled water in duplicate. The resultant solutions were monitored in a scintillation counter. The solutions were added, in duplicate, to an accurate mass of the POP-Sc support **156** (~2 mg) and POP support **154** (~2 mg) and were monitored in a scintillation counter (4 min). The maximum number of counts that can be obtained from the system was determined by the addition of an aliquot of [^{14}C]benzoic acid dissolved in the appropriate volume of water to commercial scintillation fluid (5 mL) and monitoring the samples in a scintillation counter (4 min) **Table 21**.

Water / μL	[^{14}C]benzoic acid / cpm	154 + [^{14}C]benzoic acid / cpm [a]	156 + [^{14}C]benzoic acid / cpm [a]	Scintillation fluid + [^{14}C]benzoic acid / cpm [a]
10	28.75	572.13	27832.93	115789.63
10	40.00	581.63	25949.93	116051.63
20	29.75	323.25	17028.30	121204.00
20	28.25	238.50	23265.80	120096.00
30	30.00	230.13	14051.88	120938.00
30	22.25	378.88	16375.38	119404.00
40	28.00	275.00	15638.25	128704.25
40	25.50	170.25	3683.50	124610.25
50	34.50	187.38	8679.13	121982.13
50	25.25	183.63	-	122292.13

Table 21: Effect of assay volume upon observed scintillation. Mean error = $^{+}$/-11%.

[a] Cpm values are background corrected.

Assay to Determine the Optimal Scintillant Content

A stock solution was prepared by dissolving [^{14}C]benzoic acid in distilled water (450 μL). An aliquot of this stock solution (20 μL) was monitored in a scintillation counter in duplicate/triplicate. The maximum number of counts that can be obtained from the system was determined by the addition of an aliquot of [^{14}C]benzoic acid (20 μL) to commercial scintillation fluid (5 mL) in triplicate and monitoring the samples in a scintillation counter (4 min) **Table 22**.

Stock solution	[^{14}C]benzoic acid stock (20 μL) / cpm	[^{14}C]benzoic acid stock (20 μL) + scintillation fluid (5 mL) / cpm
A	22.5	148605.0
	40.5	150802.0
	-	149891.0
Average	31.5	149766.0
B	174.3	33650.0
	35.8	33818.3
	145.0	32462.3
Average	118.4	33310.2
C	27.50	82557.0
	23.00	83319.3
	-	84185.5
Average	25.25	83328.7

Table 22: Scintillation counts of [^{14}C]benzoic acid stock solutions **A**, **B** and **C**. Mean error = $^{+}$/-14%.

The [^{14}C] benzoic acid solutions **A-C** (20 μL) were added, in triplicate, to an accurate mass (~2 mg) of POP-Sc supports **155-160** and in duplicate to POP support **154 Table 23**.

Polymer	Mass / mg	cpm	Background corrected / cpm	Background corrected / cpm mg^{-1}	Percentage efficiency	Percentage efficiency [d]
154[a]	2.2	379.50	348.0	158.18	0.11	
154[a]	2.2	428.25	396.75	180.34	0.12	
Average					0.115	0.16
155[a]	2.3	12966.8	12935.3	5624.05	3.76	
155[a]	2.2	11317.8	11317.8	5374.43	3.59	
155[a]	2.0	8222.75	8222.75	4095.63	2.74	
Average					3.36	4.8
156[a]	2.3	15192.0	15160.5	6591.52	4.40	
156[a]	2.0	14969.0	14937.5	7468.75	4.99	
156[a]	2.0	18373.0	18341.5	9170.75	6.12	
Average					5.17	7.4
157[b]	2.2	4692.00	4573.67	2078.94	6.24	
157[b]	2.3	5204.50	5086.12	2211.38	6.64	
157[b]	2.2	4015.25	3896.92	1771.33	5.32	
Average					6.07	8.7
158[a]	1.9	19872.8	19841.3	10442.79	6.97	
158[a]	1.7	21258.0	21226.5	12486.18	8.34	
158[a]	2.2	22896.8	22865.3	10393.32	6.94	
Average					7.42	10.6
159[c]	1.8	7945.75	7920.5	4400.28	5.28	
159[c]	2.3	10160.5	10135.25	4406.63	5.29	
159[c]	2.6	11030.8	11005.55	4232.90	5.08	
Average					5.22	7.5
160[b]	2.3	4159.00	4040.67	1756.81	5.27	
160[b]	2.2	4264.25	4145.92	1884.51	5.66	
160[b]	2.4	4358.00	4239.67	1766.53	5.30	
Average					5.41	7.7

Table 23: Observed scintillation counts of [^{14}C]benzoic acid stock solutions **A**, **B** and **C** added to polymers **154-160**. Mean error = $^{+}$/-7%.

[a] Values are background corrected and percentage efficiency determined using Table 22 (A) average value. [b] Values are background corrected and percentage efficiency determined using Table 22 (B) average value. [c] Values are background corrected and percentage efficiency determined using Table 22 (C) average value. [d] All values have been adjusted to accommodate the fact that a fluor based solely on 2,5-diphenyloxazole **1** gives only 70% of the cpm obtained with a multi-fluor scintillation fluid.[215]

POP-Sc support 161: Fmoc-Gly-OH coupling to POP-Sc support 158

2,6-Dichlorobenzoylchloride (0.05 mL, 0.3 mmol), pyridine (anhydrous, 0.07 mL, 0.8 mmol), POP-Sc support **158** (0.050 g, 0.13 mmol) and Fmoc-Gly-OH (0.112 g, 0.38 mmol) in DMF (anhydrous, 2.0 mL) were combined according to General Procedure 3 to give, after washing, POP-Sc support **161** as a yellow polymer (0.064 g). IR (gel compressed between NaCl discs): ν_{max}/cm^{-1} 3421 (s, N-H), 3069 (w, C-H aromatic), 3042 (w, C-H aromatic), 2924 (s, C-H aliphatic), 2865 (s, C-H aliphatic), 1750 (s), 1720

(s, C=O), 1652 (m), 1608 (m, C=C aromatic), 1581 (m, C=C aromatic), 1537 (m), 1510 (s, C=C aromatic), 1452 (s), 1350 (m), 1244 (s), 1191 (s), 1106 (s, C-O), 1054 (s), 947 (m), 830 (m) and 740 (m).

POP-Sc support 162: Fmoc-release assay of POP-Sc support 161

POP-Sc support **161** was weighed accurately, in quadruplicate, into a sample vial and treated according to General Procedure 4 **Table 24**.

Mass / g	Absorption @ 290 nm	Absorption @ 290 nm / mg
0.0016	2.298	1.436
0.0021	2.469	1.176
0.0019	2.414	1.271
0.0014	2.027	1.448
Average		1.333

Table 24: Fmoc-release assay of POP-Sc support **161**. Mean error = $^{+}$/-8%.

The average loading of POP-Sc support **158** was established to be 0.81 mmol/g (32%).[235]

20% piperidine/DMF (10 mL) was added to polymer resin **161** (0.057 g) and the resultant mixture stirred (1 hr). The polymer was collected by filtration and washed *in-situ* with DCM (3 x 30 mL), DCM/MeOH 1:1 (30 mL) and MeOH (3 x 30 mL). The polymer was pre-dried under suction before being dried to constant mass to give polymer **162** (0.050 g). IR (gel compressed between NaCl discs): ν_{max}/cm^{-1} 3356 (s, N-H), 2924 (s, C-H aliphatic), 2847 (s, C-H aliphatic), 1732 (m), 1710 (m), 1692 (m), 1665 (m), 1647 (m), 1630 (m), 1608 (m, C=C aromatic), 1555 (m), 1537 (m), 1510 (m), 1537 (m), 1510 (m, C=C aromatic), 1453 (m), 1430 (m), 1249 (m), 1111 (m, C-O), 1071 (m) and 1036 (m).

POP-Sc support 163: Fmoc-Gly-OH coupling to POP-Sc support 162

2,6-Dichlorobenzoylchloride (0.05 mL, 0.3 mmol), pyridine (anhydrous, 0.07 mL, 0.8 mmol), POP-Sc support **162** (0.050 g, 0.13 mmol) and Fmoc-Gly-OH (0.112 g, 0.38 mmol) in DMF (anhydrous, 2.0 mL) were combined according to General Procedure 3 to give, after washing, POP-Sc support **163** as a yellow polymer (0.036 g). IR (gel compressed between NaCl discs): ν_{max}/cm^{-1} 3424 (m, N-H), 3060 (w, C-H), 3016 (w, C-H), 2925 (s, C-H aliphatic), 2856 (s, C-H aliphatic), 1741 (m), 1719 (m), 1705 (m), 1683 (m), 1657 (m), 1634 (m), 1603 (m, C=C aromatic), 1577 (m, C=C aromatic), 1559 (m), 1541 (m), 1510 (m, C=C aromatic), 1444 (m), 1404 (w), 1382 (w), 1346 (w), 1244 (m), 1191 (m), 1093 (s, C-O), 947 (m), 827 (w), 761 (w), 734 (w) and 668 (w).

Fmoc-release assay of POP-SC support 163

POP-Sc support **163** was weighed accurately, in quadruplicate, into a sample vial and treated according to General Procedure 4 **Table 25.**

Mass / g	Absorption @ 290 nm	Absorption @ 290 nm / mg
0.0009	1.594	1.771
0.0015	1.673	1.115
0.0024	2.255	0.940
0.0011	1.503	1.366
Average		1.298

Table 25: Fmoc-release assay of POP-Sc support **163**. Mean error = $^{+}$/-21%.

The average efficiency of the second Fmoc-Gly-OH coupling to polymer **158** was established to be 0.79 mmol/g (98%).[235]

4.7 Scintillation Proximity Hydrolysis Assay

Polymer resin 164: Wang derivatisation of polymer resin 121

Polymer resin **121** (150–75 μm) (2.000 g, theoretically 0.96 mmol/g chloride groups), hydroxybenzyl alcohol (0.730 g, 5.76 mmol) and sodium methoxide (0.320 g, 5.63 mmol) were combined and stirred in DMF (40 mL) overnight (50 °C). The reaction mixture was cooled to room temperature and the polymer resin separated from the reaction mixture by filtration and then washed with dioxane (50 mL), dioxane/water 3:1 (50 mL), dioxane (50 mL) and MeOH (50 mL). The resin was dried under reduced pressure to constant mass to provide polymer resin **164** (1.780 g, 82%). IR (KBr disc): ν_{max}/cm^{-1} 3447 (m, O-H), 3064 (m, C-H aromatic) , 3023 (m, C-H aromatic), 2920 (s, C-H aliphatic), 2850 (s, C-H aliphatic), 1947 (w), 1871 (w), 1805 (w), 1769 (w), 1754 (w), 1733 (w), 1718 (w), 1698 (w), 1686 (w), 1657 (w), 1600 (m, C=C aromatic), 1544 (w), 1540 (w), 1510 (m, C=C aromatic), 1492 (m), 1423 (m), 1377 (m), 1347 (m), 1306 (w), 1286 (w), 1221 (m), 1174 (m), 1118 (w), 1067 (w), 1005 (m, C-O), 904 (w), 869 (w), 820 (w), 754 (m), 693 (s) and 533 (m).

Polymer resin 165: Fmoc-Gly-OH coupling to polymer support 164

2,6-Dichlorobenzoylchloride (0.04 mL, 0.3 mmol), pyridine (anhydrous, 0.05 mL, 0.6 mmol), polymer resin **164** (0.100 g, theoretically 0.96 mmol/g hydroxyl groups) and Fmoc-Gly-OH (0.086 g, 0.29 mmol) in DMF (anhydrous, 5.0 mL) were combined according to General Procedure 3 to give polymer resin **165** (0.080 g, 62%). IR (KBr disc): ν_{max}/cm^{-1} 3422 (m, N-H), 3053 (m, C-H aromatic), 3023 (m, C-H aromatic), 2922 (s, C-H aliphatic), 2840 (m, C-H aliphatic), 1728 (s, C=O), 1720 (s, C=O), 1698 (m), 1652 (m), 1601 (m, C=C aromatic), 1586 (m, C=C aromatic), 1560 (m), 1544 (m), 1510 (s, C=O aromatic), 1493 (s), 1448 (s), 1377 (w), 1342 (w), 1245 (m), 1171 (s, C-O), 1052 (w), 1026 (w), 1006 (w), 904 (w), 818 (w), 758 (s), 698 (s) and 537 (m).

Fmoc-release assay of polymer resin 165

Polymer resin **165** (1-2 mg) was weighed accurately, in quadruplicate, into a sample vial and treated according to General Procedure 4 **Table 26**.

Mass / g	Absorption @ 290 nm	Absorption @ 290 nm / mg
0.0014	1.405	1.004
0.0012	1.338	1.115
0.0016	1.742	1.089
0.0014	1.525	1.089
Average		1.074

Table 26: Fmoc-release assay of POP-Sc support **165**. Mean error = $^{+}/_{-}$3%.

The average loading of polymer resin **164** was established to be 0.65 mmol / g (68%).[235]

POP-Sc support 166: [^{3}H]Acetylation of POP-Sc support 158

A sample of POP-Sc support **158** (0.010 g, theoretically 2.5 mmol/g hydroxyl groups) was weighed accurately into a polypropylene centrifuge tube (0.5 mL). DMAP (catalytic amount) in DCM (200 μL) was added to the tube. To the swollen gel was added pyridine (2.54 μL, 30.0 μmol) and [^{3}H]acetic anhydride (2.36 μL, 30.0 μmol). The contents of the tube were mixed and then concentrated to the bottom of the tube by pulsing in a centrifuge (10,000 rpm, 10 s). The reaction mixture was left to stand at room temperature (4 days). The [^{3}H]acetylated POP-Sc support **166** was transferred to a polypropylene micro centrifuge filter tube (0.4 μm) and washed with DCM (40 μL). The polymer was separated from the washing solution by pulsing in the centrifuge (10,000 rpm, 10 s). The polymer was then washed with MeOH (40 μL). This procedure was repeated six times. The polymer was then dried, at room temperature, to constant mass (0.008 g).

Polymer resin 167: [^{3}H]Acetylation of polymer resin 164

Using the same procedure as described for POP-Sc support **166**, Polymer resin **164** (0.010 g, theoretically 0.96 mmol/g hydroxyl groups), DMAP (catalytic amount), pyridine (0.97 μL, 12.0 μmol) and [^{3}H]acetic anhydride (0.91 μL, 10 μmol) in DCM (200 μL) were combined to give polymer resin **167** (0.008 g).

POP-Sc support 168: [^{1}H]Acetylation of POP-Sc support 158

Using the same procedure as described for POP-Sc support **166**, POP-Sc support **158** (0.010 g, 0.03 mmol), DMAP (catalytic amount), pyridine (2.54 μL, 30.0 μmol) and acetic anhydride (2.36 μL, 25.0 μmol) in DCM (200 μL) were combined to give, after washing, POP-Sc support **168** as a clear gel. IR (gel compressed between NaCl discs): ν_{max}/cm^{-1} 3381 (s, O-H), 3060 (w, C-H aromatic), 3024 (w, C-H aromatic), 2920 (s, C-H aliphatic), 2847 (m, C-H aliphatic), 1714 (m), 1692 (m), 1661 (m), 1644 (m), 1630 (m), 1607 (m, C=C aromatic), 1586 (m), 1550 (m), 1537 (m), 1510 (m, C=C aromatic), 1493 (m), 1484 (m), 1470 (s), 1453 (s), 1417 (m), 1249 (m) and 1102 (s, br, C-O).

Polymer resin 169: [^{1}H]Acetylation of polymer resin 164

Using the same procedure as described for POP-Sc support **166**, Polymer resin **164** (0.500 g, theoretically 0.96 mmol/g hydroxyl groups), DMAP (catalytic amount), pyridine (17.7 mL, 218 mmol) and acetic anhydride (1.8 mL, 19 mmol) in DCM (10 mL) were combined to give polymer resin **169** (0.327 g, 63%). IR (gel compressed between NaCl discs): ν_{max}/cm^{-1} 3060 (m, C-H aromatic), 3023 (m, C-H aromatic), 2922 (s, C-H aliphatic), 2847 (m, C-H aliphatic), 1735 (s, C=O), 1719 (m), 1686 (m), 1654 (m), 1637 (w), 1600 (m, C=C aromatic), 1560 (m), 1542 (w), 1509 (s, C=C aromatic), 1491 (s), 1449 (s), 1376 (m), 1302 (w), 1218 (s), 1173 (s), 1111 (m), 1067 (m), 1017 (m), 960 (m), 903 (m), 820 (m), 754 (s) and 692 (s).

Scintillation counting of polymer supports 158, 164 and 166-169

An aliquot of the polymer supports **158**, **164** and **166-169** (1-2 mg) were weighed accurately into glass scintillation vials. These polymer support samples were counted in a scintillation counter (1 min). Commercial scintillation fluid (5 mL) was added to each sample and subsequently counted in a scintillation counter (1 min) **Table 27**.

Polymer	Mass / g	Polymer only / cpm	Polymer + scintillation fluid / cpm
158	0.0008	31.0	40.0
158	0.0007	74.0	70.0
158	0.0004	10.0	37.0
164	0.0018	11.0	17.0
164	0.0013	30.0	26.0
166	0.0016	53102.0	125501.0
166	0.0018	64627.0	159296.0
166	0.0009	44602.0	107372.0
167	0.0007	10916.0	23824.0
167	0.0007	6385.0	10926.0
168	0.0007	11.0	19.0
168	0.0007	39.0	53.0
168	0.0013	8.0	23.0
169	0.0022	11.0	16.0
169	0.0018	5.0	21.0

Table 27: Scintillation counting of polymers **158**, **164** and **166-169**. **166-167** mean error = $^{+}$/-23%.

Resin 169 incubated with KOH/benzene/18-crown-6 and subsequent IR-spectroscopic analysis

Polymer resin **169** (0.008 g) was weighed into five glass reaction tubes. To each tube was added a solution of KOH dissolved in benzene (1 mL, 10 M, 18-C-6 catalytic amount) and the resultant suspension stirred. After 3, 11.5, 26, 52.5, and 72 hr., the polymer resin was collected by filtration and washed with water (40 mL), MeOH (40 mL), DCM/MeOH 1:1 (40 mL) and DCM (40 mL). The polymer was dried to constant mass and then combined with KBr, pressed into a disc and analysed by IR-spectroscopy (Table 9).

Polymers 166 and 167 incubated with both KOH/benzene/18-crown-6 and KOH/water/18-crown-6, whilst scintillation counting

Polymer supports **166** (0.003 g), (0.001 g) and **167** (0.003 g), (0.003 g) were weighed accurately into a glass scintillation vial. To each vial was added separately an aqueous solution of KOH (10 mL, 0.18 M, 18-crown-6 catalytic amount) and a solution of KOH dissolved in benzene (10 mL, 0.18 M, 18-crown-6 catalytic amount). The assay mixtures were counted in a scintillation counter immediately after the addition of the KOH solution (15 min/hr. for 74 hr.) (Appendix D, Table 46).

4.8 Scintillation Proximity Hybridisation Assay

Poly(oxyethylene glycol)$_{350}$ monomethyl ether *p*-toluene sulfonate 170

Using the same procedure as described for triethylene glycol di-*p*-toluene sulfonate **128**, a solution of TsCl (27.792 g, 143.00 mmol) in DCM (80 mL) was added to a solution of poly(oxyethylene glycol)$_{350}$ monomethyl ether (50.000 g, 143.00 mmol), triethylamine (40.30 mL, 290.0 mmol) and DMAP (0.177 g, 1.4 mmol) in DCM (75 mL) to give a yellow oil. This oil was dissolved in hexane (3 x 200 mL) and the unreacted TsCl separated from the reaction mixture by filtration. The filtrate was concentrated under reduced pressure to provide poly(oxyethylene glycol)$_{350}$ monomethyl ether *p*-toluene sulfonate as a pale yellow oil (64.494 g, 90%), which was reacted on without further purification. IR (thin film): ν_{max}/cm^{-1} 3064 (w, C-H aromatic), 3042 (w, C-H aromatic), 2873 (s, C-H aliphatic), 1731 (w), 1598 (m, C=C aromatic), 1574 (w, C=C aromatic), 1494 (m, C=C aromatic), 1454 (m), 1355 (s), 1292 (m), 1248 (s), 1189 (s), 1177 (s), 1106 (s, C-O), 1018 (m), 924 (s), 818 (m), 777 (m), 758 (m), 706 (w), 691 (w) and 664 (m). ^{1}H NMR (300 MHz, $CDCl_3$): δ_H 2.25 (3H, s), 3.17 (3H, s), 3.34-5.50 (32H, m), 3.96 (2H, t, *J*=5.6), 7.17 (2H, d, *J*=9.6) and 7.59 (2H, d, *J*=9.6). ^{13}C NMR (75 MHz, $CDCl_3$, PENDANT)[270]: δ_C 21.0 (CH_3), 58.4 (CH_3), 66.4 (CH_2), 68.0 (CH_2), 68.8 (CH_2), 69.9 (CH_2), 70.1 (CH_2), 71.3 (CH_2), 127.4 (CH), 129.3 (CH), 132.4 (C) and 144.3 (C). LRMS (APCI): *m/z* 583 (100%, $[M + H]^+$), 627 (100%, $[M + C_2H_4O + H]^+$), 539 (81%, $[M - C_2H_4O + H]^+$), 671 (75%, $[M + 2(C_2H_4O) + H]^+$), 715 (48%, $[M + 3(C_2H_4O) + H]^+$), 495 (47%, $[M - 2(C_2H_4O) + H]^+$), 759 (31%, $[M + 4(C_2H_4O) + H]^+$), 451 (21%, $[M - 3(C_2H_4O) + H]^+$), 803 (14%, $[M + 5(C_2H_4O) + H]^+$). $]^+$). HRMS (EI): *m/z* 605.2584 ($[M + Na]^+$); calculated for $C_{26}H_{46}O_{12}NaS$ 605.2608.

α-Styryl-poly(oxyethylene glycol)$_{350}$ monomethyl ether 171

Using the same procedure as described for α,ω-bis-styryl-triethylene glycol **129**, 4-acetoxystyrene (10.0 mL, 63 mmol) was reacted with an ethanolic solution of potassium hydroxide (7.823 g, 125.50 mmol). An ethanolic solution of poly(oxyethylene glycol)$_{350}$ monomethyl ether *p*-toluene sulfonate (37.934 g, 75.24 mmol) was added to the refluxing reaction mixture to give α-styryl-poly(oxyethylene glycol)$_{350}$ monomethyl ether **171**, after flash column chromatography (EtOAc), as a pale yellow oil (12.176 g, 43%). IR (thin film): ν_{max}/cm^{-1} 3065 (w, C-H aromatic), 3033 (w, C-H aromatic), 2871 (s, C-H aliphatic), 1627 (w), 1607 (m, C=C aromatic), 1574 (w, C=C aromatic), 1510 (s, C=C aromatic), 1454 (m), 1349 (m), 1301 (m), 1249 (s), 1199 (m), 1176 (m), 1110 (s, C-O), 992 (m), 947 (m) and 838 (m). ^{1}H NMR (300 MHz, $CDCl_3$): δ_H 3.34 (3H, s), 3.49-4.11 (38H, m), 5.08 (1H, dd, *J*=13.1 1.2), 5.57 (1H, dd, *J*=21.2 1.2), 6.62 (1H, dd, *J*=21.2 13.1), 6.83 (2H, d, *J*=10.4) and 7.29 (2H, d, *J*=10.4). ^{13}C NMR (75 MHz, $CDCl_3$, PENDANT)[270]: δ_C 59.0 (CH_3), 63.6 (CH_2), 67.4 (CH_2), 69.6 (CH_2), 70.5 (CH_2), 70.8 (CH_2), 71.9 (CH_2), 111.6 (CH_2), 114.4 (CH), 114.5 (CH), 127.3 (CH), 130.5 (C), 136.1 (CH) and 158.5 (C). LRMS (APCI): *m/z* 563 (100%, $[M - H]^+$), 607 (90%, $[M + C_2H_4O - H]^+$), 519 (69%, $[M - C_2H_4O -$

$H]^+$), 651 (43%, $[M + 2(C_2H_4O) - H]^+$), 475 (12%, $[M - 2(C_2H_4O) – H]^+$). $]^+$). HRMS (EI): *m/z* 553.2997 ($[M + Na]^+$); calculated for $C_{27}H_{46}O_{10}Na$ 553.2989.

Poly(oxyethylene glycol)$_{2000}$ di-*p*-toluenesulfonate 172

Using the same reaction procedure as described for triethylene glycol di-*p*-toluene sulfonate **128**, a solution of TsCl (3.891 g, 20.00 mmol) in DCM (60 mL) was added to a solution of poly(oxyethylene glycol)$_{2000}$ (10.000 g, 5.00 mmol), triethylamine (5.60 mL, 40.0 mmol) and DMAP (0.006 g, 0.05 mmol) in DCM (100 mL) to give a yellow oil following concentration under reduced pressure. In a modified work-up procedure, the oil was resuspended in the minimum volume of DCM and the resultant suspension separated by filtration and the filtrate concentrated under reduced pressure. This procedure was repeated four times. The resultant oil was dissolved in water (200 mL) and washed with Et_2O (3 x 30 mL). The aqueous phase was concentrated under reduced pressure to give poly(oxyethylene glycol)$_{2000}$ di-*p*-toluenesulfonate **172** as a colourless oil (11.332 g, 98%). IR (thin film): ν_{max}/cm^{-1} 2869 (s, C-H aliphatic), 1457 (w), 1350 (m, -SO_2O-), 1297 (w), 1249 (w), 1177 (m, -SO_2O-), 1105 (s, C-O), 1036 (w), 948 (w), 876 (w), 846 (w), 819 (w), 777 (w) and 668 (m). ^{1}H NMR (300 MHz, $CDCl_3$): δ_H 2.45 (6H, s), 3.55-3.69 (208H, m), 4.14 (4H, t, *J*=4.9), 7.48 (4H, d, *J*=8.3) and 7.78 (4H, d, *J*=8.3). ^{13}C NMR (75 MHz, $CDCl_3$, PENDANT)[270]: δ_C 20.7 (CH_3), 67.7 (CH_2), 68.5 (CH_2), 69.6 (CH_2), 127.0 (CH), 129.0 (CH), 132 (C) and 143 (C). LRMS (MALDI-TOF): *m/z* 2201 (100%, $[M + H]^+$), 2290 (97%, $[M + 2(C_2H_4O) + H]^+$), 2157 (96%, $[M - C_2H_4O + H]^+$), 2113 (95%, $[M - 2(C_2H_4O) + H]^+$), 2245 (94%, $[M + C_2H_4O + H]^+$), 2334 (89%, $[M + 3(C_2H_4O) + H]^+$), 2069 (87%, $[M - 3(C_2H_4O) + H]^+$), 2378 (86%, $[M + 4(C_2H_4O) + H]^+$), 2422 (86%, $[M + 5(C_2H_4O) + H]^+$), 2021 (76%, $[M - 4(C_2H_4O) + H]^+$), 1977 (69%, $[M - 5(C_2H_4O) + H]^+$), 2466 (61%, $[M + 6(C_2H_4O) + H]^+$), 2511 (60%, $[M + 7(C_2H_4O) + H]^+$), 1932 (54%, $[M - 6(C_2H_4O) + H]^+$), 2555 (47%, $[M - 8(C_2H_4O) + H]^+$), 1888 (42%, $[M - 7(C_2H_4O) + H]^+$), 2599 (38%, $[M + 9(C_2H_4O) + H]^+$), 1844 (34%, $[M - 8(C_2H_4O) + H]^+$).

α,ω-Bis-styryl-poly(oxyethylene glycol)$_{2000}$ 173

Using the same reaction procedure as described for α,ω-bis-styryl-tri(ethylene glycol) **129**, 4-acetoxystyrene (3.45 mL, 21.7 mmol) was reacted with an ethanolic solution of potassium hydroxide (2.701 g, 43.33 mmol). An ethanolic solution of poly(oxyethylene glycol)$_{2000}$ di-*p*-toluenesulfonate **172** (5.132 g, 2.22 mmol) was added to the refluxing reaction mixture. The reaction mixture was concentrated under reduced pressure, resuspended in DCM (150, 50, 30, mL) and then filtered. The filtrate was concentrated under reduced pressure to give brown oil. The oil was dissolved in water (100 mL) and neutralized with 20% $HCl_{(aq)}$. The solution was concentrated under reduced pressure to give brown oil. The oil was suspended in DCM (30 mL) and filtered. The solution was concentrated under reduced pressure and dissolved in water (100 mL) and washed with Et_2O (3 x 100 mL). The aqueous fraction was concentrated under reduced pressure to give yellow solid (2.382 g, 49%). Mp 47-48 °C. IR (thin film): ν_{max}/cm^{-1} 2936 (w, C-H aliphatic), 2882 (w, C-H aliphatic), 1606 (w, C-H aromatic), 1510 (w,

C-H aromatic), 1466 (m), 1408 (w), 1359 (w), 1344 (w), 1280 (m), 1248 (w), 1147 (m), 1114 (s), 1060 (m), 945 (w), 842 (m) and 668 (w). ^{1}H NMR (300 MHz, $CDCl_3$): δ_H 3.64-3.71 (216H, m), 3.85 (2H, t, *J*=4.6), 4.13 (4H, t, *J*=4.6), 5.11 (2H, d, *J*=10.9), 5.60 (2H, d, *J*=17.8), 6.65 (2H, dd, *J*=17.8 10.9), 6.87 (4H, d, *J*=8.6) and 7.32 (4H, d, *J*=8.6). ^{13}C NMR (75 MHz, $CDCl_3$, PENDANT)[270]: δ_C 67.2 (CH_2), 69.5 (CH_2), 70.3 (CH_2), 114.4 (CH), 127.1 (CH), 129.4 (CH_2), 130.3 (C), 136.0 (CH), Remaining quaternary signals remain too small to be resolved. LRMS (MALDI-TOF): *m/z* 2201 (100%, $[M + H]^+$), 2245 (91%, $[M + C_2H_4O + H]^+$), 2157 (91%, $[M - C_2H_4O + H]^+$), 2113 (89%, $[M - 2(C_2H_4O) + H]^+$), 2069 (77%, $[M - 3(C_2H_4O) + H]^+$), 2333 (75%, $[M + 3(C_2H_4O) + H]^+$), 2025 (68%, $[M - 4(C_2H_4O) + H]^+$), 2377 (62%, $[M + 4(C_2H_4O) + H]^+$), 1981 (61%, $[M - 5(C_2H_4O) + H]^+$), 2421 (52%, $[M + 5(C_2H_4O) + H]^+$), 1936 (47%, $[M - 6(C_2H_4O) + H]^+$), 1893 (39%, $[M - 7(C_2H_4O) + H]^+$).

POP-Sc support 174: α-styryl-poly(oxyethylene glycol)$_{350}$ monomethyl ether 171, 5 mole percent α-styryl-poly(oxyethylene glycol)$_{300}$ 153, 6 mole percent (4'vinyl)-4-benzyl-2,5-diphenyloxazole 101, cross-linked with 2 mole percent α,ω-bis-styryl-poly(oxyethylene glycol)$_{2000}$ 173

α-styryl-poly(oxyethylene glycol)$_{350}$ monomethyl ether **171** (0.550 g, 0.98 mmol), α-styryl-poly(oxyethylene glycol)$_{300}$ **153** (0.026 g, 0.06 mmol), (4'vinyl)-4-benzyl-2,5-diphenyloxazole **101** (0.022 g, 0.07 mmol), α,ω-*bis*-styryl-poly(oxyethylene glycol)$_{2000}$ **173** (0.049 g, 0.02 mmol), and AIBN **7** (0.001 g, 0.01 mmol) were combined according to General Procedure 5 to give, after washing, polymer **174** as a clear gel (0.306 g, 47%). IR (gel compressed between NaCl discs): ν_{max}/cm^{-1} 3512 (s, O-H), 3033 (m, C-H aromatic), 2917 (s, br, C-H aliphatic), 2599 (w), 2546 (w), 2484 (w), 2422 (w), 2235 (w), 2129 (w), 2058 (w), 1964 (m), 1887 (w), 1732 (w), 1714 (w), 1659 (m), 1650 (s), 1644 (s), 1614 (s, C=C aromatic), 1584 (s), 1556 (m), 1514 (s), 1504 (s, C=C aromatic), 1486 (s), 1470 (s), 1454 (s) and 696 (s).

Solvent swelling assay upon POP-Sc support 174

POP-Sc support **174** was packed into the bottom of a polypropylene disposable syringe (1 mL), with the tip removed, housing a nylon frit (0.45 μm). A reservoir containing solvent was placed below the syringe and the reservoir raised until the solvent was just brought into contact with the bottom of the syringe. A volume reading was recorded when there was no further volume increase (Appendix B, Table 41).

POP-Sc-PNA(T_1)-Fmoc: Coupling of the first Fmoc-PNA(T)-OH to POP-Sc support 174

A solution of Fmoc-PNA(T)-OH (0.005 g, 0.01 mmol) in DMF (500 μL) and *N*-methylimidazole (NMI) (2.96 μL, 37.2 μmol) was added to MSNT (0.003 g, 0.01 mmol) ,the resultant mixture was added to the polymer (0.051 g, 0.01 mmol), contained in a Bio-rad, polypropylene mesh (10 μm) filter tube and

incubated (30 min). A further aliquot of DMF (410 μL) was added to the reaction mixture and incubated (2.5 hr.). The polymer was collected by filtration and washed *in-situ* with DCM (3 mL), DCM/MeOH 1:1 (3 mL) and MeOH (3 mL). This procedure was repeated three times. The PNA-derived polymer was placed in a vacuum oven at 35 °C for 3 hours and dried to constant mass to give POP-Sc-PNA(T_1)-Fmoc as a clear polymer gel (0.047 g).

Acetylated POP-Sc-PNA(T_1)-Fmoc: Acetylation of POP-Sc-PNA(T_1)-Fmoc.

The stock solutions acetic anhydride (0.0010 mmol/μL), DMAP (0.0001 mmol/μL) and pyridine (0.0010 mmol/μL) in DCM were prepared. Accordingly, aliquots of these stock solutions were combined: acetic anhydride (15 μL, 15 μmol), DMAP (5 μL, 0.5 μmol), pyridine (38 μL, 38 μmol) and DCM (542 μL). The resultant mixture was added to POP-Sc-PNA(T_1)-Fmoc (0.047 g, 0.01 mmol) and incubated for 2 hours. The polymer was collected by filtration and washed with DCM (3 mL), DCM/MeOH 1:1 (3 mL) and MeOH (3 mL). This procedure was repeated twice. The polymer was placed in a vacuum oven at 35 °C and dried to constant mass to provide acetylated POP-Sc-PNA(T_1)-Fmoc (0.047 g).

General Procedure 8: Fmoc-PNA(T)-OH Coupling to POP-Sc-PNA(T_{1-9})

A solution of Fmoc-PNA-OH (0.005 g, 0.01 mmol) in DMF (577 μL) and *N,N*-diisopropylethylamine (DIPEA) (3.08 μL, 17.6 μmol) was added to PyBOP (0.005 g, 0.01 mmol). The resultant mixture was added to the PNA-derived polymer (~0.04 g, theoretical loading 0.093 mmol/g) and incubated (2 hr.). The polymer was separated from the reaction mixture by filtration and washed *in-situ* with DCM (3 mL), DCM/MeOH 1:1 (3 mL) and MeOH (3 mL). This filtration-washing procedure was repeated three times. The PNA-derived polymer was placed in a vacuum oven at 35 °C overnight and dried to constant mass to give polymer as a clear gel. The whole of general procedure 8 was repeated nine times sequentially, followed by General Procedure 9, to give POP-Sc-PNA(T_{10}) **175**.

General Procedure 9: Fmoc Release Assay

Following each Fmoc-PNA(T)-OH coupling, the entire polymer sample was accurately weighed (~0.04 g). A 20% piperidine/DMF solution (500 μL) was added to the filter tube and the resultant suspension agitated. The filtrate was separated from the polymer by filtration. This procedure was repeated six times. The assay solutions were combined in a quartz cuvette (3 mL). The absorption of the Fmoc/piperidine adduct **74** was measured at 290 nm against a 20% piperidine/DMF blank. The absorbance per mg was calculated. The loading (mmol/g) of each polymer was determined by dividing the average absorbance per mg at 290 nm by 1.65 **Table 28**.[235] The polymer was collected by filtration and washed *in-situ* with DCM (3 mL), DCM/MeOH 1:1 (3 mL) and MeOH (3 mL). This filtration-washing procedure was repeated three times. The PNA-derived polymer was placed in a vacuum oven at 35 °C

and dried to constant mass. This entire procedure was repeated following the coupling of each of the ten Fmoc-PNA(T)-OH coupling reactions (general procedure 8)

POP-Sc-PNA(T_x)	Mass / g	Abs @ 290 nm	Abs @ 290 nm / mg	Loading / mmolg^{-1}
POP-Sc-PNA(T_1)-Fmoc	0.0473	2.602	0.055	0.03
POP-Sc-PNA(T_2)-Fmoc	0.0500	2.373	0.048	0.03
POP-Sc-PNA(T_3)-Fmoc	0.0510	2.492	0.049	0.03
POP-Sc-PNA(T_4)-Fmoc	0.0511	2.552	0.050	0.03
POP-Sc-PNA(T_5)-Fmoc	0.0476	2.325	0.049	0.03
POP-Sc-PNA(T_6)-Fmoc	0.0460	2.222	0.048	0.03
POP-Sc-PNA(T_7)-Fmoc	0.0356	1.826	0.051	0.03
POP-Sc-PNA(T_8)-Fmoc	0.0334	1.787	0.054	0.03
POP-Sc-PNA(T_9)-Fmoc	0.0402	2.049	0.051	0.03
POP-Sc-PNA(T_{10})-Fmoc	0.0412	1.843	0.045	0.03

Table 28: Fmoc Release Assay following the ten sequential couplings of Fmoc-PNA(T)-OH to POP-Sc support **174**. Mean estimated error = $^{+}$/-20%.

Radio-labelling DNA (T_{10}) and DNA(A_{10}) at the 5' termini with ^{33}P from [γ-^{33}P]ATP using PNK

Three assay solutions were prepared containing **A**) DNA(A_{10}) (2 µL, 40 pmol), **B**) DNA(T_{10}) (2 µL, 40 pmol) and **C**) water (2 µL). To each assay solution was added water (13 µL), PNK 10 x buffer (2 µL), [γ^{33}P]ATP (2 µL, 0.37 MBq/µL) and PNK (1 µL, 5 µ/µL). The assay solutions were incubated at 37 °C (56 min). The temperature was then increased to 65 °C (20 min). An aliquot of water (180 µL) was added to each tube.

General Procedure 10: DE81 Assay

For each assay solution A-C two pieces of DE81 paper (Whatman) were marked 'Total' and two marked 'Incorporated'. An aliquot of the assay mixtures **A-B** (10 µL) (0.2 pmol DNA) and **C** (10 µL) was pipetted onto each piece of paper and air dried (10 min). the pieces of paper marked 'Incorporated' were washed in Na_2HPO_4 (5 x 10 mL, 150 nM) for 5 minutes, water (10 mL), ethanol (10 mL), acetone (10 mL) and then air dried. The pieces of paper marked 'Incorporated' and 'Total' were placed in scintillation vials with scintillation fluid (1 mL) and then monitored in a scintillation counter **Table 29**.

Tube	DE81 Total	DE81 Incorporation
A	1634300	852005
A	1697060	869747
B	1602800	555810
B	1723740	550767
C	1674830	22990
C	1774860	29567

Table 29: Scintillation counting data for DE81 assay of **A)** ^{33}P-DNA(A_{10}), **B)** ^{33}P-DNA(T_{10}) and **C)** ^{33}P-blank control. Mean error = $^{+}$/-4%.

Scintillation Hybridisation Assay of POP-Sc-PNA(T_{10}) 175

The polymers POP-Sc-PNA(T_{10}) **175** (6 x 0.0014 g) and POP-Sc **174** (6 x 0.0014 g) were subjected to a washing (6 x SSPE {3 x 500 µL}) / centrifugation (10000 rpm, 5 sec) procedure and then counted in a scintillation counter (Appendix E, Table 48).

To each assay solution **A-C** (135 µL) was added 6 x SSPE (2115 µL). An aliquot (100 µL, 0.02 MBq) of each assay solution was added to scintillation fluid (5 mL) in duplicate and then monitored in a scintillation counter **Table 30**.

Tube	Sc-fluid / cpm
A	872390
A	819305
B	1011525
B	1016794
C	1071620
C	1077167

Table 30: Scintillation counting data for assay tube **A)** ^{33}P-DNA(A_{10}), **B)** ^{33}P-DNA(T_{10}) and **C)** ^{33}P-blank control. Mean error = $^{+}$/-1%.

An aliquot of the diluted assay solutions **A-C** (500 µL) was added to POP-Sc-PNA(T_{10}) **175** and POP-Sc **174** in duplicate and incubated (25 min). These assay mixtures were then monitored in a scintillation counter (Appendix E, Table 48). The polymers were isolated by centrifugation (5000 rpm, 30 sec) and monitored in a scintillation counter (Appendix E, Table 48). The polymer samples were sequentially washed-monitored and centrifuged (5000 rpm, 30 sec)-monitored using 4 x SSPE (500 µL), 2 x SSPE (500 µL) and water (500 µL) (Appendix E, Table 48). The polymers were then immersed in scintillation fluid (10 mL) and monitored in a scintillation counter (Appendix E, Table 48).

PNK-Assay

Seven samples of POP-Sc-PNA(T_{10}) **175** were accurately weighed (0.0015 g, 45000 pmol) into Whatman, polypropylene (0.45 µm) vecta spin micro centrifuge filter tubes. These polymer samples

were subjected to a washing (6 x SSPE {2 x 300 µL}) / centrifugation (13200 rpm, 30 sec) procedure. An aliquot of DNA(A_{10}) (6 pmol) in 6 x SSPE (100 µL) was added to 6 samples of the POP-Sc-PNA(T_{10}) **175**. As a negative control, an aliquot of DNA(T_{10}) (6 pmol) in 6 x SSPE (100 µL) was added to a sample of POP-Sc-PNA(T_{10}) **175**. After, 30 minutes the polymers were separated from the reaction mixture by centrifugation (5000 rpm, 30 sec) and washed with water (3 x 300 µL).

A solution was prepared containing water (1074.6 µL), PNK 10 x buffer (120 µL), [γ^{33}P]ATP (3.6 µL, 0.37 MBq/µL) and PNK (1.8 µL, 5 µ/µL). An aliquot of this assay solution (100 µL. 0.11 MBq) was added to scintillation fluid (5 mL) in duplicate and monitored in a scintillation counter **Table 31**.

[γ^{33}P]ATP + Sc-fluid / cpm
5358100
5492534

Table 31: Duplicate scintillation counting data for [γ^{33}P]ATP, PNK, 10 x PNK buffer aqueous solution (100 µL) in scintillation fluid (5 mL). Mean error = $^{+}$/-1%.

An aliquot of the assay solution (100 µL, 0.11 MBq) was added to the polymer samples **175** and then placed in an oven (37 °C). Once the assay mixtures temperature had reached 37 °C the first tube was removed (20 min) and then a tube was removed after 30, 40, 50 and 70 minutes. The assay mixtures were subjected to a centrifugation/washing procedure with water (2 x 300 µL, 37 °C) and then monitored in a scintillation counter **Table 32**.

Time / min	cpm
20	7841
30	11472
40	15421
50	16694
70	24656
70[a]	6753

Table 32: Scintillation counting data for *in-situ* [γ^{33}P]ATP-phosphorylation of DNA(A_{10}) hybridised to POP-Sc-PNA(T_{10}) **175** using PNK. Deviation from linear plot mean error = $^{+}$/-7%.
[a] Corresponding data for DNA(T_{10}).

4.9 Scintillation Proximity Hybridisation Assay of POP-Sc-PNA Library

α-Styryl-poly(oxyethylene glycol)$_{300}$ *p*-toluene sulfonate 176

Using the same procedure as described for triethylene glycol di-*p*-toluene sulfonate **128**, a solution of TsCl (1.091 g, 5.61 mmol) in DCM (15 mL) was added to a solution of α-styryl-poly(oxyethylene glycol)$_{300}$ **153** (2.000 g, 4.67 mmol), triethylamine (1.6 mL, 11 mmol) and DMAP (0.006 g, 0.05 mmol) in DCM (15 mL) to give a yellow oil. This oil was dissolved in DCM (30 mL) and stirred with Polymer Laboratories PL-EDA (ethylenediamine) MP-resin (0.85 g, >3.3 mmol/g) for four hours. The resin was separated from the reaction mixture by filtration and washed with DCM (3 x 20 mL). The filtrates were combined with the reaction mixture and concentrated under reduced pressure and then dried in-vacuo overnight to constant mass to give α-styryl-poly(oxyethylene glycol)$_{300}$ *p*-toluene sulfonate **176** as a slight yellow oil (2.538 g, 93%), which was reacted on without further purification. IR (thin film): ν_{max}/cm^{-1} 3060 (w, C-H aromatic), 3055 (w, C-H aromatic), 2871 (s, C-H aliphatic), 1627 (w), 1606 (m, C=C aromatic), 1510 (s, C=C aromatic), 1454 (m), 1355 (m, -SO_2O-), 1291 (w), 1249 (s), 1189 (m), 1177 (s, -SO_2O-), 1098 (s, C-O), 1018 (w), 923 (m), 838 (w), 818 (w), 777 (w) and 664 (m). ^{1}H NMR (300 MHz, $CDCl_3$): δ_H 2.33 (3H, s), 3.46-3.60 (26H, m), 3.74 (2H, t, *J*=6.5), 4.02 (2H, t, *J*=7.3), 4.04 (2H, t, *J*=6.5), 5.01 (1H, d, *J*=13.1), 5.50 (1H, d, *J*=21.2), 6.64 (1H, dd, *J*=13.1 21.2), 6.76 (2H, d, *J*=10.3), 7.22 (2H, d, *J*=10.3), 7.23 (2H, d, *J*=9.8) and 7.69 (2H, d, *J*=9.8). ^{13}C NMR (75 MHz, $CDCl_3$, PENDANT)[270]: δ_C 21.3 (CH_3), 61.3 (CH_2), 63.2 (CH_2), 63.6 (CH_2), 67.0 (CH_2), 68.2 (CH_2), 69.0 (CH_2), 69.3 (CH_2), 69.9 (CH_2), 70.1 (CH_2), 70.2 (CH_2), 70.3 (CH_2), 70.4 (CH_2), 72.1 (CH_2), 76. 5 (CH_2), 77.0 (CH_2), 77.5 (CH_2), 111.2 (CH_2), 114.1 (CH), 127.0 (CH), 127.6 (CH), 129.5 (CH), 130.1 (C), 132.5 (C), 135.8 (CH), 144.5 (C) and 158.2 (C). LRMS (APCI): *m/z* 583 (100%, $[M + H]^+$), 539 (53%, $[M - C_2H_4O + H]^+$), 627 (51%, $[M + C_2H_4O + H]^+$), 495 (42%, $[M - 2(C_2H_4O) + H]^+$) and 451 (23%, $[M - 3(C_2H_4O) + H]^+$). $]^+$). HRMS (EI): *m/z* 605.2413 ($[M + Na]^+$); calculated for $C_{29}H_{42}O_{10}NaS$ 605.2396.

α-Styryl-poly(oxyethylene glycol)$_{300}$ phthalimide 177

To a solution of α-styryl-poly(oxyethylene glycol)$_{300}$ *p*-toluene sulfonate **176** (1.621 g, 2.79 mmol) in DMF (15 mL) and water (2 mL) was added potassium phthalimide (0.790 g, 4.18 mmol). The reaction mixture was placed in an oven (80 °C) overnight. The reaction mixture was allowed to cool to room temperature and then dissolved in DCM (100 mL) and washed sequentially with, water (3 x 500 mL), saturated brine (6 x 1 L), dried over anhydrous magnesium sulphate and concentrated under reduced pressure to give yellow oil. The oil was dissolved in the minimum volume of DCM, filtered and then concentrated under reduced pressure to give α-styryl-poly(oxyethylene glycol)$_{300}$ phthalimide **177** as a slight yellow oil with crystal formation (1.185 g, 76%), which was reacted on without further purification. IR (thin film): ν_{max}/cm^{-1} 2871 (m, C-H aliphatic), 1772 (w), 1713 (s, C=O), 1627 (w, C=C), 1606 (m, C=C

aromatic), 1510 (m, C=C aromatic), 1467 (w), 1394 (m), 1351 (w), 1301 (w), 1249 (m), 1176 (w), 1114 (s, C-O), 946 (w), 838 (w), 721 (w) and 668 (w). ^{1}H NMR (300 MHz, $CDCl_3$): δ_H 3.45-3.70 (39H, m), 4.07 (2H, t, *J*=5.8), 5.06 (1H, d, *J*=13.1), 5.54 (1H, d, *J*=21.1), 6.59 (1H, dd, *J*=21.1, 13.1), 6.81 (2H, d, *J*=9.5), 7.3 (2H, d, *J*=9.5) and 7.63-7.79 (4H, m). ^{13}C NMR (75 MHz, $CDCl_3$, PENDANT)[270]: δ_C 61.3 (CH_2), 63.3 (CH_2), 63.7 (CH_2), 67.1 (CH_2), 67.6 (CH_2), 69.0 (CH_2), 69.4 (CH_2), 69.8 (CH_2), 70.0 (CH_2), 70.1 (CH_2), 70.3 (CH_2), 70.5 (CH_2), 72.3 (CH_2), 11.3 (CH_2), 114.1 (CH), 114.3 (CH), 122.9 (CH), 123.0 (CH), 127.0 (CH), 130.2 (CH), 131.8 (CH), 132.5 (CH), 133.8 (CH), 135.9 (CH), 158.3 (C) and 167.9 (C). LRMS (APCI): *m/z* 558 (100%, $[M + H]^+$), 514 (68%, $[M - C_2H_4O + H]^+$), 602 (54%, $[M + C_2H_4O + H]^+$) and 470 (29%, $[M - 2(C_2H_4O) + H]^+$). $]^+$). HRMS (EI): *m/z* 580.2516 ($[M + Na]^+$); calculated for $C_{30}H_{39}NO_9Na$ 580.2523.

POP-Sc support 178: α-styryl-poly(oxyethylene glycol)$_{350}$ monomethyl ether 171, 6 mole percent α-styryl-poly(oxyethylene glycol)$_{300}$ phthalimide 177, 6 mole percent (4'vinyl)-4-benzyl-2,5-diphenyloxazole 101, 2 mole percent α,ω-bis-styryl-poly(oxyethylene glycol)$_{2000}$ 173

α-Styryl-poly(oxyethylene glycol)$_{350}$ monomethyl ether **171** (1.007 g, 1.79 mmol), α-styryl-poly(oxyethylene glycol)$_{300}$ phthalimide **177** (0.071 g, 0.13 mmol), (4'vinyl)-4-benzyl-2,5-diphenyloxazole **101** (0.042 g, 0.12 mmol), α,ω-bis-styryl-poly(oxyethylene glycol)$_{2000}$ **173** (0.091 g, 0.04 mmol) and AIBN 7 (0.005 g, 0.03 mmol) were combined according to General Procedure 5 to give, after washing, polymer **178** as a yellow gel (0.532 g, 44%). IR (gel compressed between NaCl discs): ν_{max}/cm^{-1} 3060 (w, C-H aromatic), 3025 (w, C-H aromatic), 2919 (s, C-H aliphatic), 2847 (s, C-H aliphatic), 1971 (m), 1772 (w), 1714 (s, C=O), 1692 (m), 1661 (m), 1647 (s), 1639 (s), 1614 (s, C=C aromatic), 1581 (m, C=C aromatic), 1556 (m), 1532 (m), 1519 (m), 1504 (s, C=C aromatic), 1484 (m), 1470 (s), 1448 (m), 1435 (m), 1413 (m), 1395 (m), 1373 (m), 1355 (m), 1244 (m), 1178 (w), 1111 (s, C-O) and 1045 (m)

POP-Sc support 179: Hydrazinolysis of POP-Sc support 178

A solution of hydrazine hydrate (2454 μL, 49440 μmol) in dioxane (10 mL) was added to POP-Sc support **178** (1.200 g, 0.10 mmol/g). The reaction mixture was placed in an oven (50 °C) overnight. The polymer was separated from the supernatant by filtration and washed with dioxane/20% HCl 4:1 (25 mL), dioxane/water 4:1(25 mL), 10% TEA/DMF (25 mL), DMF (25 mL), DCM (25 mL) and MeOH (25 mL). This filtration and washing procedure was repeated twice. The polymer was dried in an oven at 35 °C *in-vacuo* to give POP-Sc support **179** as a colourless opaque polymer gel (0.434 g, 37%). IR (thin film): ν_{max}/cm^{-1} 3454 (m, N-H), 3060 (w, C-H aromatic), 3025 (w, C-H aromatic), 2921 (s, C-H aliphatic), 2847 (s, C-H aliphatic), 1745 (w), 1728 (w), 1710 (w), 1674 (m), 1660 (m), 1639 (m), 1614 (m, C=C aromatic), 1586 (m, C=C aromatic), 1550 (w), 1515 (m, C=C aromatic), 1497 (m), 1479 (m), 1466 (m), 1448 (m), 1377 (m), 1346 (m), 1297 (m), 1249 (m), 1104 (s, C-O), 947 (w) and 827 (w).

Solvent swelling assay upon POP-Sc support 179

POP-Sc support **179** was packed into the bottom of a polypropylene disposable syringe (1 mL), with the tip removed, housing a nylon frit (0.45 μm). A reservoir containing solvent was placed below the syringe and the reservoir raised until the solvent was just brought into contact with the bottom of the syringe. A volume reading was recorded when there was no further volume increase (Appendix B, Table 42).

POP-Sc Support 180: Fmoc-Gly-OH Coupling to POP-Sc support 179

The stock solutions PyBOP (1.8×10^{-5} mmol/μL), Fmoc-Gly-OH (3.3×10^{-5} mmol/μL) and DIPEA (5.7×10^{-4} mmol/μL) in DMF were prepared. Accordingly, aliquots of these stock solutions were combined: PyBOP (455.6 μL, 8.2 μmol), Fmoc-Gly-OH (257.8 μL, 8.5 μmol) and DIPEA (29.5 μL, 16.8 μmol). The resultant mixture was added to POP-Sc support **179** (0.021 g, 0.002 mmol), contained in a Bio-Rad filter syringe and incubated for 2 hours. The polymer was separated from the reaction mixture by filtration and washed *in-situ* with DCM (3 mL), DCM/MeOH 1:1 (3 mL) and MeOH (3 mL). This washing-filtration procedure was repeated twice. The polymer was placed in a vacuum oven at 35 °C and dried to constant mass to give Fmoc-derived polymer (0.021 g). IR (thin film): ν_{max}/cm^{-1} 3521 (m, N-H), 3060 (w, C-H aromatic), 3025 (w, C-H aromatic), 2954 (s, C-H aliphatic), 2921 (s, C-H aliphatic), 2847 (s, C-H aliphatic), 1967 (w), 1731 (m), 1714 (w), 1682 (w), 1648 (w), 1634 (w), 1614 (m, C-C aromatic), 1581 (w, C=C aromatic), 1555 (w), 1537 (w), 1515 (m), 1504 (m, C=C aromatic), 1466 (m), 1454 (m), 1351 (m), 1324 (m), 1302 (m), 1244 (m), 1195 (m), 1102 (m, C-O), 952 (w), 834 (w), 774 (w), 761 (w), 730 (m), 699 (m) and 663 (s).

POP-Sc Support 181: Acetylation of POP-Sc support 180

The stock solutions acetic anhydride (1.06×10^{-4} mmol/μL), DMAP (6.48×10^{-6} mmol/μL) and pyridine (1.2×10^{-4} mmol/μL) in DCM were prepared. Accordingly, aliquots of these stock solutions: acetic anhydride (25.5 μL, 2.7 μmol), DMAP (13.9 μL, 0.1 μmol), pyridine (56.7 μL, 6.8 μmol), DCM (200 μL) and POP-Sc support **180** (0.009 g, 0.001 mmol) were combined according to General Procedure 7 to give POP-Sc support **181** (0.009 g). IR (thin film): ν_{max}/cm^{-1} 3362 (m, N-H), 3069 (w, C-H aromatic), 3033 (w, C-H aromatic), 2945 (s, C-H aliphatic), 2922 (s, C-H aliphatic), 2847 (s, C-H aliphatic), 1732 (m, C=O), 1714 (w), 1696 (w), 1683 (w), 1652 (m), 1630 (w), 1614 (m, C=C aromatic), 1581 (w, C=C aromatic), 1568 (w), 1550 (w), 1537 (m), 1519 (m), 1506 (m), 1488 (m), 1455 (m), 1435 (m), 1373 (m), 1302 (m), 1249 (m), 1200 (w), 1151 (m), 1106 (m, C-O), 1071 (m, C-O), 1045 (m, C-O), 952 (w), 836 (w) and 668 (s).

POP-Sc Support 182: Fmoc-release assay of POP-Sc support 181

POP-Sc support **181** (0.0095 g), in a Bio-Rad filter syringe, was treated with 20% piperidine/DMF solution (3 x 1.00 mL) for 3 minutes. The polymer was seperated from the supernatant by filtration and then subjected to a washing-filtration procedure with DCM (3 mL), DCM/MeOH 1:1 (3 mL), MeOH (3 mL), DCM/MeOH 1:1 (3 mL) and DCM (3 mL). The polymer was dried under vacuum (35 °C, 1 hr) to give polymer **181** (0.010 g): ν_{max}/cm^{-1} 3584 (m, N-H), 3512 (m, N-H), 3060 (w, C-H aromatic), 3033 (w, C-H aromatic), 2945 (s, C-H aliphatic), 2922 (s, C-H aliphatic), 2847 (s, C-H aliphatic), 1976 (w), 1738 (w), 1706 (w), 1667 (m), 1639 (m), 1614 (m, C=C aromatic), 1581 (m, C=C aromatic), 1550 (w), 1515 (m, C=C aromatic), 1484 (m), 1470 (m), 1454 (m), 1439 (m), 1368 (m), 1356 (m), 1328 (m), 1302 (m), 1244 (m), 1200 (m), 1156 (m), 1107 (m, C-O), 1071 (m, C-O), 1045 (m, C-O), 956 (m), 836 (m), 779 (w) and 690 (m).

The piperidine-DMF supernatant was analysed in a uv-spectrometer at 290 nm **Table 33**.

Mass / g	Absorption @ 290 nm	Absorption @ 290 nm / mg
0.0095	2.038	0.22

Table 33: Fmoc release assay for POP-Sc support **181**. Estimated error = $^{+}$/-3%.

The loading of POP-Sc support **179** was established to be 0.13 mmol/g (126%).[235]

POP-Sc 183: Fmoc-Gly-OH Coupling to POP-Sc support 182

A solution of PyBOP (0.003 g, 0.005 mmol), Fmoc-Gly-OH (0.002 g, 0.005 mmol) and DIPEA (1.68 µL, 9.6 µmol) in DMF (200 µL) was added to POP-Sc support **182** (0.010 g, 0.001 mmol), in a Bio-Rad filter syringe and incubated for 2 hours. The polymer was separated from the reaction mixture and washed *in-situ* with DCM (3 mL), DCM/MeOH 1:1 (3 mL) and MeOH (3 mL). This washing filtration procedure was repeated twice. The polymer was placed in a vacuum oven at 35 °C and dried to constant mass to give polymer **183** (0.010 g). IR (thin film): ν_{max}/cm^{-1} 3441 (m, br, N-H), 3060 (w, C-H aromatic), 3025 (w, C-H aromatic), 2921 (s, C-H aliphatic), 2847 (s, C-H aliphatic), 1731 (m), 1682 (m), 1661 (m), 1643 (m), 1614 (s, C-H aromatic), 1586 (m, C=C aromatic), 1568 (w), 1550 (m), 1532 (m), 1515 (s, C=C aromatic), 1504 (s, C=C aromatic), 1488 (m), 1470 (s), 1461 (s), 1454 (m), 1351 (m), 1302 (m), 1249 (m), 1195 (m), 1156 (s, C-O), 1095 (s, C-O), 1071 (s, C-O), 1040 (s, C-O), 952 (m), 836 (m) and 668 (s).

Fmoc-release assay of POP-Sc support 183

POP-Sc support **183** (0.0032 g), in a Bio-Rad filter syringe, was treated with a 20% piperidine/DMF solution (3 x 1.00 mL) for 3 minutes. The polymer was separated from the supernatant by filtration. The supernatant was analysed in a uv-spectrometer at 290 nm **Table 34**.

Mass / g	Absorption @ 290 nm	Absorption @ 290 nm / mg
0.0032	0.703	0.22

Table 34: Fmoc release assay for POP-Sc support **183**. Estimated error = $^{+}$/-3%.

The efficiency of the second Fmoc-Gly-OH coupling to polymer **179** was established to be 0.13 mmol/g (100%).

General Procedure 11: Fmoc-PNA-OH coupling in the POP-Sc-PNA-library construction

Stock solutions of Fmoc-PNA-OH (5.2 x 10^{-5} mmol/μL), PyBOP (4.9 x 10^{-5} mmol/μL) and DIPEA (1.0 x 10^{-4} mmol/μL) were prepared. An aliquot (10.0 μL) of each of these stock solutions was dissolved in DMF (70.0 μL), the resultant mixture was added to the polymer sample (0.002 g, ~0.26 μmol) and incubated (3 hr.). The polymer was separated from the reaction mixture by centrifugation (132000 rpm, 30 sec) and then subjected to a washing-centrifugation procedure using DCM (500 μL), DCM/MeOH 1:1 (500 μL), MeOH (500 μL), DCM/MeOH 1:1 (500 μL) and DCM (500 μL). The PNA-derived polymer was dried at room temperature overnight. Following Fmoc-cleavage (General procedure 13), this procedure was repeated using the appropriate Fmoc-PNA-OH monomers to generate PNA-oligomers 9 base units in length.

General Procedure 12: Acetylation of the POP-Sc-PNA library

Stock solutions of acetic anhydride (7.8 x 10^{-5} mmol/μL), DMAP (2.6 x 10^{-6} mmol/μL) and pyridine (2 x 10^{-4} mmol/μL) were prepared. An aliquot (10.0 μL) of each stock solution was dissolved in DMF (70.0 μL), the resultant mixture was added to the polymer sample (~0.002 g, ~0.26 μmol), following the first Fmoc-PNA-OH coupling-reaction and incubated (2 hr.). The polymer was separated from the reaction mixture by centrifugation (132000 rpm, 30 sec) and then subjected to a washing-centrifugation (132000 rpm, 30 sec) procedure using DCM (500 μL), DCM/MeOH 1:1 (500 μL), MeOH (500 μL), DCM/MeOH 1:1 (500 μL) and DCM (500 μL). The polymer was dried at room temperature (1 hr.).

General Procedure 13: Fmoc cleavage of POP-Sc-PNA library compounds

Each polymer sample (~0.002 g, ~0.26 μmol) was treated with 20% piperidine/DMF (2 x 300 μL) for 3 minutes. The polymer was isolated from the supernatant by centrifugation (132000 rpm, 30 sec) and then subjected to a washing-centrifugation (132000 rpm, 30 sec) procedure using DCM (500 μL),

DCM/MeOH 1:1 (500 μL), MeOH (500 μL), DCM/MeOH 1:1 (500 μL) and DCM (500 μL). The PNA-derived polymer was dried at room temperature (1 hr.). This procedure was repeated following every Fmoc-PNA-OH coupling-reaction (General Procedure 11).

Radio-labelling DNA(A_9) at the 5' termini with ^{33}P from [γ-^{33}P]ATP using PNK

A mixture containing DNA(A_9) (9.0 μL, 180 pmol), water (58.5 μL), PNK 10 x buffer (9.0 μL), [$\gamma^{33}P$]ATP (9.0 μL, 3.33 MBq) and PNK (4.5 μL, 5 μ/μL) was incubated at 37 °C (45 min). The temperature was then increased to 65 °C (20 min). An aliquot of water (810.0 μL) was added to the mixture.

DE81 Assay of ^{33}P-DNA(A_9)

An aliquot of the assay mixture ^{33}P-DNA(A_9) (10.0 μL, 2 pmol, 0.037 MBq) was analysed, in duplicate, according to General Procedure 10 **Table 35**.

Total / cpm	Incorporated / cpm
353183	154787
320102	162914

Table 35: Scintillation counting data for DE81 assay of ^{33}P-DNA(A_9). Mean error = $^{+}/_{-}$4%.

Hybridisation of the POP-Sc-PNA library with ^{33}P-DNA(A_9)

The POP-Sc-PNA library was initially subjected to a washing (6 x SSPE (2 x 500 μL))-centrifugation (13200 rpm, 30 sec) procedure using. An aliquot of the ^{33}P-DNA(A_9) assay solution (800.0 μL) was added to 6 x SSPE (39200.0 μL). An aliquot (100.0 μL, 0.4 pmol, 0.0074 MBq) of this diluted assay solution was added to scintillation fluid (5 mL) in quadruplet and then monitored in a scintillation counter **Table 36**.

[$\gamma^{33}P$]ATP + Sc-fluid / cpm
62008
47320
59594
61879

Table 36: Quadruplicate scintillation counting data for [$\gamma^{33}P$]ATP (0.0074 MBq), ^{33}P-DNA(A_9), PNK, 10 x PNK buffer aqueous solution (100.0 μL) in scintillation fluid (5 mL). Mean error = $^{+}/_{-}$9%.

An aliquot of the diluted assay solution (500.0 μL, 2.0 pmol, 0.037 MBq) was added to each member of the POP-Sc-PNA library. The polymer was separated from the assay solution by centrifugation (13200 rpm, 30 sec) and then monitored in a scintillation counter (Appendix F, Table 50). The POP-Sc-PNA library was subjected to a washing-centrifugation (13200 rpm, 30 sec)-counting procedure using 4 x SSPE (500 μL) (Appendix F, Table 51), 2 x SSPE (500 μL) (Appendix F, Table 52), and water (500 μL)

(Appendix F, Table 53), water (500 µL, 25 °C) (Appendix F, Table 54), water (500 µL, 30 °C) (Appendix F, Table 55), water (500µL, 40 °C) (Appendix F, Table 56) and 3 x 50% formamide/2 x SSPE (250 µL, 40 °C) (Appendix F, Table 57-59).

Chapter 5

References

[1] J. Nielsen, *Chem. Ind.*, 1994, 902.

[2] C. G. Lerner and A. Y. Chiang Saiki, *Anal. Biochem.,* 1996, **240**, 185.

[3] M. A. Crook, P. Johnson and B. Scales, *Liquid Scintillation Counting*, Heyden, London, p. 23.

[4] S. W. Wunderly, *Appl. Radiat. Isot.*, 1989, **40**, 569.

[5] K. D. Neame and C. A. Homewood, *Introduction to Liquid Scintillation Counting*, Butterworths, London, 1974, p. 145.

[6] K. D. Neame and C. A. Homewood, *Introduction to Liquid Scintillation Counting*, Butterworths, London, 1974, p. 4.

[7] K. D. Neame and C. A. Homewood, *Introduction to Liquid Scintillation Counting*, Butterworths, London, 1974, p. 6.

[8] K. D. Neame and C. A. Homewood, *Introduction to Liquid Scintillation Counting*, Butterworths, London, 1974, p. 7.

[9] K. D. Neame and C. A. Homewood, *Introduction to Liquid Scintillation Counting*, Butterworths, London, 1974, p.9.

[10] J. B. Birks, *The Theory and Practice of Scintillation Counting*, Pergamon Press, London, p. 4.

[11] J. B. Birks, *The Theory and Practice of Scintillation Counting*, Pergamon Press, London, p. 8.

[12] A. Dyer, *Liquid Scintillation Counting Practice*, Heyden, London, p. 24.

[13] J. B. Birks, The Theory and Practice of Scintillation Counting, Pergamon Press, London, p. 9.

[14] J. B. Birks, *The Theory and Practice of Scintillation Counting*, Pergamon Press, London, p. 96.

[15] K. D. Neame and C. A. Homewood, *Introduction to Liquid Scintillation Counting*, Butterworths, London, 1974, p. 31.

[16] A. H. Snell, *Nuclear Instruments and their Uses*, John Wiley and Sons, London, 1962, pp. 132-136.

[17] F. N. Haynes and R. G. Gould, *Science (Washingto, D. C.)*, 1953, **117**, 480.

[18] *The Principles of Proximity your Guide to SPA* (CD-ROM), Amersham Biosciences Ltd, 2002.

[19] K. D. Neame and C. A. Homewood, *Introduction to Liquid Scintillation Counting*, Butterworths, London, 1974, p. 30, fig. 3.1.

[20] K. D. Neame and C. A. Homewood, *Introduction to Liquid Scintillation Counting*, Butterworths, London, 1974, p. 56, fig. 4.5.

[21] K. D. Neame and C. A. Homewood, *Introduction to Liquid Scintillation Counting*, Butterworths, London, 1974, p. 83.

[22] K. D. Neame and C. A. Homewood, *Introduction to Liquid Scintillation Counting*, Butterworths, London, 1974, p. 88.

[23] K. D. Neame and C. A. Homewood, *Introduction to Liquid Scintillation Counting*, Butterworths, London, 1974, p. 91.

[24] K. D. Neame and C. A. Homewood, *Introduction to Liquid Scintillation Counting*, Butterworths, London, 1974, p. 49.

[25] A. H. Snell, *Nuclear Instruments and their Uses*, John Wiley and Sons, London, 1962, p. 167.

[26] M. A. Crook, P. Johnson and B. Scales, *Liquid Scintillation Counting*, Heyden, London, p. 170.

[27] K. D. Neame and C. A. Homewood, *Introduction to Liquid Scintillation Counting*, Butterworths, London, 1974, p. 131.

[28] K. D. Neame and C. A. Homewood, *Introduction to Liquid Scintillation Counting*, Butterworths, London, 1974, p. 170.

[29] K. D. Neame and C. A. Homewood, *Introduction to Liquid Scintillation Counting*, Butterworths, London, 1974, p. 32.

[30] A. Dyer, *Liquid Scintillation Counting Practice*, Heyden, London, p. 24.

[31] A. Pla-Dalmau, *J. Org. Chem.*, 1995, **60**, 5468.

[32] R. P. Wayne, *Photochemistry*, Butterworths, London, 1970, p. 5.

[33] J. A. Barltrop and J. D. Coyle, *Principles of Photochemistry*, John Wiley and Sons, London, 1978.

[34] R. P. Wayne, *Photochemistry*, Butterworths, London, 1970, p. 131.

[35] A. Dyer, *Liquid Scintillation Counting Practice*, Heyden, London, p. 1.

[36] K. D. Neame and C. A. Homewood, *Introduction to Liquid Scintillation Counting*, Butterworths, London, 1974, p. 1.

[37] J. B. Birks, *The Theory and Practice of Scintillation Counting*, Pergamon Press, London, p. 39.

[38] H. J. Meyer, F. Hoffmann and T. Wolff, *Helv. Chim. Acta.*, 2001, **84**, 3600.

[39] B. Clapham, Thesis: *Scintillation Counting in Molecular Recognition and combinatorial chemistry*, Aston University, Birmingham, 1999, p.14.

[40] K. D. Neame and C. A. Homewood, *Introduction to Liquid Scintillation Counting*, Butterworths, London, 1974, p. 68.

[41] J. B. Birks, *The Theory and Practice of Scintillation Counting*, Pergamon Press, London, p. 292, fig. 8.6.

[42] J. B. Birks, *The Theory and Practice of Scintillation Counting*, Pergamon Press, London, pp. 277-288.

[43] J. B. Birks, *The Theory and Practice of Scintillation Counting*, Pergamon Press, London, p. 289.

[44] H. Ross, J. E. Noakes and J. D. Spaulding, *Liquid Scintillation Counting and Organic Scintillators*, Lewis Publishers INC, Michigan, 1991, p. 3.

[45] R. A. Jessop, *P. SPIE.*, 1998, **3259**, 228.

[46] K. D. Neame and C. A. Homewood, *Introduction to Liquid Scintillation Counting*, Butterworths, London, 1974, p. 13.

[47] J. B. Birks, *The Theory and Practice of Scintillation Counting*, Pergamon Press, London, p. 54.

[48] K. D. Neame and C. A. Homewood, *Introduction to Liquid Scintillation Counting*, Butterworths, London, 1974, p. 70.

[49] J. B. Birks, *The Theory and Practice of Scintillation Counting*, Pergamon Press, London, p. 295, fig. 8.12.

[50] J. B. Birks, *The Theory and Practice of Scintillation Counting*, Pergamon Press, London, p. 292, fig. 8.6.

[51] D. Steinberg, *Nature (London)*, 1958, **182**, 740.

[52] J. B. Birks, *The Theory and Practice of Scintillation Counting*, Pergamon Press, London, p. 10.

[53] C. R. Hurlbut, *Trans. Amer. Nucl. Soc.,* 1985, **50**, 20.

[54] J. B. Birks, *The Theory and Practice of Scintillation Counting*, Pergamon Press, London, p. 321.

[55] K. D. Neame and C. A. Homewood, *Introduction to Liquid Scintillation Counting*, Butterworths, London, 1974, p. 79.

[56] H. E. Hart and E. G. Greenwald, *Mol. Immunol.,* 1979, **16**, 265.

[57] J. H. Bertaglio-Matte, 1986, US patent no. 4,568,649.

[58] Amersham Life Science Catalogue, 1996, pp. 252-266.

[59] Amersham Biosciences Catalogue, 2002, p. 10, 17-18, 24-41.

[60] R. A. Jessop, *Radiocarbon*, 1993, 285.

[61] B. Jessop and T. Smith, *Phys. World*, 1997, **10**, 26.

[62] R. A. Jessop, *Radiocarbon*, 1996, 175.

[63] Amersham Pharmacia Biotech Catalogue, 1998, p.11.

[64] N. D. Cook, *D.D.T*, 1996, **1**, 287.

[65] Amersham Life Science Catalogue, 1996, p. 256.

[66] S. Udenfriend, L.D. Gerber, L. Brink and S. Spector, *Proc. Natl. Acad. Sci.*, 1985, **82**, 8672.

[67] S. Udenfriend, L. Gerber and N. Nelson, *Anal. Biochem.,* 1987, **161**, pp. 494-500.

[68] R. A. Jessop, Liquid scintillation spectrometry, 1992, 285.

[69] N. D. Cook, SPA: A Highly Versatile High Throughput Screening Technology, Amersham Internal document, 2003.

[70] J. Liu, P. A. Feldman, J. S. Lippy, E. Bobkova, M. G. Kurilla and T. D. Y. Chung, *Anal. Biochem.*,2001, **289**, 239.

[71] N. Bosworth and P. Towers, *Nature (London)*, 1989, **341**, 167.

[72] J. Hodgson, *BioTechnology*, 1993, **11**, 683.

[73] R. B. Merrifield, *J. Am. Chem. Soc.*, 1963, 2149.

[74] D. C. Sherrington, *Chem Commun.*, 1998, 2275.

[75] D. C. Sherrington, A. Lanver, H. G. Schmalz, B. Wilson, X. W. Ni and S. Yuan, *Angew. Chem. Int. Ed, Engl.,* 2002, **41**, 3656.

[76] D. C. Sherrington, *Brit. Polym. J.*, 1984, **16**, 164.

[77] M. Tomoi and W. T. Ford, *J. Am. Chem. Soc.*, 1981, **103**, 3821.

[78] S. S. Wang, *J. Am. Chem. Soc.*, 1973, **95**, 1328.

[79] J. S. McMurray and C. A. Lewis, *Tetrahedron Lett.*, 1993, **34**, 8059.

[80] M. Mergler, R. Tanner, J. Gosteli and P. Grogg, *Tetrahedron Lett*, 1988, **29**, 4005.

[81] A. W. Czarnik and S. H. DeWitt, *A Practical Guide to Combinatorial Chemistry*, American Chemical Society, Washington, DC, 1997, pp. 78-85.

[82] G. Jung, *Combinatorial Chemistry Synthesis, Analysis, Screening*, 1st edition, Wiley-vch, Germany, 1999, pp. 167-228.

[83] K. Barlos, D. Gatos, S. Kapolos, G. Papaphotiu, W. Schafer and Y. Wenqing, *Tetrahedron Lett.*, 1989, **30**, 3943.

[84] H. Rink, *Tetrahedron. Lett.*, 1987, **28**, 3787.

[85] P. G. Pietta, P. F. Cavallo, K. Takahashi and G. R. Marshall, *J. Org. Chem.*, 1974, **39**, 44.

[86] R. C. Orlowski and R. Walter, *J. Org. Chem.*, 1976, **41**, 3701.

[87] P. Seiber, *Terahedron. Lett.*, 1987, **28**, 2107.

[88] W. F. DeGrado and E. T. Kaiser, *J. Org. Chem.*, 1980, **45**, 1295.

[89] D. H. Rich and S. K. Gurwara, *J. Am. Chem. Soc.*, 1975, **97**, 1575.

[90] R. Santini, M. C. Griffith and M. Qi, *Tetrahedron. Lett.*, 1998, **39**, 8951.

[91] S. Zalipsky, J. L. Chang, F. Albericio and G. Barany, *React. Polym.*, 1994, **22**, 243.

[92] E. Bayer, *Angew. Chem. Int. Ed. Engl.*, 1991, **30**, 113.

[93] www.rapp-polymere.com.

[94] *The Fine Art of Solid Phase Synthesis Catalogue*, Novabiochem, Switzerland, 2002/2003, p. 2.2.

[95] *Resins and Reagents for Accelerating Synthesis and Purification Catalogue*, Argonaut Technologies, Foster City, CA, 2000, pp. 40-44.

[96] O. W. Gooding, S. Baudart, T. L. Deegan, K. Heisler, J. W. Labadie, W. S. Newcomb, J. A. Porco and P. V. Eikeren, *J. Comb. Chem.*, 1999, **1**, 113.

[97] *Resins and Reagents Technical Handbook Catalogue*, Argonaut Technologies, Foster City, CA, 2003, pp. 144-149.

[98] *Combinatorial Chemistry Catalogue*, Sigma Aldrich, St Louis, p. 133.

[99] B. G. Main, *PCT Publication No. WO 00/02953*, 2000.

[100] S. Lebreton, S. Monaghan and M. Bradley, *Aldrichim. Acta.*, 2001, **34**, 75.

[101] S. Lebreton, N. Newcombe and M. Bradley, *Tetrahedron. Lett.*, 2002, **43**, 2479.

[102] K. Kamahori, K. Ito and S. Itsuno, *J. Org. Chem.*, 1996, **61**, 8321.

[103] M. E. Wilson, K. Paech, W. Zhou and M. J. Kurth, *J. Org. Chem.*, 1998, **63**, 5099.

[104] P. H. Toy and K. D. Janda, *Tetrahedron. Lett.*, 1999, **40**, 6329.

[105] P. H. Toy, T. S. Reger and K. D. Janda, *Aldrichim. Acta.*, 2000, **33**, 87.

[106] P. H. Toy, T. S. Reger, P. Garibay, J. C. Garno, J. A. Malikayil, G. Liu and K. D. Janda, *J. Comb. Chem.*, 2001, **3**, 117.

[107] www.sigmaaldrich.com.

[108] E. Atherton, D. L. J. Clive and R. C. Sheppard, *J. Am. Chem. Soc.*, 1975, **97**, 6584.

[109] R. Arshady, E. Atherton, D. L. J. Clive and R. C. Sheppard., *J. Chem. Soc., Perkin Trans. 1*, 1981, 529.

[110] G. L. Stahl, C. W. Smith and R. Walter, *J. Org. Chem.*, 1979, **44**, 3424.

[111] G. L. Stahl, R. Walter and C. W. Smith, *J. Am. Chem. Soc.*, 1979, **101**, 5383.

[112] R. Kita, F. Svec and J. M. J. Frechet, *J. Comb. Chem.*, 2001, **3**, 564.

[113] M. Kempe and G. Barny, *J. Am. Chem. Soc.*, 1996, **118**, 7083.

[114] M. Meldel, *Tetrahedron. Lett.*, 1992, **33**, 3077.

[115] H. K. Smith and M. Bradley, *J. Comb. Chem.*, 1999, **1**, 326.

[116] J. Buchardt, C. B. Schiodt, C. K. Jensen, J. M. Delaisse, N. T. Foged and M. Meldal, *J. Comb. Chem.*, 2000, **2**, 624.

[117] P. M. St. Hilaire, M. Willert, M. A. Juliano, L. Juliano and M. Meldal, *J. Comb. Chem.*, 1999, **1**, 509.

[118] M. Meldal, F. I. Auzanneau, O. Hindsgaul and M. M. Palcic, *J. Chem. Soc., Chem. Commun.*, 1994, 1849.

[119] T. Groth, M. Grotli, W. D. Lubell, L. P. Miranda and M. Meldal, *J. Chem. Soc., Perkin Trans. 1*, 2000, **24**, 4258.

[120] M. Renil and M. Meldal, *Tetrahedron Lett.*, 1996, **37**, 6185.

[121] M. Grotli, J. Rademan, T. Groth, W. D. Lubell, L. P. Miranda and M. Meldal, *J. Comb. Chem.*, 2001, **3**, 28.

[122] J. Buchardt and M. Meldal, *Tetrahedron Lett.*, 1998, **39**, 8695.

[123] J. Rademann, M. Grotli, M. Meldal and K. Bock, *J. Am. Chem. Soc.*, 1999, **121**, 5459.

[124] L. P. Miranda, W. D. Lubell, K. M. Halkes, T. Groth, M. Grotli, J. Rademann, C. H. Gotfredsen and M. Meldal, *J. Comb. Chem.*, 2002, **4**, 523.

[125] C. W. Tornoe and M. Meldal, *Tetrahedron Lett.*, 2002, **43**, 6409.

[126] S. Leon, R. Quarrell and G. Lowe, *Bioorg. Med. Chem. Lett.*, 1998, **8**, 2997.

[127] J. Kress, R. Zanaletti, A. Amour, M. Ladlow, J. G. Frey and M. Bradley, *Chem. Eur. J.*, 2002, **8**, 3769.

[128] R. B. Merrifield, *Angew. Chem. Int. Ed. Engl.*, 1985, **24**, 799.

[129] D. Orain, J. Ellard and M. Bradley, *J. Comb. Chem.*, 2002, **4**, 1.

[130] E. Atherton, C. J. Logan and R. C. Sheppard, *J. Chem. Soc., Perkin Trans. 1*, 1981, 538.

[131] NovaBiochem catalog 2002/3, p 3.4.

[132] J. Jones, *Amino Acid and Peptide Synthesis*, Oxford Chemistry Primers, second edition, Oxford, 2002, p. 37.

[133] J. Jones, *Amino Acid and Peptide Synthesis*, Oxford Chemistry Primers, second edition, Oxford, 2002, p. 38.

[134] NovaBiochem catalog 2002/3, p. 3.1.

[135] J. C. Sheehan and G. P. Hess, *J. Am. Chem. Soc.*, 1955, **77**, 1067.

[136] S. Mojsov, A. R. Mitchell and R. B. Merrifield, *J. Org. Chem.*, 1980, **45**, 555.

[137] L. Kisfaludy and I. Schon, *Synthesis*, 1983, 325.

[138] G. W. Anderson, J. E. Zimmerman and F. M. Callahan, *J. Am. Chem. Soc.*, 1964, **86**, 1839.

[139] B. Castro, J. R. Dormoy, G. Evin and C. Selve, *Tetrahedron. Lett.*, 1975, **14**, 1219.

[140] R. Knorr, A. Trzeciak, W. Bannwarth and D. Gillessen, *Tetrahedron Lett.*, 1989, **30**, 1927.

[141] C. B. Reese, R. C. Titmas and L. Yau, *Tetrahedron Lett.*, 1978, **19**, 2727.

[142] B. B. Blankemeyer-Menge, M. Nimtz and R. Frank, *Tetrahedron. Lett.*, 1990, **31**, 1701.

[143] P. E. Nielsen, M. Egholm, R. H. Berg and O. Buchardt, *Science (Washington, D. C.)*, 1991, **254**, 1497.

[144] M. Egholm, O. Buchardt, L. Christensen, C. Behrens, S. M. Freier, D. A. Driver, R. H. Berg, S. K. Kim, B. Norden and P. E. Nielsen, *Nature (London)*, 1993, **365**, 566.

[145] J. A. Ellman, *Chemtracts: Org. Chem.*, 1995, **8**, 1.

[146] R. Storer, *D.D.T.*, 1996, **1**, 248.

[147] N. K. Terret, M. Gardener, D. W. Gordon, R. J. Kobylecki and J. Steele, *Tetrahedron*, 1995, **51**, 8135.

[148] L. A. Thompson and J. A. Ellman, *Chem Rev.*, 1996, **96**, 555.

[149] F. Balkenhohl, C. von dem Bussche-Hunnefeld, A. Lansky and C. Zechel, *Angew. Chem. Int. Ed. Engl.*, 1996, **35**, 2288.

[150] H. An and P. D. Cook, *Chem. Rev.*, 2000, **100**, 3311.

[151] N. Bailey, A. W. Dean, D. B. Judd, D. Middlemiss, R. Storer and S. P. Watson, *Bioorg. Med. Chem. Lett.* 1996, **6**, 1409.

[152] E. Peisach, D. Casebier, S. L. Gallion, P. Furth, G. A. Petsko, J. C. Hogan and D. Ringe, *Science (Washington, D. C.)*, 1995, **269**, 66.

[153] D. L. Boger, C. M. Tarby, P. L. Myers and L. H. Caporale, *J. Am. Chem. Soc.*, 1996, **118**, 2109.

[154] S. Cheng, D. D. Comer, J. P. Williams, P. L. Myers and D. L. Boger, *J. Am. Chem. Soc.*, 1996, **118**, 2567.

[155] P. W. Smith, J. Y. Q. Lai, A. R. Whittington, B. Cox, J. G. Houston, C. H. Stylli, M. N. Banks and P. R. Tiller, *Bio. Med. Chem. Lett.*, 1994, **4**, 2821.

[156] T. Carell, E. A. Wintner, A. Bashir-Hashemi and J. Rebek, *Angew. Chem. Int. Ed. Engl.*, 1994, **33**, 2059.

[157] T. Carell, E. A. Wintner, A. J. Sutherland, J. Rebek, Y. M. Dunayevskiy and P. Vourous, *Chem. Biol.*, 1995, **2**, 171.

[158] Y. M. Dunayevskiy, P. Vourous, T. Carell, E. A. Wintner and J. Rebek, *Anal. Chem.*, 1995, **67**, 2906.

[159] T. Carell, E. A. Wintner and J. Rebek, *Angew. Chem. Int. Ed. Engl.*, 1994, **33**, 2061.

[160] S. V. Ley, I. R. Baxendale, R. N. Bream, P. S. Jackson, A. G. Leach, D. A. Longbottom, M. Nesi, J. S. Scott, R. I. Storer and S. J. Taylor, *J. Chem. Soc., Perkin Trans. 1*, 2000, **23**, 3815.

[161] A. Studer, S. Hadida, R. Ferritto, S. Y. Kim, P. Jeger, P. Wipf and D. P. Curran, *Science (Washington D. C.)*, 1997, **275**, 823.

[162] D. P. Curran and S. Hadida, *J. Am. Chem. Soc.*, 1996, **118**, 2531.

[163] D. J. Gravert and K. D. Janda, *Chem. Rev.*, 1997, **97**, 489.

[164] H. Han, M. M. Wolfe, S. Brenner and K. D. Janda, *Proc. Natl. Acad. Sci. USA.*, 1995, **92**, 6419.

[165] R. M. Kim, M. Manna, S. M. Hutchins, P. R. Griffin, N. A. Yates, A. M. Bernick and K. T. Chapman, *Proc. Natl. Acad. Sci. USA*, 1996, **93**, 10012.

[166] S. H. DeWitt, J. S. Kiely, C. J. Stankovic, M. C. Schroeder, D. M. Reynolds Cody and M. R. Pavia, *Proc. Natl. Acad. Sci. USA*, 1993, **90**, 6909.

[167] H. V. Meyers, G. J. Dilley, T. L. Durgin, T. S. Powers, N. A. Winssinger, H. Zhu and M. R. Pavia, *Mol. Diversity*, 1995, **1**, 13.

[168] B. Atrash, M. Bradley, R. Kobylecki, D. Cowell and J. Reader, *Angew. Chem. Int. Ed. Engl.*, 2001, **40**, 938.

[169] H. M. Geysen, R. H. Meloen and S. J. Barteling, *Proc. Natl. Acad. Sci. USA*, 1984, **81**, 3998.

[170] H. M. Geysen, S. J. Barteling and R. H. Meloen, *Proc. Natl, Acad. Sci. USA*, 1985, **82**, 178.

[171] A. M. Bray, N. J. Maeji and H. M. Geysen, *Tetrahedron Lett.*, 1990, **31**, 5811.

[172] A. M. Bray, N. J. Maeji, R. M. Valerio, R. A. Campbell and H. M. Geysen, *J. Org. Chem.*, 1991, **56**, 6659.

[173] A. M. Bray, N. J. Maeji, A. G. Jhingran and R. M. Valerio, *Tetrahedron Lett*, 1991, **32**, 6163.

[174] www.chiron.com

[175] www.mimotopes.com

[176] M. C. Pirrung, *Chem. Rev.*, 1997, **97**, 473.

[177] U. Maskos and E. M. Southern, *Nuc. Acids. Res.*, 1992, **20**, 1675.

[178] U. Maskos and E. M. Southern, *Genomics*, 1992, **13**, 1008.

[179] S. P. A. Fodor, J. Leighton Read, M. C. Pirrung, L. Stryer, A. Tsai Lu and D. Solas, *Science (Washington D. C.)*, 1991, **251**, 767.

[180] C. A. Patchnornik, B. Amit and R. B. Woodward, *J. Am. Chem. Soc.*, 1970, **92**, 6333.

[181] N. K. Terrett, *Combinatorial Chemistry*, Oxford University Press, Oxford, 1998, p. 42.

[182] R. Frank, *Tetrahedron*, 1992, **48**, 9217.

[183] A. Roda, M. Guardigli, C. Russo, P. Pasini and M. Baraldini, *BioTechniques*, 2000, **28**, 492.

[184] R. A. Houghten, *Proc. Natl. Acad. Sci. USA.*, 1985, **82**, 5131.

[185] H. M. Geysen, S. J. Rodda and T. J. Mason, *Mol. Immunology*, 1986, **23**, 709.

[186] K. S. Lam, M. Lebl and V. Krchnak, *Chem. Rev.*, 1997, **97**, 411.

[187] K. Burgess, A. I. Liaw and N. Wang, *J. Med. Chem.*, 1994, **19**, 2985.

[188] C. P. Holmes and D. G. Jones, *J. Org. Chem.*, 1995, **60**, 2318.

[189] J. J. Baldwin, J. J. Burbaum, I. Henderson and M. H. J. Ohlmeyer, *J. Am. Chem. Soc.*, 1995, **117**, 5588.

[190] S. E. Salmon, K. S. Lam, M. Lebl, A. Kandola, P. S. Khattri, S. Wade, M. Patek, P. Kocis, V. Krchnak and D. Thorpe, *Proc. Natl. Acad. Sci. USA*, 1993, **90**, 11708.

[191] P. Kocis, V. Krchnak and M. Lebl, *Tetrahedron Lett.*, 1993, **34**, 7251.

[192] M. C. Needels, D. G. Jones, E. H. Tatye, G. L. Heinkel, L. M. Kochersperger, W. J. Dower, R. W. Barrett and M. A. Gallop, *Proc. Natl. Acad. Sci. USA*, 1993, **90**, 10700.

[193] R. J. Fulton, R. L. McDade, P. L. Smith, L. J. Kienker and J. R. Kettman Jr. *Clin. Chem.,* 1997, **43**, 1749.

[194] *Combinatorial and Solid Phase Organic Chemistry Handbook*, Advanced Chemtech, 1998, Kentucky, USA, p. 17.

[195] R. A. Houghton, C. Pinilla, S. E. Blondelle, J. R. Appel, C. T. Dooley and J. H. Cuervo, *Nature (London)*, 1991, **354**, 84.

[196] E. Erb, K. D. Janda and S. Brenner, *Proc. Natl. Acad. Sci. USA.*, 1994, **91**, 11422.

[197] C. T. Dooley, N. N. Chung, P. W. Schiller and R. A. Houghten, *Proc. Natl. Acad. Sci. USA.*, 1993, **90**, 10811.

[198] C. T. Dooley, N. N. Chung, B. C. Wilkes, P. W. Schiller, J. M. Bidlack, G. W. Pasternak and R. A. Houghten, *Science (Washington D. C.)*, 1994, **266**, 2019.

[199] S. Brenner and R. Lerner, *Proc. Natl. Acad. Sci. USA*, 1992, **89**, 5381.

[200] J. Nielson, S. Brenner and K. D. Janda, *J. Am. Chem. Soc.*, 1993, **115**, 9812.

[201] J. M. Kerr, S. C. Banville and R. N. Zuckermann, *J. Am. Chem. Soc.*, 1993, **115**, 2529.

[202] Z. J. Ni, D. Maclean, C. P. Holmes, M. M. Murphy, B. Ruhland, J. W. Jacobs, E. M. Gordon and M. A. Gallop, *J. Med. Chem.*, 1996, **39**, 1601.

[203] H. P. Nestler, P. A. Barlett and W. C. Still, *J. Org. Chem.*, 1994, **59**, 4723.

[204] M. H. J. Ohlmeyer, R. N. Swanson, L. W. Dillard, J. C. Reader, G. Asouline, R. Kobayashi, M. Wigler and W. C. Still, *Proc. Natl. Acad. Sci. USA*, 1993, **90**, 10922.

[205] A. Borchardt and W. C. Still, *J. Am. Chem. Soc.*, 1994, **116**, 373.

[206] P. Eckes, *Angew. Chem. Int. Ed. Engl.*, 1994, **33**, 1573.

[207] H. Fenniri, L. Ding, A. E. Ribbe and Y. Zyrianov, *J. Am. Chem. Soc.*, 2001, **123**, 8151.

[208] B. J. Egner, S. Rana, H. Smith, N. Bouloc, J. G. Frey, W. S. Brocklesby and M. Bradley, *Chem. Commun.*, 1997, 735.

[209] R. H. Scott and S. Balasubramanian, *Bioorg. Med. Chem. Lett.*, 1997, **7**, 1567.

[210] J. A. Ferguson, F. J. Steemers and D. R. Walt, *Anal. Chem.*, 2000, **72**, 5618.

[211] M. Han, X. Gao, J. Z. Su and S. Nie, *Nature biotech.,* 2001, **19**, 631.

[212] K. C. Nicolaou, X. Y. Xiao, Z. Parandoosh, A. Senyei and M. P. Nova, *Angew. Chem. Int. Ed. Engl.*, 1995, **34**, 2289.

[213] E. J. Moran, S. Sarshar, J. F. Cargill, M. M. Shahbaz and A. Lio, *J. Am. Chem. Soc.*, 1995, **117**, 10787.

[214] X. Y. Xiao, C. Zhao, H. Potash and M. P. Nova, *Angew. Chem. Int. Ed. Engl.*, 1997, **36**, 780.

[215] B. Clapham, A. J. Richards, M. L. Wood, A. J. Sutherland, *Tetrahedron. Lett.*, 1997, **38**, 9061.

[216] S. E. Whitney and B. Rickborn, *J. Org. Chem.*, 1991, **56**, 3058.

[217] S. J. Culliford, P. McCauley, A. J. Sutherland, M. C. McCairn, J. Sutherland, J. Blackburn, R. Z. Kozlowski, *Biochem. Biophys. Res. Commun.*, 2002, **296**, 857.

[218] B. Clapham and A. J. Sutherland, *J. Org. Chem.*, 2001, **66**, 9033.

[219] S. W. Chaikin and W. G. Brown, *J. Am. Chem. Soc.*, 1949, **71**, 122.

[220] L. K. Mahal, K. J. Yarema and C. R. Bertozzi, *Science (Washington D. C.)*, 1997, **276**, 1125.

[221] J. March, *Advanced Organic Chemistry*, John Wiley and Sons, London, 1992, p. 386.

[222] A. Rodrigue, J. W. Bovenkamp, B. V. Lacroix and R. A. B. Bannard, *Can. J. Chem.*, 1986, **64**, 808.

[223] L. M. Harwood and C. J. Moody, *Experimental Organic Chemistry*, 1994, Blackwell Scientific Publications, London, p. 663.

[224] M. L. Waters, *Curr. Opin.Chem. Biol.*, 2002, **6**, 1.

[225] E. J. Corey and A. Venkateswarlu, *J. Am. Chem. Soc.*, 1972, **94**, 6190.

[226] D. J. Shaw, *Introduction to Colloid and Surface Chemistry*, 4th edition, Butterworth-Heinemann Ltd., Oxford, 1992, pp. 84-93.

[227] E. J. Corey and J. W. Suggs, *Tetrahedron. Lett.*, 1975, 2647.

[228] T. G. Clarke, N. A. Hampson, J. B. Lee, J. R. Morley and B. Scanlon, *Tetrahedron. Lett.*, 1968, 5685.

[229] J. March, *Advanced Organic Chemistry*, John Wiley and Sons, London, 1992, p. 903.

[230] G. W. Anderson, J. E. Zimmerman and F. M. Callahan, *J. Am. Chem. Soc.*, 1964, **86**, 1839.

[231] J. C. Sheehan, *J. Am. Chem. Soc.*, 1955, **77**, 1067.

[232] U.K. application number 0020503.9, U.S. application number 60/247994.

[233] R. Arshady and G. W. Kenner, *J. Polym. Sci.*, 1974, **12**, 2017.

[234] H. Deleuze and D. C. Sherrington, *J. Chem. Soc., Perkin Trans. 2,* 1995, 2217.

[235] NovaBiochem Catalog and Peptide Synthesis Handbook, NovaBiochem, La Jolla, CA, 1998, p S37.

[236] S. Itsuno, Y. Sakurai, K. Ito, T. Maruyama, S. Nakahama and J. M. J. Frechet, *J. Org. Chem.*, 1990, **55**, 304.

[237] B. Clapham and A. J. Sutherland, *Tetrahedron Lett.*, 2000, **41**, 2253.

[238] B. Clapham and A. J. Sutherland, *Tetrahedron Lett.*, 2000, **41**, 2257.

[239] B. Clapham and A. J. Sutherland, *PCT Publication No. WO 00/20475*, 2000.

[240] S. Inokuma, T. Yamamoto and J. Nishimura, *Tetrahedron Lett.,* 1990, **31**, 97.

[241] www.swpolymers.com

[242] J. W. Cornforth, E. D. Morgan, K. T. Potts and R. J. W. Rees, *Tetrahedron,* 1973, **29**, 1659.

[243] L. Borjesson and C. J. Welch, *Acta Chemica Scandinavica,* 1991, **45**, 621.

[244] D. J. Shaw, *Introduction to Colloid and Surface Chemistry*, 4th edition, Butterworth-Heinemann Ltd., Oxford, 1992, pp. 151-168.

[245] C. Rulison, *Krüss Technical Note #302*. 1996 (www.kruss.de; e-mail. info@kruss.de).

[246] E. W. Washburn, *Phys. Rev.*, 1921, **17**, 374.

[247] Amersham Life Science Catalogue, 1996, p. 190.

[248] D. L. Horrocks, *Applications of Liquid Scintillation Counting*, Academic Press, 1974, pp. 51-57.

[249] M. A. Gallop and W. L. Fitch, *Curr. Opin. Chem. Biol.*, 1997, **1**, 94.

[250] W. Li and B. Yan, *J. Org. Chem.*, 1998, **63**, 4092.

[251] B. Yan, Q. Sun, J. R. Wareing and C. F. Jewell, *J. Org. Chem.*, 1996, **61**, 8765.

[252] B. Yan, G. Kumaravel, H. Anjaria, A. Wu, R. C. Petter, C. F. Jewell and J. R. Wareing, *J. Org. Chem.*, 1995, **60**, 5736.

[253] B. D. Larsen, D. H. Christensen, A. Holm, R. Zillmer and O. F. Nielsen, *J. Am. Chem. Soc.*, 1993, **115**, 6247.

[254] B. Schneider, D. Doskocilova and J. Dybal, *Polymer*, 1985, **26**, 253.

[255] W. L. Fitch, G. Detre, C. P. Holmes, J. N. Shoolery and P. A. Keifer, *J. Org. Chem.*, 1994, **59**, 7955.

[256] S. L. Manatt, C. F. Amsden, C. A. Bettison, W. T. Frazer, J. T. Gudman, B. E. Lenk, J. F. Lubetich, E. A. McNelly, S. C. Smith, D. J. Templeton and R. P. Pinnell, *Tetrahedron Lett.*, 1980, **21**, 1397.

[257] B. J. Egner, G. J. Langley and M. Bradley, *J. Org. Chem.*, 1995, **60**, 2652.

[258] M. S. Bernatowicz, S. B. Daniels and H. Koster, *Tetrahedron Lett.*, 1989, **30**, 4645.

[259] D. P. Walsh, C. Pang, P. B. Parikh, Y. Kim and Y. Chang, *J. Comb. Chem.*, 2002, **4**, 204.

[260] M. Egholm, P. E. Nielsen, O. Buchardt and R. H. Berg, *J. Am. Chem. Soc.*, 1992, **114**, 9677.

[261] M. Egholm, C. Behrens, L. Christiensen, R. H. Berg, P. E. Nielsen and O. Buchardt, *J. Chem. Soc., Chem. Commun.*, 1993, 800.

[262] www.appliedbiosystems.com

[263] S. A. Thomson, J. A. Josey, R. Cadilla, M. D. Gaul, F. Hassman, M. J. Luzzio, A. J. Pipe, K. L. Reed, D. J. Ricca, R. W. Wiethe and S. A. Noble, *Tetrahedron*, 1995, **51**, 6179.

[264] Personnel communication, M. Bradley.

[265] J. Nielsen and L. O. Lyngs, *Tetrahedron Lett.*, 1996, **37**, 8439.

[266] J. Sambrook, E. F. Fritsch and T. Maniatis, *Molecular Cloning A Laboratory Manual 2*, Second Edition, 1989, Cold Spring Harbour, New York, p. 11.31.

[267] J. Sambrook, E. F. Fritsch and T. Maniatis, *Molecular Cloning A Laboratory Manual 3*, Second Edition, 1989, Cold Spring Harbour, New York, p. E.19.

[268] www.promega.com

[269] Personal communication M. Hughes.

[270] J. Homer and M. C. Perry, *J. Chem. Soc., Chem. Commun.* 1994, 373.

Chapter 6

Appendix

6.1 Appendix A

Scintilipid	Percentage efficiency [a,b]	PC : Scintilipid / cpm [a, c]	DOTAP : Scintilipid / cpm [a, c]	DOTAP : DOPE : Scintilipid / cpm [a, c]
104	0.1	12	10	8
106	0.6	3	3	10
109	14	214	469	506
110	11	8	234	146
111	19	308	128	518
112	0.9	96	76	62
114	93	12	58	20
116	9	32	12	10
117	17	18	30	44
118	13	9	20	66
119	21	161	129	172

Table 37: Scintillation counting efficiency of scintilipid compounds and the counts per minute (cpm) of the corresponding scintiliposomes (lipid:scintilipid, 10:1).

[a] Values are background corrected. [b] To a solution of scintilipid compound in toluene (200 µL, 20 mM) was added [^{3}H]hexadecane (200 µL, 0.5 µCi/mL), followed by monitoring in a scintillation counter. Values correspond to the cpm as a percentage of the cpm detected with the addition of commercial scintillation fluid Microscint 20. All values have been adjusted to accommodate the fact that a system based solely on 2,5-diphenyloxazole **1** gives approximately 70% scintillation counting efficiency when compared with commercial scintillation fluid. [c] [^{14}C]taurine (0.1 µCi) is added to scintiliposome preparation (500 µL, 10 mg/mL, 10:1, lipid:scintilipid) and the assay solution monitored in a scintillation counter.

Polymer	DCM			THF			DMF			water			toluene		
	Initial / mL	Final / mL	%	Initial / mL	Final / mL	%	Initial / mL	Final / mL	%	Initial / mL	Final / mL	%	Initial / mL	Final / mL	%
121	0.10	0.39	290	0.10	0.38	280	0.10	0.21	110	0.10	0.10	0	0.10	0.41	310
122	0.05	0.14	180	0.05	0.14	180	0.05	0.07	40	0.05	0.05	0	0.05	0.11	120
123	0.10	0.39	290	0.10	0.39	290	0.10	0.20	100	0.10	0.10	0	0.10	0.35	250
124	0.05	0.11	120	0.05	0.12	140	0.05	0.07	40	0.05	0.05	0	0.05	0.07	40
125	0.10	0.30	200	0.10	0.33	230	0.10	0.18	80	0.10	0.10	0	0.10	0.34	240

Table 38: Percentage volume increase of polymer resins **121-125** upon contact with DCM, THF, DMF, water and toluene. Mean estimated error = $^{+}$/-23%.

Polymer	DCM			THF			DMF			water			toluene		
	Initial / mL	Final / mL	%	Initial / mL	Final / mL	%	Initial / mL	Final / mL	%	Initial / mL	Final / mL	%	Initial / mL	Final / mL	%
9	0.04	0.14	250	0.04	0.13	225	0.04	0.09	125	0.04	0.04	0	0.04	0.14	250
27	0.03	0.04	33	0.03	0.05	67	0.03	0.09	200	0.03	0.06	100	0.03	0.08	167
29	0.03	0.08	167	0.03	0.13	333	0.03	0.11	267	0.035	0.06	71	0.03	0.08	167
135	-	-	-	-	-	-	0.05	0.12	140	0.05	0.05	0	0.05	0.19	280
136	-	-	-	-	-	-	0.03	0.04	33	0.04	0.04	0	0.03	0.07	133
137	-	-	-	-	-	-	0.04	0.05	25	0.04	0.04	0	0.04	0.09	125
138	-	-	-	-	-	-	0.05	0.10	100	0.05	0.05	0	0.05	0.15	200
139	-	-	-	-	-	-	0.02	0.09	350	0.02	0.04	100	0.02	0.07	250
140	0.02	0.15	650	0.02	0.14	600	0.02	0.19	850	0.02	0.12	500	0.02	0.06	200
141	0.02	0.19	850	0.02	0.16	700	0.02	0.2	900	0.02	0.12	500	0.02	0.06	200
142	0.02	0.19	850	0.02	0.12	500	0.02	0.20	900	0.02	0.15	650	0.02	0.06	200

Table 39: Percentage volume increase of polymer resins **9**, **27**, **29**, **135-142** upon contact with DCM, THF, DMF, water and toluene. Mean estimated error = $^{+}$/-43%.

Polymer	DCM			THF			DMF			water			toluene		
	Initial / mL	Final / mL	%	Initial / mL	Final / mL	%	Initial / mL	Final / mL	%	Initial / mL	Final / mL	%	Initial / mL	Final / mL	%
154	0.02	0.24	1100	0.02	0.19	850	0.02	0.23	1050	0.02	0.20	900	0.02	0.05	150
155	0.02	0.22	1000	0.02	0.17	750	0.02	0.23	1050	0.02	0.15	650	0.02	0.05	150
156	0.02	0.22	1000	0.02	0.16	700	0.02	0.20	900	0.02	0.145	600	0.02	0.06	200
157	0.02	0.21	950	0.02	0.16	700	0.02	0.18	800	0.02	0.13	550	0.02	0.06	200
158	0.02	0.20	900	0.02	0.15	650	0.02	0.17	750	0.02	0.13	550	0.02	0.07	250
159	0.02	0.20	900	0.02	0.15	650	0.02	0.15	650	0.02	0.12	500	0.02	0.07	250
160	0.02	0.12	500	0.02	0.14	600	0.02	0.12	500	0.02	0.12	500	0.02	0.09	350

Table 40: Percentage volume increase of polymer resins **154-160** upon contact with DCM, THF, DMF, water and toluene.

Mean estimated error = $^{+}$/-47%.

Polymer	DCM			THF			DMF			water			toluene		
	Initial / mL	Final / mL	%	Initial / mL	Final / mL	%	Initial / mL	Final / mL	%	Initial / mL	Final / mL	%	Initial / mL	Final / mL	%
174	0.04	0.59	1375	0.04	0.43	975	0.04	0.37	825	0.04	0.30	650	0.04	0.41	925

Table 41: Percentage volume increase of polymer resin **174** upon contact with DCM, THF, DMF, water and toluene.

Mean estimated error = $^{+}$/-17%.

Polymer	DCM			THF			DMF			water			toluene		
	Initial / mL	Final / mL	%	Initial / mL	Final / mL	%	Initial / mL	Final / mL	%	Initial / mL	Final / mL	%	Initial / mL	Final / mL	%
178	0.02	0.25	1150	0.02	0.20	900	0.02	0.20	900	0.02	0.20	900	0.02	0.19	850

Table 42: Percentage volume increase of polymer resin **178** upon contact with DCM, THF, DMF, water and toluene.

Mean estimated error = $^{+}$/-47%.

6.3 Appendix C

Time / sec	Mass / mg						
	Blank	9	29	27	140	141	142
0	0.0	0.0	1.8	0.0	0.0	0.0	0.8
30	65.0	29.0	70.8	50.4	48.5	50.9	104.0
60	66.3	36.1	99.6	54.7	83.3	56.2	117.7
90	66.3	41.1	112.5	89.5	106.4	65.0	126.0
120	66.5	44.8	117.0	99.8	115.5	82.7	132.8
180	67.4	49.8	117.0	101.6	127.1	100.4	140.8
240	67.9	51.6	117.0	102.1	135.1	110.1	147.1
300	67.9	53.6	117.0	102.6	140.8	115.1	150.8
360	68.4	55.7	117.3	103.1	144.3	117.9	153.3
420	68.4	57.6	117.5	103.6	146.2	120.8	156.4
480	68.4	58.6	118.0	103.6	147.8	122.9	157.7
540	68.4	59.3	118.0	103.6	148.8	124.9	159.8
600	68.4	59.5	118.0	103.8	150.4	126.7	161.5
660	68.4	60.4	118.3	104.1	151.6	128.3	164.2
720	68.4	60.8	118.6	104.7	152.6	129.5	164.8
780	68.4	61.4	119.0	104.7	153.5	130.7	165.6
840	68.4	61.7	119.0	105.2	154.6	132.3	166.5
900	68.4	62.5	119.0	105.2	155.5	133.0	167.6
960	68.4	63.0	119.0	105.5	156.5	134.4	168.5
1020	68.4	63.3	119.0	105.5	156.5	135.6	169.0
1080	68.4	63.4	119.2	105.5	157.4	136.5	169.5
1140	68.4	63.9	119.5	105.5	158.4	137.5	170.6
1200	68.4	64.4	120.1	105.5	158.6	138.6	171.0
1260	68.4	64.4	120.1	106.0	159.9	139.5	171.6
1320	68.4	65.5	120.1	106.0	160.2	140.4	172.5
1380	68.4	65.5	120.6	106.0	160.3	140.6	172.5
1440	68.4	65.6	120.6	106.5	161.2	141.4	172.5
1500	68.4	66.4	120.6	106.5	161.6	142.3	173.3
1560	68.4	66.4	121.1	106.5	162.4	142.8	173.4
1620	68.4	67.4	121.1	106.5	162.4	143.9	174.4
1680	68.4	67.4	121.1	107.0	163.4	144.4	174.4
1740	68.4	67.4	121.1	107.6	163.4	144.8	174.6
1800	68.4	67.5	121.1	107.6	164.3	146.4	175.5
1860	68.4	67.8	121.2	107.6	164.3	146.5	175.9
1920	68.4	68.3	121.4	107.6	164.3	147.8	176.4
1980	68.4	68.3	121.4	107.6	164.7	148.3	176.4
2040	68.4	68.9	121.8	107.6	165.2	148.7	176.6
2100	68.4	69.2	121.9	107.6	165.3	149.7	176.8
2160	68.4	69.2	121.9	107.6	166.2	150.2	177.2
2220	68.4	69.2	121.9	107.9	166.2	151.3	177.3
2280	68.4	69.5	122.4	108.6	166.2	152.0	177.4
2340	68.4	70.3	123.0	108.6	166.6	152.1	178.4
2400	68.5	70.3	123.0	108.6	167.3	153.0	178.4

Table 43: Mass-water up-take versus time data for polymers **9**, **27**, **29**, **140-142** and a blank control.

Time / sec	Mass / mg						
	Blank	9	29	27	140	141	142
0	0.0	0.0	0.0	0.0	0.0	0.0	0.0
30	71.4	131.5	161.1	120.1	126.6	119.8	155.2
60	72.3	139.7	164.2	144.5	156	133.2	173.2
90	72.9	138.7	164.2	144.4	163.8	141.2	184.7
120	73.3	139.7	164.2	143.0	169.4	146.9	191.2
180	74.4	139.7	163.2	142.7	177.5	155.8	203.4
240	74.4	139.7	163.2	142.7	189.0	161.1	212.3
300	75.3	139.7	163.2	142.7	199.7	165.3	216.3
360	75.3	139.7	163.2	142.7	204.7	168.4	221.6
420	75.3	139.7	163.2	142.7	206.5	171.9	225.0
480	75.8	139.7	163.2	142.7	207.6	174.4	227.9
540	75.8	138.6	163.2	142.7	208.7	175.9	229.8
600	76.0	138.6	163.2	142.7	208.7	177.2	232.0
660	76.3	138.6	163.2	142.7	209.7	180.0	233.7
720	76.3	138.4	163.2	142.7	210.2	182.2	235.2
780	76.3	138.1	163.2	142.7	212.4	186.1	237.5
840	76.3	137.7	163.2	142.7	212.5	188.9	238.6
900	76.3	137.6	163.2	142.7	212.7	192.0	239.6
960	76.3	137.6	163.2	142.2	213.1	192.8	241.1
1020	76.3	137.5	163.2	142.2	213.6	194.5	241.6
1080	76.3	137.2	162.7	142.2	213.6	195.8	242.5
1140	76.3	137.2	162.7	142.2	214.1	197.3	243.6
1200	76.3	136.7	162.7	142.2	214.1	198.0	244.6
1260	76.3	136.1	162.7	142.2	214.6	199.5	245.1
1320	76.3	135.6	162.2	141.7	214.6	201.3	245.4
1380	76.3	135.6	162.3	141.7	214.6	203.2	245.7
1440	76.3	135.6	162.3	141.7	214.6	204.1	246.4
1500	76.3	135.6	162.2	141.7	214.6	205.7	247.4
1560	76.5	134.6	162.7	141.7	214.6	207.1	247.4
1620	76.5	134.6	162.6	141.7	214.6	208.5	248.5
1680	76.5	134.2	163.2	141.7	214.6	211.3	249.0
1740	76.5	133.7	163.2	141.7	214.6	213.6	249.0
1800	76.5	133.7	163.2	141.7	214.6	216.2	249.2
1860	76.7	133.7	163.2	141.7	214.6	218.4	249.3
1920	76.7	133.5	163.2	141.1	214.6	219.3	249.6
1980	76.7	133.5	163.2	140.8	214.6	220.1	249.8
2040	76.7	133.5	163.2	140.8	214.6	221.2	250.3
2100	76.7	133.5	163.2	140.7	214.6	222.7	250.3
2160	76.7	133.5	163.2	140.7	214.6	223.1	250.6
2220	76.7	133.5	163.2	140.7	214.6	223.6	251.4
2280	76.7	133.5	163.2	140.7	214.6	224.3	251.4
2340	76.7	133.5	163.2	140.7	214.6	225.5	251.4
2400	76.7	133.6	163.2	140.7	214.6	228.0	251.4

Table 44: Mass-DMF up-take versus time data for polymers **9**, **27**, **29**, **140-142** and a blank control.

Time / sec	Mass / mg						
	Blank	9	29	27	140	141	142
0	0.0	0.0	0.0	0.0	0.0	0.0	0.0
30	77.3	154.0	126.6	104.5	91.9	97.8	90.8
60	77.5	154.5	128.8	127.6	94.4	97.9	92.8
90	77.5	154.5	128.8	128.0	96.0	99.3	93.9
120	77.3	152.5	129.1	128.0	97.6	99.6	94.8
180	77.6	153.5	129.3	128.0	98.7	100.6	97.2
240	77.6	154.0	129.8	128.2	100.0	101.9	97.8
300	77.6	154.5	129.8	128.5	101.2	103.2	98.8
360	78.1	154.5	130.1	128.5	101.7	103.6	99.7
420	78.1	154.6	130.4	128.9	102.1	104.1	100.7
480	78.6	155.3	130.8	128.9	103.2	104.5	101.1
540	78.6	155.3	130.8	128.9	103.5	105.6	101.5
600	78.9	156.3	130.8	129.6	103.8	105.6	101.5
660	79.3	156.3	131.0	130.0	104.6	105.8	102.1
720	79.6	157.0	131.3	130.0	105.1	106.6	102.5
780	79.6	157.9	131.9	130.0	105.6	107.1	103.1
840	79.6	158.4	131.9	130.0	105.6	107.1	103.3
900	79.8	158.4	132.4	130.0	105.6	107.3	103.5
960	80.5	158.5	132.4	130.2	105.7	107.5	103.5
1020	80.7	159.2	132.5	131.0	106.0	107.5	103.7
1080	81.2	159.6	132.6	131.0	106.5	107.7	103.9
1140	81.6	160.3	132.7	131.0	106.5	107.9	104.2
1200	81.6	160.3	132.7	131.5	106.7	108.4	104.6
1260	81.6	161.3	132.7	132.0	107.6	108.4	104.6
1320	81.6	162.3	133.0	132.0	107.6	108.7	104.6
1380	81.6	162.3	133.2	132.0	107.6	109.0	105.0
1440	81.6	162.3	133.2	132.0	107.6	109.4	105.0
1500	81.6	162.4	133.7	132.0	107.6	109.4	105.0
1560	81.6	163.2	133.7	132.0	107.7	109.4	105.0
1620	81.6	163.6	133.7	132.1	108.6	109.4	105.0
1680	81.6	163.6	134.0	132.3	108.6	109.5	105.0
1740	81.6	163.6	134.8	132.3	108.6	109.7	105.0
1800	81.6	163.7	134.8	132.8	109.0	110.0	105.0
1860	81.6	163.7	134.8	132.8	109.0	110.5	105.0
1920	81.6	163.7	134.8	132.8	109.0	110.5	105.3
1980	81.6	163.8	134.8	132.8	109.3	111.0	105.3
2040	81.6	163.8	134.8	133.3	109.3	111.0	105.3
2100	81.6	163.8	134.9	133.7	109.4	111.5	105.4
2160	81.6	163.9	135.8	133.8	109.4	111.5	105.4
2220	81.6	163.9	135.8	133.8	109.4	111.5	105.4
2280	81.6	163.9	135.8	133.8	109.4	111.5	105.4
2340	81.6	163.9	135.8	134.0	109.4	111.5	105.4
2400	81.6	164.0	136.3	134.0	109.9	111.6	105.4

Table 45: Mass-toluene up-take versus time data for polymers **9**, **27**, **29**, **140-142** and a blank control.

6.4 Appendix D

Time / hr	166,water,18-C-6 / cpm mg^{-1}	166,benzene,18-C-6 / cpm mg^{-1}	167,water,18-C-6 / cpm mg^{-1}	167,benzene,18-C-6 / cpm mg^{-1}
0	227920	305994	29762	30021
1	227920	172618	29483	13179
2	219201	178789	29308	6157
3	218290	159996	29004	3055
4	218095	142971	28773	1652
5	215645	130014	28497	1043
6	216345	119019	28282	781
7	209655	111433	27996	661
8	198192	100040	27809	598
9	194248	94694	27725	543
10	187220	83996	27422	505
11	185741	73501	27240	484
12	184352	69077	27039	460
13	179837	64680	26974	450
14	172816	56673	26829	442
15	175403	54216	26731	434
16	171719	52235	26485	428
17	169830	50660	26323	416
18	173767	49013	26087	405
19	170513	47652	26118	394
20	168394	49097	25970	386
21	165968	51354	25862	386
22	161024	49478	25869	375
23	159881	51633	25608	369
24	151008	50390	25547	369
25	145432	49834	25448	368
26	141468	45921	25361	365
27	139795	48600	25249	366
28	144072	46878	25192	357
29	134979		25163	
30	138428		24938	
31	133569		24778	
32	132041		24669	
33	127150		24657	
34	125347		24509	
35	123207		24541	
36	120699		24423	
37	117066		24302	
38	110029		24283	
39	106660		24204	
40	106163		24065	
41	106539		24023	
42	104518		23956	
43	102119		23849	

44	100422		23894	
45	96292		23693	
46	92760		23554	
47	91820		23493	
48	89238		23490	
49	87035		23424	
50	85488		23238	
51	82864		23200	
52	80689		23094	
53	79027		23044	
54	72218		22983	
55	72130		22937	
56	72526		22834	
57	71356		22766	
58	70226		22700	
59	70018		22671	
60	69154		22645	
61	68766		22569	
62	67280		22503	
63	66525		22429	
64	63863		22347	
65	62617		22251	

Table 46: Scintillation counting data for polymer supports **166** and **167** during incubation with a solution of KOH/benzene/18-crown-6 (cat) (0.18 M) and KOH/water/18-crown-6 (cat) (0.18 M). According to Table 23, Mean error = $^{+}$/-7%.

Time / hrs	166,water,18-C-6 % cpm	166,benzene,18-C-6 % cpm	167,water,18-C-6 % cpm	167,benzene,18-C-6 % cpm
0	100	100	100	100
1	100	56	99	44
2	96	58	98	21
3	96	52	97	10
4	96	47	97	6
5	95	42	96	3
6	95	39	95	3
7	92	36	94	2
8	87	33	93.	2
9	85	31	93	2
10	82	27	92	2
11	81	24	92	2
12	81	23	91	2
13	79	21	91	1
14	76	19	91	1
15	77	18	90	1
16	75	17	89	1
17	75	17	88	1
18	76	16	88	1
19	75	16	88	1

20	74	16	87	1
21	73	17	87	1
22	71	16	87	1
23	70	17	86	1
24	66	16	86	1
25	64	16	86	1
26	62	15	85	1
27	61	16	84	1
28	63	15	85	1
29	59		85	
30	61		84	
31	59		83	
32	58		83	
33	56		83	
34	55		82	
35	54		82	
36	53		82	
37	51		82	
38	48		82	
39	47		81	
40	47		81	
41	47		81	
42	46		80	
43	45		80	
44	44		80	
45	42		80	
46	41		79	
47	40		79	
48	39		79	
49	38		79	
50	38		78	
51	36		78	
52	35		78	
53	35		77	
54	32		77	
55	32		77	
56	32		77	
57	31		76.	
58	31		76	
59	31		76	
60	30		76	
61	30		76	
62	30		76	
63	29		75	
64	28		75	
65	27		75	

Table 47: Percentage scintillation counting data for polymers **166-167** during incubation with a solution of KOH/benzene/18-crown-6 (cat) (0.18 M) and KOH/water/18-crown-6 (cat) (0.18 M).

Polymer	Polymer (6 x SSPE) x 3	6xSSPE	centrifuge	4xSSPE	centrifuge	2xSSPE	centrifuge	water	centrifuge	Sc-fluid
175+^{33}P-DNA(A_{10})	23	31419	38194	29339	28770	26059	26629	24674	24377	62257
175+^{33}P-DNA(A_{10})	26	36514	44832	35543	34396	32571	31047	29757	29845	68644
175+^{33}P-DNA(T_{10})	33	24938	15756	1185	481	116	89	47	60	934
175+^{33}P-DNA(T_{10})	25	25053	15429	1114	534	130	91	49	54	905
175+[γ^{33}P]ATP	22	31806	20761	1854	883	242	313	494	252	4548
175+[γ^{33}P]ATP	24	27624	17838	1345	690	259	277	526	243	7470
174+^{33}P-DNA(A_{10})	20	23429	13546	1221	481	138	87	51	77	521
174+^{33}P-DNA(A_{10})	30	22410	12210	1318	474	137	132	55	58	808
174+^{33}P-DNA(T_{10})	22	31957	18871	1781	578	89	456	37	40	891
174+^{33}P-DNA(T_{10})	23	28749	18921	1199	516	72	60	51	44	592
174+[γ^{33}P]ATP	18	27662	19530	3106	930	380	198	138	122	1959
174+[γ^{33}P]ATP	20	25503	15448	1469	752	166	224	117	131	2196

Table 48: Scintillation counting data for POP-Sc-PNA(T_{10}) **175** and POP-Sc **174** incubated with ^{33}P-DNA(A_{10}), ^{33}P-DNA(T_{10}) and ^{33}P[ATP] blank control. Scintillation counts over 10000 cpm have a mean error = $^{+}$/-10%.

Polymer	Polymer (6 x SSPE) x 3	6xSSPE	centrifuge	4xSSPE	centrifuge	2xSSPE	centrifuge	water	centrifuge	Sc-fluid
175+^{33}P-DNA(A_{10})	24	33967	41513	32441	31583	29315	28838	27216	27111	65450
175+^{33}P-DNA(T_{10})	29	24996	15593	1149	508	123	90	48	57	920
175+^{33}P[ATP]	23	29715	19299	1600	786	250	295	510	248	6009
174+^{33}P-DNA(A_{10})	25	22919	12878	1269	478	138	110	53	68	665
174+^{33}P-DNA(T_{10})	23	30353	28331	1490	547	81	258	44	42	741
174+^{33}P-[ATP]	19	26582	17489	2288	841	273	211	128	127	2078

Table 49: Averaged scintillation counting data for POP-Sc-PNA(T_{10}) **175** and POP-Sc **174** incubated with ^{33}P-DNA(A_{10}), ^{33}P-DNA(T_{10}) and ^{33}P[ATP] blank control. Scintillation counts over 10000 cpm have a mean error = $^{+}$/-10%.

6.6 Appendix F

	1	2	3	4	5	6	7	8
A	5527	4608	808	850	3956	4436	3663	4263
B	5614	6703	3221	1850	5609	4437	3913	4795
C	4379	2585	4375	3546	3673	5988	8045	978
D	2101	5044	6154	1204	5066	4656	4748	3637
E	5799	3815	8109	3991	7054	6127	4853	3871
F	6401	6219	7614	5394	9898	6000	8143	6057
G	8150	5505	7006	5593	7337	3896	6536	2679
H	7038	7150	6472	4391	5686	5741	5216	4814
I	1389	2872	2220					

Table 50: Scintillation counting data (cpm) for POP-Sc-PNA library incubated with ^{33}P-DNA(A_9) in 6 x SSPE following centrifugation.

	1	2	3	4	5	6	7	8
A	1774	3611	124	294	3129	2936	4850	2586
B	2414	4411	2213	1418	3017	3403	4428	4606
C	313	1611	2806	3340	2771	4034	5462	511
D	1320	2835	4107	408	4736	2962	3913	3212
E	2481	2036	6740	3536	4947	3636	2885	2685
F	4912	4506	6576	4964	7343	5733	11167	5578
G	5324	2840	4884	5750	4935	2425	4394	2198
H	7106	5748	4564	4340	4427	3613	4391	3639
I	647	2336	2106					

Table 51: Scintillation counting data (cpm) for POP-Sc-PNA library following washing with 4 x SSPE and centrifugation.

	1	2	3	4	5	6	7	8
A	1926	2296	82	227	3846	2302	5836	1494
B	4111	2096	4910	1336	2965	3109	3869	3958
C	1961	1487	2477	2247	1869	3406	4087	404
D	1577	2098	3230	351	4643	1813	2583	3273
E	1380	1472	5125	1670	1534	3192	3672	1859
F	5714	3713	4307	4715	6621	4777	7422	5459
G	4747	1464	4184	3286	4671	2790	2897	1287
H	6330	3749	3734	3849	3700	1628	2041	3856
I	706	1947	1711					

Table 52: Scintillation counting data (cpm) for POP-Sc-PNA library following washing with 2 x SSPE and centrifugation.

	1	2	3	4	5	6	7	8
A	2321	5792	117	227	5244	3500	6040	5296
B	4687	2714	2769	1317	3340	2963	4507	5533
C	3551	1398	2518	3516	2372	4277	5025	458
D	1691	2687	3464	287	5086	2853	2944	2827
E	2210	1342	5453	2029	1494	2887	6257	2405
F	6483	3772	4833	5241	5895	5811	6919	6899
G	4820	1906	4790	4974	4825	2299	3597	1856
H	7009	3687	3817	3659	4503	2835	3902	2985
I	365	1226	2532					

Table 53: Scintillation counting data (cpm) for POP-Sc-PNA library following washing with water and centrifugation.

	1	2	3	4	5	6	7	8
A	2988	6786	181	260	8035	3646	6561	8653
B	9653	4663	4308	1310	4870	3151	6769	4985
C	4697	1352	5421	4719	2675	4516	7344	460
D	2655	4199	4917	423	7345	5298	5615	2865
E	3633	2312	6366	4691	2156	4343	7368	3266
F	7176	6061	4696	7481	8236	9639	8237	7418
G	5680	3101	4945	6202	4658	2275	5153	2111
H	8298	3261	4313	5408	5309	6353	6715	4322
I	716	2771	3409					

Table 54: Scintillation counting data (cpm) for POP-Sc-PNA library following washing with water (25 °C, 15 min) and centrifugation.

	1	2	3	4	5	6	7	8
A	3702	6825	220	286	9357	3759	8025	9361
B	10431	4995	4390	1101	6181	3049	7205	9535
C	5657	1341	5787	5488	3217	5640	9336	605
D	3108	4617	5069	585	6563	5338	6552	2623
E	3833	3238	7837	5216	2915	4803	7316	3396
F	8146	5723	4904	8267	7128	11058	7901	8648
G	6090	3166	5002	7152	5609	2377	4818	2483
H	8245	3379	2854	5841	5440	6044	7577	4906
I	667	3012	3747					

Table 55: Scintillation counting data (cpm) for POP-Sc-PNA library following washing with water (30 °C, 15 min) and centrifugation.

	1	2	3	4	5	6	7	8
A	4474	6745	189	322	9388	3881	7257	9466
B	9923	5861	4972	1221	6159	3360	7634	8378
C	5749	1740	6340	6163	3292	5571	9277	523
D	3098	5440	5281	658	6496	6264	6207	2741
E	3723	3774	7371	6815	2748	5264	9776	3826
F	7021	6824	5226	8343	8219	10222	8666	9683
G	5102	3988	5621	10003	5325	2582	6008	2494
H	8996	3951	5234	6178	6338	7260	7773	4775
I	722	3230	4307					

Table 56: Scintillation counting data (cpm) for POP-Sc-PNA library following washing with water (40 °C, 15 min) and centrifugation.

	1	2	3	4	5	6	7	8
A	582	1228	37	83	784	1924	3296	862
B	456	1058	480	114	493	2528	412	614
C	1777	992	1354	3566	1349	7349	1126	206
D	402	1085	967	100	1907	2293	758	395
E	699	400	1479	1018	820	1011	993	704
F	3080	1371	4328	1453	6728	1152	2091	1145
G	1347	672	2921	1117	4764	527	902	378
H	1377	1330	946	914	953	1328	1309	885
I	75	321	223					

Table 57: Scintillation counting data (cpm) for POP-Sc-PNA library following first washing with 50% formamide/2 x SSPE (40 °C, 15 min) and centrifugation.

	1	2	3	4	5	6	7	8
A	340	773	41	62	560	1360	1160	637
B	434	677	395	73	362	1352	341	426
C	1311	847	799	2479	850	5369	648	96
D	171	471	806	86	1279	1666	449	260
E	465	259	876	587	421	548	517	368
F	1697	492	3392	679	4872	581	975	542
G	800	408	1929	681	3272	377	269	701
H	636	895	489	486	541	651	619	605
I	36	158	135					

Table 58: Scintillation counting data (cpm) for POP-Sc-PNA library following second washing with 50% formamide/2 x SSPE (40 °C, 15 min) and centrifugation.

	1	2	3	4	5	6	7	8
A	329	742	36	56	478	1524	810	616
B	260	523	311	79	289	1275	282	296
C	1113	857	682	2227	801	5015	550	83
D	163	441	381	85	1169	1442	431	241
E	281	210	769	568	342	536	445	323
F	1664	514	3410	547	3952	600	763	588
G	730	306	1836	573	2779	310	621	203
H	467	1008	456	431	607	525	575	615
I	52	147	114					

Table 59: Scintillation counting data (cpm) for POP-Sc-PNA library following third washing with 50% formamide/2 x SSPE (40 °C, 15 min) and centrifugation.

Washing and centrifugation procedure	POP-Sc-PNA(T_4AT_4) + ^{33}P-DNA(A_9) / cpm	POP-Sc-PNA($T_4A_2T_3$) + ^{33}P-DNA(A_9) / cpm
6 x SSPE	8415	5142
4 x SSPE	5196	4248
2 x SSPE	4845	7180
water	5780	5104
water (25 °C, 15 min)	8510	8774
water (30 °C, 15 min)	7716	7042
water (40 °C, 15 min)	8588	7347
1st 50 % formamide/2 x SSPE (40 °C, 15 min)	1384	843
2nd 50 % formamide/2 x SSPE (40 °C, 15 min)	776	497
3rd 50 % formamide/2 x SSPE (40 °C, 15 min)	741	484

Table 60: Scintillation counting data for POP-Sc-PNA(T_4AT_4) and POP-Sc-PNA($T_4A_2T_3$) hybridised with ^{33}P-DNA(A_9) following sequential washing and centrifugation.

Acording to Table 48, Tables 50-60 have a mean error = $^{+}$/-10%.